NATURAL KILLER CELLS, HYPOXIA, AND EPIGENETIC REGULATION OF HEMOCHORIAL PLACENTATION

BY

Damayanti Chakraborty

Submitted to the graduate degree program in Pathology and Laboratory Medicine and the Graduate Faculty of the University of Kansas in partial fulfillment ofthe requirements for the degree of Doctor of Philosophy.

_____

Chair: Michael J. Soares, Ph.D.

_____

Jay Vivian, Ph.D.

_____

Patrick Fields, Ph.D.

_____

Soumen Paul, Ph.D.

_____

Michael Wolfe, Ph.D.

_____

Adam J. Krieg, Ph.D.

Date Defended: 04/01/2013

The Dissertation Committee for Damayanti Chakraborty

certifies that this is the approved version of the following dissertation:

NATURAL KILLER CELLS, HYPOXIA, AND EPIGENETIC REGULATION OF HEMOCHORIAL PLACENTATION

_____

Chair: Michael J. Soares, Ph.D.

Date approved: 04/01/2013

ABSTRACT

During the establishment of pregnancy, uterine stromal cells differentiate into decidual cells and recruit natural killer (NK) cells. These NK cells are characterized by low cytotoxicity and distinct cytokine production. In rodent as well as in human pregnancy, the uterine NK cells peak in number around mid-gestation after which they decline. NK cells associate with uterine spiral arteries and are implicated in pregnancy associated vascular remodeling processes and potentially in modulating trophoblast invasion. Failure of trophoblast invasion and vascular remodeling has been shown to be associated with pathological conditions like preeclampsia syndrome, hypertension in mother and/or fetal growth restriction.

We hypothesize that NK cells fundamentally contribute to the organization of the placentation site. In order to study the *in vivo* role of NK cells during pregnancy, gestation stage-specific NK cell depletion was performed in rats using anti asialo GM1 antibodies. Robust endovascular trophoblast invasion and vascular remodeling were observed in NK cell depleted animals. This depletion affected mesometrial vasculature, lowered relative oxygen concentrations at the placentation site and altered trophoblast lineage commitment at gestation d9.5. There was also a significant change in the organization of the chorioallantoic placenta on d13.5. Delivery of oxygen appears to be a key signal influencing both trophoblast cell differentiation and organization of the placentation site.

Hypoxia promotes development of the invasive trophoblast lineage. We next evaluated the impact of hypoxia on the trophoblast stem (TS) cell transcriptome. DNA microarray analysis was performed on rat TS cells exposed to atmospheric and low oxygen (0.5%). Upregulation of genes characteristic of an invasive phenotype and a marked downregulation of stem state-associated genes were observed. Matrix metalloproteinase 12 (*Mmp12*) and lysine demethylase

3A (*Kdm3a*) were markedly upregulated in response to low oxygen, while E-cadherin (*Cdh1*) expression was dramatically decreased. These responses were dependent upon hypoxia inducible factor (HIF) signaling. Several of the HIF targets were identified to be *Kdm3a* targets. KDM3A acts on dimethyl and monomethyl histone H3K9 substrates, which prompted an examination of global histone H3K9 methylation status of trophoblast cells developing *in vitro* and *in vivo*. Hypoxia significantly impacted histone H3K9 methylation. Knockdown of KDM3A in TS cells inhibited hypoxia-induced *Mmp12* gene expression and disrupted histone H3K9 methylation status at the *Mmp12* locus.

Ectopic expression of KDM3A stimulated MMP12 expression. KDM3A knockdown also significantly decreased hypoxia-activated TS cell invasion through Matrigel chambers. Finally, blastocysts transduced with *Kdm3a* shRNA expressing lentiviral particles showed reduced outgrowth when exposed to low oxygen tensions. In summary, NK cells impact oxygen delivery and uteroplacental adaptive responses, influencing critical lineage decisions affecting trophoblast differentiation and the ultimate structure and function of the chorioallantoic placenta. Hypoxia/HIF-directed epigenetic remodeling via KDM3A contributes to the control of TS cell adaptations during placentation modulating trophoblast lineage commitment and invasion.

ACKNOWLEDGEMENTS

I would like to thank my family for the unrestrained support, guidance, and encouragement that I have received from them over all these years. My father Mr. Janak Chakraborty has always instilled in me a love for science, and encouraged me to pursue my dreams of becoming a scientist wholeheartedly. My mother, Ms. Swati Chakraborty has been instrumental in imparting strong values, both moral and ethical, and an unflinching sense of commitment and integrity. I shall be forever grateful to the both of them. Special thanks to my brother Mr. Arnab Chakraborty (Tito), for helping me realize the spirit of sharing and teamwork, which was extremely valuable during my tenure as a graduate student in the laboratory. I would like to thank my best friend and collaborator, Dr. Aritra Bhattacherjee, for some very stimulating scientific discussions and brainstorming sessions, which contributed significantly towards designing experiments and interpreting experimental outcomes.

I would like to thank my mentor Dr. Michael J. Soares, for supporting me, and nurturing and shaping my scientific endeavors. Without his support, this work would scarcely have been possible. His scientific spirit and enthusiasm has been quite infectious, and I hope to carry on my future research activities based on his foundation of strong scientific ethic and commitment. I would also like to thank Dr. Mohammad Rumi for his help and advice with Molecular Biology and his superior guidance in helping me delve into unchartered scientific territories fearlessly.

My heartfelt thanks to Dr. Toshihiro Konno, for his advice on histological techniques, and on developing a camaraderie amongst fellow lab members. I would like to thank my committee members, for their continuous help and advice in guiding my research project. I would also like to thank Ms. Stacy McClure, Ms. Jackie Jorland and Ms. Lesley Shriver for their

support and administrative help. Special thanks to Ms. Jorland for helping me acquire the tools and reagents for my experiments, without which all of the research work would not have been possible. I would like to acknowledge all members of the Soares Laboratory (past and present), who helped me with their scientific and non-scientific advice, making me a better scientist in the process.

I would like to thank Dr. Sumedha Gunewardena and Clark Bloomer in the Bioinformatics core (University of Kansas Medical Center) for helping me with generation and analysis of microarray data. I would like to thank my collaborators Dr. Kunio Shiota from University of Tokyo, Japan and Dr. Christopher Mack from University of North Carolina, Chapel Hill for kindly providing me with reagents that were valuable for my research. Last but not the least, I would like to acknowledge American Heart Association and Biomedical Research Training Grant Program (University of Kansas Medical Center) for providing me with fellowship which has partially supported my research activities.

TABLE OF CONTENTS

LIST OF FIGURES AND TABLES

List of Figures

CHAPTER1: GENERAL INTRODUCTION

CHAPTER 2: NATURAL KILLER CELL REGULATION OF HEMOCHORIAL PLACENTATION

CHAPTER 3: EPIGENETIC INVOLVEMENT OF THE HISTONE H3K9 DEMETHYLASE KDM3A IN TROPHOBLAST STEM CELL ADAPTATIONS TO HYPOXIA

CHAPTER 4: GENERAL DISCUSSION

APPENDICES

APPENDIX A:

List of Tables

CHAPTER1:

GENERAL INTRODUCTION

The maternal –fetal interface

The maternal fetal interface is a dynamic site undergoing pregnancy associated adaptations (Enders and Welsh, 1993). The most important adaptation is extensive vascular remodeling of the maternal spiral arteries to facilitate nutrient flow and gas exchange in the growing fetus (Adamson et al., 2002; Kaufmann et al., 2003; Red-Horse et al., 2004; Vercruysse et al., 2006). An elaborate arterial-venous network is established that supplies the placenta. As gestation progresses, small uterine spiral arteries supplying the placenta are modified creating flaccid, low resistance blood vessels (Adamson et al., 2002; Christofferson, 1993; Pijnenborg et al., 2006; Takemori et al., 1984; Takemori et al., 1985). Uterine natural killer (NK) cells and invasive trophoblast cells have been identified as two key players mediating these pregnancy associated vascular changes (Croy et al., 2000; Moffett and Loke, 2006a, b; Vercruysse et al., 2006).

The rat as a model for studying biology at the maternal-fetal interface

Animal model systems are essential tools for studying and manipulating molecular mechanisms that govern cellular development. The maternal-fetal interface is no exception. The rat and the human both possess hemochorial placentation **(Fig. 1.1)**. The idea of studying any animal model system is that if the process being studied is fundamental, most likely it will demonstrate conservation across species. Although, there are some differences in the organization of the rodent versus the primate maternal-fetal interface, overriding similarities in the lineages of cells comprising the maternal-fetal interface and their functions exist. Among these are the processes and changes taking place during the last week of gestation in the rat. During this latter phase, trophoblast cells move out of the chorioallantoic placenta and invade into the uterine endometrium, where they establish intimate relationships with the uterine

vasculature (Adamson et al., 2002; Ain et al., 2003a; Caluwaerts et al., 2005; Coan et al., 2006; Vercruysse et al., 2006). These invasive events in the rat are remarkably similar to invasive events taking place during the latter stages of the first trimester and throughout the second trimester of pregnancy in the human (Kaufmann et al., 2003; Red-Horse et al., 2004; Vercruysse et al., 2006).

Placentation in the Rat

The placenta is an important organ during gestation, which functions as a conduit between the mother and the developing fetus. It is specialized to facilitate and coordinate maternal adaptations to pregnancy and fetal development. The placenta is primarily comprised of trophoblast cells, which perform a number of specialized functions. Implantation brings about differentiation of mural trophectoderm (trophectoderm not in contact with the inner cell mass) to post-mitotic trophoblast giant cells (TGC). These cells move anti mesometrially and surround the future parietal yolk sac. The polar trophectoderm (trophectoderm in direct contact with the inner cell mass) proliferates and expands to form the extraembryonic ectoderm and the ectoplacental cone (Gardner et al., 1973). Pluripotent trophoblast stem (TS) cells are found in the extraembryonic ectoderm and later on in the chorionic ectoderm (Tanaka et al., 1998; Uy et al., 2002). They supply the ectoplacental cone with precursors for the spongiotrophoblast lineage and the secondary TGC. During mid-gestation, the rodent placenta has a layer of TGC and the developing chorioallantoic placenta **(Fig. 1.2 A&B)**. The developing chorioallantoic placenta further acquires distinct structural and functional specifications as pregnancy progresses. The mature placenta is comprised of two morphologically and functionally distinct layers : the junctional zone and the labyrinth zone. Progenitor cells, spongiotrophoblasts, glycogen cells, and an outer layer of TGCs comprise the junctional zone.

Fig. 1.1 Schematic representation of the general organization of the hemochorial placenta. In hemochorial placentation trophoblast cells invade into the uterus both interstitially and endovascularly. Uterine NK cells and invasive trophoblast cells are two key players at the maternal fetal interface.

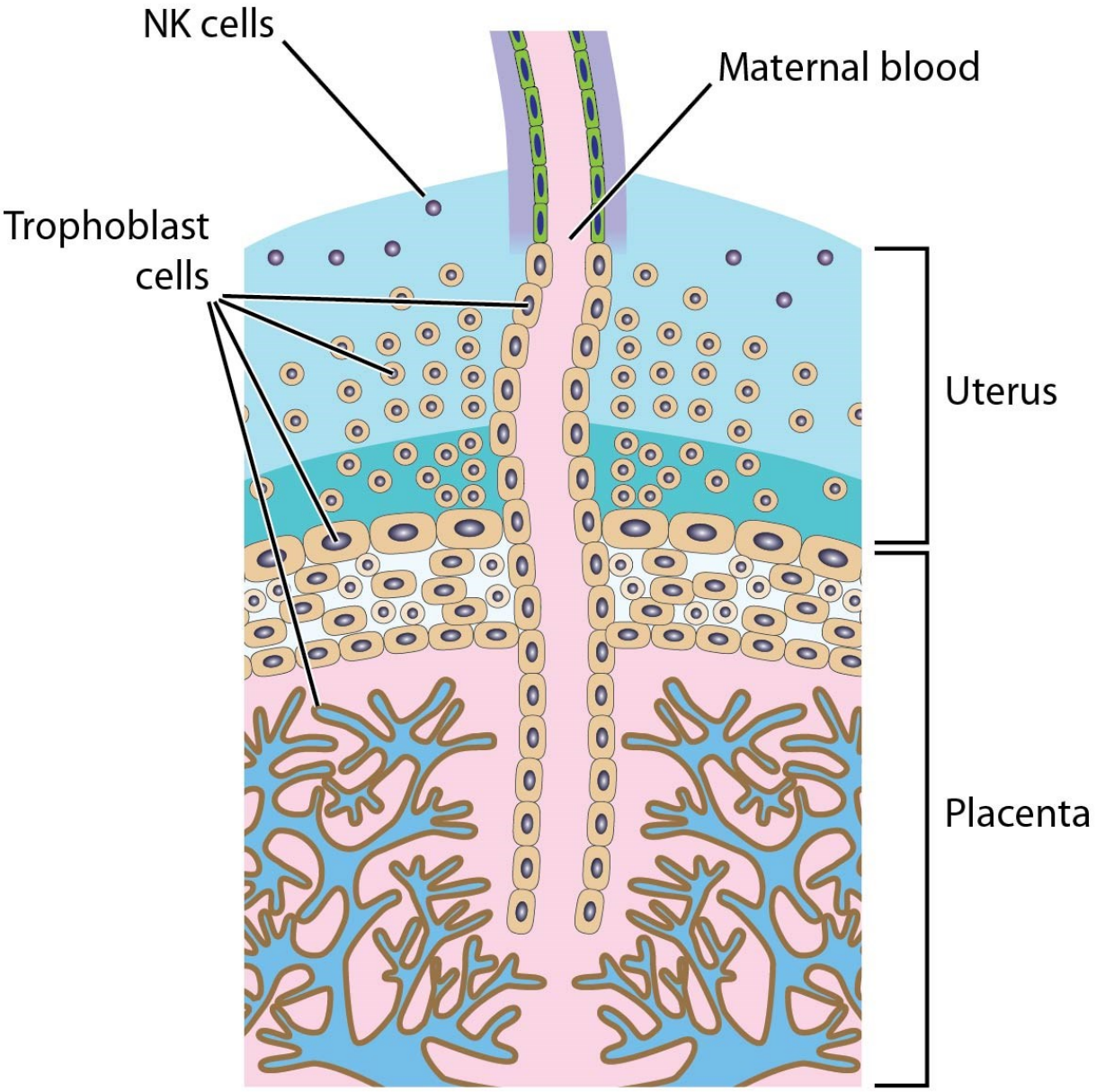
NK cells
Maternal blood
Trophoblast cells
Uterus
Placenta

The invasive trophoblast lineage is known to arise from progenitors within the junctional zone region (Wiemers et al., 2003). During the last week of gestation, these cells move out of the placenta and invade into the maternal uterine mesometrial compartment. The innermost layer of the placenta is the labyrinth zone which consists of trophoblast cells and fetal vasculature derived from the allantois. Progenitor trophoblast cells within the labyrinth zone fuse to form syncytia, which provide barriers between maternal and fetal compartments. The labyrinth zone consists of an elaborate branched structure, providing a large surface area for nutrient, waste and gas exchange with the fetus.

Blastocyst derived rat trophoblast stem (TS) cell

Rat trophoblast stem cells **(Fig. 1.3)** represent an excellent model system to study effects of low oxygen signaling *in vitro*. These cells were derived from d4.5 rat blastocysts cultured on rat embryonic fibroblasts (REFs) in RPMI-1640 culture medium supplemented with 20% FBS, FGF4, and heparin. Once cell lines were established, the REF feeder layers could be replaced with REF conditioned medium (Asanoma et al., 2012).

In the proliferative state, cells express established markers of TS cells, including Cdx2 and Eomes. Cells ceased proliferation and differentiated when FGF4, heparin, and REF conditioned medium were removed. Differentiation was characterized by the decline of Cdx2 and Eomes expression, the appearance of large polyploid cells (trophoblast giant cells), and the expression of trophoblast differentiation-associated genes, including Prl3b1 (PL-II, trophoblast giant cells), Tpbpa (spongiotrophoblast), Cx31 (glycogen cells), Prl5a1 (PLP-L, invasive trophoblast), and Gcm1 (syncytial trophoblast). The capacity of rat TS cells to express different lineage associated genes which are also observed *in vivo* during trophoblast differentiation and

Fig 1.2A Multi-lineage trophoblast cell differentiation. In mouse and rat, trophoblast cells differentiate into several lineages. Junctional zone precursor cells can give rise to trophoblast giant cells, spongiotrophoblast and glycogen cells. Labyrinth zone precursor cells differentiate into syncytial trophoblast. **Fig 1.2 B Organization of a mature rat placenta.** Beginning midgestation the placenta is comprised of two distinct zones, the junctional zone harboring the precursors of invasive trophoblast lineage and the labyrinth zone composed of syncytiotrophoblast cells.

A

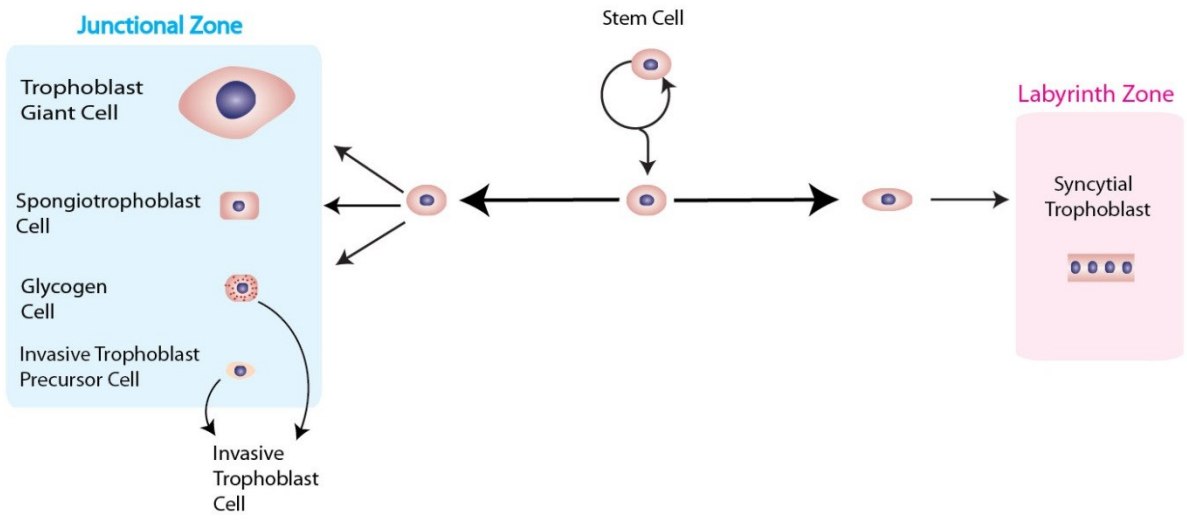
Junctional Zone
Trophoblast Giant Cell
Spongiotrophoblast Cell
Glycogen Cell
Invasive Trophoblast Precursor Cell
Invasive Trophoblast Cell
Stem Cell
Labyrinth Zone
Syncytial Trophoblast

B

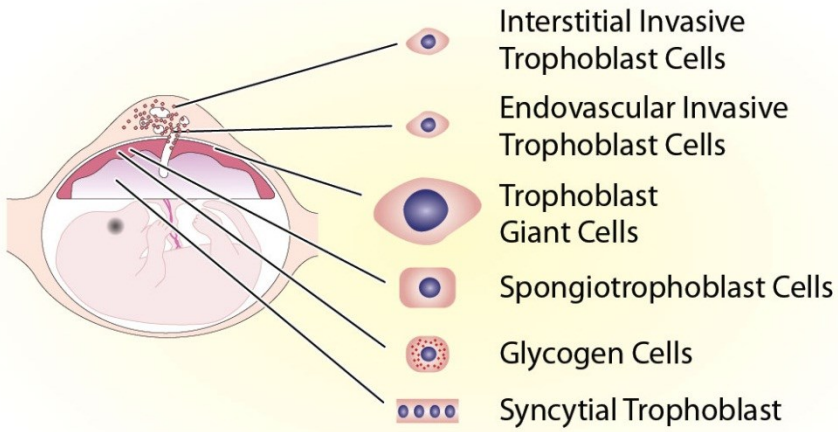
Interstitial Invasive Trophoblast Cells
Endovascular Invasive Trophoblast Cells
Trophoblast Giant Cells
Spongiotrophoblast Cells
Glycogen Cells
Syncytial Trophoblast

placenta formation, makes them an excellent tractable model to study hypoxia dependent adaptations *in vitro*.

NK cells and the uterine vasculature

Pregnancy results in a highly regulated allocation of immune cells to the uterus (Bulmer and Lash, 2005; Croy et al., 2002; Croy et al., 2003; Head, 1996; Hunt et al., 2000; Kruse et al., 1999; Kruse et al., 2002; Moffett-King, 2002). Following embryo implantation most leukocytes are excluded from the maternal uterus except for NK cells which constitute almost 70% of the leukocyte population in the uterus during pregnancy.

NK cells are conspicuous cellular constituents of uteroplacental compartments from rodents and primates (Bulmer and Lash, 2005; Croy et al., 1996; Dosiou and Giudice, 2005; Hanna and Mandelboim, 2007; Head, 1996; Liu and Young, 2001; Moffett-King, 2002; Moffett and Loke, 2006a; Parham, 2004; Sargent et al., 2006). Implantation associated decidualization in the rat and mouse, results in expansion of NK cell numbers in the maternal uterine mesometrial decidua (Ain et al., 2003a; Croy et al., 1996; Head, 1996). The uterine mesometrial compartment receives the mesenteric blood flow and it is the region overlying the developing chorioallantoic placenta. By midgestation, NK cells migrate away from the decidual region and associate with the mesometrial vasculature **(Fig. 1.4)**. The mesometrial vasculature is organized in a triangular shaped area between the mesometrial decidua and the mesometrial surface of the uterus and has been referred to as the metrial gland, and several other terms (Ain and Soares, 2004; Peel, 1989). These mesometrial blood vessels are responsible for the nutrient flow to the placenta and fetus.

Fig. 1.3. Overview of rat trophoblast stem cell model. The rat trophoblast stem (TS) cells can be maintained in a stem cell state or induced to differentiate by removal of FGF4 and rat embryonic fibroblast (REF) conditioned media. Differentiated cells have distinct cellular morphology comprising of various lineages.

Stem

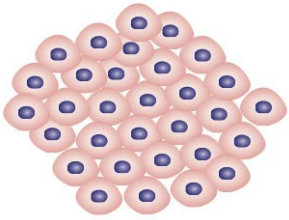

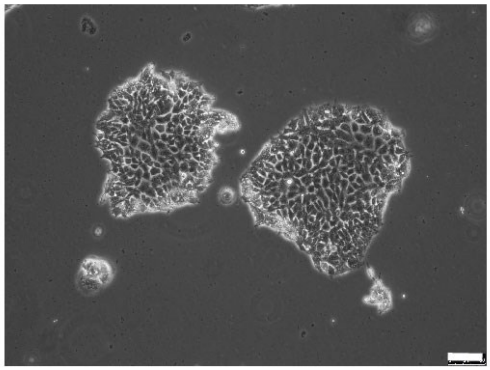

Removal of FGF4, HEPARIN
and REF conditioned media

Differentiated

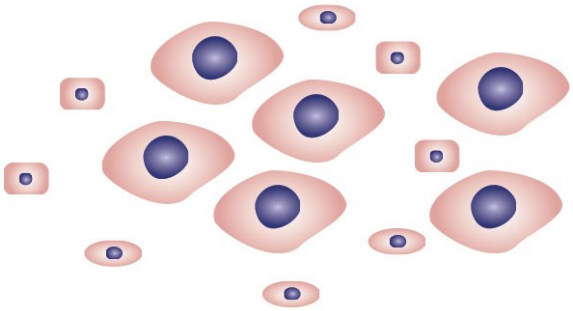

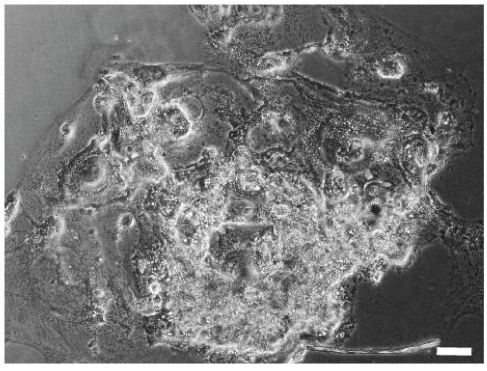

NK cells are implicated in uterine vascular development (Croy et al., 2002). Lack of NK cells is associated with profound alterations in the uterine mesometrial vasculature. Several mouse models of NK cell deficiency (transgenic mice expressing a human CD3ε gene, Tgε26, recombinase activating gene-2 null/common cytokine receptor chain γ null double mutant mice, IL-15 null mice) have been studied during pregnancy. Genetic deficiency of uterine NK cells causes a lack of remodeling of the uterine vasculature resulting in hypertrophied vascular media, swollen endothelial cells, and narrow vessel lumens (Ashkar and Croy, 2001; Barber and Pollard, 2003; Croy et al., 2002; Guimond et al., 1997). NK cell-mediated effects on the uterine vasculature may be directed by NK cell production of an assortment of angiogenic growth factors, including vascular endothelial growth factor A (VEGF A) (Hanna et al., 2006; Lash et al., 2006b; Li et al., 2001; Wang et al., 2000) nitric oxide (NO) (Ain and Soares, 2004; Burnett and Hunt, 2000; Burnett et al., 2002; Hunt et al., 1997; Hunt et al., 2000) and pro-inflammatory cytokine interferon γ (IFNγ) (Ashkar et al., 2003; Ashkar et al., 2000; Monk et al., 2005; Murphy et al., 2009).

Uterine NK cell-invasive trophoblast cell interactions

The nature of the interaction between uterine NK cells and trophoblast cells is not clearly understood. At the onset of uterine NK cell recruitment, NK cells are positioned in close contact with growing trophoblast cells (gestation d7.5 to d 9.5; **Fig. 1.4**). As gestation proceeds, NK cells exit the decidua. By gestation d13.5 NK cells are numerous and are concentrated in the metrial gland region. As gestation proceeds further, uterine NK cell number decreases. The movement of invasive trophoblast cells into the metrial gland is initiated as NK cell numbers decrease. A reciprocal relationship exists in rat and mouse between the disappearance of the NK cells and initiation of trophoblast invasion (Ain et al., 2003a).

Fig. 1.4. Natural killer cell, uterine spiral artery, and trophoblast cell dynamics within rat placentation sites throughout gestation. The schematic diagram highlights the reciprocal relationship between the uterine natural killer cells and the invasive trophoblast cells through different time-points of gestation. Two waves of uterine spiral artery remodeling are executed through the actions of natural killer cells (first wave) and invasive trophoblast cells (second wave).

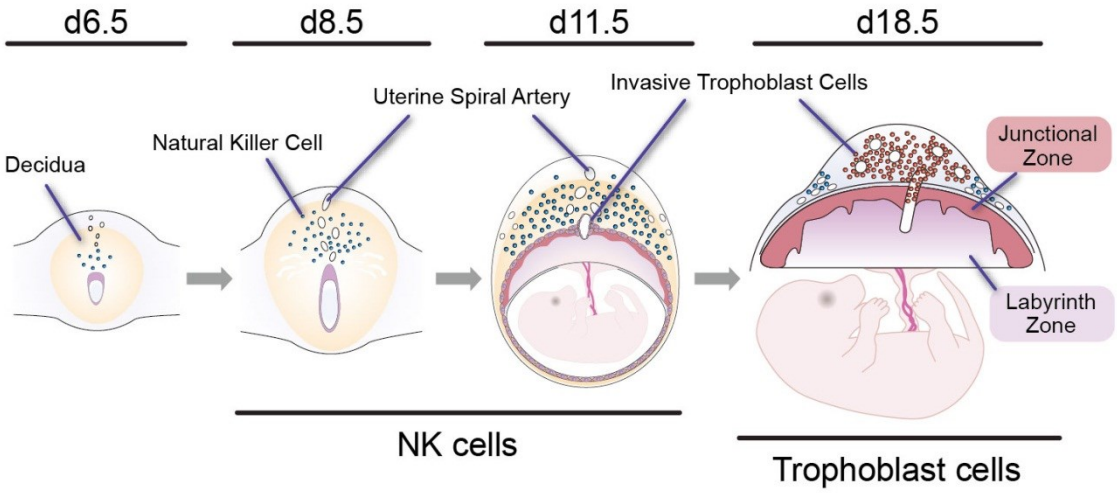
d6.5
d8.5
d11.5
d18.5
Decidua
Natural Killer Cell
Uterine Spiral Artery
Invasive Trophoblast Cells
Junctional Zone
Labyrinth Zone
NK cells
Trophoblast cells

This reciprocal relationship is also supported by observations with an NK deficient mouse model (Ain et al., 2003a). Trophoblast cell invasion has been investigated in wild type and in Tgε26 transgenic (deficient in NK cells) mice. Pregnant Tgε26 transgenic mice possess very few NK cells in their mesometrial decidua and metrial gland on gestation d12.5, in contrast to the large number of NK cells in these compartments of the wild type mouse. NK cell deficiency is correlated with an accelerated migration of cytokeratin-positive trophoblast cells into the mesometrial decidua. This observation contrasted with minimal trophoblast cell invasion in wild type mice on gestation d12.5.

The reciprocal relationship between NK cells and invasive trophoblast cells is further demonstrated in the Brown Norway (BN) rat strain (Konno et al., 2007). The late gestation invasion of trophoblast cells into the metrial gland of BN rats is decreased in comparison to other strains. The decreased trophoblast invasion is associated with a prominent retention of NK cells. The retained NK cells are prominently arranged in close proximity to the uterine mesometrial vasculature of the late gestation stage placentation site.

Evidence exists that human uterine NK cells may be the source of regulatory molecules that may promote (e.g.IL8, IP10) (Hanna et al., 2006; Hanna and Mandelboim, 2007) or inhibit (e.g. IFN γ) trophoblast cell invasion (Ain et al., 2003a; Hu et al., 2006b; Hu et al., 2008; Lash et al., 2006a). NK cells may have a direct effect on trophoblast cells or alternatively indirect effects via actions on other constituents of the uterine mesometrial compartment. The latter may include uterine NK cell products targeting the uterine mesometrial endothelium, which represent the guidance system for the movement of invasive endovascular trophoblast cells.

Hypoxia and HIF signaling

Hypoxia is defined as a condition of reduced oxygen pressure below a critical threshold which brings about restriction of proper functioning of organs, tissues or cells (Hockel and Vaupel, 2001). The concept of hypoxia is context dependent. Normoxic conditions for embryonic or adult cells vary between 2-9% of oxygen. Certain regions in thymus, medulla of kidney and bone marrow can exist in as low as 1% oxygen due to their specialized, atypical vascular networks (Simon and Keith, 2008). Early embryonic development takes place in low oxygen (1-2%). Balance in oxygen levels is maintained by cells primarily through induction of specialized transcription factors known as hypoxia inducible factors (HIFs).

HIFs are basic Per-Arnt/AhR-Sim basic helix loop helix (bHLH-PAS) transcription factors (Gu et al., 2000). The HIFs form heterodimers with aryl hydrocarbon receptor nuclear translocator (ARNT); also known as HIF1β and bind to specific DNA sequences known as hypoxia responsive elements (HREs) which are located in the promoter, introns and 3' enhancers of a large number of oxygen regulated target genes (Wang et al., 1995; Wang and Semenza, 1995). Three separate genes code for HIF1α, HIF2α and HIF3α. HIF1α is ubiquitously expressed, whereas HIF2α and HIF3α show more tissue specific expression (Wiesener et al., 2003). HIF3α has multiple splice variants (Gu et al., 1998).

HIFα subunits are regulated by oxygen tension, whereas the ARNT subunit is insensitive to changes in oxygen concentration (**Fig. 1.5**). Under normoxic conditions HIFα subunits are hydroxylated on two conserved proline residues, P402 and P564 (Ivan et al., 2001; Jaakkola et al., 2001a) by a family of three prolyl hydroxylases (PHD1, PHD2 and PHD3) (Bruick and McKnight, 2001; Epstein et al., 2001). Hydroxylated HIFα proteins are degraded by mechanisms

involving von Hippel Lindau (pVHL) tumour suppressor proteins, which covalently tag HIF proteins with polyubiquitin and lead them to proteasome mediated degradation (Schofield and Ratcliffe, 2004). Under hypoxic conditions HIFα proteins are not hydroxylated and are therefore not degraded (Simon and Keith, 2008). The accumulated HIFα proteins translocate into the nucleus where they dimerize with ARNT and bind to the HREs (RCGTG motif where R is any purine residue). The heterodimer further binds to a transcriptional coactivator, CREB binding protein (CBP)/ p300, for full functional activation of HIF signaling (Ema et al., 1999). Downstream target genes of HIF signaling are stress response gene families such as glucose transporters, glycolytic enzymes, angiogenic factors, hematopoietic growth factors and gene families which affect cell growth, survival and motility (Schofield and Ratcliffe, 2004; Semenza, 2000, 2001).

Hypoxia signaling and trophoblast cell development

Oxygen is an essential nutrient for cells. Oxygen is delivered to tissues via red blood cells through the vasculature. Molecular mechanisms mediating cellular responses to low oxygen tension have been identified. HIFs are activated by low oxygen and promote transcriptional regulation of downstream effector genes, which lead to cellular adaptations to hypoxia (Wang et al., 1995; Wang and Semenza, 1995).

Placental and fetal development rely on oxygen availability. Uterine oxygen concentrations are low (1-2%) before chorioallantoic placenta formation (Rodesch et al., 1992). Before gestation d9.5, the mouse embryo is heavily dependent on glycolysis for ATP generation (Simon and Keith, 2008). However, by gestation d10.5-d11.5, establishment of placental circulation increases intrauterine oxygen concentrations. Once the hemochorial placenta is

established, oxygen concentrations increase to approximately 8%. *In vitro* studies demonstrated that low oxygen tension can modulate trophoblast differentiation (Adelman et al., 2000; Alsat et al., 1996; Caniggia et al., 2000; Genbacev et al., 1996; James et al., 2006a, b; Jiang et al., 2000; Nelson et al., 1999). An oxygen gradient has also been proposed to be the primary effector regulating gestation dependent vascular remodeling (Burton and Jaunaiux, 2001; Caniggia et al., 2000; Fryer and Simon, 2006; Genbacev et al., 1996). Mutagenesis of components of HIF signaling in mice (Arnt, Vhl, Phd2, HIF1α and HIF2α) results in aberrant placental phenotypes and disruptions in trophoblast lineage commitment (Adelman et al., 2000; Cowden Dahl et al., 2005; Gnarra et al., 1997; Maltepe et al., 2005; Takeda et al., 2006). An appropriate balance between trophoblast proliferation and differentiation is required to produce a functional placenta (Fryer and Simon, 2006).

Oxygen concentration and trophoblast cell invasion

Low oxygen tension or exposure of trophoblast cells to gradients of oxygen concentrations have been shown to both activate and inhibit trophoblast invasion (Caniggia et al., 2000; Crocker et al., 2005; Genbacev et al., 1996; Graham et al., 2000; Hayashi et al., 2005; James et al., 2006a, b; Kadyrov et al., 2003; Kilburn et al., 2000; Robins et al., 2007; Rosario et al., 2008; Zhou et al., 1997). These studies have used different experimental procedures, cell types, duration and concentration of oxygen exposure. A study looked at the effects of low oxygen tension on four different transformed trophoblast cell lines; HTR-8/SVneo, SGHPL-4, JEG3 and JAR (Lash et al., 2007). These cell populations exhibited pronounced differences in the extent of invasiveness upon exposure to low oxygen tensions (3%).

Fig. 1.5. Schematic of the hypoxia inducible factor (HIF) signaling pathway. The HIFs form heterodimers with aryl hydrocarbon receptor nuclear translocator (ARNT); also known as HIF1β and bind to specific DNA sequences known as hypoxia responsive elements (HREs) which are located in the promoter, introns and 3' enhancers of a large number of oxygen regulated target genes. HIFα subunits are regulated by oxygen tension, whereas the ARNT subunit is insensitive to changes in oxygen concentration.

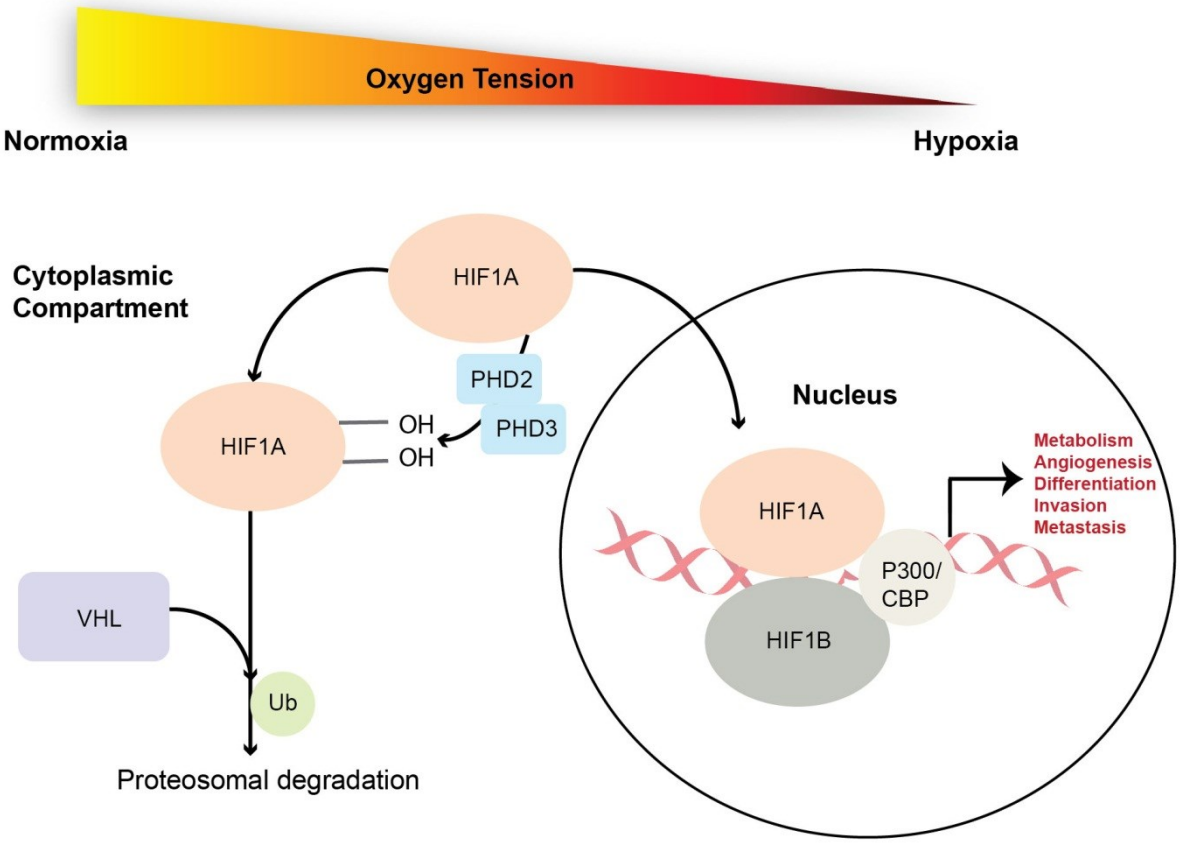
Oxygen Tension
Normoxia
Hypoxia
Cytoplasmic Compartment
HIF1A
PHD2
PHD3
HIF1A
OH
OH
VHL
Ub
Proteosomal degradation
Nucleus
HIF1A
P300/ CBP
HIF1B
Metabolism
Angiogenesis
Differentiation
Invasion
Metastasis

The impact of oxygen tension on development of invasive trophoblast lineages from trophoblast stem cell populations has received little attention. Our laboratory has identified two reproducible *in vivo* methods for perturbing the development of the placentation site (Ain et al., 2004; Alam et al., 2007; Ho-Chen et al., 2006; Ho-Chen et al., 2007; Rosario et al., 2008); see Preliminary Data). Exposure of pregnant rats to hypobaric-hypoxia during the establishment of the placenta (gestation d6.5 to d13.5) or NK cell depletion during the same phase of pregnancy results in profound structural changes: 1) activation of intrauterine endovascular trophoblast invasion; 2) alteration in chorioallantoic placental organization (Rosario et al., 2008;summarized in Fig. 4).

Hypoxia activation of epigenetic regulators

Hypoxia signaling mediated by HIF transcription factors are known to modulate adaptations by epigenetic regulators. Regulation of histone methylation by low oxygen signaling is an area of active research. Although it has been observed that under low oxygen exposure (0.2%) hypoxia promotes increase in H3K9 trimethylation marks and global deacetylation, promoters of hypoxia regulated genes have been shown to have increased H3K4 tri-methylation and decreased H3K27 trimethylation (Johnson et al., 2008).

Under low oxygen, stabilized HIF transcription factors increase their repertoire of downstream players by regulating chromatin modifiers which then are targeted to different regulatory regions and control cellular adaptations to low oxygen. So apart from transcriptional regulation, epigenetic regulation is another rapid regulatory device that the cells utilize to adapt to low oxygen environment. Histone lysine demethylases consists of two different groups: flavin adenine dinucleotide (FAD)-dependent enzyme and the Jmjc domain containing demethylases

(Mosammaparast and Shi, 2010). Jmjc domain containing demethylases are dioxygenases whose activities require Fe(II), a-ketoglutarate, and oxygen. There are 30 known jmjc domain containing proteins out of which some are hypoxia responsive(Pollard et al., 2008). Based on gene expression analysis, it has been identified that JMJD1A, JMJD2B as well as JMJD1B, JMJD2C, JMJD6, PLU-1, SMCX, RBP2, and KIAA1718, could be upregulated by hypoxia (Yang et al., 2009). ChIP seq studies in human cell lines have identified several JmJc family members which are direct targets of HIF transcription factors which include PLU-1, JMJD1A, JMJD2B, JMJD2C(Yang et al., 2009).

Epigenetics, Hypoxia and Cell invasion

Hypoxia signaling through HIF transcription factors upregulate a number of JmJc domain containing proteins, out of a which a subset of them are involved in cell invasion particularly in cancer cell metastases. *Jmjd2c* or *Kdm4c* has long been shown to be amplified in different types of cancers like squamous cell carcinoma, medulloblastoma and in prostrate carcinomas. In colorectal cancer (CRC) cells, *Jmjd2c* is upregulated on hypoxia exposure and regulates cell proliferation, apoptosis, cell cycle arrest and invasion. JMJD2B was overexpressed in CRC tissues and had positive correlation with deeper depth of invasion and advanced clinical stages (Fu et al., 2012).

Recently, the mechanism of *Jmjd2c* mediated regulation of invasion and metastasis has been shown in breast cancer cells (Luo et al., 2012). JMJD2C interact with HIF1A and is preferentially recruited to the response elements of a subset of hypoxia responsive genes involved in metabolic switch and metastatic invasion in lung cancer cells. Disruption of Jmjd2c

significantly downregulated metastasis and also caused reduction of tumor growth in a mouse model.

Epigenetically altered VHL-HIF pathway has been implicated in metatstatic pathology of clear cell renal carcinoma (Vanharanta et al., 2013). Studying two pro metastatic VHL-HIF targets CXCR4 and CYTIP genes, the authors show that that loss of Polycomb repressive complex 2 (PRC2)-dependent histone H3 Lys27 trimethylation (H3K27me3) upregulates HIF-driven chemokine (C-X-C motif) receptor 4 (CXCR4) expression, promoting chemotactic cell invasion. Loss of promoter DNA methylation resulted in upregulation of HIF target CYTIP gene. Results from the study elucidate a clear mechanism of HIF driven epigenetic amplification of tumor initiating pathways, resulting in tumor metastasis.

Epigenetic regulation of trophoblast cell invasion

Histone deacetylation has been linked to HIF mediated effector functions in other systems. ARNT null TS cells have been shown to have significantly lower HDAC activity characterized by differentiation independent induction of H4acetylation and altered class 2 HDAC subcellular localization. Inhibition of HDAC activity in TS cells mimics the trophoblast differentiation defects observed in ARNT null TS cells implying greater roles of HIF mediated signaling pathway and HDACs in the process of trophoblast differentiation and invasion (Maltepe et al., 2005).

Trophoblast cells show increased invasiveness on differentiation. They undergo epethilial to mesenchymal transition with a marked loss of e cadherin. Abell et al. very elegantly probe mechanisms underlying this epithelial mesenchymal transition (Abell et al., 2011). MAP3K4 kinase deficient TS cells show increased invasiveness with loss of apical basal polarity, gain of

mesenchymal front-back polarity , significant loss of ecadherin expression and concomitant gain of mesenchymal markers like N-Cadherin and Vimentin. However this acquisition of mesenchymal characteristics do not alter the "stemness" of the trophoblast cells as they can equally contribute to placentas when injected in blastocysts. Histone acetylation has been shown to be a regulator of gene activation. Global loss of histone acetylation has been observed when TS cells differentiate. MAP3K4 regulation of CBP acetyl transferase is pivotal in maintenance of the epithelial phenotype of the trophoblast stem cells.

Research Objectives

During pregnancy, the maternal fetal interface is a dynamic site undergoing pregnancy associated adaptations. Vascular remodeling of the maternal uterine spiral arteries facilitates nutrient flow and gas exchange in the growing fetus represents a critical event in the establishment of the hemochorial placenta. Failure in this process results in unmodified vessels and gives rise to a number of pregnancy associated diseases like preeclampsia (affects 5-7% of all pregnancies), intra uterine growth restriction (IUGR) and pre-term birth. The rat and the human both possess hemochorial placentation and overriding similarities exist between the species, especially in the process wherein trophoblast cells move out of the chorioallantoic placenta and invade into the uterine endometrium and establish intimate relationships with the uterine vasculature (Harris, 2010; Pijnenborg et al., 1981b; Pijnenborg et al., 2006). Uterine NK cells and invasive trophoblast cells have been identified as two key players mediating pregnancy associated vascular changes.

Disrupted oxygen delivery to the fetus retards somatic growth and brain development. In some situations it can also lead to fetal death. NK cells have been implicated in preeclampsia.

Aberrant NK cell number, activation and signaling have been related to failure of pregnancy associated vascular remodeling. Chronic placental hypoxia and altered hypoxia signaling have been proposed to be major players in the pathogenesis of preeclampsia. Thus, understanding the regulation of uterine vascular remodeling and trophoblast invasion is critical in deciphering the molecular mechanisms of the pathogenesis of pregnancy associated disorders.

There are two specific aims in this research project (**Fig. 1.6**), they are:

1. To investigate NK cell regulation of hemochorial placentation
2. To examine epigenetic regulation of TS cell adaptations to hypoxia through activation of KDM3A

Experimental findings related to Specific Aim 1 are presented in Chapter 2 and those associated with Specific Aim 2 are presented in Chapter 3.

Fig. 1.6. Schematic diagram describing the objectives of the research. NK cells regulate uterine vascular development, which impacts oxygen delivery (ΔO_2), activates HIF signaling, and modulates trophoblast lineage development.

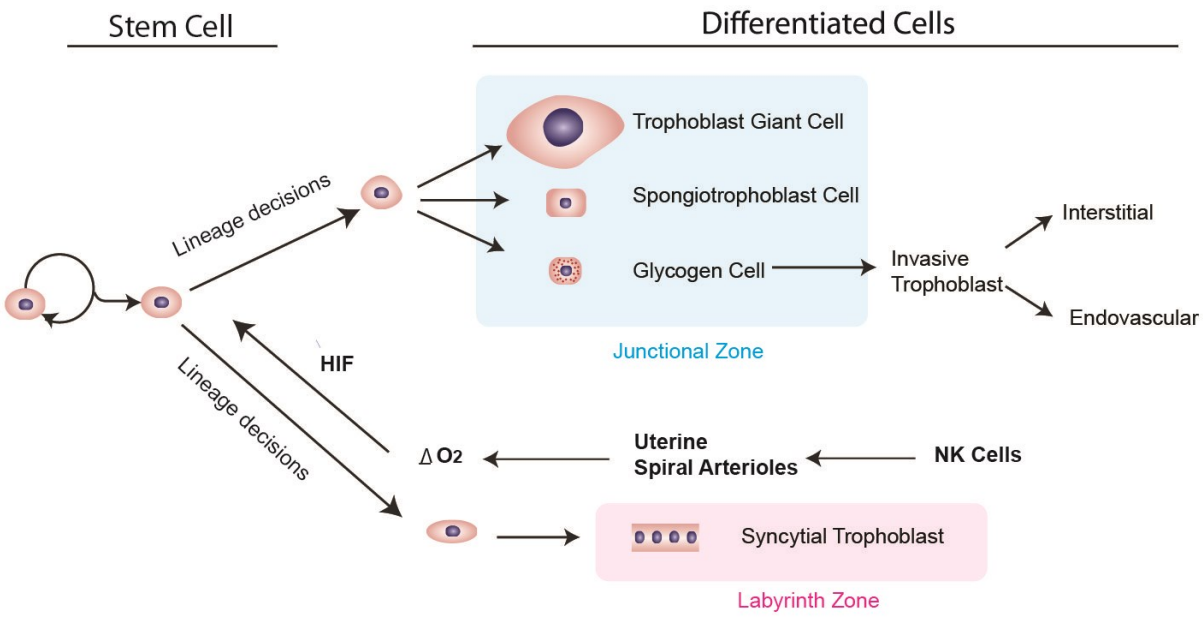
Stem Cell
Differentiated Cells
Trophoblast Giant Cell
Spongiotrophoblast Cell
Glycogen Cell
Invasive Trophoblast
Interstitial
Endovascular
Junctional Zone
Lineage decisions
HIF
Lineage decisions
ΔO2
Uterine Spiral Arterioles
NK Cells
Syncytial Trophoblast
Labyrinth Zone

CHAPTER 2:

NATURAL KILLER CELL REGULATION OF HEMOCHORIAL PLACENTATION

ABSTRACT

During the establishment of pregnancy, uterine stromal cells differentiate into decidual cells and recruit a population of lymphocytes called natural killer (NK) cells. This process is conserved in laboratory rodents, humans, and other species with hemochorial placentation. NK cells associate with uterine spiral arteries, the conduit for nutrient delivery to the placenta and fetus, and are hypothesized to contribute to the regulation of pregnancy-dependent uterine spiral artery remodeling. Failures in uterine spiral artery remodeling are associated with diseases of pregnancy, such as preeclampsia and intrauterine growth restriction. This prompted an investigation of NK cells as potential regulators of hemochorial placentation. NK cell depletion within the uterus decreased the delivery of pro-angiogenic factors and delayed uterine spiral artery development leading to decreased oxygen tension at the placentation site, stabilized hypoxia inducible factor (HIF) 1A protein within the primordial placenta, and re-directed trophoblast cell differentiation to junctional zone/invasive trophoblast cell lineages. Invasive endovascular trophoblast cells replaced the endothelium of uterine spiral arteries extending the depth of the placental vascular bed and accelerating vessel remodeling. Hypoxia-regulated trophoblast lineage decisions, including expansion of invasive trophoblast cells, could be reproduced *in vitro* using rat trophoblast stem cells; and were dependent on hypoxia-inducible factor signaling. We conclude that NK cells guide hemochorial placentation through controlling a hypoxia-sensitive adaptive reflex regulating trophoblast lineage decisions.

INTRODUCTION

Hemochorial placentation is shared by many mammalian species, including humans, some nonhuman primates and rodents (Davies and Glasser, 1968; Enders and Welsh, 1993; Georgiades et al., 2002). The hemochorial placenta is organized into two distinct compartments. Each compartment provides a specialized function, which includes: i) delivery of maternal nutrients to the placenta; and ii) transfer of nutrients from the placenta to the developing fetus. These functionally distinct placental compartments are under different regulatory programs. The maternal-fetal interface is a dynamic site undergoing pregnancy-associated adaptations (Enders and Welsh, 1993). A critical adaptation is the extensive vascular remodeling of the maternal uterine spiral arteries, which facilitates nutrient flow and gas exchange with the growing fetus (Adamson et al., 2002; Kaufmann et al., 2003; Pijnenborg et al., 2006; Red-Horse et al., 2004). Failures in this process result in unmodified vessels and give rise to pregnancy-associated diseases such as preeclampsia, intrauterine growth restriction (IUGR), and pregnancy termination (Kaufmann et al., 2003; Pijnenborg et al., 2006; Redman and Sargent, 2005). The mechanisms controlling uterine vascular remodeling are poorly understood. Putative regulators include natural killer (NK) cells and a specialized lineage of trophoblast cells referred to as invasive or extravillous trophoblast (Croy et al., 2003; Moffett and Loke, 2006a; Pijnenborg et al., 2006).

Uterine adaptations to pregnancy include highly regulated immune cell trafficking (Croy et al., 2003; Erlebacher, 2010; Hunt et al., 2000). Following embryo implantation most leukocytes are excluded from uterine tissue proximal to the placentation site except for NK cells, a process evident in rodents and primates (Bulmer et al., 2010; Croy et al., 2003; Moffett and Loke, 2006a; Zhang et al., 2011). Implantation associated decidualization in the rat and mouse,

results in the accumulation of NK cell numbers in the uterine mesometrial decidua (Ain et al., 2003a; Croy et al., 2003; Zhang et al., 2011). NK cells have been implicated in pregnancy-associated uterine vascular development (Croy et al., 2003; Lash et al., 2010; Smith et al., 2009; Zhang et al., 2011). Genetic deficiency of uterine NK cells results in a lack of remodeling of the uterine vasculature resulting in hypertrophied vascular media, swollen endothelial cells, and narrow vessel lumens(Ashkar and Croy, 2001; Barber and Pollard, 2003; Guimond et al., 1997). NK cell-mediated effects on the uterine vasculature may be directed by NK cell production of an assortment of angiogenic growth factors and vasoactive molecules (Hanna et al., 2006; Hunt et al., 2000; Kalkunte et al., 2009; Lash et al., 2006a; Li et al., 2001; Monk et al., 2005; Wang et al., 2003; Wang et al., 2000). Aberrant NK cell number, activation, and signaling have been implicated in pregnancy complications (Dosiou and Giudice, 2005; Lash and Bulmer, 2011; Trowsdale and Moffett, 2008; Zhang et al., 2011).

The invasive trophoblast lineage arises from trophoblast stem (TS) cells through an as yet unknown differentiation process(Roberts and Fisher, 2011). This differentiated cell lineage possesses a unique gene expression profile and is specialized for adhesion, degradation, and migration through uterine stromal extracellular matrices and restructuring uterine spiral arteries(Ain et al., 2003a; Apps et al., 2011; Bilban et al., 2010; Harris, 2010; Red-Horse et al., 2004). Invasive trophoblast cells take two routes as they penetrate into the uterus. They move between spiral arteries (interstitial invasive trophoblast) or alternatively they move within spiral arteries, replacing the endothelium and in some instances acquiring a pseudo-endothelial phenotype as they proceed (Damsky and Fisher, 1998; Pijnenborg et al., 2006; Red-Horse et al., 2004; Zhou et al., 1997). Rat and human placentation sites exhibit deep intrauterine trophoblast cell invasion (Ain et al., 2003a; Caluwaerts et al., 2005; Kaufmann et al., 2003; Pijnenborg et al.,

2006; Vercruysse et al., 2006), which contrasts with mouse placentation(Adamson et al., 2002; Ain et al., 2003a; Coan et al., 2006). Shallow trophoblast invasion is linked to poor spiral artery remodeling and diseases of pregnancy (Kaufmann et al., 2003; Red-Horse et al., 2004; Whitley and Cartwright, 2010).

A potential interaction between uterine NK cells and trophoblast cells is not clearly understood. A reciprocal relationship exists in rat and mouse regarding the presence of NK cells and invasive trophoblast cells within the uterine mesometrial compartment (Ain et al., 2003a; Konno et al., 2007). NK cells represent effectors directing the first wave of vascular modification. Their disappearance after midgestation marks the entry of invasive trophoblast cells and initiation of the second wave of vascular modification. The reciprocal relationship of NK cells and trophoblast cells is also supported by observations with an NK deficient mouse model (Ain et al., 2003a) and the Brown Norway rat (Konno et al., 2007). NK cells may directly act on trophoblast cells (Ain et al., 2003a; De Oliveira et al., 2010; Hanna et al., 2006; Hu et al., 2006b; Hu et al., 2010) or alternatively they may possess indirect effects on trophoblast cells via actions on other constituents of the uterine mesometrial compartment(Hanna and Mandelboim, 2007; Zhang et al., 2011). The latter may include uterine NK cell products targeting uterine spiral arteries and their delivery of nutrients, including oxygen to the developing placenta.

Placental development is sensitive to oxygen availability. Oxygen tension at the maternal-fetal interface changes with gestation and is affected by placentation (Burton, 2009; Caniggia et al., 2000; Cartwright et al., 2007; Fryer and Simon, 2006; Genbacev et al., 1997). Oxygen tensions tend to be lower during early pregnancy and increase following the establishment of the hemochorial placenta (Fischer and Bavister, 1993; Rodesch et al., 1992; Zamudio, 2003). Insights about the role of oxygen as an intrinsic regulator of placentation have

been derived from mutagenesis of genes in the mouse genome controlling cellular responses to hypoxia. Central to the cellular response to hypoxia is a transcription factor complex referred to as hypoxia inducible factor (HIF; (Dunwoodie, 2009; Majmundar et al., 2010; Semenza, 2010)). Phenotypes of placentas with null mutations for several genes encoding components of the HIF signaling pathway are associated with failures in placentation, including the HIF1A, HIF2A, HIF1B (dimerization partner for HIF1A and HIF2A), prolyl hydroxylase domain protein 2 (PHD2; also known as EGLN1), and von Hippel-Lindau genes (Adelman et al., 2000; Cowden Dahl et al., 2005; Gnarra et al., 1997; Maltepe et al., 2005; Takeda et al., 2006). Exposure of pregnant rats to a hypoxic environment leads to alterations in placentation, especially expansion of the invasive trophoblast lineage (Rosario et al., 2008). This is a conserved adaptive response. Maternal anemia (human) and chronic constriction of the lower aorta (rhesus monkey), which lead to hypoxia at the maternal-fetal interface, are also triggers for increasing intrauterine trophoblast invasion (Kadyrov et al., 2003; Zhou et al., 1993).

In this study, we investigated the role of NK cells on placentation in the rat. Depletion of NK cells affected uterine spiral artery development, oxygen delivery, HIF-dependent trophoblast lineage decisions, and trophoblast-directed uterine spiral artery remodeling. The results indicate that NK cells fundamentally contribute to the organization of the hemochorial placentation site.

MATERIALS AND METHODS

Animals and tissue collection

Holtzman Sprague Dowley (HSD) and Dahl Salt Sensitive (DSS) rats were acquired from Harlan Laboratories (Indianapolis, IN). Brown Norway (BN) and Fischer F344 (F344) rats were obtained from Charles River Laboratories (Wilmington, MA). Transgenic rats expressing

enhanced green fluorescence protein (EGFP) driven by a chicken β-actin promoter (chbA-EGFP; (Ikawa et al., 1999)) were obtained from Masaru Okabe (Osaka University, Osaka, Japan) and used to establish a colony. Animals were housed in an environmentally controlled facility with lights on from 0600-2000 h and allowed free access to food and water. Virgin female rats 8-10 weeks of age were cohabited with adult males (>3 months of age) of the same strain. Mating was assessed by inspection of vaginal lavages. The presence of sperm in the vaginal lavage was considered d0.5 of pregnancy.

An immunodepletion strategy was used to ablate NK cells (Barlozzari et al., 1987; Barlozzari et al., 1985; Murphy et al., 2005). Pregnant rats received intraperitoneal injections of anti-asialo GM1 (0.5 ml/injection; Wako Chemicals, Richmond, VA) on gestation d4.5, d6.5, and d9.5. Control pregnant rats received the same volume of normal rabbit serum.

Some pregnant rats were placed in a hypoxic (8.5% oxygen) gas-regulated chamber (BioSpherix, Lacona, NY) from gestation d8.5 to d9.5. Pair-fed and ad libitum-fed pregnant rats exposed to ambient conditions (normoxia) served as controls.

Oxygen tensions at placentation sites were estimated by pimonidazole-protein adduct formation (Pringle et al., 2007; Samoszuk et al., 2004). Gestation d9.5 animals were weighed and injected intraperitoneally with pimonidazole hydrochloride (Hypoxyprobe™-1, HPI Inc.; Burlington, MA) at a concentration of 60mg/kg of body weight and sacrificed 90 min later by cervical dislocation.

Rat placental tissues were collected on gestation d9.5, d11.5, and d13.5. The primordial placental structure at gestation d9.5 is referred to as the ectoplacental cone. At gestation day 13.5, the placenta is comprised of two distinct dissectible compartments: the junctional zone,

which establishes the border with maternal uterine structures; and the labyrinth zone, which represents the interface with the fetus. Placentation site dissections were performed as previously described (Ain et al., 2006). Tissues for histological analysis were frozen in dry-ice cooled heptane and stored at -80°C. Tissue samples for protein or RNA extraction were frozen in liquid nitrogen and stored at -80°C until processed.

The University of Kansas Animal Care and Use Committee approved protocols for the care and use of animals.

Flow cytometry

Dissociated splenocytes were subjected to density gradient centrifugation with Ficoll Hypaque solution (GE Amersham, Piscataway, NJ) for enrichment of lymphocytes. Enriched cell preparations ($1x10^6$) were labeled with phycoerythrin (PE) conjugated mouse anti-CD161 (BD Pharmingen, San Diego, CA; Cat. No. 555009) and fluorescein (FITC) conjugated mouse anti-CD3 (BD Pharmingen; Cat. No.554832). Cells were analyzed by flow cytometry with a BD LSRII (BD Biosciences San Jose, CA).

Immunocytochemistry and histochemistry

Immunocytochemical analyses were performed on 10 μm frozen tissue sections using Histostain-AEC-plus kits (Zymed, San Francisco, CA) or indirect immunofluorescence detection using goat anti-mouse IgG tagged with Alexa 488 (Invitrogen, Carlsbad, CA, Cat. No. A11029; 1:1000 dilution), goat anti-mouse IgG tagged with Alexa 568 (Invitrogen, Cat. No. A11031; 1:400 dilution), or goat anti-rabbit IgG tagged with cyanine 3 (Cy3; Jackson ImmunoResearch Laboratories, West Grove, PA, Cat. No. 111-165-003; 1:250 dilution). Nuclei were visualized with 4',6-diamidino-2-phenylindole (DAPI, Molecular Probes, Carlsbad, CA). Negative controls

were performed with normal rabbit serum or isotype-specfic control mouse IgG and did not exhibit positive reactivity in the tissue sections. Processed tissue sections were inspected and images recorded with a Leica MZFLIII stereomicroscope equipped with a charge-coupled device (CCD) camera (Leica, Welzlar, Germany).

Trophoblast cells. Trophoblast cells were detected using a mouse anti-pan cytokeratin antibody (Sigma-Aldrich, St.Louis, MO; Cat. No. C2931) at a dilution of 1:400 (Konno et al., 2007). Immunofluorescence detection was performed with a mouse monoclonal antibody to pan cytokeratin tagged with FITC (Sigma-Aldrich; Cat. No. F3418); and used at a dilution of 1:200.

NK cells. NK cells were detected with antibodies against Perforin (PRF1) and ANK61 antigen. Rabbit anti-rat PRF1 antibodies (Torrey Pines Biolabs, Houston, TX; Cat. No. TP251) were used at a concentration of 2.5 μg/ml. Immunoreactivity was visualized using alkaline phosphatase conjugated goat anti-rabbit immunoglobulin (Sigma-Aldrich; Cat. No. A3687) and nitro blue tetrazolium/bromochloroindoyl phosphate (Hu et al., 2006b). Mouse anti rat ANK61 antibodies (Santa Cruz Biotechnology, Santa Cruz, CA; Cat. No. sc-59340) were used at 1:100 dilution. Uterine NK cells present in the uterine mesometrial compartment specifically bind prolactin-like protein-A (PLP-A; (Muller et al., 1999)). Consequently, we also used a fusion protein containing human placental alkaline phosphatase (AP) and PLP-A (AP-PLP-A) as a ligand for detection of PLP-A binding to uterine NK cells, as previously described (Muller et al., 1999). AP was used as a negative control.

Endothelial cells. Mouse antibodies to a rat platelet/ endothelial cell adhesion molecule1 (PECAM1) (Serotec, Oxford, UK; Cat. No. MCA970) were used to identify endothelial cells (1:20 dilution).

Smooth muscle cells. Smooth muscle cells were monitored with a mouse smooth muscle α actin (ACTA2) antibody (Sigma-Aldrich; Cat. No. A2547) using a dilution of 1:400. Immunofluorescence detection was performed with mouse monoclonal antibody to ACTA2 tagged with Cy3 (Sigma-Aldrich; Cat. No. C6198); and used at a dilution of 1:300.

Junctional zone trophoblast lineages. TPBPA localizes to junctional zone progenitor cell population and some of its differentiated derivatives (77). Rabbit polyclonal antibodies were generously provided by Dr. Kunio Shiota (University of Tokyo, Japan) and used at a dilution of 1:1000.

Placental compartments. Regions of the placentation sites were determined by vimentin immunostaining. A mouse monoclonal antibody to vimentin (Sigma-Aldrich; Cat. No. V6389) was used at a dilution of 1:500.

HIF1A. HIF1A stabilization was monitored with a mouse anti-HIF1A antibody (BD Biosciences; Cat. No. 610959) and used at a dilution of 1:200.

Pimonidazole-protein adducts. Oxygen tension within placentation sites was estimated by detection of pimonidazole-protein adducts. The 4.3.11.3 mouse monoclonal antibody supplied with the Hypoxyprobe kit (HPI Inc.) was used at a dilution of 1:50.

Western blot analysis

HIF1B and β-actin (ACTB) protein levels were evaluated by western blot analysis. Rat TS cell lysates were prepared in radioimmunoprecipitation assay (RIPA) buffer (10 mM Tris-HCl, pH 7.2, 1% Triton X-100 or 1% Nonidet P-40, 1% sodium deoxycholate, 0.1% SDS, 150 mM NaCl, 5 mM EDTA, 1 mM sodium orthovanadate, 1 mM phenylmethylsulfonyl fluoride, 10

μg/ml aprotinin). Protein concentrations were determined by the DC protein assay (Bio-Rad, Hercules, CA). Proteins were separated by SDS-PAGE and transferred onto nitrocellulose membranes. Immunoreactive proteins were detected with mouse antibodies to HIF1B (BD Pharmingen; Cat. No. 611079; 1:1000 dilution) and ACTB (Sigma-Aldrich; Cat. No. A5228; 1:5000 dilution). Immunoreactive proteins were visualized by enhanced chemiluminescence according to the manufacturer's instructions (Amersham Biosciences, Piscataway, NJ).

qRT-PCR

Total RNA was extracted from cells and tissues using TRIzol reagent (Invitrogen). cDNAs were synthesized from total RNA (1 μg) for each sample using Superscript 2 reverse transcriptase (Invitrogen), diluted five times with water, and subjected to qRT-PCR to estimate mRNA levels. Primers were designed using Beacon primer designer (Applied Biosystems, Foster City,CA). Primer sequences can be found in **Table 1**. Real-time PCR amplification of cDNAs was carried out in a reaction mixture (20 μl) containing SYBR GREEN PCR Master Mix (Applied Biosystems) and primers (250 nM each). Amplification and fluorescence detection were carried out using the ABI Prism 7500 real time PCR system (Applied Biosystems). Cycling conditions included an initial hold step (95 °C for 10 min) and 40 cycles of a two-step PCR (92 °C for 15 sec, then 60 °C for 1 min), followed by a dissociation step (95 °C for 15 sec, 60 °C for 15 sec, and then 95 °C for 15 sec). The comparative cycle threshold method was used for relative quantification of the amount of mRNA for each sample normalized to 18S RNA.

In situ hybridization

Transcripts were localized at placentation sites using nonradioactive in situ hybridization as previously described (Ain et al., 2003a). Ten μm cryosections were prepared and stored at

Table2.1. Primer sequences used for qRT-PCR

Symbol	Accession no.	Forward primer	Reverse primer
Prf1	NM_017330	ATCAGGACCAATACAACT	CCATAGGAAGAGATGAGT
Prl7b1	NM_153738	AACAATGCCTCTGGCCACTGC	AGGCCATTGATGTGCTGAGACAGT
Vegfa	NM_0001110334	GCTCTGGGATTTGATATTC	TCTTTCCTCTGCTGATTT
Vegfb	NM_053549	GGCTTTACACGATAGATATF	TCACTATGGAACAGAGAA
Vegfc	NM_053653	GAAATTACAGTGCCTCTCTC	CGTCTAATAATTGAATGAACTTG
Tpbpa	NM_172073	GCAAGAGCAGAAGGGTAAAGAAGG	TTTCTATGTCGAGCTCCTCCTCCT
Gjb3	NM_019240	TGTGAACCAGTACTCCACCGCATT	GCTGCCTGGTGTTACAGTCAAAGT
Prl5a1	NM_138527	TCCACACCAGACATTCCAGA	TTTCCAGGAAGCCAACATTC
Prl3d1	NM_017363	TCGCGCCTCTGGTATGCAAC	TGGACACAATGGCAGTTGGTTTGG
Tfeb	NM_001025707	ACTCAGTTTCTCCTTATGC	AGACAGGTCCATGAAGTA
Hif1b	NM_012780	GTCCAGAGGGCTATTAAG	CTCATCGTCACATCTCAA
Ankrd37	NM_001108400	TGAGACAGAAGCGGAGTT	TGCCCAACAAGACATCATC
Egln1	BC081694	GACCTGTCACCTAACTGAG	AATAGCATGAAGAGGTTTACAAA
Bhlhe40	NM_053328	CTTAGAAACCAAAGACTA	CTATAAACACACATACAAG
Cdh1	NM_031334	AAGATCACGTATCGGATT	CAATGATGAGAGCTGTATA
Mmp9	NM_031055	TACTGCTGGTCCTTCTGA	CCGTCCTTGAAGAAATGC
Mmp12	NM_053963	GCTGGTTCGGTTGTTAGG	GTAGTTACACCCTGAGCATAC
18S rRNA	M11188	GCAATTATTCCCCATGAACG	GGCCTCACTAAACCATCCAA

-80°C until used. A plasmid containing a cDNA for Prl7b1(Wiemers et al., 2003) was used as a template to synthesize sense and antisense digoxigenin-labeled riboprobes according to the manufacturer's instructions (Roche Molecular Biochemicals, Indianapolis, IN). Tissue sections were air dried and fixed in ice cold 4% paraformaldehyde in phosphate buffered saline. Prehybridization, hybridization, and detection of alkaline phosphatase conjugated anti-digoxigenin were performed as previously reported (Ain et al., 2003b). Images were captured using a Leica MZFLIII stereomicroscope equipped with a Leica CCD camera.

Morphological measurements of placentation sites

Measurements of the depth of trophoblast invasion, the sizes of placental compartments, and blood vessel and uterine mesometrial compartment cross-sectional areas were performed with National Institutes of Health Image J software as previously described (Konno et al., 2007; Rosario et al., 2008). Definitions of each compartment within the rat placentation site (uterine mesometrial compartment, metrial gland, mesometrial deciduum, junctional zone, and labyrinth zone) have been described (Ain et al., 2006).

VEGFA protein measurements

VEGFA was measured in decidual lysates by enzyme-linked immunosorbent assay (ELISA) according to the manufacturer's (RayBiotech Inc., Norcross, GA) instructions. Gestation d9.5 mesometrial decidua samples were dissected and lysates prepared in extraction buffer provided by the manufacturer. Measurements were normalized to protein concentration.

Rat TS cell culture

Blastocyst-derived rat TS cells (Asanoma et al., 2011) were used to evaluate the effects of low oxygen on trophoblast lineage decisions. TS cells were cultured in Basal Culture Medium [RPMI 1640 (Cellgro, Herndon, VA), 20% fetal bovine serum (FBS; Atlanta Biologicals, Norcross, GA), 100 μM 2-mercaptoethanol (Sigma), 1 mM sodium pyruvate (Cellgro), 50 μM penicillin and 50 U/ml streptomycin (Cellgro)] supplemented with 70% rat embryonic fibroblast (REF) conditioned medium, FGF4 (25 ng/ml; Sigma) and heparin (1 mg/ml; Sigma). TS cells maintained in the basal culture medium (stem cell/proliferative state) were exposed to a range of oxygen tensions (0.5 to 2%) and 5% CO2 using a NAPCO Series 8000WJ incubator (Thermo Scientific, Pittsburgh, PA) for 24 h and then harvested for cell and molecular analyses.

Matrigel invasion assay

The invasive ability of rat TS cells was measured as previously described (Peters et al., 1999). Rat TS cells were placed in Matrigel invasion chambers (BD Biosciences) at a density of 2 x 10^4 cells per chamber. Cells were allowed to invade for 24 h. Membranes were collected and stained with Diff-Quick (Dade Behring, Newark, DE). Invading cells were visualized by light microscopy and counted.

Short- hairpin RNA (shRNA) constructs and production of lentivirus

Hif1b shRNA constructs in the pLKO.1 vector were obtained from Open Biosystems (Huntsville, AL). Several shRNAs were tested for each gene. The *Hif1b* shRNA sequences used in this analysis are as follows: i) *Hif1b* shRNA-1: 5'GAGAAGTCAGAAGGTCTCTTTTCTCGAGTAAAGAGACCTTCTGACTTCTC3'; ii) *Hif1b* shRNA-2:

5’CCAGACAAGCTAACCATCTTACTCGAGTAAGATGGTTAGCTTGTCTGG3’. The control shRNA, which targets no known mammalian gene, pLKO.1-shSCR (Plasmid 1864), was obtained from Addgene (Cambridge, MA) and has the following sequence 5’CCTAAGGTTAAGTCGCCCTCGCTCTAGCGAGGGCGACTTAACCTTAGG3’ (Sarbassov et al., 2005b). Third generation lentiviral packaging vectors were purchased from Addgene and included: pMDLg/pRRE (Plasmid 12251), pRSV-Rev (Plasmid 12253) and pMD2.G (Plasmid 12259). Lentiviral particles were produced as previously reported (Lee et al., 2009). In brief, 293FT cells (Invitrogen) were transiently transfected using Lipofectamine 2000 (Invitrogen) with the following plasmids: shRNA containing transducing vector, third-generation packaging system plasmids (pMDLg/pRRE and pRSV-Rev; 104), and a VSVG envelope plasmid (pMD2.G). After transfection, cells were maintained in 50% DMEM with high glucose (Cellgro), 45% Opti-MEM I (Invitrogen) and 5% FBS. Culture supernatants containing lentiviral particles were harvested every 24 h for two to three days. Supernatants were centrifuged to remove cell debris, filter sterilized, concentrated by ultracentrifugation, and stored at -80°C until used.

Statistical analyses

Data analyses were performed using SigmaPlot 11.2 statistical software package (Systat Software, Inc, San Jose, CA). Specific details of the analyses are presented in the figure legends.

RESULTS

Depletion of uterine NK cells

In vivo depletion of NK cells can be achieved by treatment with anti-asialo GM1 antibodies (Barlozzari et al., 1987; Barlozzari et al., 1985; Murphy et al., 2005). HSD rats were

injected intraperitoneally with 500 µl of anti-asialo GM1 antibodies (Wako Chemicals, Richmond, VA) or normal rabbit serum (control) on gestation d4.5 or gestation d4.5 and d9.5. Placentation sites were collected on gestation d9.5 or d13.5 and examined for the presence of NK cells using PRF1 immunostaining. A single injection of anti-asialo GM1 at gestation d4.5 depleted NK cells from placentation sites at gestation day 9.5 (**Fig. 2.1 A-F**) and decreased uterine NK cell numbers on gestation d13.5, indicating evidence of recovery (**Fig. 2.2 A**). A combination of two injections of anti-asialo GM1 (one at gestation d4.5 and the second at d9.5) was effective in depleting uterine NK cells at gestation d13.5 (**Fig. 2G-L**). qRT-PCR analysis of d9.5 uterine mesometrial decidua for *Prf1* mRNA verified the depletion of NK cells (Fig. 1.2 B). Successful NK cell depletion was confirmed through the use of other strategies to detect NK cells (ANK61 immunostaining and AP-PLP-A binding; **Fig. 2.3**). The immunodepletion treatment was also effective in depleting systemic NK cells as assessed by flow cytometric analysis of splenocytes with NK1.1 antibodies (also known as NKRP1 or CD161; **Fig. 2.4**). Controls exhibited the expected full complement of systemic and uterine NK cells. Delaying the initiation of anti-asialo GM1 antibody treatment until gestation d6.5 was less effective in depleting NK cells (**Fig. 1.5**). Thus, we have a protocol for preventing the colonization of the placentation site with NK cells and a tool for investigating the role of NK cells on hemochorial placentation.

NK cells, endovascular trophoblast invasion, and uterine spiral artery remodeling

The placentation site at gestation d13.5 is well defined but lacks penetration of invasive trophoblast cells beyond the decidual compartment (Ain et al., 2003a). In contrast, gestation d13.5 placentation sites from NK cell depleted rats exhibited distinct changes in their placental

Fig. 2.1 NK cell depletion from d9.5 and d13.5 placentation sites. A) Rats were treated on gestation d4.5 with normal rabbit serum (Control) or anti-asialo GM1 on gestation d4.5 (Anti-aGM1-1$_{(4.5)}$) and sacrificed on gestation d9.5. This treatment strategy effectively depleted NK cells from placentation sites on gestation d9.5 **(B-F)**. **D and E** are high magnification images of boxed regions in **B and C**, respectively. **G)** Rats were treated on gestation d4.5 and d9.5 with normal rabbit serum (Control) or anti-asialo GM1 (Anti-aGM1-2$_{(4.5, 9.5)}$) and sacrificed on gestation d13.5. This treatment strategy effectively depleted NK cells from placentation sites on gestation d13.5 (**H-L**). **J and K** are high magnification images of boxed regions in **H and I**, respectively. NK cells were identified using PRF1 immunocytochemistry. Quantification of relative depletion (% of control) is shown in panels **F** (n=6 per group, $P<0.02$; Mann-Whitney Rank Sum Test) and **L** (n=5 per group, $P<0.001$; Student's *t*-test). Scale bars=0.25mm.

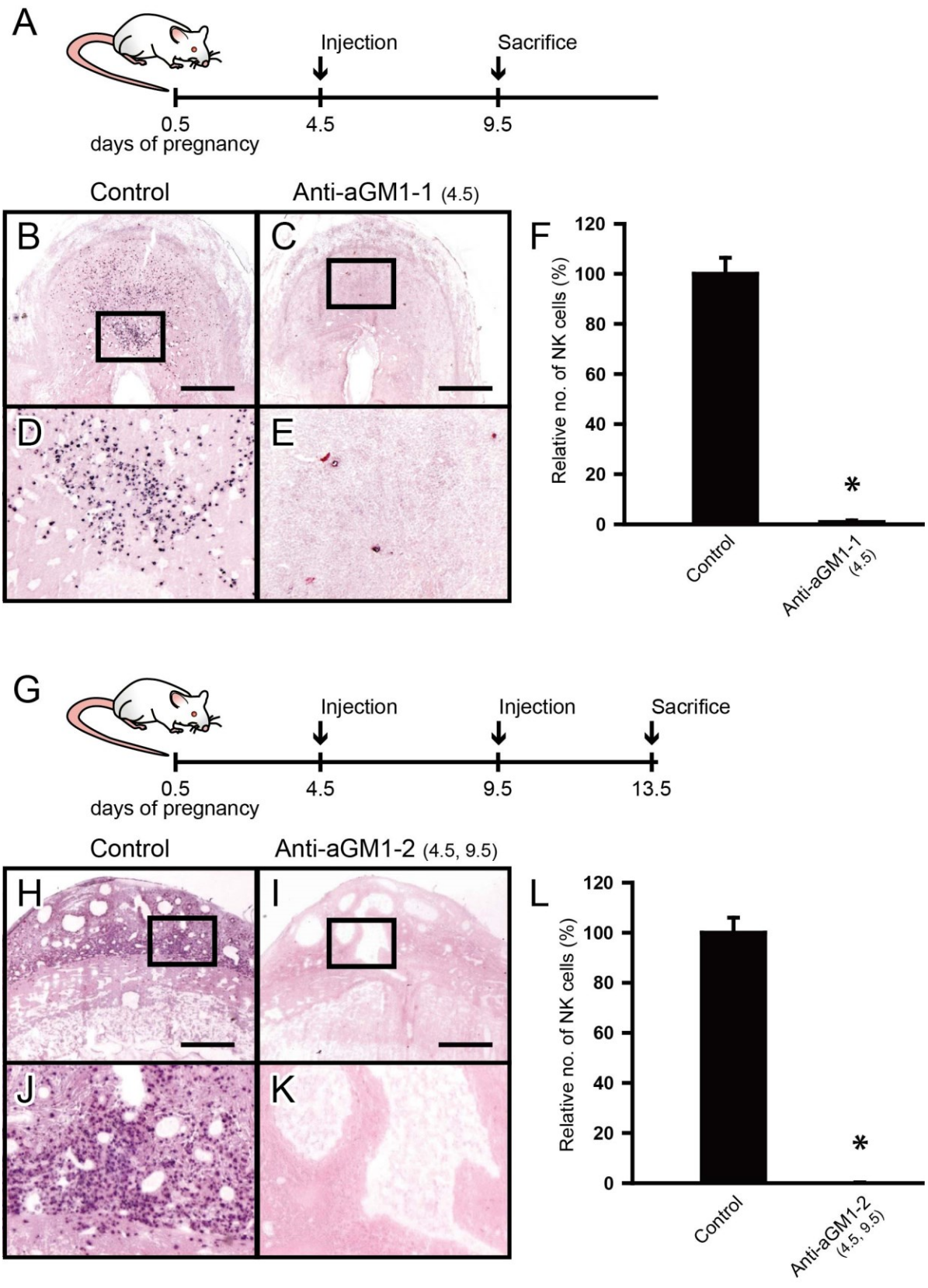
A
Injection
Sacrifice
0.5
days of pregnancy
4.5
9.5
Control
Anti-aGM1-1 (4.5)
B
C
D
E
F
Relative no. of NK cells (%)
120
100
80
60
40
20
0
*
Control
Anti-aGM1-1 (4.5)
G
Injection
Injection
Sacrifice
0.5
days of pregnancy
4.5
9.5
13.5
Control
Anti-aGM1-2 (4.5, 9.5)
H
I
J
K
L
Relative no. of NK cells (%)
120
100
80
60
40
20
0
*
Control
Anti-aGM1-2 (4.5, 9.5)

Fig. 2.2. NK cell numbers in gestation d13.5 placentation sites following a single injection of anti-asialo GM1 on gestation d4.5. A) Rats were treated on gestation d4.5 with a single dose of normal rabbit serum (Control) or antiasialo GM1 (Anti-aGM1-$1_{(4.5)}$) and sacrificed on gestation d13.5. This treatment strategy significantly decreased NK cell numbers but did not eliminate them from the placentation site on gestation d13.5 (**B-F**). **D and E** are high magnification images of boxed regions in **B and C**, respectively. NK cells were identified using PRF1 immunocytochemistry. **F)** Quantification of PRF1 positive cells (number/mm^2; n=5 per group). Asterisks indicate significant differences from controls (n=5 per group, $P<0.01$; Mann-Whitney Rank Sum Test). Scale bars=0.25 mm. **G)** *Prf1* transcript levels in gestation d9.5 decidual tissues dissected from rats treated on gestation d4.5 with normal rabbit serum (Control) or anti-asialo GM-1 (anti-aGM1-$1_{(4.5)}$). *Prf1* transcript levels were measured by qRT-PCR (SYBR Green, ΔΔCT method). 18S rRNA served as an internal control. Asterisks indicate significant differences (Control, n=5 and anti-aGM1- $1_{(4.5)}$, n=5; $P<0.05$, Mann-Whitney Rank Sum Test).

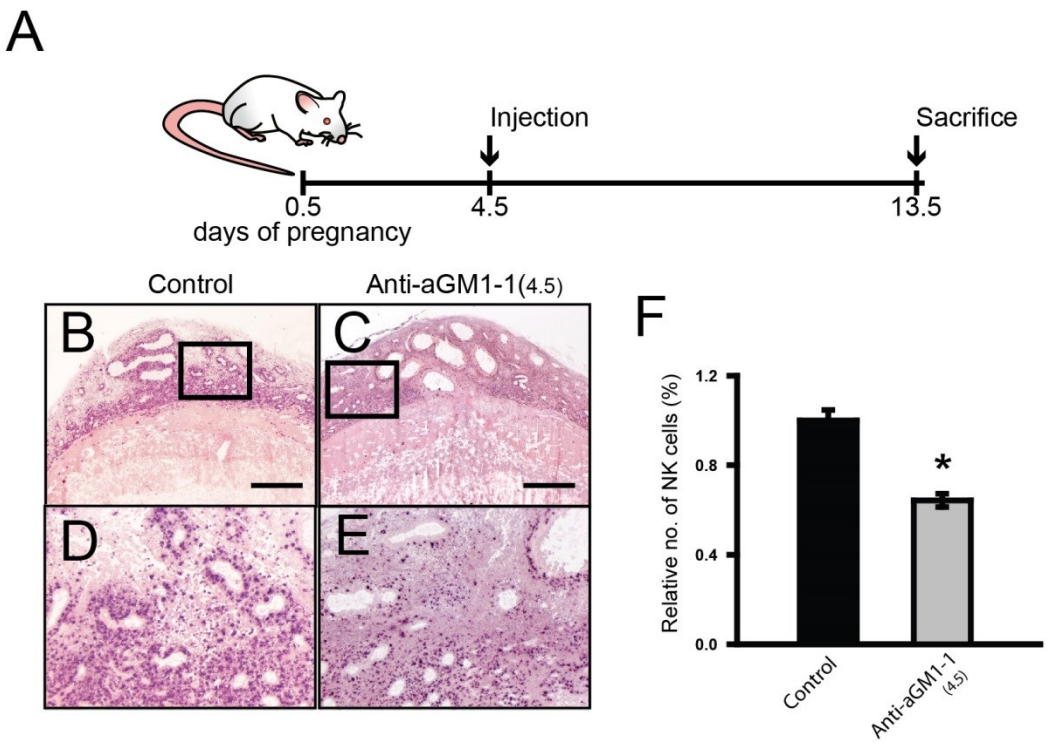
A
Injection
Sacrifice
0.5
4.5
13.5
days of pregnancy
Control
Anti-aGM1-1(4.5)
B
C
D
E
F
Relative no. of NK cells (%)
1.2
0.8
0.4
0.0
*
Control
Anti-aGM1-1 (4.5)

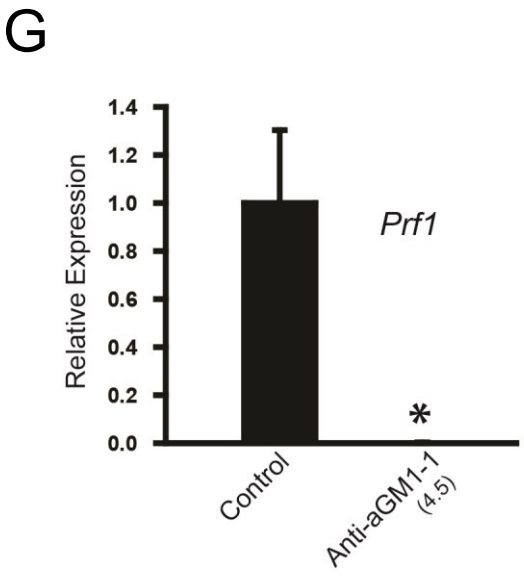
G
Relative Expression
1.4
1.2
1.0
0.8
0.6
0.4
0.2
0.0
Prf1
*
Control
Anti-aGM1-1 (4.5)

Fig.2.3 Assessment of NK cell depletion in gestation d9.5 and d13.5 placentation sites using PRF1 and ANK61 immunoreactivity and AP-PLP-A binding. A) Schematic representation of treatment on gestation d4.5 and sacrifice on gestation d9.5. Rats were treated with a single dose of normal rabbit serum (Control: **B-E**) or anti-asialo GM1 (Anti-aGM1-1$_{(4.5)}$: **F-I**). **J**) Schematic representation of treatment on d4.5 and d9.5 and sacrifice on gestation d13.5. Rats were treated with two doses of normal rabbit serum (Control: **K-N**) or antiasialo GM1 (Anti-aGM1-2$_{(4.5,9.5)}$: **O-R**). NK cells were identified using PRF1 immunocytochemistry (**B, C, F, G, K, L, O, and P**), ANK61 immunocytochemistry (**D, H, M, and Q**), or AP-PLP-A binding (**E, I, N, and R**). **C, G, L, and P** are high magnification images of boxed regions in **B, F, K, and O**, respectively. Please note that these treatment regimens effectively depleted NK cells as determined by each of the three NK cell detection methods. Scale bars=0.25 mm.

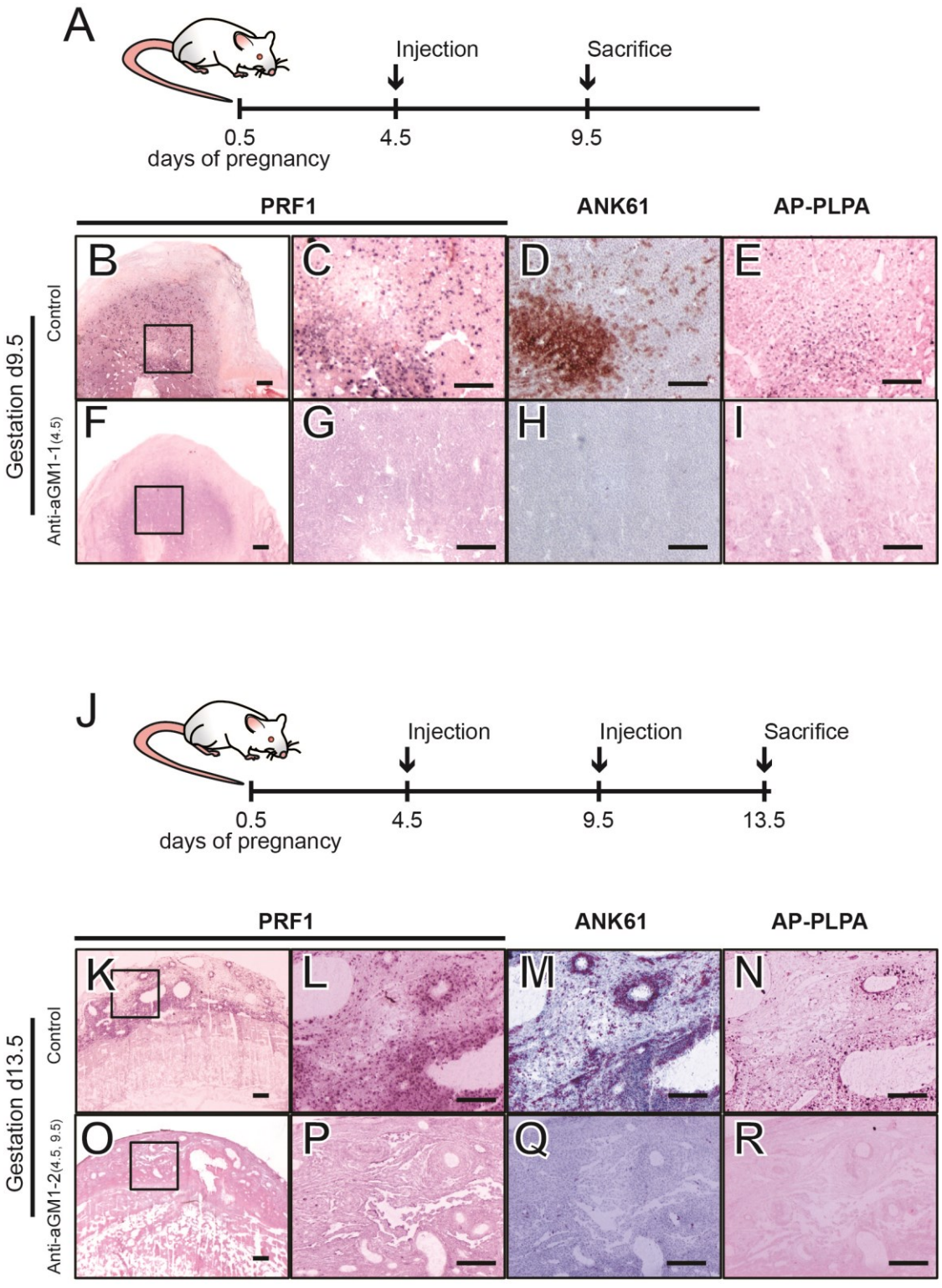
A
Injection
Sacrifice
0.5
days of pregnancy
4.5
9.5
PRF1
ANK61
AP-PLPA
B
C
D
E
F
G
H
I
Gestation d9.5
Control
Anti-aGM1-1(4.5)
J
Injection
Injection
Sacrifice
0.5
days of pregnancy
4.5
9.5
13.5
PRF1
ANK61
AP-PLPA
K
L
M
N
O
P
Q
R
Gestation d13.5
Control
Anti-aGM1-2(4.5, 9.5)

Fig. 2.4. Splenic NK cell depletion. A) Schematic representation of treatment on gestation d4.5 and sacrifice on gestation d9.5. Rats were treated with a single dose of normal rabbit serum (Control, **B**) or anti-asialoGM1 (Anti-aGM1-1$_{(4.5)}$, **C**).Spleens were dissected, mechanically dissociated, and processed for flow cytometry using CD3-FITC and CD161-PE antibodies. Please note that the antiasialoGM1 treatment effectively depleted NK cells from the spleen.

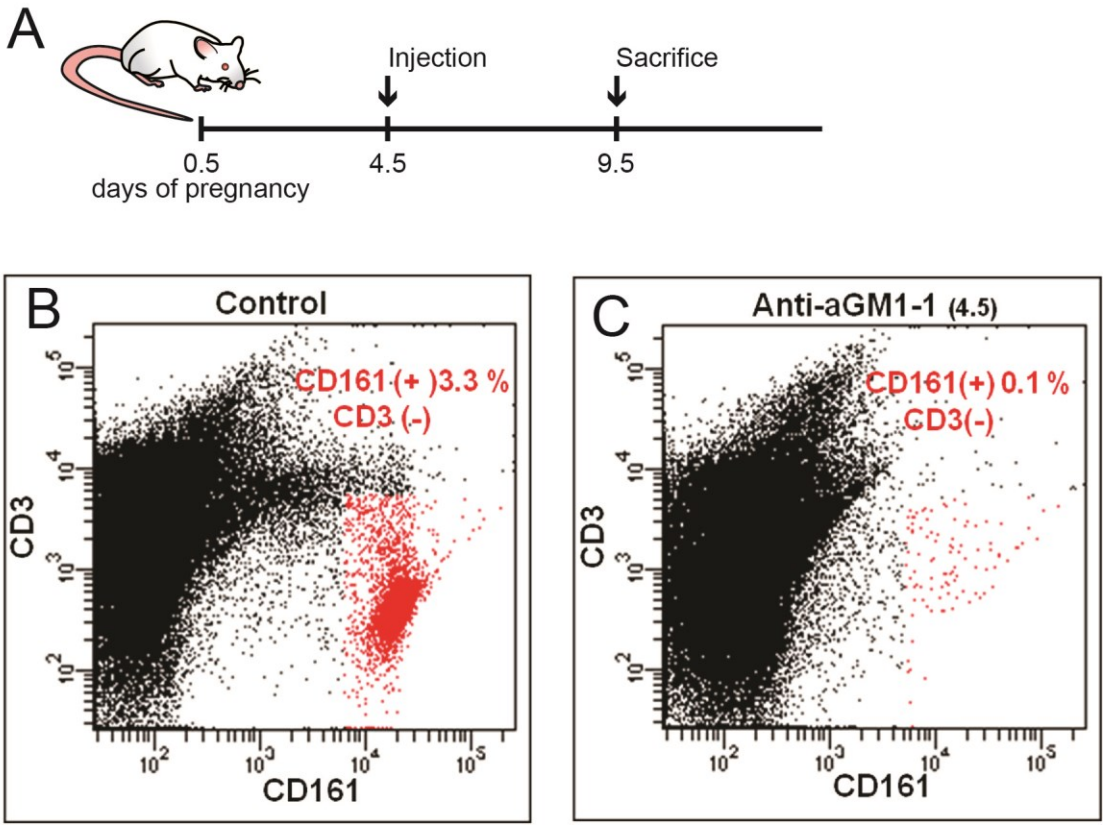
A
Injection
Sacrifice
0.5
days of pregnancy
4.5
9.5
B
Control
CD161 (+)3.3 %
CD3 (-)
CD3
CD161
C
Anti-aGM1-1 (4.5)
CD161(+) 0.1 %
CD3(-)
CD3
CD161

Fig. 2.5. NK cell numbers in gestation d9.5 placentation sites following a single injection of anti-asialo GM1 on gestation d6.5. A) Rats were treated on gestation d6.5 with a single dose of normal rabbit serum (Control) or antiasialoGM1 (Anti-aGM1-1$_{(6.5)}$) and sacrificed on gestation d9.5. This treatment strategy significantly decreased NK cell numbers but did not eliminate them from the placentation site on gestation d9.5 (**B-F**). **D and E** are high magnificationMimages of boxed regions in **B and C**, respectively. Controls were treated with normal rabbit serum. NK cells were identified using PRF1 immunohistochemistry. **F)** Quantification of PRF1 positive cells (number/mm$_2$; n=5 per group). The asterisk indicates a significant difference between Control and Anti-aGM1-1$_{(6.5)}$ groups (n=5; $P<0.05$). Scale bars=0.5 mm. **G)** *Prf1* transcript levels in decidual tissues dissected from gestation d9.5 decidual tissue following treatment with normal rabbit serum (Control) or anti-asialo GM-1 on gestation day 6.5 (anti-aGM1-1$_{(6.5)}$). *Prf1* transcript levels were measured by qRT-PCR (SYBR Green, $\Delta\Delta$CT method). 18S rRNA served as an internal control.

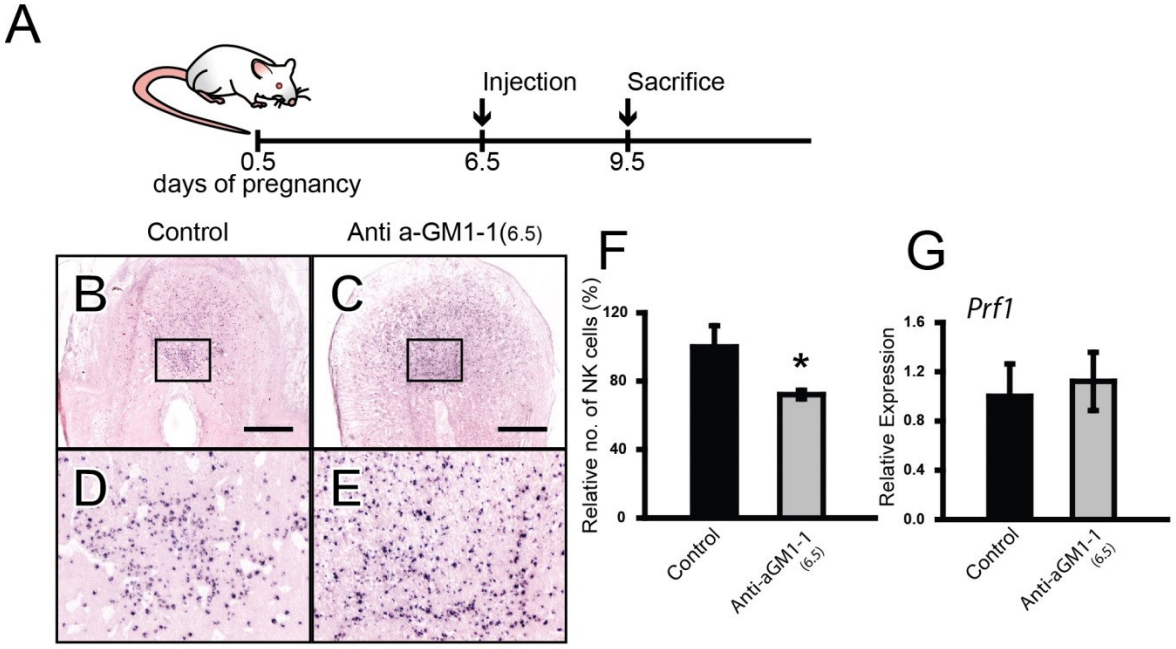
A
Injection
Sacrifice
0.5
6.5
9.5
days of pregnancy
Control
Anti a-GM1-1(6.5)
B
C
D
E
F
Relative no. of NK cells (%)
120
80
40
0
*
Control
Anti-aGM1-1 (6.5)
G
Prf1
Relative Expression
1.6
1.2
0.8
0.4
0.0
Control
Anti-aGM1-1 (6.5)

vascular beds, including deep intrauterine endovascular trophoblast invasion (**Fig. 2.6**). Uterine spiral arteries were lined with cuboidal-shaped cells, which stained positive for cytokeratin (**Fig. 2.6 B and D**) and expressed prolactin family 7, subfamily b, member 1 (*Prl7b1*; also known as prolactin-like protein-N) mRNA (**Fig. 2.6 F and G**). *Prl7b1* transcripts are restricted to the invasive trophoblast cell lineage (Konno et al., 2007; Rosario et al., 2008; Wiemers et al., 2003). The effects of NK cell depletion on placentation were not unique to the HSD rat. Three additional inbred strains (BN; DSS; F344) showed similar increases in endovascular trophoblast invasion following NK cell depletion (**Fig. 2.7**). We also verified the extraembryonic origin of the endovascular invasive trophoblast cells using a transgenic rat model expressing enhanced green fluorescent protein (EGFP) under the control of the chicken β-actin promoter (chbA-EGFP; (Ikawa et al., 1999; Rosario et al., 2008). NK cell depletion similarly stimulated EGFP-expressing extraembryonic cells to invade into the uterine vasculature of wild-type HSD females (**Fig. 2.6 J**). As indicated above, a single injection of anti-asialo GM1 on gestation d4.5 depleted NK cells at d9.5 with some recovery by d13.5 (**Fig. 2.2**). This treatment strategy was effective in stimulating endovascular trophoblast cell invasion on d13.5 (**Fig. 2.8**), suggesting that NK cell depletion was not required throughout the eight-day interval. Delaying the initiation of anti-asialo GM1 treatment until gestation d6.5 did not effectively deplete uterine NK cells (**Fig. 2.5**) nor did it promote endovascular trophoblast invasion (**Fig. 2.8**).

Additional insights into the role of NK cells and endovascular trophoblast in uterine spiral artery remodeling were obtained through immunohistological analysis. Three types of centrally located uterine spiral arteries were observed at gestation d13.5: i) vessels surrounded by NK cells; ii) vessels devoid of NK cells; iii) vessels devoid of NK cells but containing endovascular trophoblast cells. The presence of NK cells led to disruptions in the integrity of the

Fig 2.6 NK cell depletion leads to activation of endovascular trophoblast invasion on gestation d13.5. Rats were treated on gestation d4.5 and d9.5 with normalrabbit serum (Control) or anti-asialo GM1 (NK cell depleted) and sacrificed on gestation d13.5. Invasive endovasacular trophoblast cells were identified by pan cytokeratin immunocytochemistry (**A-D**). **E**) Quantification of the depth ofcytokeratin positive cell penetration into the uterine mesometrial vasculature.Values are means ± the standard error of each mean. **Invasion index** = Distanceof endovascular cytokeratin positive cell location relative relative to the trophoblast giant cell layer of the chorioallantoic placenta ÷ Total distance from the trophoblast giant cell layer to the mesometrial surface of the uterus. The asterisk indicates a significant difference between Control and NK cell depleted (n=5 per group; P<0.001; Student's *t*-test). **F and G**) In situ hybridization of *Prl7b1* mRNA incontrol and NK cell depleted d13.5 placentation sites. **H**) *Prl7b1* transcript levels in gestation d13.5 metrial gland tissues dissected from control and NK cell depleted rats. *Prl7b1* transcript levels were measured by qRT-PCR (SYBR Green, ΔΔCT method). 18S rRNA served as an internal control. The asterisk indicates a significant difference between Control and NK cell depleted (n=4; P<0.001; Student's *t*-test). **I and J**) Representative images showing EGFP expressing endovascular trophoblast cells at gestation d13.5 placentation sites of Control (**I**) and NK cell depleted (**J**) wild-type female rats mated to chβA-EGFP transgenic male rats. Please note that NK cell depletion stimulated the invasion of EGFP-positive trophoblast cells into the maternal uterine vasculature. Scale bars=0.25 mm.

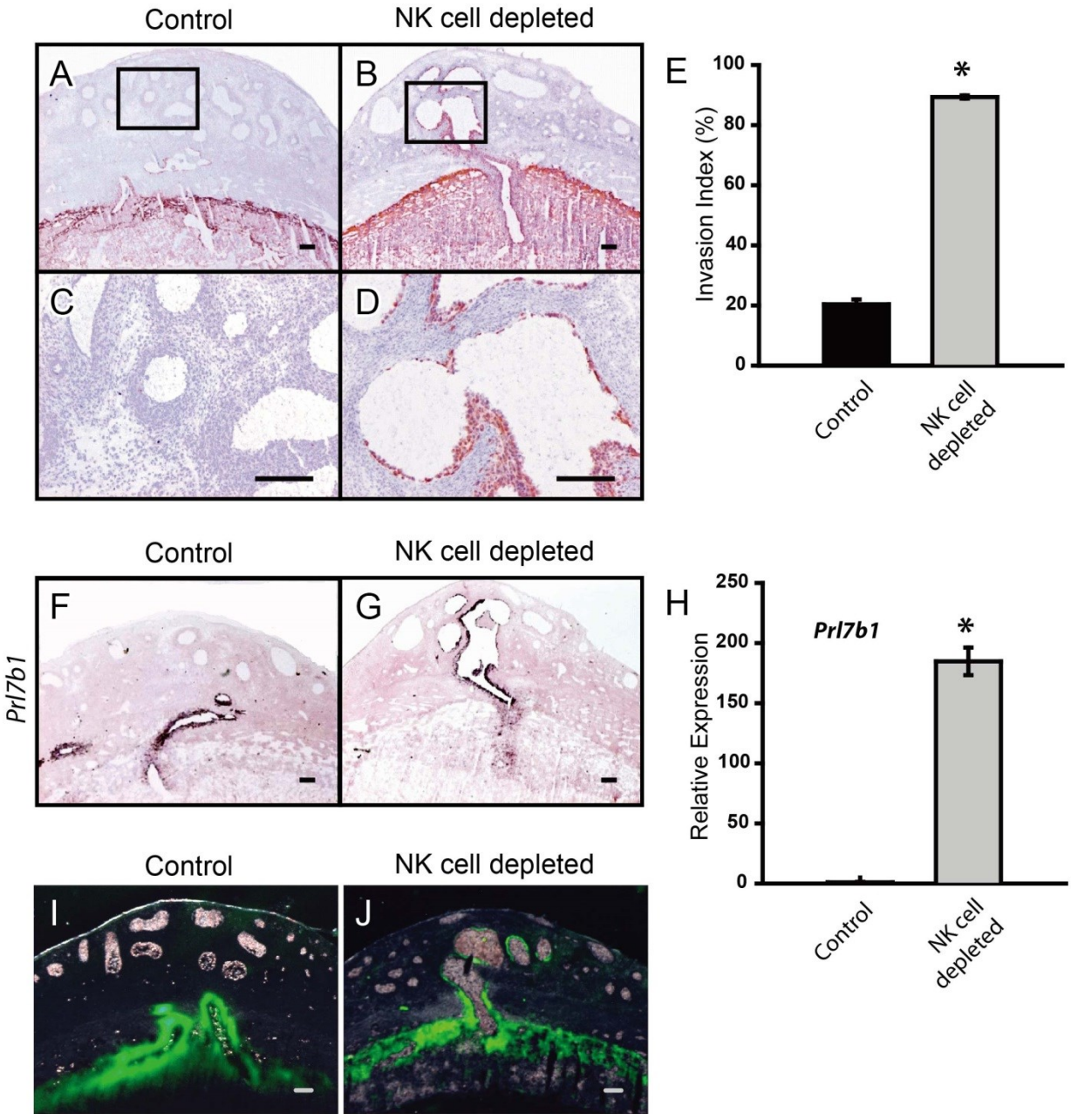
Control
NK cell depleted
A
B
C
D
E
Invasion Index (%)
100
80
60
40
20
0
*
Control
NK cell depleted
Control
NK cell depleted
F
G
Prl7b1
H
Prl7b1
Relative Expression
250
200
150
100
50
0
*
Control
NK cell depleted
Control
NK cell depleted
I
J

Fig. 2.7. NK cell depletion leads to activation of endovascular trophoblast invasion on gestation d13.5 in F344, DSS, and BN inbred rat strains. A) Schematic representation of treatments on gestation d4.5 and d9.5 and sacrifice on gestation d13.5. Rats were treated with normal rabbit serum (Control: **B**, F344; **D**, DSS; **F**, BN) or anti-asialo GM1 (NK cell depleted: **C**, F344; **E**, DSS; **G**,BN). Invasive endovascular trophoblast cells were identified by pan-cytokeratin immunocytochemistry. **H-J**) Quantification of the depth of cytokeratin positive cell penetration into the uterine mesometrial vasculature (**H**, F344; **I**, DSS; **J**, BN). Values are means ± the standard error of each mean. Asterisks indicate significant differences between Control and NK cell depleted ($P<0.001$; Student's *t*-test).

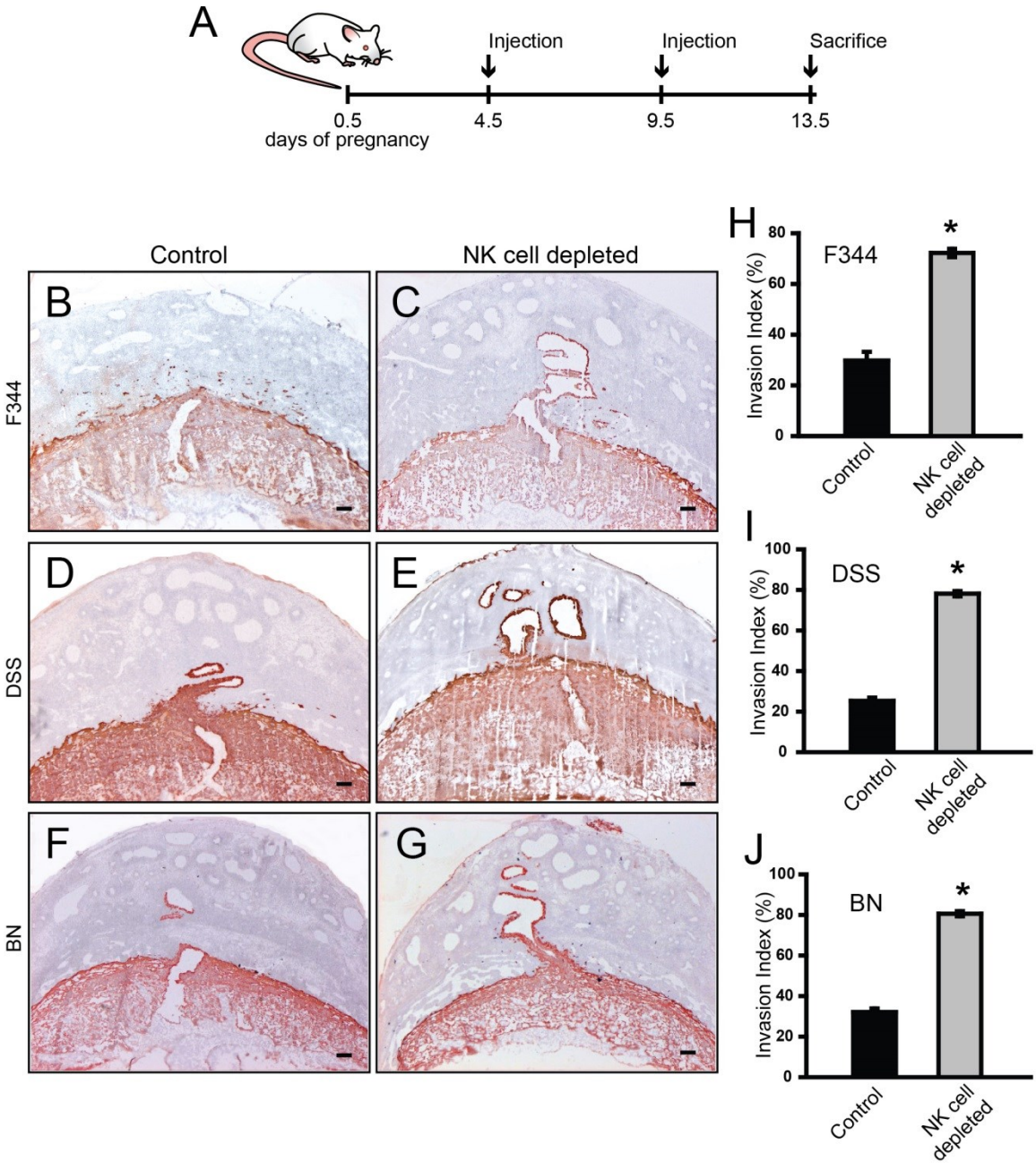
A
Injection
Injection
Sacrifice
0.5
days of pregnancy
4.5
9.5
13.5
Control
NK cell depleted
F344
DSS
BN
B
C
D
E
F
G
H
I
J
Invasion Index (%)
F344
DSS
BN
Control
NK cell depleted
*

Fig 2.8 Effects of single injections of anti-asialo GM1 on endovascular trophoblast invasion on gestation d13.5. A) Schematic representation of treatment on gestation d4.5 and sacrifice on gestation d13.5. **B**) Schematic representation of treatment on gestation d6.5 and sacrifice on gestation d13.5.Rats were treated with normal rabbit serum (Control: **C**) or anti-asialo GM1 (AntiaGM1-1$_{(4.5)}$: **D**; Anti-aGM1-1$_{(6.5)}$: **E**). Invasive endovascular trophoblast cells were identified by pan-cytokeratin immunocytochemistry. **F**) Quantification of the depth of cytokeratin positive cell penetration into the uterine mesometrial vasculature. Values are means ± the standard error of each mean. The Invasion Index is described in **Fig. 2**. Asterisks indicate significant differences between Control and anti GM1 treated rats (n=5 per group; $P<0.001$; analysis of variance with Holm-Sidak method for comparisons).

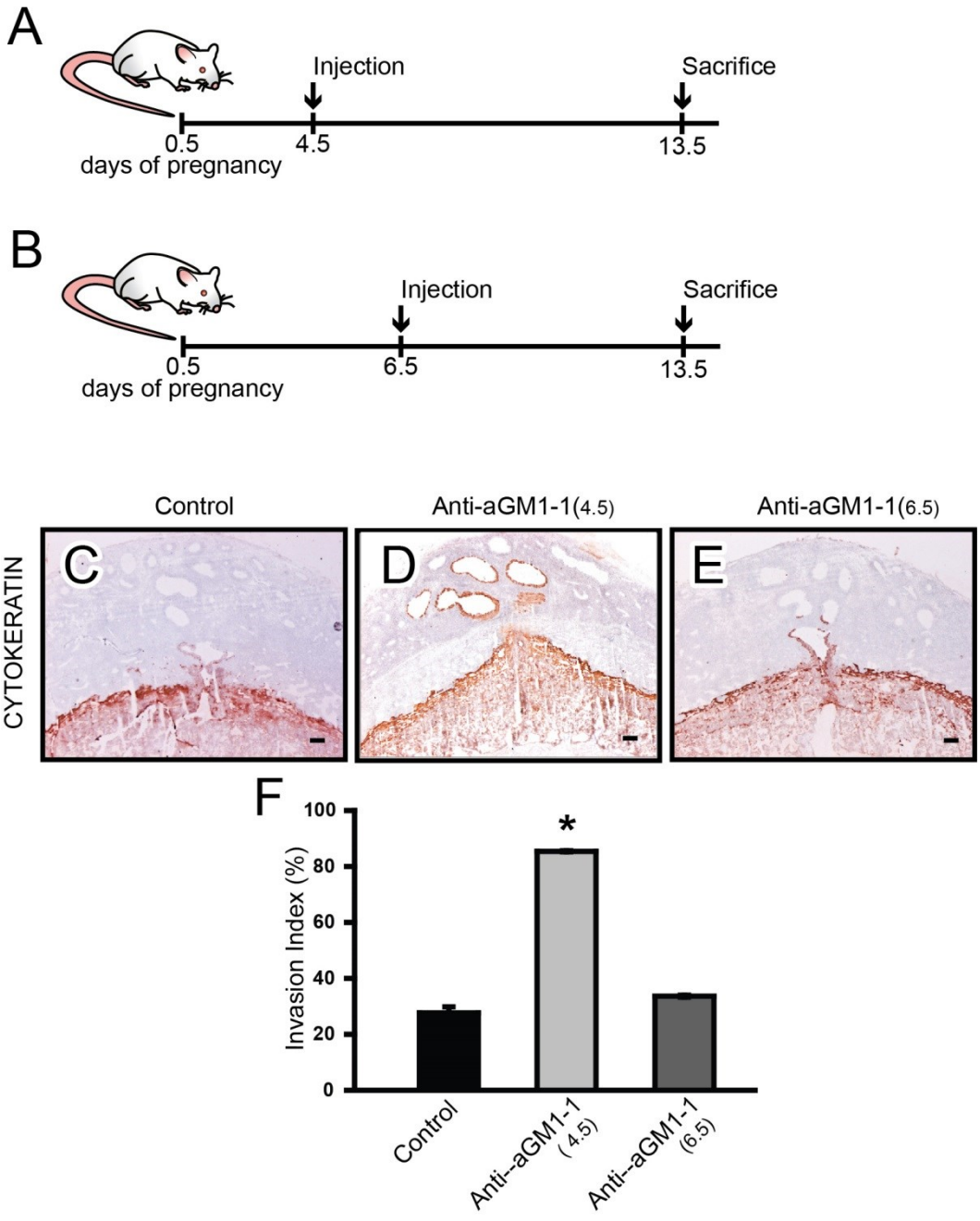
A
Injection
Sacrifice
0.5
4.5
13.5
days of pregnancy
B
Injection
Sacrifice
0.5
6.5
13.5
days of pregnancy
Control
Anti-aGM1-1(4.5)
Anti-aGM1-1(6.5)
CYTOKERATIN
C
D
E
F
Invasion Index (%)
100
80
60
40
20
0
*
Control
Anti--aGM1-1 (4.5)
Anti--aGM1-1 (6.5)

smooth muscle layer surrounding spiral arteries (**Fig. 2.9A and C**). These modifications were not observed in spiral arteries devoid of NK cells (**Fig. 2.9B**). The endovascular trophoblast-bearing (cytokeratin positive) uterine spiral arteries of NK cell depleted rats exhibited additional changes (**Fig. 2.9 D**). These vessels contained diminished ACTA2 and in many instances complete loss of the smooth muscle layer. PECAM 1 immunostaining was absent from some modified uterine spiral arteries, reflecting the disappearance of the endothelium (**Fig. 2.9F**), but present in others containing endovascular trophoblast (**Fig. 2.9 G**) indicative of their acquisition of a pseudo-endothelial phenotype (Damsky and Fisher, 1998; Zhou et al., 1997). Trophoblast cells are proposed to activate endothelial cell apoptosis (Ashton et al., 2005; Red-Horse et al., 2006). NK cells reappear in the uterine mesometrial compartment in rats receiving a single injection of anti-asialo GM1 on gestation d4.5 but not in rats receiving injections on both gestation d4.5 and d9.5 (**Fig. 2.1, Fig. 2.2**). The pseudo-endothelial trophoblast phenotype was much easier to identify following the latter treatment (**Fig. 2.9 G**). Partial and complete NK cell depletion result in distinct endovascular trophoblast phenotypes on gestation d13.5 and suggest that NK cells may modulate the appearance of the pseudo-endothelial phenotype.

Collectively, the results indicate that NK cells regulate uterine spiral artery remodeling through several mechanisms, including: i) through direct actions on the smooth muscle tunica media; ii) via restraining endovascular trophoblast invasion; iii) by modulating the endovascular trophoblast cell phenotype.

NK cells modulate uterine spiral arteries and oxygen delivery

The effects of NK cell depletion on placentation closely resembled our earlier observations on the effects of maternal hypoxia on placentation (Rosario et al., 2008). Maternal

Fig. 2.9. NK cells and endovascular trophoblast cells contribute to remodeling uterine spiral artery structure. Rats were treated on gestation d4.5 and d9.5 with normal rabbit serum (Control) or anti-asialo GM1 (NK cell depleted) and sacrificed on gestation d13.5. Double immunofluorescence staining for ANK61 and ACTA **(A and B)** and cytokeratin and ACTA2 **(C and D)** on representative uterine mesometrial regions are shown. **A and C**) Asterisks demarcate blood vessels possessing interruptions (arrowheads) in the tunica media. **B**) Asterisks identify blood vessels with intact tunica media. In panels **E-G**, rats were treated on d4.5 and d9.5 with normal rabbit serum (Control, **E**) or anti-asialo GM1 (Anti aGM1-1$_{(4.5)}$, **F**; aGM1-2$_{(4.5,9.5)}$, **G**). Double immunofluorescence staining for cytokeratin and PECAM1 (**E-G**) on representative uterine mesometrial regions are shown. **G**) The asterisk indicates the location of a blood vessel lined by cells doubly positive for cytokeratin and PECAM1 (yellow). Scale bars=0.25 mm.

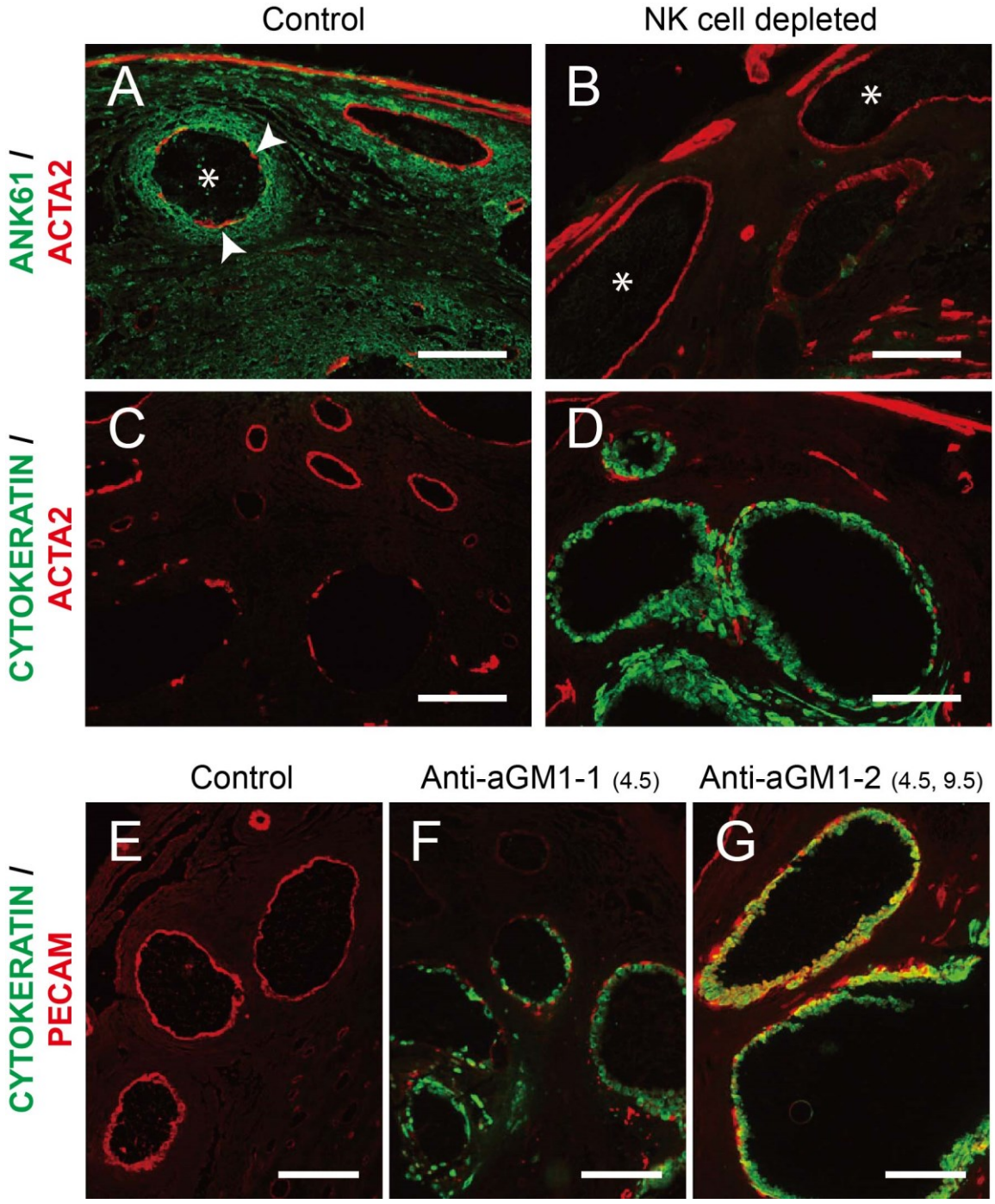
Control
NK cell depleted
A
B
C
D
E
F
G
ANK61 / ACTA2
CYTOKERATIN / ACTA2
CYTOKERATIN / PECAM
Anti-aGM1-1 (4.5)
Anti-aGM1-2 (4.5, 9.5)

hypoxia activates endovascular trophoblast invasion, uterine spiral artery remodeling, and placental reorganization. A 24 h interval of sensitivity to maternal hypoxia was noted between gestation d8.5 and d9.5 (Rosario et al., 2008). This prompted an investigation of NK cell depleted and control placentation sites at gestation d9.5. A prominent difference in the distribution of uterine spiral arteries (detected by ACTA2 and PECAM1 immunostaining) was observed at gestation d9.5 (**Fig. 2.10 A-D**). NK cell depleted placentation sites showed significantly less development of uterine spiral arteries, especially their progression toward developing trophoblast (ectoplacental cone). The difference in vascular development between control and NK cell depleted was not evident by gestation d11.5 (**Fig. 2.11**). Since uterine NK cells are potential sources of angiogenic factors such as vascular/endothelial growth factors (VEGFs; (Kalkunte et al., 2009; Lash et al., 2006b; Li et al., 2001; Wang et al., 2003; Wang et al., 2000)), we investigated Vegf transcript and VEGFA protein concentrations in the mesometrial compartment where NK cells normally reside. Transcript levels for *Vegfa*, *Vegfb*, and *Vegfc* and VEGFA protein concentrations were all significantly lower in the NK cell depleted rats. Decreases in *Vegf* transcripts and VEGFA protein are consistent with poor uterine spiral artery development.

We next investigated whether the attenuated uterine spiral artery development impacted oxygen delivery to the placentation site. Pimonidazole hydrochloride forms adducts with proteins in tissues experiencing low oxygen tensions (<10 mm of Hg). Pimonidazole-protein adducts can be immunohistochemically detected and used for assessment of relative tissue oxygen concentrations (Samoszuk et al., 2004), including murine placentation sites (Pringle et al., 2007). NK cell depletion at the placentation site was associated with an increase in the accumulation of pimonidazole-protein adduct formation and thus indicative of oxygen tensions

Fig. 2.10. NK cells and uterine spiral artery development. Rats were treated on gestation d4.5 with normal rabbit serum (Control) or anti-asialo GM1 (NK cell depleted) and sacrificed on gestation day 9.5. Blood vessels were identified by PECAM1 (**A and B**) and ACTA2 (**C and D**) immunocytochemistry. **E**) Numbers of ACTA2 positive vessels within the uterine mesometrial compartment were quantified. The asterisk indicates significant differences between Control and NK cell depleted (n=5; P<0.001; Student's *t*-test). **F-H**) Transcript levels for *Vegfa* (**F**), *Vegfb* (**G**), and *Vegfc* (**H**) were measured in gestation d9.5 mesometrial decidual tissue dissected from Control and NK cell depleted rats. Transcript levels were measured by qRT-PCR (SYBR Green, ΔΔCT method). 18S rRNA served as an internal control. Asterisks indicate significant differences between Control and NK cell depleted (n=5; P<0.02 for each gene; Mann-Whitney Rank Sum Test). **I**) VEGFA protein levels were measured in gestation d9.5 mesometrial decidual tissue dissected from Control and NK cell depleted rats by ELISA and normalized to protein concentration. The asterisk indicates a significant difference between Control and NK cell depleted tissues (n=10; P<0.05; Mann-Whitney Rank Sum Test).

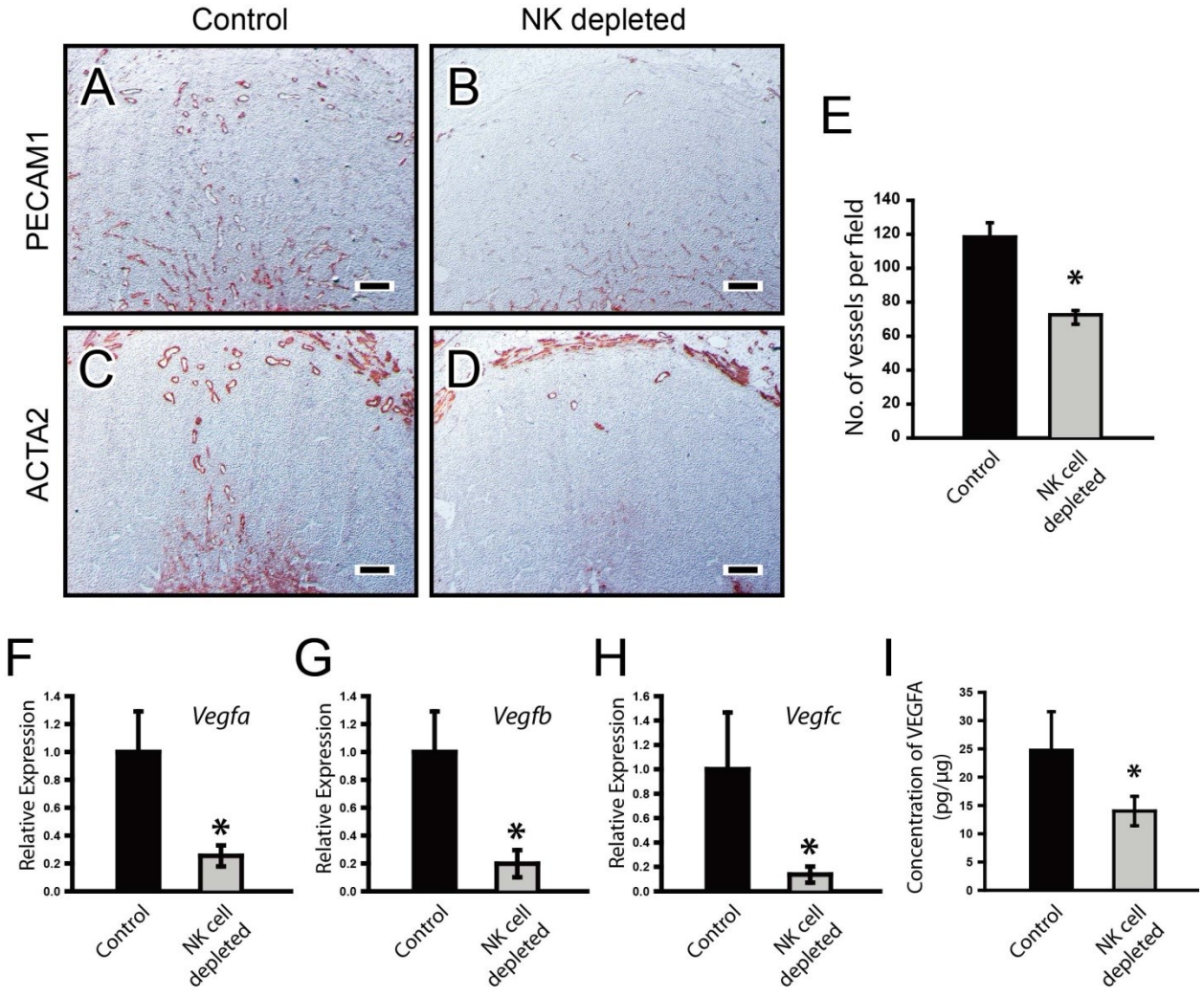
Control
NK depleted
A
B
C
D
PECAM1
ACTA2
E
No. of vessels per field
140
120
100
80
60
40
20
0
*
Control
NK cell depleted
F
Vegfa
Relative Expression
1.4
1.2
1.0
0.8
0.6
0.4
0.2
0.0
*
Control
NK cell depleted
G
Vegfb
Relative Expression
1.4
1.2
1.0
0.8
0.6
0.4
0.2
0.0
*
Control
NK cell depleted
H
Vegfc
Relative Expression
1.6
1.4
1.2
1.0
0.8
0.6
0.4
0.2
0.0
*
Control
NK cell depleted
I
Concentration of VEGFA (pg/µg)
35
30
25
20
15
10
5
0
*
Control
NK cell depleted

Fig. 2.11. Role of NK cells on uterine spiral artery development at gestation d11.5. A) Schematic representation of treatment on gestation d4.5 and d9.5 and sacrifice on gestation d11.5. Rats were treated with normal rabbit serum (Control: **B**) or anti-asialo GM1 (NK cell depleted: **C**). Blood vessels were identified by PECAM1 immunocytochemistry. Please note that uterine spiral arteries are well developed in both Control and NK cell depleted tissues. Scale bars=0.25 mm.

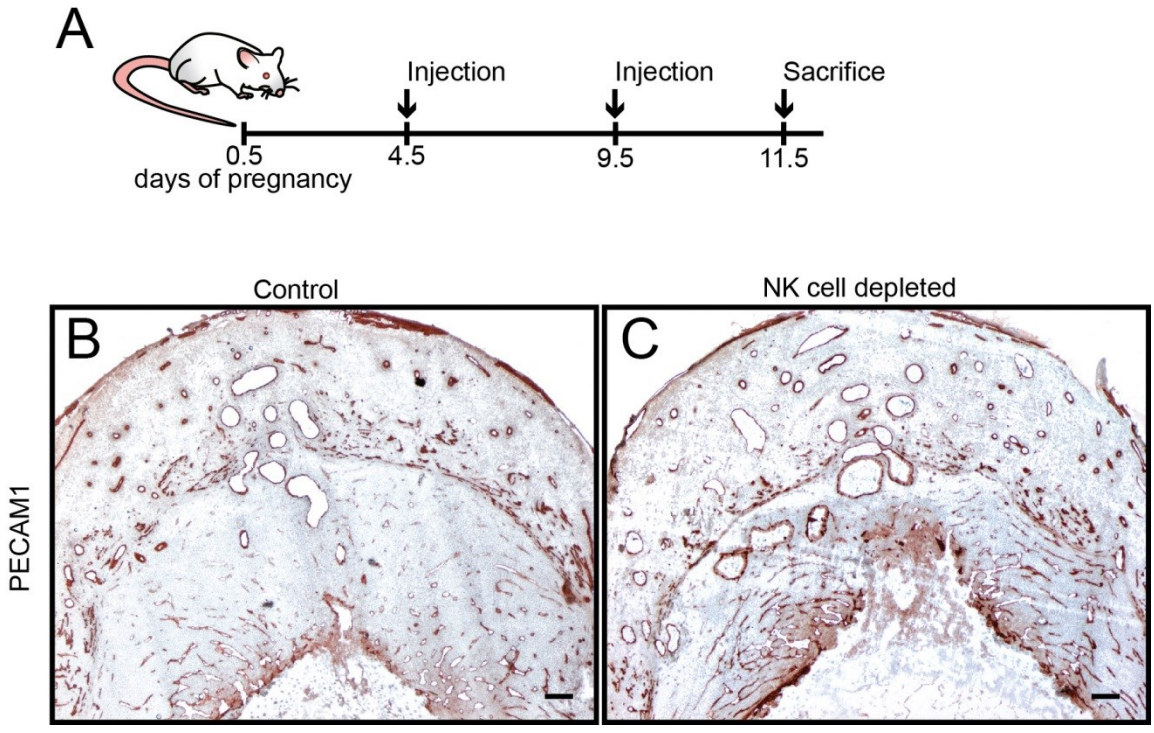
A
Injection
Injection
Sacrifice
0.5
4.5
9.5
11.5
days of pregnancy
Control
NK cell depleted
B
C
PECAM1

below 10 mm of Hg (**Fig. 2.12 A and B**). These results were suggestive of a local hypoxia but contrary to an earlier report, which failed to observe increased pimonidazole-protein adduct formation at the maternal-fetal interface in mice possessing genetic NK cell deficiencies (Leno-Duran et al., 2010).

Cellular responses to low oxygen are regulated by activation of a hypoxia signaling pathway controlled by specialized transcription factors known as HIFs (Semenza, 2010). HIFs are basic helix-loop-helix Per-Arnt/AhR-Sim (bHLH-PAS) transcription factors (Zhang et al., 2011) and consist of an oxygen-labile α subunit and the aryl hydrocarbon receptor nuclear translocator (ARNT, also known as HIF1B). This heterodimer acts to regulate a number of hypoxia-sensitive target genes (Kanasaki et al., 2008). Activation of a cellular response to low oxygen is associated with stabilization of the HIF1A subunit protein, formation of a heterodimers with HIF1B, and modulation of gene transcription. Consequently, we assessed HIF1A protein in NK cell depleted and control placentation sites on gestation d9.5 using immunocytochemistry. NK cell depletion was associated with stabilization of the HIF1A protein within cells of the ectoplacental cone (**Fig. 2.12 E-H**). These results support the idea that NK cell depletion is leading to activation of the hypoxia-signaling pathway within trophoblast cells of the ectoplacental cone.

Collectively, these experiments indicate that NK cells regulate development of uterine spiral arteries and oxygen delivery to the developing placenta.

NK cells, hypoxia, and trophoblast lineage decisions within the placenta

Maternal hypoxia during the labile period of placental morphogenesis activates invasive trophoblast cells, resulting in formation of a placenta that is adept at uterine vascular

Fig. 2.12 NK cells regulate oxygen tension and stabilization of HIF1A at the d9.5 placentation site. Representative images are presented of pimonidazole protein adduct (PIM) immunostaining within d9.5 placentation sites from Control (**A**) and NK cell depleted (**B**) rats. Staining was consistently greater in NK cell depleted rat placentation sites (n=5 per group). Representative images are shown of cytokeratin (**C and D**) and HIF1A (**E-H**) immunolocalization. Ectoplacental cone regions react positively with antibodies to pan-cytokeratin (**C and D**). The boxed areas in panels **C** and **D** are shown in **E and G** and **F and H**,respectively. Panels **G and H** contain a counterstain with DAPI. HIF1A immunofluorescence was consistently stronger in NK cell depleted rat ectoplacental cone areas (n=5 per group). Scale bars=0.25 mm.

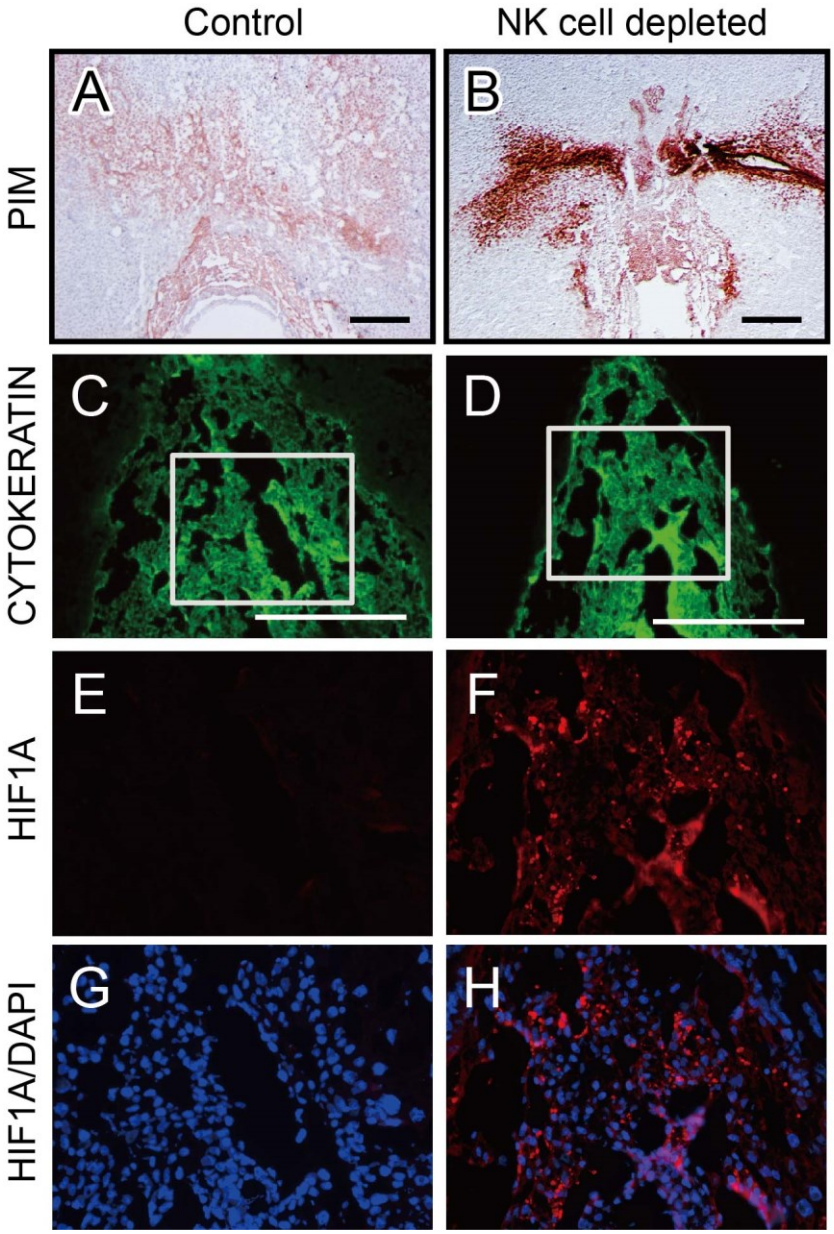
Control
NK cell depleted
PIM
CYTOKERATIN
HIF1A
HIF1A/DAPI
A
B
C
D
E
F
G
H

modification; whereas later exposure to hypoxia is entirely ineffective (Rosario et al., 2008). This infers a critical developmental window of sensitivity to low oxygen that impacts trophoblast cell lineage decisions. In the next series of experiments, we compared the effects of NK cell depletion (as described above; **Fig. 2.13A**) and maternal hypoxia (exposure to 8.5% oxygen from gestation d8.5 to d9.5; Fig. **2.13B**) on the expression of trophoblast cell lineage markers within ectoplacental cone tissues isolated on gestation d9.5. Transcripts for a series of junctional zone-specific trophoblast markers (*Prl3d1*: trophoblast giant cells; *Tpbpa*: junctional zone precursor and differentiated trophoblast; *Prl5a1* and *Prl7b1*: invasive trophoblast) were significantly upregulated, whereas a glycogen cell marker (*Gjb3*) and a labyrinthine trophoblast-specific transcript (*Tfeb*) were not affected (**Fig. 2.13 A and B**). The response was similar in the NK cell depleted and hypoxia exposed tissues. *Tpbpa* is expressed in the earliest cell populations committed to junctional zone trophoblast lineages and many of their descendants (Iwatsuki et al., 2000; Simmons and Cross, 2005). TPBPA protein expressing cells in the ectoplacental cone were also upregulated following NK cell depletion or exposure to maternal hypoxia (**Fig. 2.14**).

The hemochorial placenta is organized into two compartments, which reflect trophoblast interactions with two vascular beds. Trophoblast cells connected to the maternal vasculature specialize in facilitating nutrient flow to the placenta. This compartment is referred to as the junctional zone in the rat and extravillous trophoblast in the human. Invasive trophoblast cells of the rat arise from the junctional zone (Ain et al., 2006; Simmons and Cross, 2005). Trophoblast cells developing in proximity to the fetal vasculature promote nutrient transfer to the fetus and constitute the labyrinth zone in the rat and villous trophoblast in the human. We investigated the organization of gestation d13.5 placentation sites in control and NK cell depleted rats using vimentin immunostaining. This technique permits effective demarcation of junctional (negative)

Fig. 2.13. ***In vivo*** **analysis of the role of NK cells and oxygen on trophoblast cell lineage allocation. A**) Rats were treated on gestation d4.5 with normal rabbit serum (Control) or anti asialo GM1 (NK cell depleted) and sacrificed on gestation d9.5. **B**) Rats were exposed to 8.5% oxygen for 24 h beginning on d8.5 and sacrificed on gestation d9.5. Gestation d9.5 ectoplacental cone tissues were dissected, RNA extracted, and trophoblast lineage-associated transcripts measured by qRT-PCR. qRT-PCR measurements (SYBR Green) were performed using the ΔΔCT method). 18S rRNA served as an internal control. Asterisks indicate significant differences among groups (n=5; $P<0.01$ for each gene; Mann-Whitney Rank Sum Test). **C and D**) Effects of NK cells on the organization of the gestation d13.5 chorioallantoic placenta. Rats were treated on gestation d4.5 and d9.5 with normal rabbit serum (Control) or anti-asialo GM1 (NK cell depleted) and sacrificed on gestation d13.5. Placentation sites were sectioned and immunostained for vimentin (labyrinth zone and uterine mesometrial compartment positive, junctional zone negative). **C**) Representative localization of vimentin in placentation sites from controls. **D**) Representative localization of vimentin in placentation sites of NK cell depleted rats. Scale bar = 1 mm. The dashed black lines on panels C and D demarcate the positioning of the junctional zone, relative the underlying labyrinth zone. **E**) Ratio of cross sectional areas for junctional zone versus labyrinth zone from Control (n=5) and NK cell depleted (n=5) placentation sites. Values are means ± the standard error of each mean. Please note the relative enlargement of the JZ from NK cell depleted placentation sites (asterisk; $P<0.001$; Student's *t*-test).

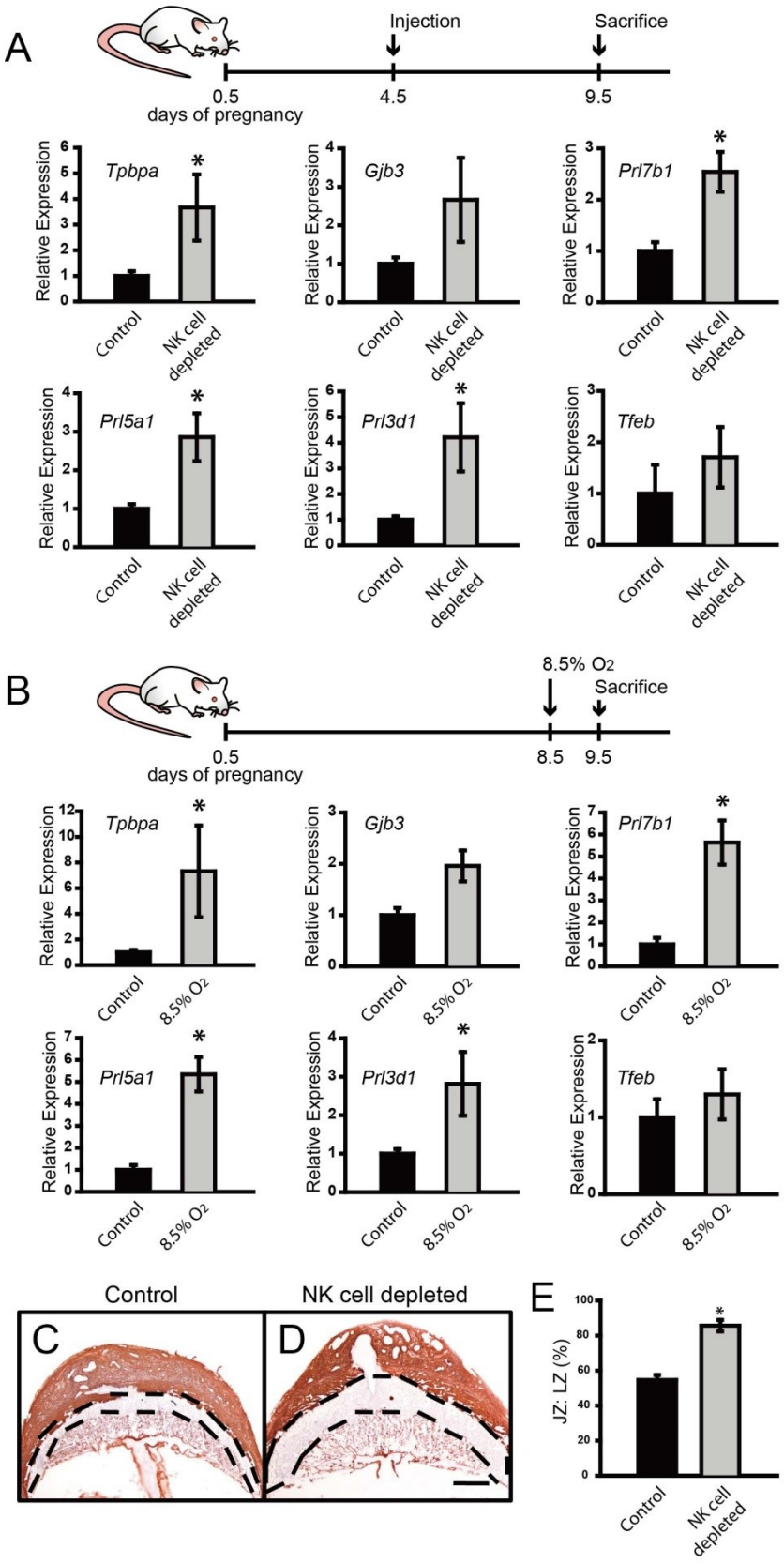
A
Injection
Sacrifice
0.5
4.5
9.5
days of pregnancy
Relative Expression
Tpbpa
Gjb3
Prl7b1
Prl5a1
Prl3d1
Tfeb
Control
NK cell depleted
B
8.5% O2
Sacrifice
0.5
8.5
9.5
days of pregnancy
Control
8.5% O2
C
D
Control
NK cell depleted
E
JZ: LZ (%)

Fig.2.14. Role of NK cells and hypoxia on TPBPA protein-positive cell distribution within the ectoplacental cone. A) Rats were treated on gestation d4.5 with normal rabbit serum (Control) or anti asialo GM1 (NK cell depleted), or **B**) exposed to 8.5% oxygen for 24 h beginning on d8.5. All animals were sacrificed on gestation d9.5. Representative sections through ectoplacental cones immunostained for cytokeratin (**C-E**), TPBPA (**F-H**), or TPBPA counterstained with DAPI (**I-K**). Sections from ectoplacental cones of Control (**C, F, and I**), NK cell depleted (**D, G, and J**), or 8.5% hypoxia exposed (**E, H, and K**) rats. Scale bars=0.125 mm.

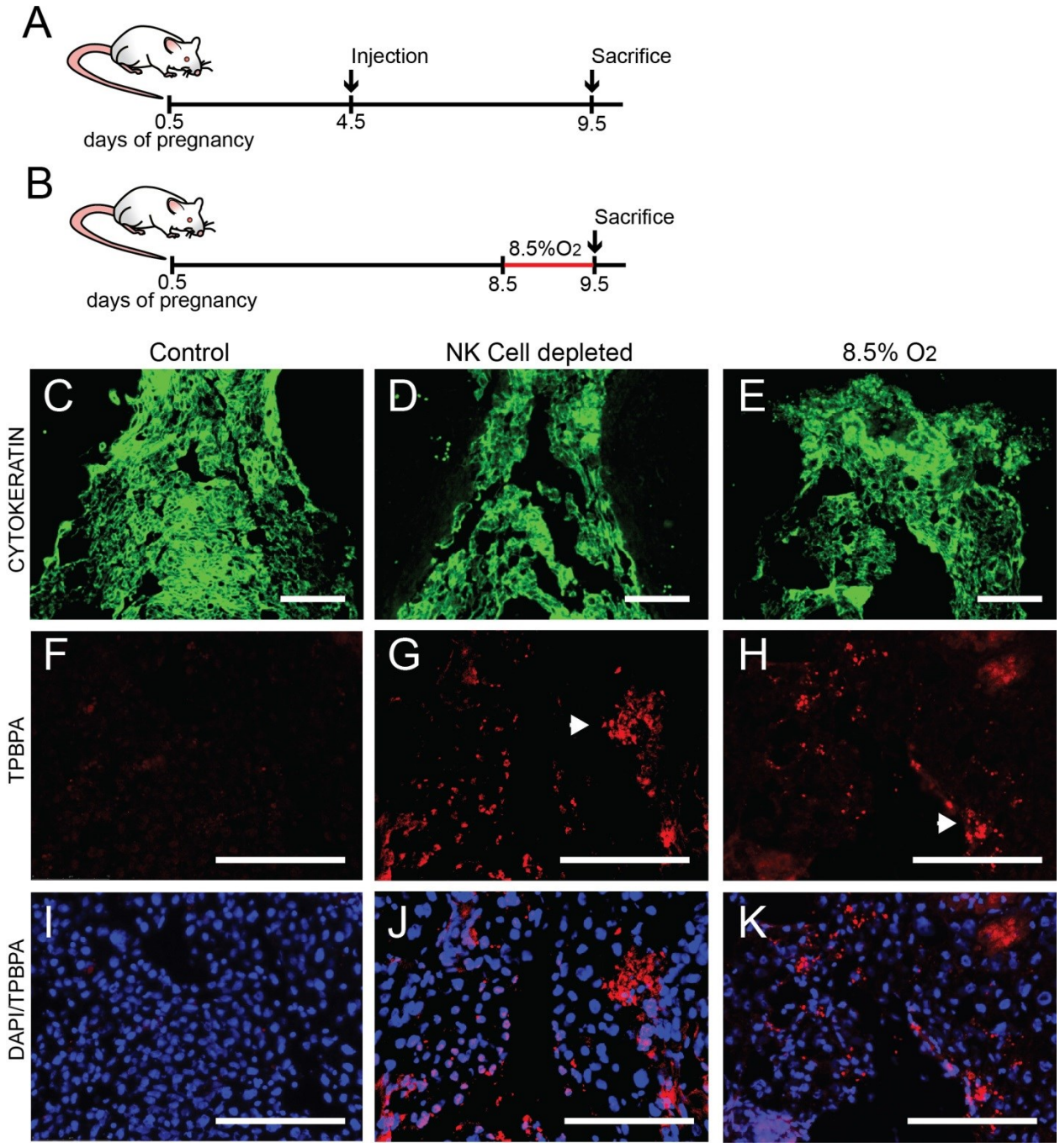
A
Injection
Sacrifice
0.5
days of pregnancy
4.5
9.5
B
Sacrifice
8.5%O2
0.5
days of pregnancy
8.5
9.5
Control
NK Cell depleted
8.5% O2
CYTOKERATIN
TPBPA
DAPI/TPBPA
C
D
E
F
G
H
I
J
K

and labyrinth (positive) zones. NK cell depletion resulted in an expansion of the junctional zone (**Fig. 2.13D**). A similar placental response occurs following maternal hypoxia exposure (Rosario et al., 2008). Although the junctional zone expanded following NK cell depletion, junctional zone and labyrinth zone-specific gene expression patterns were similar between NK cell depleted and controls (**Fig. 2.15**).

We conclude from these experiments that NK cells and hypoxia modulate trophoblast cell lineage decisions and organization of the developing placenta.

Hypoxia signaling regulates trophoblast cell lineage decisions

We next determined whether the impact of hypoxia on development of junctional zone-specific trophoblast cell lineages was a direct action on the TS cell population and whether the response was dependent on HIF1B signaling. For these experiments, we utilized TS cells derived from rat blastocysts (Asanoma et al., 2011). We first evaluated the effects of a range of oxygen concentrations (0.5 to 2%) on *Tpbpa* gene expression by TS cells maintained in the stem cell state. A 24 h interval was selected since it is sufficient to elicit *in vivo* trophoblast responses (**Fig.2.13**). An oxygen concentration of 0.5% was a reliable activator of *Tpbpa* gene expression and TPBPA protein accumulation (**Fig.2.17**) and was used in all subsequent experiments. TS cells were exposed to low oxygen for 24 h, harvested, and cellular phenotypes assessed. HIF signaling was disrupted through targeting HIF1B, the binding partner for HIF1A, with specific shRNAs. shRNAs were delivered to TS cells in lentiviral vectors. *Hif1b* shRNAs significantly decreased *Hif1b* mRNA and HIF1B protein levels, whereas control shRNAs showed no significant disruption of HIF1B expression (**Fig. 2.18 A and B**). Transcript concentrations for known hypoxia responsive genes (*Ankrd37*, *Egln1*, and *Bhlhe40*; Benita et al., 2009; Semenza,

Fig. 2.15. Effects of NK cell depletion on gestation d13.5 placental zonespecific gene expression. A) Rats were treated on gestation d4.5 and d9.5 with normal rabbit serum (Control) or anti asialo GM1 (NK cell depleted) and sacrificed on gestation d13.5. Junctional and labyrinth zones were dissected, RNA extracted, and qRT-PCR analyses (**B**) performed on genes expressed in the junctional zone (*Tpbpa, Gjb3, Prl5a1, Prl7b1*) and labyrinth zone (*Tfeb*). Sample size: n=4 per group. Transcript levels were measured by qRT-PCR (SYBR Green, ΔΔCT method). 18S rRNA served as an internal control.

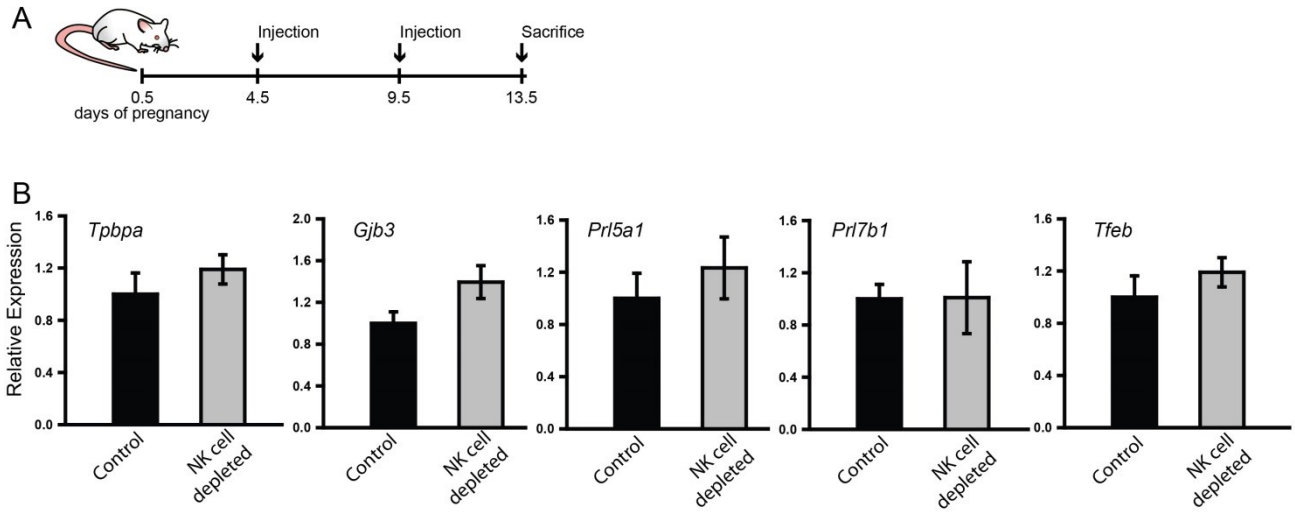
A
Injection
Injection
Sacrifice
0.5
days of pregnancy
4.5
9.5
13.5
B
Relative Expression
Tpbpa
Gjb3
Prl5a1
Prl7b1
Tfeb
Control
NK cell depleted

Fig. 2.16. Effects of low oxygen on TS cell responses. TS cells maintained in stem cell conditions were exposed to low oxygen (0.5%) for 24 h. **A**) qRT-PCR analyses for selected trophoblast cell lineage markers (*Tpbpa, Prl3d1,* and *Tfeb*) in TS cells exposed to ambient or low oxygen. qRT-PCR measurements (SYBR Green) were performed using the ΔΔCT method). 18S rRNA served as an internal control. Asterisks indicate significant differences among groups ($P<0.05$ for each gene; Mann Whitney Rank Sum Test). All experiments were performed in triplicate. **B-E**) Immunofluorescence staining for TPBPA in TS cells exposed to ambient or low oxygen. **F, G**) Assessment of the effects of oxygen tension on TS cell invasion. Cells penetrating Matrigel-coated filters were counted after staining with Diff Quick. Representative images of TS cells from the following conditions are shown: **F**) exposure to ambient oxygen, **G**) exposure to low oxygen. Arrowheads show the location of cells penetrating through the Matrigel. **H**) Quantification of TS cell invasion. All experiments were performed in triplicate. Asterisks indicate significant differences among groups ($P<0.05$; analysis of variance with Tukey's Test for comparisons).

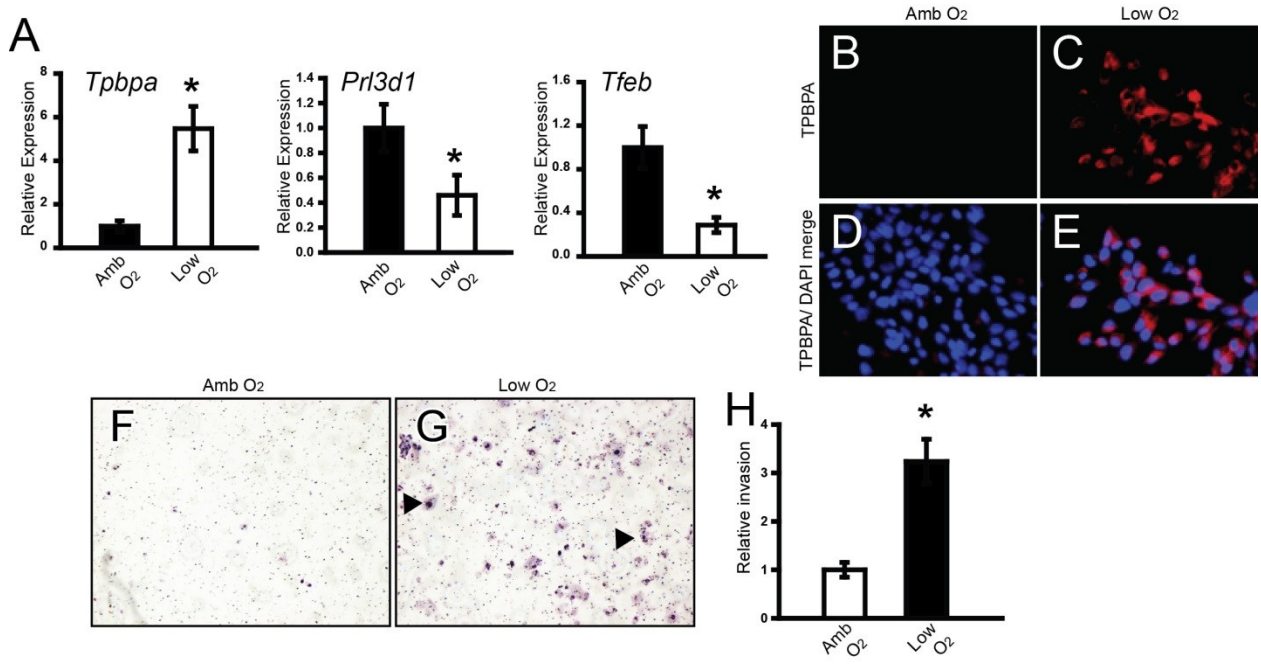
A
Tpbpa
Prl3d1
Tfeb
Relative Expression
Amb O2
Low O2
B
C
D
E
TPBPA
TPBPA/ DAPI merge
F
G
H
Relative invasion

2010) and trophoblast lineage-specific transcripts were evaluated. *Ankrd37*, *Egln1*, and *Bhlhe40* transcript concentrations were increased in response to low oxygen (**Fig. 2.18C**), as was *Tpbpa*, a transcript expressed by junctional zone precursors and some of their derivatives (**Fig. 2.18D**). In contrast, concentrations of *Prl3d1* transcripts, a trophoblast giant cell-specific transcript, and *Tfeb*, a labyrinthine trophoblast-specific transcript, were significantly decreased (**Fig. 2.18D**). All low oxygen-sensitive cellular measures were dependent upon HIF1B except for the *Tfeb* response (**Fig. 2.18C and D**). Hypoxia-mediated inhibition of gene expression is more frequently associated with HIF-independence (Semenza, 2010). Concentrations of other trophoblast-associated transcripts (*Gjb3*, *Prl5a1*, *Prl7b1*) were not reproducibly affected by low oxygen. The number of TS cells expressing TPBPA protein was increased by exposure to low oxygen and reversed by knockdown of HIF1B (Fig. 1.18E). Similar results were observed with a second independent *Hif1b* shRNA (**Fig. 2.19**). Mouse TS cells exposed to low oxygen also show an upregulation of *Tpbpa* gene expression (Adelman et al., 2000; Cowden Dahl et al., 2005; Zhang et al., 2011).

Oxygen tension also promoted the invasive phenotype of TS cells. Expression of mRNA for proteins implicated in trophoblast invasion and trophoblast-directed spiral artery remodeling (*Cdh1*, *Mmp9*, and *Mmp12*; Harris et al., 2010; Librach et al., 1991; Peters et al., 1999; Vicovac and Aplin, 1996) and trophoblast movement through Matrigel were evaluated. *Cdh1* transcript levels were decreased in response to low oxygen (**Fig. 2.20F**), while *Mmp9* and *Mmp12* transcript levels were stimulated by low oxygen. Low oxygen stimulated trophoblast invasion through Matrigel (**Fig. 2.20G**). Each of these TS cell responses to low oxygen was dependent on HIF1B (**Fig. 2.20F and G**).

Fig. 2.17. Oxygen tension, HIF1B signaling, and trophoblast cell lineage decisions.

TS cells maintained in stem cell conditions were exposed to low oxygen (0.5%) for 24 h in the presence of Control (Cntrl) shRNA or *Hif1b* shRNA-1. **A**) qRT-PCR analysis for *Hif1b* in TS cells exposed to ambient or low oxygen and control shRNA or *Hif1b* shRNA-1. **B**) Western blot analysis for TS cells exposed to ambient or low oxygen and control shRNA or *Hif1b* shRNA-1. **C**) qRT-PCR analyses for known hypoxia responsive genes (*Ankrd37, Egln1,* and *Bhlhe40*) TS cells exposed to ambient or low oxygen and control shRNA or *Hif1b* shRNA-1. All experiments were performed in triplicate. Asterisks indicate significant differences among groups ($P<0.01$ for *Ankrd37* and *Egln1*, $P<0.05$ for *Bhlhe40*; analysis of variance with Tukey's Test for comparisons). **D**) qRT-PCR analyses for trophoblast cell lineage markers (*Tpbpa, Prl3d1,* and *Tfeb*) in TS cells exposed to ambient or low oxygen and control shRNA or *Hif1b* shRNA-1. **A, C, and D**) qRT-PCR measurements (SYBR Green) were performed using the ΔΔCTmethod). 18S rRNA served as an internal control. All experiments were performed in triplicate. Asterisks indicate significant differences among groups ($P<0.01$ for each gene; analysis of variance with Tukey's Test for comparisons).**E-G)** Immunofluorescence staining for TPBPA in TS cells exposed to ambient or low oxygen and control shRNA or *Hif1b* shRNA-1.

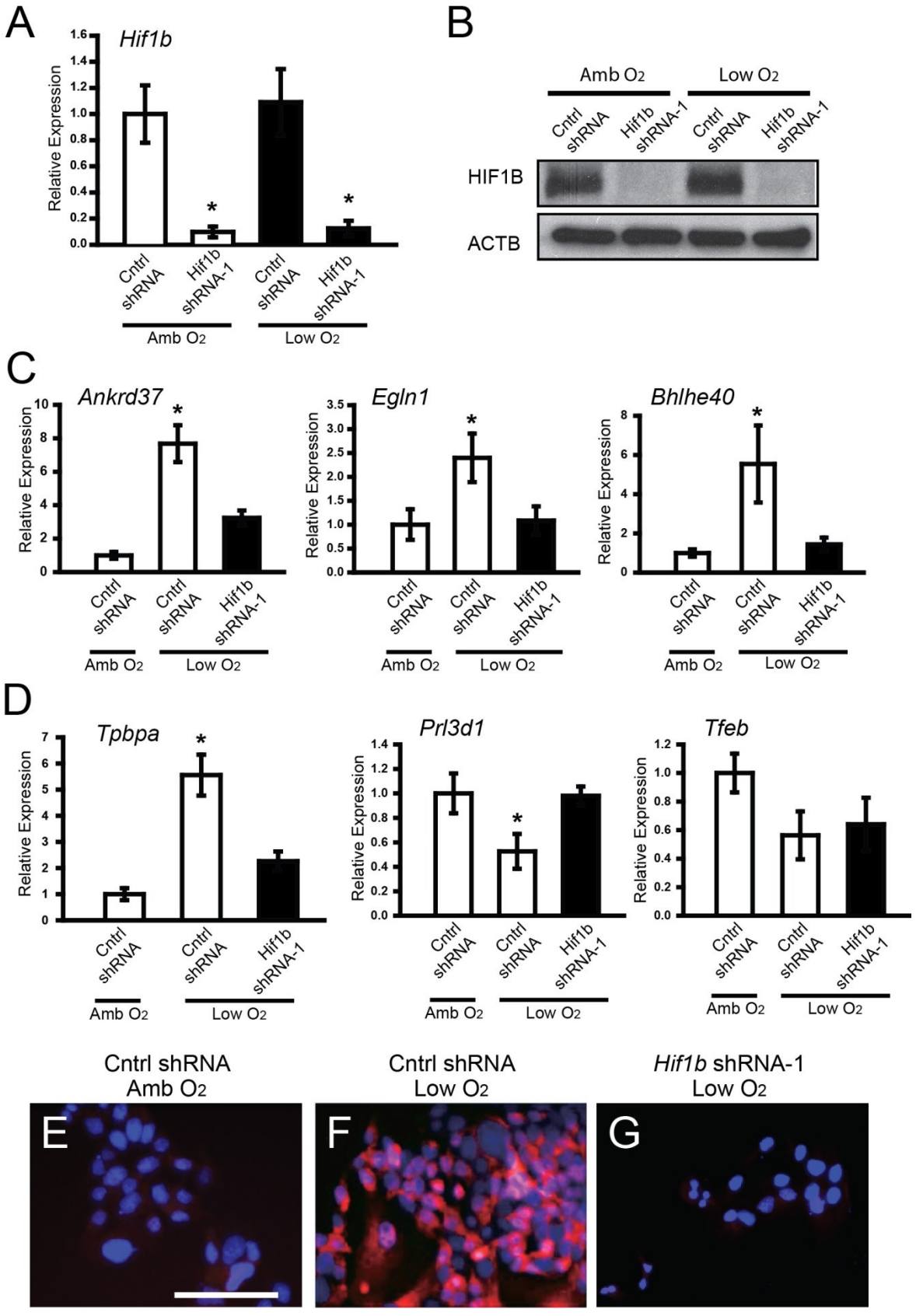
A
Hif1b
Relative Expression
Cntrl shRNA
Hif1b shRNA-1
Amb O2
Low O2
B
Amb O2
Low O2
HIF1B
ACTB
C
Ankrd37
Egln1
Bhlhe40
D
Tpbpa
Prl3d1
Tfeb
Cntrl shRNA
Amb O2
Cntrl shRNA
Low O2
Hif1b shRNA-1
Low O2
E
F
G

Fig 2.18 Examination of the effects of *Hif1b* shRNA-2 on TS cell responses to low oxygen. TS cells maintained in stem cell conditions were exposed to low oxygen (0.5%) for 24 h in the presence of Control (Cntrl) shRNA or *Hif1b* shRNA-2. **A**) qRT-PCR analysis for *Hif1b* in TS cells exposed to ambient or low oxygen and control shRNA or *Hif1b* shRNA-2. **B**) Western blot analysis for TS cells exposed to ambient or low oxygen and control shRNA or *Hif1b* shRNA-2. **C**)**.** qRT-PCR analyses for *Ankrd37*, a known hypoxia responsive gene. **D**) qRTPCR analysis for *Tpbpa*, a junctional zone lineage marker, in TS cells exposed to ambient or low oxygen and control shRNA or *Hif1b* shRNA-2. **A, C, and D**) qRTPCR measurements (SYBR Green) were performed using the ΔΔCT method).18S rRNA served as an internal control. Asterisks indicate significant differences among groups (*Hif1b* transcript measurements: *P<0.05, control shRNA vs *Hif1b* shRNA-2 in ambient conditions; **P<0.01, control shRNA vs *Hif1b* shRNA in low oxygen conditions; *Ankrd37* and *Tpbpa* transcript measurements: control shRNA vs *Hif1b* shRNA-2, *P<0.05). All experiments were performed in triplicate.Analysis of variance and the Holm-Sidak method for multiple comparisons were used for all data analyses.

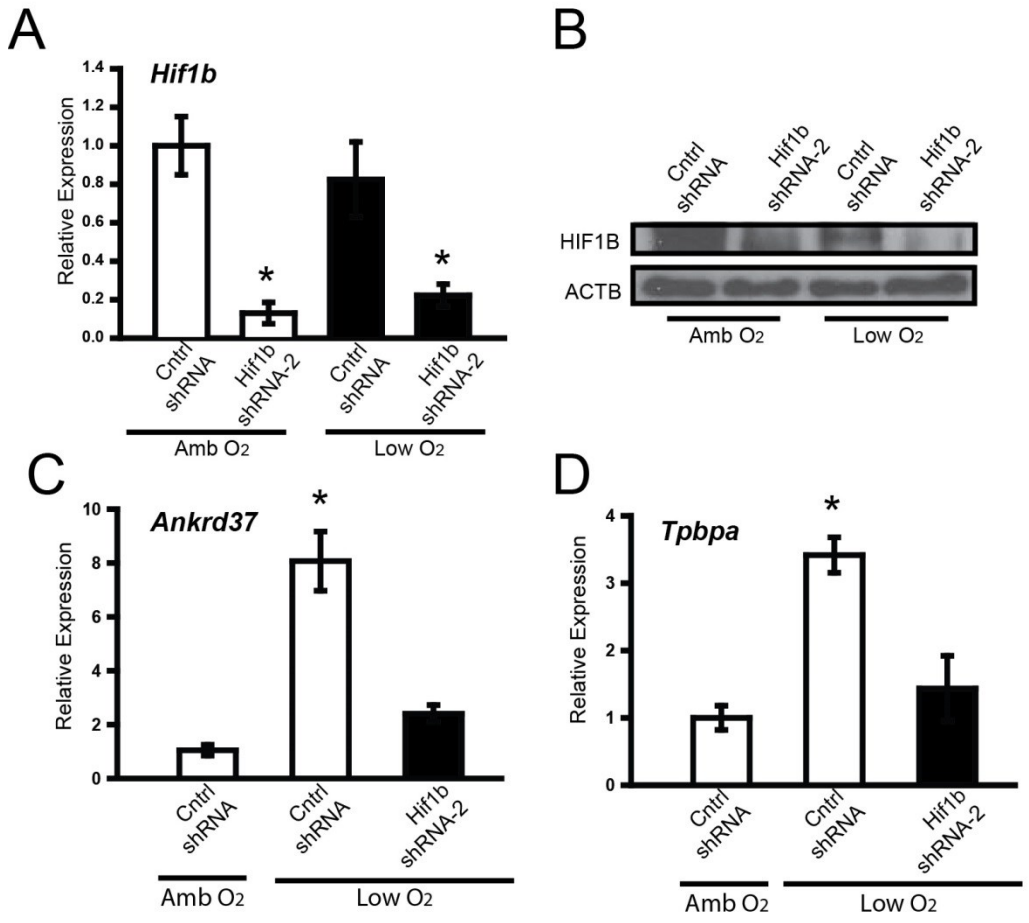
A
Hif1b
Relative Expression
1.4
1.2
1.0
0.8
0.6
0.4
0.2
0.0
*
*
Cntrl shRNA
Hif1b shRNA-2
Cntrl shRNA
Hif1b shRNA-2
Amb O2
Low O2
B
Cntrl shRNA
Hif1b shRNA-2
Cntrl shRNA
Hif1b shRNA-2
HIF1B
ACTB
Amb O2
Low O2
C
Ankrd37
Relative Expression
10
8
6
4
2
0
*
Cntrl shRNA
Cntrl shRNA
Hif1b shRNA-2
Amb O2
Low O2
D
Tpbpa
Relative Expression
4
3
2
1
0
*
Cntrl shRNA
Cntrl shRNA
Hif1b shRNA-2
Amb O2
Low O2

Fig. 2.19. Oxygen tension, HIF1B signaling, and trophoblast cell invasion. TS cells maintained in stem cell conditions were exposed to low oxygen (0.5%) for 24 h in the presence of Control (Cntrl) or *Hif1b* shRNA-1. **A**) qRT-PCR analyses for known hypoxia responsive genes (*Cdh1, Mmp9, Mmp12*) in TS cells exposed to ambient or low oxygen and control shRNA or *Hif1b* shRNA-1. qRT-PCR measurements (SYBR Green) were performed using the ΔΔCT method). 18S rRNA served as an internal control. All experiments were performed in triplicate. Asterisks indicate significant differences among groups ($P<0.05$ for each gene; analysis of variance with Tukey's Test). **B-D**) Assessment of the effects of oxygen tension and HIF1B signaling on TS cell invasion. Cells penetrating Matrigel-coated filters were counted after staining with Diff Quick. Representative images of TS cells from the following conditions are shown: **B**) control shRNA and exposure to ambient oxygen, **C**) control shRNA and exposure to low oxygen, and **D**) *Hif1b* shRNA-1 and exposure to low oxygen. Arrows in **B** and **D** show the locations of invaded cells. **E**) Quantification of TS cell invasion. All experiments were performed in triplicate. Asterisks indicate significant differences among groups ($P<0.05$; analysis of variance with Tukey's Test for comparisons). **F**) Schematic representation of the effects of NK cells on uterine spiral artery development, oxygen delivery to trophoblast stem cells, and HIF-dependenttrophoblast differentiation.

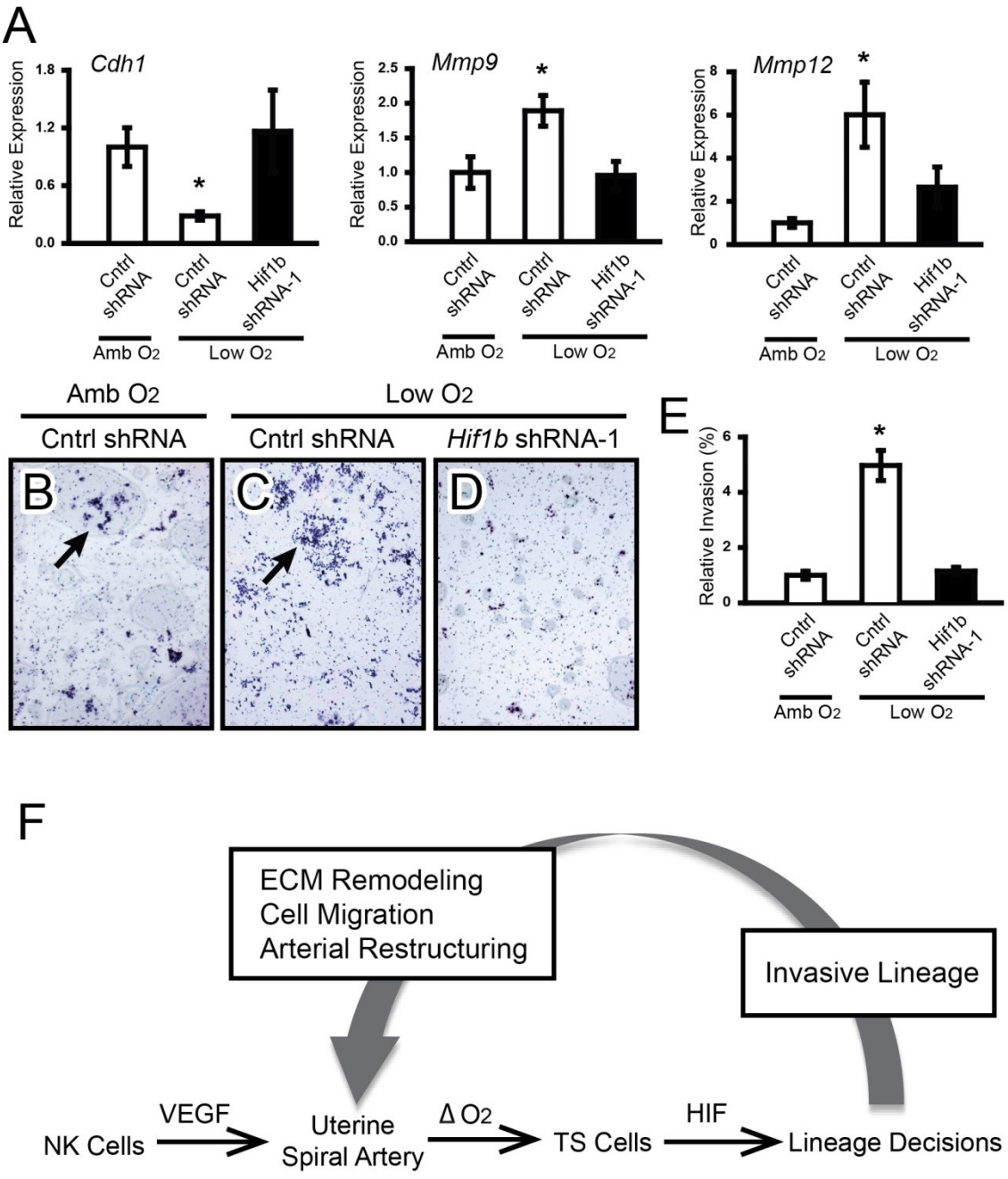
A
Cdh1
Mmp9
Mmp12
Relative Expression
Cntrl shRNA
Hif1b shRNA-1
Amb O2
Low O2
B
C
D
Amb O2
Low O2
Cntrl shRNA
Cntrl shRNA
Hif1b shRNA-1
E
Relative Invasion (%)
F
ECM Remodeling
Cell Migration
Arterial Restructuring
Invasive Lineage
NK Cells
VEGF
Uterine
Spiral Artery
Δ O2
TS Cells
HIF
Lineage Decisions

Collectively, the results indicate that trophoblast lineage decisions are sensitive to oxygen tension. Hypoxia exposed TS cells are directed to differentiate towards a unique invasive and non-giant cell and non-labyrinthine trophoblast phenotype. This process is regulated by HIF1B.

DISCUSSION

The accumulation of NK cells in the uterus during pregnancy is a well-conserved biological event (Zhang et al., 2011). In this report, we investigated the role of uterine NK cells in the rat, a species with hemochorial placentation and deep intrauterine trophoblast invasion (Ain et al., 2003a). Our research demonstrates that NK cells act as regulators of hemochorial placentation. NK cells influence the development of uterine spiral arteries, at least in part, through their production of proangiogenic factors, such as VEGFs. Uterine spiral arteries deliver nutrients including oxygen to the developing placenta. Oxygen tension at the placentation site influences adaptive responses, which include trophoblast lineage decisions. Depending upon the internal milieu, trophoblast cells are differentially allocated to the uteroplacental vascular bed versus the placental–fetal interface, resulting in the creation of placentas with specialized properties for acclimation to specific environmental challenges. These experimental findings provide an important physiological link between the work of Croy and her colleagues demonstrating a role for NK cells in uterine spiral artery remodeling (Guimond et al., 1997; Zhang et al., 2011) and the efforts of Simon and coworkers elucidating the involvement of HIF signaling in the regulation of placentation (Adelman et al., 2000; Fryer and Simon, 2006).

There are temporal and quantitative features associated with the activities of NK cells and invasive trophoblast cells in uterine spiral artery maturation. NK cells promote uterine spiral artery growth toward the ectoplacental cone, a key event in the establishment of the hemochorial

placenta, and cause at least a partial disruption of spiral artery tunica media integrity. All NK cells are not the same and differentially contribute to the establishment of the maternal–fetal interface (Madeja et al., 2011). In the absence of NK cells, spiral artery extension is delayed and the tunica media initially remains intact. These observations are consistent with an angiogenic/ vascular remodeling role for NK cells. The actions of NK cells on uterine spiral artery and stromal cell compartments are not a prerequisite for endovascular trophoblast invasion. This process is actually accelerated and more robust in the absence of NK cells. Although NK cell and invasive trophoblast cell populations are each sufficient to facilitate establishment of the hemochorial placenta, there are quantitative differences in the extent of spiral artery remodeling achieved by each cell population. NK cell actions on spiral arteries can be viewed as modest, especially in comparison with the substantial actions of endovascular invasive trophoblast cells on uterine spiral artery structure and nutrient delivery to the placenta. The latter actions are exaggerated in the absence of NK cells. By promoting spiral artery development, oxygen delivery, and establishing the hemochorial placenta, NK cells effectively delay endovascular trophoblast invasion. Delaying trophoblast entry into spiral arteries and the concomitant enhanced flow of maternal resources to the placenta is protective to the mother and can be viewed as a maternal adaptive strategy.

How do NK cells communicate with the developing placenta? Previous *in vitro* experimentation indicated that NK cells produce factors that directly affect the behavior of trophoblast cells, including the invasive trophoblast lineage (Hanna et al., 2006; Lash et al., 2010; Zhang et al., 2011). Some reports suggested that NK cell secretory products stimulate trophoblast invasion, whereas others concluded the opposite action. Differences in the findings are probably related to methodological issues, such as the origin of NK cell and trophoblast cell

preparations used in the analyses and/or other procedural considerations; however, they belie the most relevant mode of communication between NK cells and trophoblast cells, which is the delivery of oxygen. This view is supported by the similar placentation responses observed with two distinct *in vivo* manipulations: (i) NK cell depletion and (ii) maternal hypoxia(Rosario et al., 2008). Our results indicate that the direct actions of NK cells on trophoblast cells are of secondary consideration to the fundamental role of NK cells in the development of the vasculature and oxygen delivery.

Oxygen tension is a regulator of trophoblast cell function (Burton, 2009; Fryer and Simon, 2006; Genbacev et al., 1996; Zhou et al., 2011). A number of reports have demonstrated that trophoblast cells respond to oxygen restriction (Tuuli et al., 2011). *In vitro* experimentation has yielded a range of responses, some of which are contradictory, but, again, methodological differences are the likely cause for the discrepancies. Our *in vivo* findings led us to a critical window during placental morphogenesis (E8.5–E9.5 in the rat) that is especially sensitive to oxygen tension (Rosario et al., 2008). This is an interval where critical trophoblast lineage decisions are being finalized. These decisions impact morphogenesis of the placenta. Low oxygen favors TS cell and/or trophoblast precursor cell allocation to the junctional zone, a structure that establishes the placental interface with the uterus, including maternal vascular connectivity. Placentation sites are constructed to meet proximal challenges presented during the critical phase of their development, with the expectation that these challenges will continue throughout pregnancy and into postnatal extrauterine life. Problems and potentially disease arise when adaptations are ineffective and/or mismatches occur with the original environmental challenge directing placentation and subsequent prenatal and postnatal exposures. These

postulates are consistent with central roles for the placenta in fetal programming and the development of adult health and disease (Myatt, 2006).

In vivo placental adaptive responses can be simulated *in vitro* and include oxygen-sensitive lineage decisions. TS cell lineage responses are dependent upon HIF1B signaling pathways. HIF1B can interact with oxygen-sensitive HIF1A or HIF2A subunits or alternatively with other members of the bHLH-PAS family (Semenza, 2010). The HIF1A–HIF1B heterodimer is a transcription factor complex controlling expression of genes that are vital to cell survival under conditions of oxygen deprivation (Semenza, 2010). HIF1B binding partners and transcriptional targets in TS cells are unknown. Presumably, HIF1B is participating in transcriptional regulation of genes required for metabolic adaptations and also those controlling lineage decisions. The latter are keys to understanding how the invasive trophoblast cell lineage develops and potentially gaining insights about disorders that adversely affect placentation. In conclusion, hypoxia-activated trophoblast invasion/uterine spiral artery remodeling is an adaptive response regulated by NK cells that ensures appropriate placentation and protects pregnancy.

CHAPTER 3:

EPIGENETIC INVOLVEMENT OF THE HISTONE H3K9 DEMETHYLASE KDM3A IN TROPHOBLAST STEM CELL ADAPTATIONS TO HYPOXIA

ABSTRACT

Delivery of oxygen is a key signal influencing both trophoblast cell differentiation and organization of the placentation site. Hypoxia promotes development of the invasive trophoblast lineage. In this study, we evaluated the impact of hypoxia on trophoblast stem (TS) cell differentiation. Initially, DNA microarray analyses were performed in rat TS cells exposed to ambient or low oxygen (0.5%). Hypoxia stimulated an upregulation of genes characteristic of an invasive/vascular remodeling phenotype, including matrix metalloproteinases (*Mmp9*, *Mmp12*) and a histone H3K9 demethylase (*Kdm3a*) transcript levels and a marked downregulation of stem state-associated genes, including E-cadherin (*Cdh1*). These responses were dependent upon hypoxia inducible factor (HIF) signaling. Hypoxia also induced global changes in trophoblast cell histone H3K9 methylation marks. A subset of the HIF targets was further shown to be KDM3A targets. Knockdown of KDM3A in rat TS cells inhibited *Mmp12* gene expression and disrupted histone H3K9 methylation status at the *Mmp12* locus. Conversely, ectopic expression of KDM3A in rat TS cells upregulated *Mmp12* expression in ambient conditions. KDM3A knockdown also decreased hypoxia-induced blastocyst outgrowth and reduced invasion through Matrigel-coated transwell chambers. In summary, hypoxia/HIF-directed epigenetic remodeling contributes to the control of TS cell adaptations, modulating trophoblast cell lineage development.

INTRODUCTION

Vascular remodeling in an important pregnancy associated adaptation in hemochorial placentation wherein the specialized trophoblast cell population called the invasive trophoblast lineage or alternatively extravillous trophoblast invade into the maternal spiral arterioles turning them into flaccid low resistance vessels (Georgiades et al., 2002; Red-Horse et al., 2004). Failure of trophoblast invasion and vascular remodeling is associated with pathological conditions like preeclampsia and intrauterine growth restriction (Kaufmann et al., 2003; Pijnenborg et al., 2006). The invasive trophoblast lineage arises from the trophoblast stem (TS) cells. The regulation of the differentiation program for this cell lineage is not well understood. Invasive trophoblast cells can be classified based on their route of invasion. In the rat, an initial wave of invasion consists of the endovascular invasive cell lineage, which moves within the spiral arteries, removes endothelium and often acquires a vascular endothelial phenotype known as pseudovasculogenesis (Harris, 2010; Harris et al., 2010; Pijnenborg et al., 1981b; Pijnenborg et al., 2006; Wiemers et al., 2003; Zhou et al., 1997). A second wave consists of the interstitial invasive cell lineage, which moves into the decidua and is situated between the uterine spiral arteries (Ain et al., 2003a; Pijnenborg et al., 1981a).

Oxygen tension is an important cue for placental development. During early gestation, oxygen tension at the placentation sites is low and then progressively increases with the establishment of functional placental compartments and vascular remodeling (Burton, 2009; Fryer and Simon, 2006; Genbacev et al., 1997; Rodesch et al., 1992). Cellular responses to low oxygen signaling are mediated by hypoxia inducible factor (HIF) transcription factors (Semenza, 2010). HIF transcription factors consist of heterodimer composed of oxygen sensitive HIF1A or

HIF2A and a constitutively active HIF1B (also known as aryl hydrocarbon receptor nuclear translocator, ARNT).

Under oxygen replete conditions HIFA proteins is hydroxylated by prolyl hydroxylases and targeted for degradation by the ubiquitin ligase Von Hippel Lindau protein (Ivan et al., 2001; Jaakkola et al., 2001b). Under low oxygen tensions, HIFA proteins are stabilized, dimerize with HIF1B, and bind hypoxia response elements (Wang et al., 1995). HIF1A and HIF2A are known to have unique as well as overlapping targets (Bracken et al., 2006; Hu et al., 2006a; Raval et al., 2005). Mutagenesis of genes encoding components of the HIF pathway including the *Hif1a*, *Hif2a*, *Hif1b*, prolyl hydroxylase domain protein 2 (*Phd2*; also known as *Egln1*), and Von Hippel-Lindau (*Vhl*) genes, are associated with failures in placentation (Adelman et al., 2000; Fryer and Simon, 2006). Hypoxia exposure can redirect placental organization and promote development of the invasive trophoblast cell lineage (Chakraborty et al., 2011; Rosario et al., 2008).

Cellular adaptations to hypoxia include epigenetic reorganization. Hypoxia leads to a range of histone modifications at target genes (Johnson et al., 2008; Melvin and Rocha, 2012) and specifically regulates a number of JmJc domain containing histone demethylases (Beyer et al., 2008; Krieg et al., 2010; Pollard et al., 2008; Wellmann et al., 2008). KDM3A (also known as JMJD1A) is a hypoxia responsive JmJc containing histone H3K9 demethylase, specifically acting on histone H3K9 monomethyl and dimethyl substrates (Yamane et al., 2006). KDM3A is implicated in the regulation of cell differentiation (Herzog et al., 2012; Lockman et al., 2007), maintenance of embryonic stem cell stem state (Ko et al., 2006; Loh et al., 2007), in cancer cell invasion (Guo et al., 2011; Yamada et al., 2012; Yamane et al., 2006) as well as *in vivo* tumor cell growth (Krieg et al., 2010). Targeted *in vivo Kdm3a* mutagenesis in mice is associated with

failures in male germ cell development and metabolic syndrome (Liu et al., 2010; Okada et al., 2007; Tateishi et al., 2009).

In this chapter, we examine the actions of hypoxia signaling on development of the invasive trophoblast cell lineage. Hypoxia-responsive gene expression in TS cells is elucidated and the contributions of HIF and KDM3A to hypoxia-dependent changes in TS cell biology were determined. Hypoxia exposure upregulates a signature set of genes involved in cellular movement and invasion. HIF regulated KDM3A appears to be at the center of global and genespecific epigenetic changes. In summary, HIF-directed epigenetic remodeling contributes to the control of TS cell adaptations to low oxygen and development of the invasive trophoblast cell lineage.

MATERIALS AND METHODS

Animals and tissue collection

HSD rats were acquired from Harlan Laboratories (Indianapolis, IN). Animals were housed in an environmentally controlled facility with lights on from 0600-2000 h and allowed free access to food and water. Virgin female rats 8-10 weeks of age were cohabited with adult males (>3 months of age) of the same strain. Mating was assessed by inspection of vaginal lavages. The presence of sperm in the vaginal lavage was considered gestation day (E)0.5. Rat embryos were collected by flushing uteri with M2 medium (Millipore, Temecula, CA) at E4.5.

Pregnant rats were placed in a hypoxic (8.5% oxygen) gas-regulated chamber (BioSpherix, Lacona, NY) from E8.5 to E9.5. Pair-fed and ad libitum-fed pregnant rats exposed to ambient conditions (normoxia) served as controls. Rat placental tissues were collected on E9.5. The E9.5 primordial placental structure is referred to as the ectoplacental cone. Placentation site

dissections were performed as previously described (Ain et al., 2006). Tissues for histological analysis were frozen in dry-ice cooled heptane and stored at -80°C. Tissue samples for protein or RNA extraction were frozen in liquid nitrogen and stored at -80°C until processed. The University of Kansas Animal Care and Use Committee approved protocols for the care and use of animals.

Rat TS cell culture

Blastocyst-derived rat TS cells (Asanoma et al., 2012) were used to evaluate the effects of low oxygen on trophoblast lineage decisions. TS cells were cultured in Basal Culture Medium [RPMI 1640 (Cellgro, Herndon, VA), 20% fetal bovine serum (FBS; Atlanta Biologicals, Norcross, GA), 100 μM 2-mercaptoethanol (Sigma-Aldrich, St. Louis, MO), 1 mM sodium pyruvate (Cellgro), 50 μM penicillin and 50 U/ml streptomycin (Cellgro)] supplemented with 70% rat embryonic fibroblast (REF) conditioned medium, FGF4 (25 ng/ml; Sigma-Aldrich) and heparin (1 μg/ml; Sigma-Aldrich). TS cells maintained in the stem cell/proliferative state were exposed to a range of oxygen tensions (0.5 to 2%) and 5% CO_2 using a NAPCO Series 8000WJ incubator (Thermo Scientific, Pittsburgh, PA) for 24 h and then harvested for cell and molecular analyses.

Immunocytochemistry

Immunocytochemical analyses were performed on 10 μm frozen tissue sections using indirect immunofluorescence detection using goat anti-mouse IgG tagged with Alexa 488 (Invitrogen, Carlsbad, CA, Cat. No. A11029; 1:1000 dilution), goat anti-mouse IgG tagged with Alexa 568 (Invitrogen, Cat. No. A11031; 1:400 dilution), or goat anti-rabbit IgG tagged with cyanine 3 (Cy3; Jackson ImmunoResearch Laboratories, West Grove, PA, Cat. No. 111-165-

003; 1:250 dilution). Nuclei were visualized with 4',6-diamidino-2-phenylindole (DAPI, Molecular Probes, Carlsbad, CA). Negative controls were performed with normal rabbit serum or isotype-specfic control mouse IgG and did not exhibit positive reactivity in the tissue sections. Processed tissue sections were inspected and images recorded with a Leica MZFLIII stereomicroscope equipped with a charge-coupled device (CCD) camera (Leica, Welzlar, Germany).

Western blot analysis

KDM3A, ACTB, histone H3, and histone H3K9 methylation modifications (monomethylated: H3K9me1, dimethylated: H3K9me2, trimethylated: H3K9me3) were monitored by western blot analysis. Rat TS cell lysates were prepared in radioimmunoprecipitation assay (RIPA) buffer (10 mM Tris-HCl, pH 7.2, 1% Triton X-100 or 1% Nonidet P-40, 1% sodium deoxycholate, 0.1% SDS, 150 mM NaCl, 5 mM EDTA, 1 mM sodium orthovanadate, 1 mM phenylmethylsulfonyl fluoride, 10 μg/ml aprotinin). Protein concentrations were determined by the DC protein assay (Bio-Rad, Hercules, CA). Proteins were separated by SDS-PAGE and transferred onto nitrocellulose membranes. Immunoreactive proteins were detected with rabbit antibodies to KDM3A (Sigma-Aldrich, Catalog No. SAB3500093) and ACTB (Sigma-Aldrich, Catalog No. A1978). Antibodies to histone H3 and histone H3K9 methylated isoforms were obtained from (Abcam, Cambridge, MA; histone H3, Catalog No. ab1791; H3K9me1, Catalog No.ab9045; H3K9me2, Catalog No. ab1220; H3K9me3, Catalog No.ab8898). Immunoreactive proteins were visualized by enhanced chemiluminescence according to the manufacturer's instructions (Amersham Biosciences, Piscataway, NJ).

DNA microarray

Affymetrix 230 2.0 DNA microarray chips (Affymetrix, Santa Clara, CA) were probed with cDNAs generated from rat trophoblast stem cells grown under oxygen replete conditions or low (0.5%) oxygen exposure. Each treatment group was repeated in triplicate. RNA samples were hybridized to the Affymetrix 230 2.0 DNA microarray chip using the GeneChip® Hybridization Oven 640 (Affymetrix). Washing and staining of hybridized chips were conducted using the GeneChip® Fluidics Station 450 (Affymetrix).Chips were scanned using the Affymetrix GeneChip® Scanner 3000 (Affymetrix) with autoloader by the KUMC Biotechnology Support Facility. Hybridization signals were normalized with internal controls using the Mas5 algorithm in Expression Console (Affymetrix) and fold change computed. Significant differences were determined by paired two-tailed Student t-tests. Microarray data was processed for functional analysis using Ingenuity Pathway Analysis (Redwood City, CA). Probe sets included in the analysis were restricted to those changing at least 1.5 fold between group comparisons with signal strengths of ≥ 500 for the maximal value.

Quantitative RT-PCR (qRT-PCR)

Total RNA was extracted from cells and tissues using TRIzol reagent (Invitrogen). cDNAs were synthesized from total RNA (1 μg) for each sample using Superscript 2 reverse transcriptase (Invitrogen), diluted five times with water, and subjected to qRT-PCR to estimate mRNA levels. Primers were designed using Beacon primer designer (Applied Biosystems, Foster City, CA). Primer sequences can be found in **Table 3.1**.**1** and **3.1.2.** Real-time PCR amplification of cDNAs was carried out in a reaction mixture (20 μl) containing SYBR GREEN PCR Master Mix (Applied Biosystems,) and primers (250 nM each). Amplification and fluorescence detection were carried out using the ABI Prism 7500 real time PCR system

Table 3.1.1 Primer sequences of the upregulated genes used for qRT-PCR

Gene Symbol	GenBank Accession Number	Forward Primer	Reverse Primer
Ppp1r3c	NM_001012072	TACCTGAACGACCATCTA	AAAGTGTGGCAGAAAGTT
Mmp12	NM_053963	GCTGGTTCGGTTGTTAGG	GTAGTTACACCCTGAGCATAC
Plod2	NM_175869	TGAGAAGACGAGAGGAATA	TAAACAAGATGACCAGAT
Bhlhe40	NM_053328	ACAATGAGTACAGTTCCTTA	ACCGTGATTCCATAACAG
Kdm3a	NM_175764	CTGAGATTCCTGAGCAAGTTATTC	AGCCGAAGACTGTTTACATCC
Ndrg1	NM_001011991	CCCACTAAACTCATTCCT	TCAGCATTCAGAACTCTAA
Il33	NM_001014166	CCAACATATCCGTAACAG	GCTTGTAACCAGTAAGTC
Cd200	NM_031518	TTCTCTATGTGCTTCTATGA	AGATGTGAACTACTTGCTA
Vegfa	NM_031836	GCTCTGGGATTTGATATTC	TCTTTCCTCTGCTGATTT
Dpp3	NM_053748	AGAGTTACATTGGCTTCA	CTTTGCACTCATGTCTTT
Mmp9	NM_031055	TACTGCTGGTCCTTCTGA	CCGTCCTTGAAGAAATGC
Slc2a1	NM_138827	GCTCAGTGTCATCTTCATC	ACCCTCTTCTTTCATCTCC
Comt	NM_012531	CTGACTTCCTGGCGTATG	TTCTCCAAGCCGTCTACA
Plau	NM_013085	TTGGTTCAGACTGTGAGAT	GCACTGTTCGTGAGAAAT
Loxl2	NM_001106047	GCAGAGAAGACTTACAACC	AGATGTGTGCTTCAGTTC
LOC680835 similar to Cullin 7	XM_002727163	CAAGTCATCAGACCTTCC	TTCACATCCGTTTCCATC
Ankrd37	NM_001108400	**TGAGACAGAAGCGGAGTT**	**TGCCCAACAAGACATCATC**
18S rRNA	M11188	GCAATTATTCCCCATGAACG	GGCCTCACTAAACCATCCAA

Table 3.1.2: Primer sequences of the downregulated genes used for qRT-PCR

Gene Symbol	GenBank Accession Number	Forward Primer	Reverse Primer
Cdh1	NM_031334	TTCTGAAGACTCCCGATT	ATGGACGAGAAAACTGGT
Ccdc86	NM_001006974	CAACGAGAGCAGTCATCCA	TGGGATCACCTCCTCCTTAG
Rbm3	NM_053696	TCTAGAGGTGGTGGAGAC	TCTCTAGACCGCCCATAC
Id1	NM_012797	CTACCCTGCCTCAGAACC	GCGACTTCAGACTCAGAG
Ncoa3	XM_215947	AGTGTATCGTTTCTCATT	TACATCCATTCTGTTCTC
Kat6a	NM_001100570	AATCTTGTATGCTATGGTTA	TTATCCTGATGCTGAGTA
Lin28	NM_001109269	AAACAAGTGTCAAACCAAGATTA	GCCCTGTGGAAATAACCT
Satb1	NM_001012129	GCCACTGGTATTTCCTAC	TCCTTCTGACTTCCTGTT
Hand1	NM_021592	CTCTTTGGAAATCCGAACC	CTGGAGATGACACGAAGG
Cdx2	NM_023963	CAGGAGGAAAGCTGAGTTGG	TGCTGCTGTTGCAACTTCTT

(Applied Biosystems). Cycling conditions included an initial hold step (95 °C for 10 min) and 40 cycles of a two-step PCR (92 °C for 15 sec, then 60 °C for 1 min), followed by a dissociation step (95 °C for 15 sec, 60 °C for 15 sec, and then 95 °C for 15 sec). The comparative cycle threshold method was used for relative quantification of the amount of mRNA for each sample normalized to 18S RNA.

Chromatin immunoprecipitation (ChIP)

ChIP analysis was performed according to a previously published procedure (Krieg et al. 2010). Briefly, TS cells were grown in 150-mm dishes for two days in ambient conditions and then exposed to 0.5% oxygen for 24 hours. Cells were then fixed with 1% formaldehyde, and purified nuclear lysates were sonicated using a Diagenode Bioruptor (Diagenode, Denville, NJ) to prepare DNA fragments at a size of approximately 500 bp. Lysates were immunoprecipitated with 3µg of appropriate antibody (H3K9me1, Catalog No.ab9045; H3K9me2, Catalog No. ab1220, ABCAM) or with rabbit or mouse IgG (BD Biosciences). Immunoprecipitated chromatin fragments were eluted from agarose beads. DNA-protein interactions were reverse cross-linked and purified using a QiaQuick PCR purification kit (Qiagen). Purified DNA fragments were assessed by quantitative PCR (qPCR) using *Mmp12* promoter-specific primers (**Table 3.1**) and SYBRgreen PCR master mix (Applied Biosystems). Specific primers were used for qPCR measurements of H3K9me1 and H3K9me2 enrichment site A (−459 to −322) occupancy (forward, AAGGATTCGTGTATTCTAGCA; reverse, ACGCCATTAGCAGAGTTT; 138-bp product) and site B (−207 to −10) occupancy (forward, TGAGTGATGACTTAGACAATG; reverse, TCCTTTCAGCAACAGAGT; 197-bp product) at *Mmp12* locus. Relative occupancy/enrichment was normalized to input samples by use of the ΔΔCT method.

Short hairpin RNA (shRNA) constructs and production of lentivirus

*Hif1b*shRNA constructs cloned into the pLKO.1 vector were obtained from Open Biosystems (Huntsville, AL). Several shRNAs were tested for each gene evaluated. The *Hif1b* shRNA sequences used in this analysis are as follows: i) *Hif1b* shRNA-1: 5'GAGAAGTCAGAAGGTCTCTTTTCTCGAGTAAAGAGACCTTCTGACTTCTC3'; ii) *Hif1b* shRNA-2: 5'CCAGACAAGCTAACCATCTTACTCGAGTAAGATGGTTAGCTTGTCTGG3'. The *Kdm3a* shRNA sequences used in the analysis are as follows: i) *Kdm3a* shRNA-1: 5'CCGGTGCGGGTAGAAGGCTTCTTAACTCGAGTTAAGAAGCCTTCTACCCGCATTTTTG3'; ii) *Kdm3a* shRNA-2: 5'CCGGGAAGTTCCTGAGCAAGTTATTCTCGAGAATAACTTGCTCAGGAACTTCTTTTTG3'.

The control shRNA, which targets no known mammalian gene, pLKO.1-shSCR (Plasmid 1864), was obtained from Addgene (Cambridge, MA) and has the following sequence 5'CCTAAGGTTAAGTCGCCCTCGCTCTAGCGAGGGCGACTTAACCTTAGG3' (Sarbassov et al., 2005a). Third generation lentiviral packaging vectors were purchased from Addgene and included: pMDLg/pRRE (Plasmid 12251), pRSV-Rev (Plasmid 12253) and pMD2.G (Plasmid 12259). Lentiviral particles were produced as previously reported (Lee et al., 2009). In brief, 293FT cells (Invitrogen) were transiently transfected using Lipofectamine 2000 (Invitrogen) with the following plasmids: shRNA containing transducing vector, third-generation packaging system plasmids (pMDLg/pRRE and pRSV-Rev; 104), and a VSVG envelope plasmid (pMD2.G). After transfection, cells were maintained in 50% DMEM with high glucose (Cellgro), 45% Opti-MEM I (Invitrogen) and 5% FBS. Culture supernatants containing lentiviral

particles were harvested every 24 h for two to three days. Supernatants were centrifuged to remove cell debris, filter sterilized, concentrated by ultracentrifugation, and stored at -80°C until used.

Ectopic expression of Kdm3a

Full length mouse *Kdm3a* expression vector was kindly provided by Dr. Christopher Mack, University of North Carolina, Chapel Hill, NC. Flag-tagged pcDNA3 vector expressing *Kdm3a* was transfected into rat TS cells using Lipofectamine 2000 (Lifetechnologies, NY) transfection reagent according to manufacturer's instructions. Cells were selected with Geneticin (Lifetechnologies, NY) for 5 days before experiments.

Matrigel invasion assay

The invasive ability of rat TS cells was measured as previously described (Peters et al., 1999). Rat TS cells were placed in Matrigel invasion chambers (BD Biosciences) at a density of 2 x 104 cells per chamber. Cells were allowed to invade for 24 h. Membranes were collected and stained with Diff-Quick (Dade Behring, Newark, DE). Invading cells were visualized by light microscopy and counted.

Blastocyst outgrowth assay

The blastocyst outgrowth assay was performed as reported before (Armant et al., 1986). Blastocysts were obtained from d4.5 pregnant rats by flushing them from the uterine horns with 0.1 ml DMEM medium (Lifetechnology). The embryos were cultured at 37°C in a 5% CO2 incubator for 48 hours to allow hatching from the zona pellucida. They were cultured in rat TS Basal Culture Medium. The attached blastocysts were exposed to 0.5 % oxygen for 24 hours in a NAPCO Series 8000WJ incubator (Thermo Scientific, Pittsburgh, PA) and then fixed in 4%

paraformaldehyde solution. The surface area of outgrowth was visualized using light microscopy and measured using Image J software.

Statistical analyses

Data analyses were performed using SigmaPlot 11.2 statistical software package (Systat Software, Inc, San Jose, CA). Specific details of the analyses are presented in the figure legends.

RESULTS

TS cell transcriptome responses to low oxygen

Hypoxia signaling regulates the development of the invasive trophoblast cell lineage (Chakraborty et al., 2011; Rosario et al., 2008), which can be effectively modeled *in vitro* using rat TS cells (Chakraborty et al., 2011). As a first step to identify potential regulatory mechanisms downstream of hypoxia exposure, we profiled the transcriptomes of TS cells exposed to ambient and 0.5% oxygen for 24 h using DNA microarray analysis (**Fig. 3.1A**). This culture condition activates HIF signaling pathways and promotes development of the invasive trophoblast cell lineage (Chakraborty et al., 2011). All DNA microarray data will be deposited in the Gene Expression Omnibus (GEO) repository. Appendix Tables **A 2.1** and **A 2.2** show abbreviated lists of hypoxia-regulated transcripts. Genes listed in these tables are those with arbitrary expression signal strengths of ≥ 500, a fold change of ≥ 1.5, and a P value ≤ 0.05. Similar numbers of transcripts were significantly upregulated (n=786) or downregulated (n=838) by low oxygen exposure (**Fig. 3.1B**). We utilized Ingenuity Pathway Analysis software (Ingenuity Systems, Redwood City, CA) to evaluate signaling pathways affected by exposure to low oxygen. Functions associated with general cellular movement and survival were upregulated

Fig3.1. Analysis of microarray data. A) Schematic showing the experimental plan of hypoxia exposure of rat TS cells. **B)** Scatter graph showing the signal intensity probe sets.

A

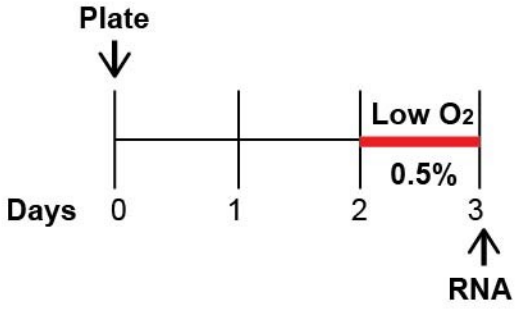
Plate
Low O2
0.5%
Days 0 1 2 3
RNA

B

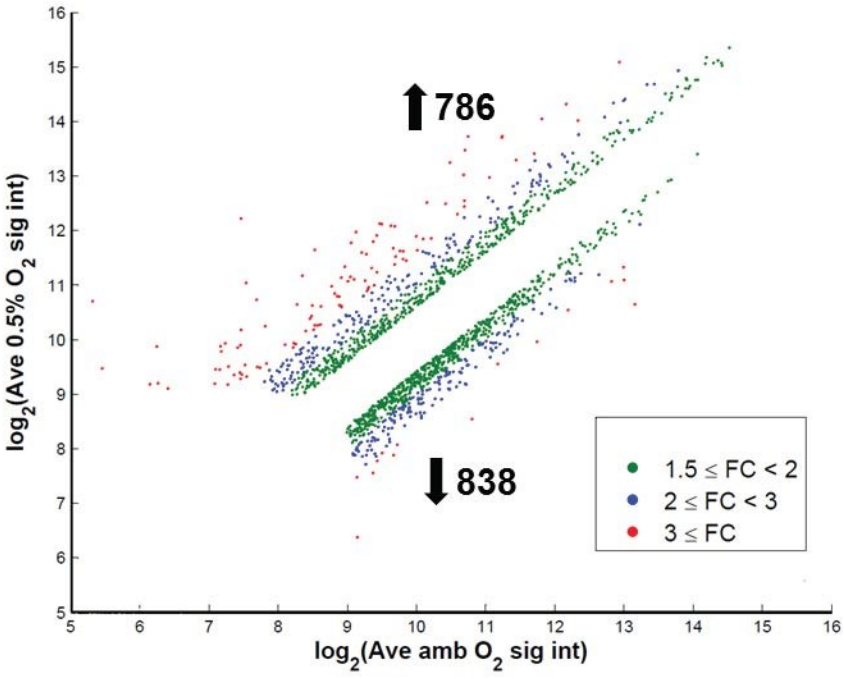
786
838
1.5 ≤ FC < 2
2 ≤ FC < 3
3 ≤ FC
log2(Ave 0.5% O2 sig int)
log2(Ave amb O2 sig int)

Fig3.2. Ingenuity Pathway Analysis of microarray data. Functional analysis of ambient oxygen exposed rat TS cell genes and 0.5% oxygen exposed rat TS cell genes using Ingenuity Pathway Analysis software.

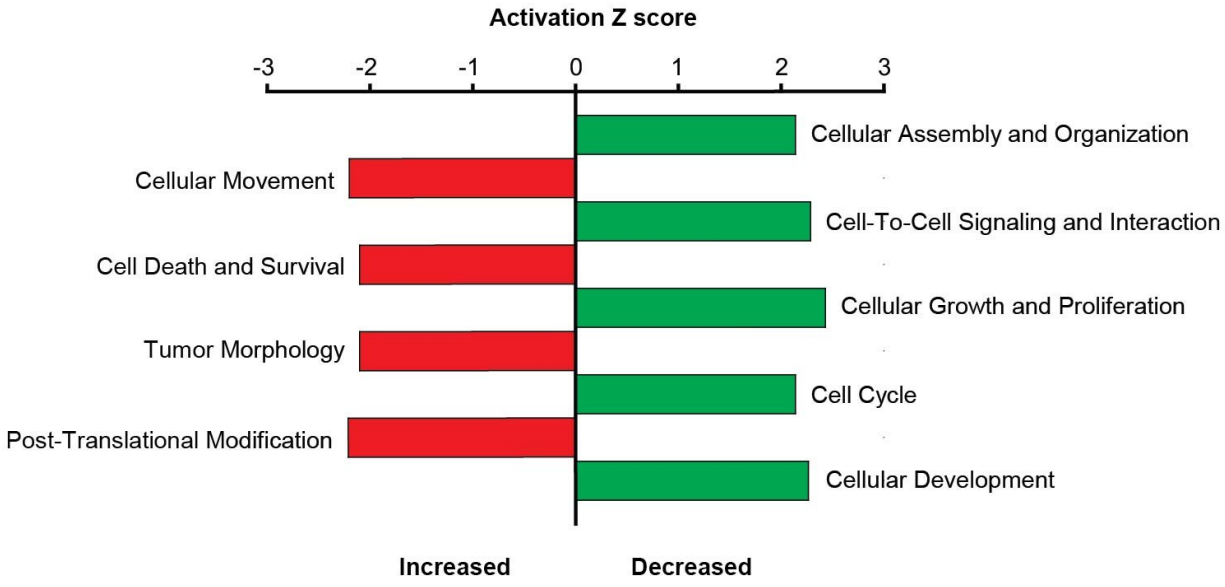
Activation Z score
-3
-2
-1
0
1
2
3
Cellular Assembly and Organization
Cellular Movement
Cell-To-Cell Signaling and Interaction
Cell Death and Survival
Cellular Growth and Proliferation
Tumor Morphology
Cell Cycle
Post-Translational Modification
Cellular Development
Increased
Decreased

following exposure to low oxygen exposure, whereas cell-to-cell association and stem cell maintenance pathways were downregulated (**Fig. 3.2**). A subset of differentially regulated transcripts was further analyzed and validated using qRT-PCR. The transcripts upregulated by low oxygen included transcripts encoding extracellular matrix remodeling enzymes (*Mmp12, Mmp9, Plau, Dpp3*), a histone demethylase (*Kdm3a*), key regulators of glycogen and glucose metabolism (*Ppp1r3c*), and a number of transcripts known to be regulated by hypoxia and the HIF signaling pathway (Benita et al., 2009; Semenza, 2010) (**Table 3.2.1**). In contrast, the downregulated group included cell-cell adhesion (Cdh1), TS cell-associated (*Cdx2, Bmp4, Id2, Satb1*), cell proliferation-associated (*Rbm3, Lin28*), and trophoblast giant cell-associated (*Hand1*) transcripts (**Table 3.2.2**). In summary gene expression analysis is consistent with rat TS cells adapting to low oxygen by differentiation into an invasive trophoblast cell lineage.

HIF dependence of TS cell responses to low oxygen

Many cellular adaptations to hypoxia are mediated by the HIF signaling pathway (Semenza, 2010). Since hypoxia-activated TS cell differentiation towards an invasive trophoblast cell lineage is dependent on HIF signaling (Chakraborty et al., 2011), we next focused on identification of hypoxia-responsive TS cell transcripts, which were dependent on HIF signaling. In order to determine the involvement of the HIF signaling pathway in the regulation of TS cell adaptations to low oxygen, HIF1B (the common transcriptional partner for HIF1A and HIF2A) was silenced using lentiviral transduction of HIF1B-specific shRNAs (Chakraborty et al., 2011). Knockdown of HIF1B attenuated the hypoxia-dependent upregulation of several transcripts, such as: *Mmp12*, *Mmp9*, *Kdm3a*, *Ppp1r3c*, *Il33* and *Bhlhe40* (**Fig. 3.3 A**). In contrast, the HIF dependence of TS cell transcripts downregulated by low oxygen was not as

Table 3.2.1 Genes upregulated by hypoxia exposure

Gene Symbol	Function	GenBank Accession Number	Microarray fold change (*)	QRT-PCR (*)
Ppp1r3c	Glycogen metabolism	NM_001012072	41.298	29.91±4.67
Mmp12	ECM remodeling	NM_053963	12.28	18.03±2.36
Plod2	Enzyme	NM_175869	11.03	10.57±1.24
Bhlhe40	Cell differentiation	NM_053328	8.20	7.66±1.35
Kdm3a	Histone demethylase	NM_175764	7.18	7.33±0.9
Ndrg1	Stress response, Cell growth differentiation	NM_001011991	5.165	2.53±0.29
Il33	Cytokine	NM_001014166	5.05	7.51±2.37
Cd200	Cell junctional protein	NM_031518	4.434	6.47±0.49
Vegfa	Growth Factor	NM_031836	3.98	4.41±0.09
Dpp3	Serine proteases	NM_053748	3.77	4.59±0.59
Mmp9	Metallopeptidase	NM_031055	2.66	3.45±0.36
Slc2a1	Glucose transporter	NM_138827	2.37	4.64±0.56
Comt	Enzyme, neurotransmitter degrader	NM_012531	2.28	1.96±0.12
Plau	Serine protease, ECM remodeler	NM_013085	2.19	2.5±0.16
Loxl2	Lysyl oxidase	NM_001106047	2.08	5.71±0.52
LOC680835 similarto Cullin 7	Ubiquitin ligase complex	XM_002727163	2.08	1.74±0.07

(Experiment performed in triplicate; * indicates $P<0.05$, Student's t Test)

Table 3.2.2. Genes downregulated by hypoxia exposure

Gene Symbol	Function	GenBank Accession Number	Microarray fold change (*)	QRT-PCR (*)
Cdh1	Cell-cell adhesion	NM_031334	0.21	0.13±0.02
Ccdc86	Cytokine responsive gene	NM_001006974	0.29	0.35±0.14
Rbm3	Cell cycle	NM_053696	0.29	0.27±0.11
Id1	Cell growth, differentiation	NM_012797	0.31	0.24±0.02
Ncoa3	Nuclear receptor co-activator	XM_215947	0.41	0.13±0.05
Kat6a	Chromatin modifier, acetyl-transferase	NM_001100570	0.42	0.24±0.11
Lin28	Cell proliferation	NM_001109269	0.43	0.5±0.05
Satb1	Chromatin modifier	NM_001012129	0.58	0.28±0.05
Hand1	Cell development and differentiation	NM_021592	0.57	0.59±0.06
Cdx2	Development and stem cell maintenance	NM_023963	0.84	0.74±0.25

(Experiment performed in triplicate; * indicates $P<0.05$, Student's t Test)

Fig. 3.3. Validation of hypoxia responsive genes. A) qRT-PCR analyses for hypoxia responsive upregulated genes . TS cells exposed to ambient or low oxygen and 1control shRNA or *Hif1b* shRNA-1. All experiments were performed in triplicate. Asterisks indicate significant differences among groups ($P<0.05$ analysis of variance with Student-Newman-Keuls method for comparisons). **B)** qRT-PCR analyses for hypoxia responsive downregulated genes . TS cells exposed to ambient or low oxygen and 1control shRNA or Hif1b shRNA-1. All experiments were performed in triplicate. Asterisks indicate significant differences among groups ($P<0.05$ analysis of variance with Student-Newman-Keuls method for comparisons; ** indicates P,0.05 between control shRNA group in ambient conditions and control shRNA group in hypoxic conditions).

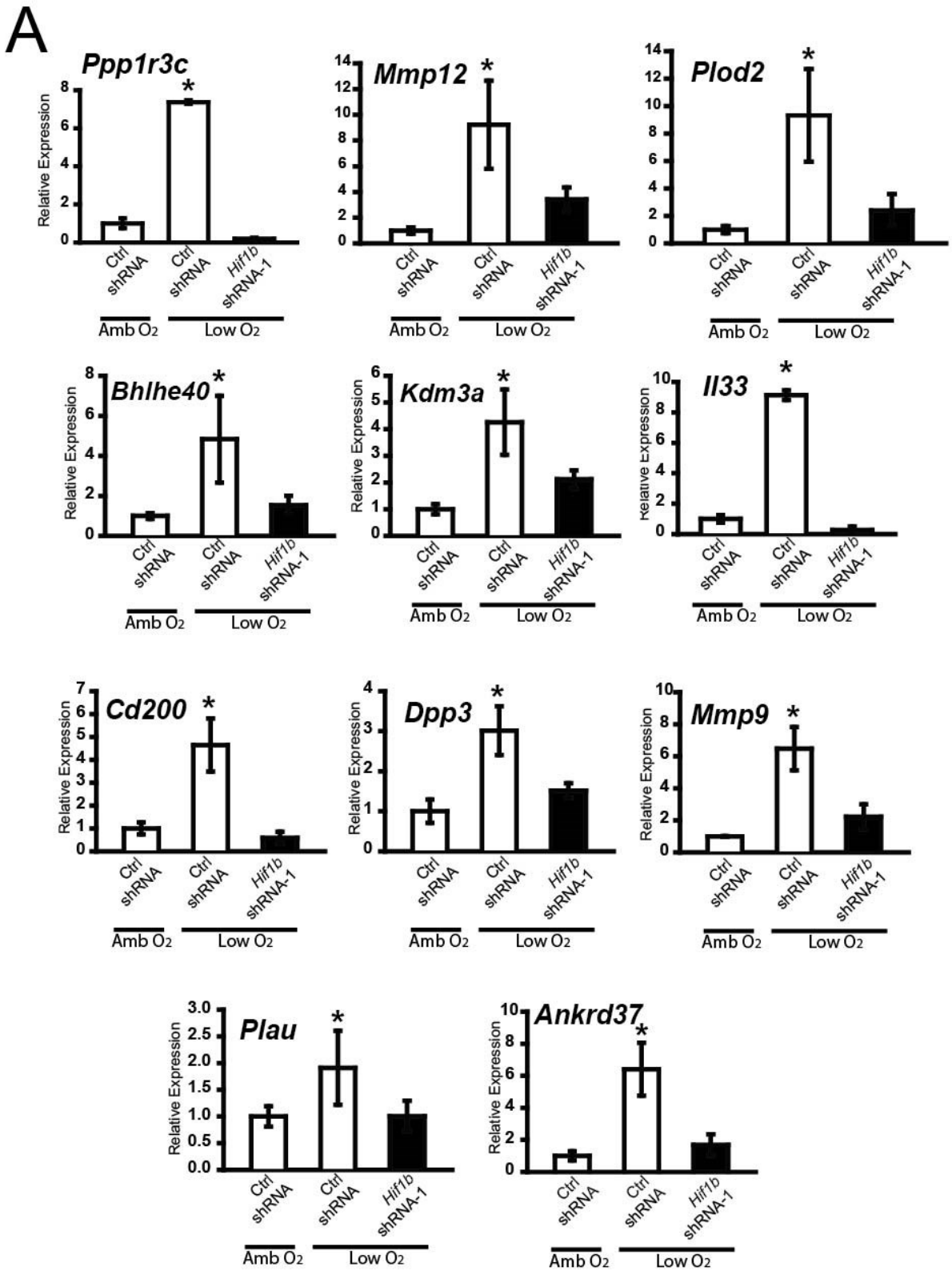
A
Ppp1r3c
Mmp12
Plod2
Bhlhe40
Kdm3a
Il33
Cd200
Dpp3
Mmp9
Plau
Ankrd37
Relative Expression
Ctrl shRNA
Hif1b shRNA-1
Amb O2
Low O2

B

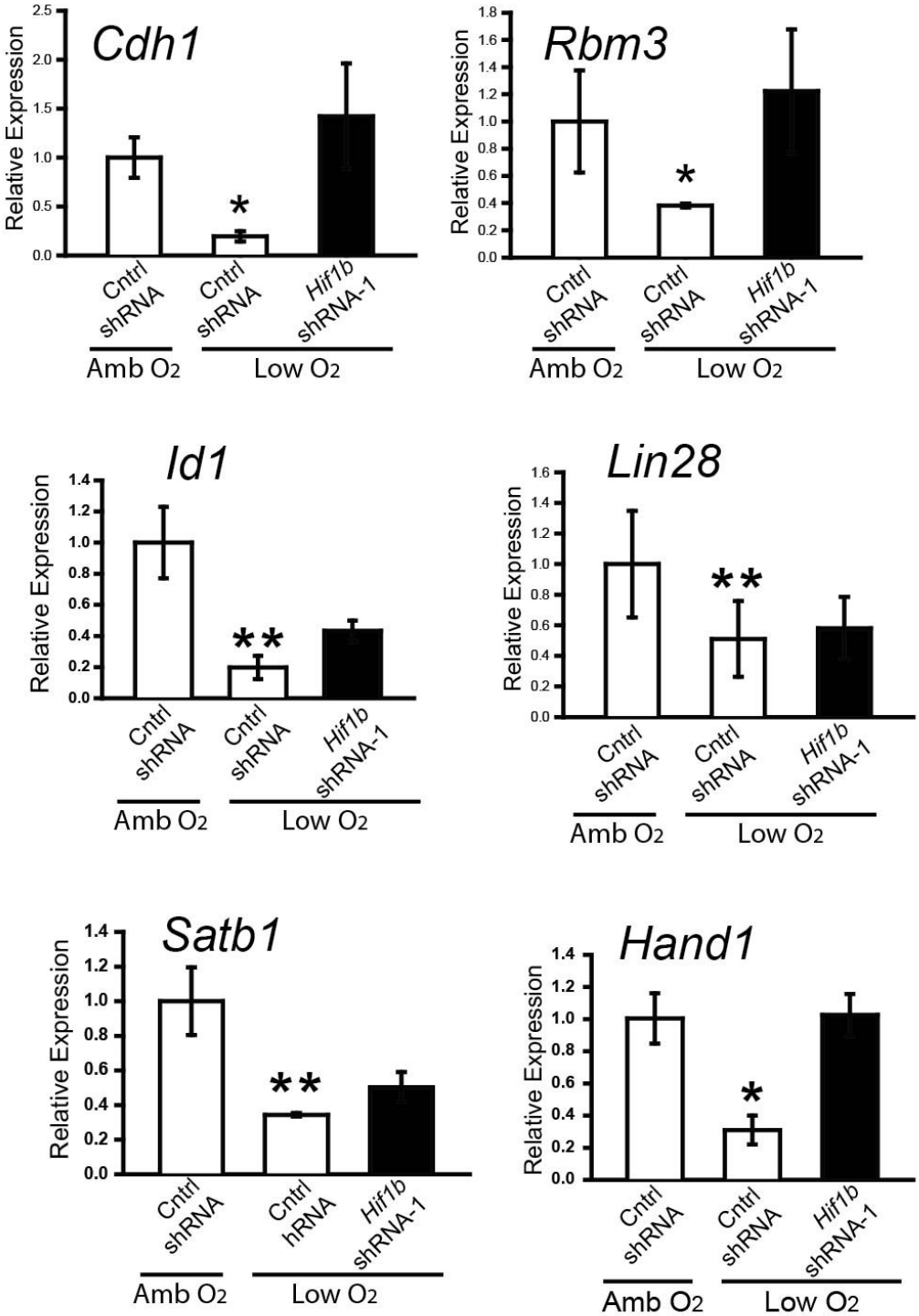
Cdh1
Relative Expression
2.5
2.0
1.5
1.0
0.5
0.0
*
Cntrl shRNA
Cntrl shRNA
Hif1b shRNA-1
Amb O2
Low O2
Rbm3
Relative Expression
1.8
1.6
1.4
1.2
1.0
0.8
0.6
0.4
0.2
0.0
*
Cntrl shRNA
Cntrl shRNA
Hif1b shRNA-1
Amb O2
Low O2
Id1
Relative Expression
1.4
1.2
1.0
0.8
0.6
0.4
0.2
0.0
**
Cntrl shRNA
Cntrl shRNA
Hif1b shRNA-1
Amb O2
Low O2
Lin28
Relative Expression
1.6
1.4
1.2
1.0
0.8
0.6
0.4
0.2
0.0
**
Cntrl shRNA
Cntrl shRNA
Hif1b shRNA-1
Amb O2
Low O2
Satb1
Relative Expression
1.4
1.2
1.0
0.8
0.6
0.4
0.2
0.0
**
Cntrl shRNA
Cntrl hRNA
Hif1b shRNA-1
Amb O2
Low O2
Hand1
Relative Expression
1.4
1.2
1.0
0.8
0.6
0.4
0.2
0.0
*
Cntrl shRNA
Cntrl shRNA
Hif1b shRNA-1
Amb O2
Low O2

uniform. *Cdh1*, *Hand1* and *Rbm3* transcript decreases in response to hypoxia were dependent upon HIF signaling but other transcripts like *Id1*, *Lin28*, and *Satb1* which downregulated in response to low oxygen were not significantly affected by HIF1B knockdown (**Fig. 3.3 B**). Similar patterns of HIF-dependence of hypoxia upregulated versus downregulated genes have been described (Semenza, 2010). The results demonstrate that HIF controls oxygen tension-sensitive genes potentially involved in regulating development of the invasive trophoblast cell lineage.

Role of KDM3A in TS cell adaptations to low oxygen

Among the candidate mediators of HIF action on trophoblast development identified by transcriptome profiling (see above), the discovery of KDM3A was compelling. Kdm3a is a known hypoxia responsive gene and is a direct target of HIF action (Beyer et al., 2008; Krieg et al., 2010; Pollard et al., 2008; Wellmann et al., 2008; Yang et al., 2009). Additionally, histone H3K9 demethylases, including KDM3A, are known regulators of differentiation of a range of cell lineages, such as embryonic stem cells, extraembryonic endoderm, neural crest, neuronal cells, mammary epithelium, and muscle (Kawazu et al., 2011; Ko et al., 2006; Lockman et al., 2007; Loh et al., 2007; Nottke et al., 2009; Pedersen and Helin, 2010; Qi et al., 2010; Strobl-Mazzulla et al., 2010; Verrier et al., 2011; Wen et al., 2009).

Hypoxia and trophoblast differentiation modulate KDM3A expression. Initially, we examined KDM3A mRNA and protein responses to hypoxia using *in vitro* and *in vivo* models. Exposure of rat TS cells to 0.5% oxygen was an effective stimulus to increase KDM3A transcript and protein levels (**Fig. 3.4 A,B &C**). KDM3A protein peaked at 16 h following initiation of the exposure to low oxygen. Two related histone H3K9 demethylases, *Kdm3b* and *Kdm3c*, were not

Fig. 3.4. KDM3A is upregulated on hypoxia exposure . TS cells maintained in stem cell conditions were exposed to low oxygen (0.5%) for 24 h. **A**) qRT-PCR analyses for *Kdm3a* in TS cells exposed to ambient or low oxygen. qRT-PCR measurements (SYBR Green) were performed using the ΔΔCT method). 18S rRNA served as an internal control. Asterisks indicate significant differences among groups ($P<0.05$ for each gene; Student's tTest). All experiments were performed in triplicate. **B)** Western blot analysis of KDM3A on rat TS cell exposed to ambient or low oxygen (collected every four hour interval upto 24 hours) conditions. **C)** Immunofluorescence staining for KDM3A in TS cells exposed to ambient or low oxygen. **D)** qRT-PCR analyses for *Kdm3b* and *Kdm3c* in TS cells exposed to ambient or low oxygen.

A

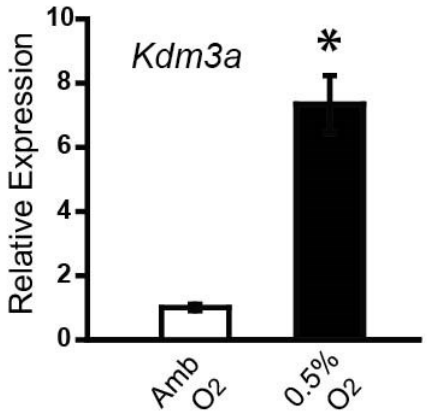
Kdm3a
*
Relative Expression
10
8
6
4
2
0
Amb O2
0.5% O2

B

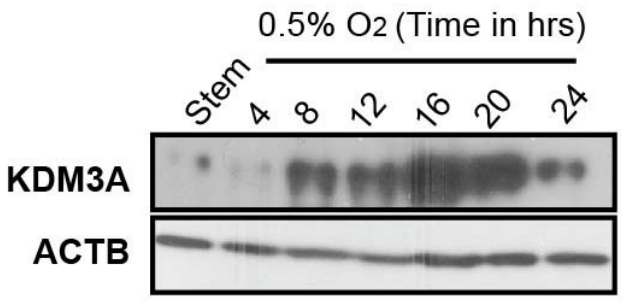
0.5% O2 (Time in hrs)
Stem
4
8
12
16
20
24
KDM3A
ACTB

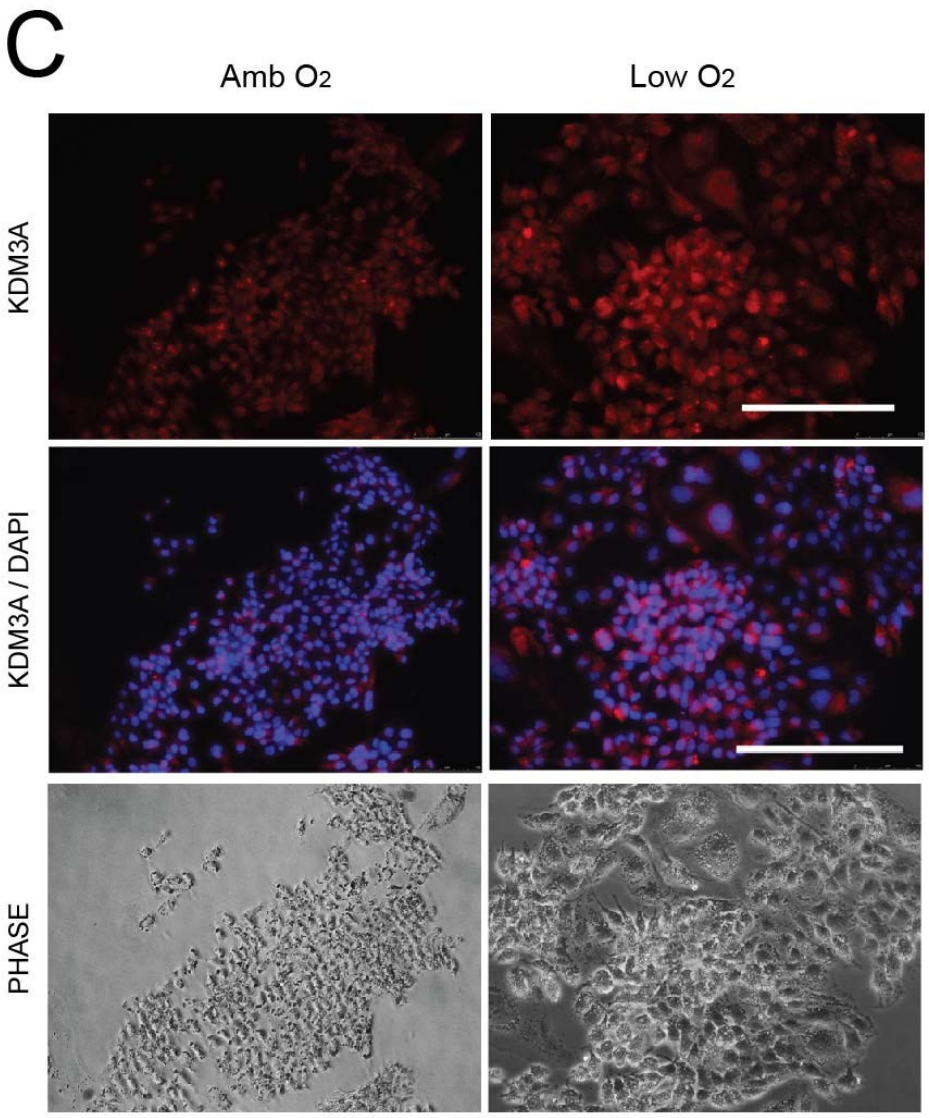
C
Amb O2
Low O2
KDM3A
KDM3A / DAPI
PHASE

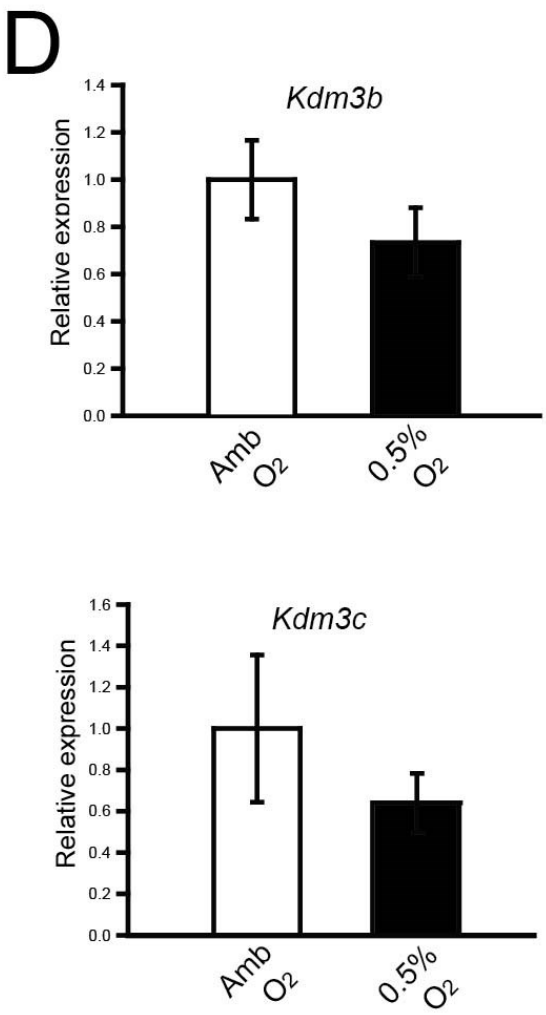
D
Kdm3b
Relative expression
1.4
1.2
1.0
0.8
0.6
0.4
0.2
0.0
Amb O2
0.5% O2
Kdm3c
Relative expression
1.6
1.4
1.2
1.0
0.8
0.6
0.4
0.2
0.0
Amb O2
0.5% O2

upregulated following rat TS cell exposure to low oxygen (**Fig. 3.4D**). KDM3A transcript and protein levels were also upregulated in the ectoplacental cone following exposure of E8.5 pregnant rats to hypoxic conditions for 24 h (**Fig. 3.5**). These *in vivo* conditions were also associated with increases in the expression of other hypoxia responsive genes, including *Mmp12* and *Ppp1r3c* (**Fig. 3.6**). Increased KDM3A expression also accompanies *in vitro* trophoblast differentiation induced by mitogen withdrawal and *in vivo* trophoblast development (**Fig. 3.7 A, B, C, D and E**). We utilized BeWo trophoblast cells as a human trophoblast cell model. BeWo trophoblast cells also respond to hypoxic conditions with increased KDM3A expression (Fig. **3.8. A&B**). KDM3A could be localized on human placentation sites (**Fig. 3.8. C**) prominently in the first trimester extra villous trophoblast (EVT) columns. A marked decrease in expression of KDM3A is observed at term placentation sites. The cytokeratin positive interstitial trophoblast cells continue to express KDM3A at term. Collectively, the results indicate that KDM3A expression is regulated by hypoxia and by developmental events leading to trophoblast cell specialization.

Identification of KDM3A responsive genes.

Since KDM3A exhibited a pronounced increase accompanying hypoxia exposure, we postulated that KDM3A might contribute to the regulation of a subset of the genes differentially regulated by exposure to low oxygen. We utilized shRNAs to disrupt KDM3A expression (**Fig. 3.9**). Knockdown of KDM3A interfered with TS cell gene expression responses to low oxygen (**Fig. 3.10**). The hypoxia responsiveness of *Mmp12*, *Ppp1r3c, Il33*, Cd200, Plod2 and LOC580835 like *Cullin 7*gene expression was attenuated by knockdown of KDM3A, whereas other hypoxia-responsive genes like *Bhlhe40*, *Plau*, *Dpp3*, *Ankrd37*, *Cdh1* and *Rbm3* were

Fig. 3.5. KDM3A is upregulated on hypoxia exposure *in vivo* . A) Rats were exposed to 8.5% oxygen for 24 h beginning on d8.5 and sacrificed on gestation d9.5. Gestation d9.5 ectoplacental cone tissues were dissected, RNA extracted, and *Kdm3a* was measured by qRT-PCR. qRT-PCR measurements (SYBR Green) were performed using the ΔΔCT method). 18S rRNA served as an internal control. Asterisks indicate significant differences among groups (n=5; $P<0.05$; Mann-Whitney Rank Sum Test). **B)** Western blot analysis of KDM3A on rat TS cell exposed to ambient or low oxygen (collected every four hour interval upto 24 hours) conditions. **C)** Rats were exposed to 8.5% oxygen or kept at ambient housing conditions for 24 h beginning on d8.5. All animals were sacrificed on gestation d9.5. Representative sections through ectoplacental cones immunostained for KDM3A counterstained with DAPI. Scale bars=0.125 mm.

A

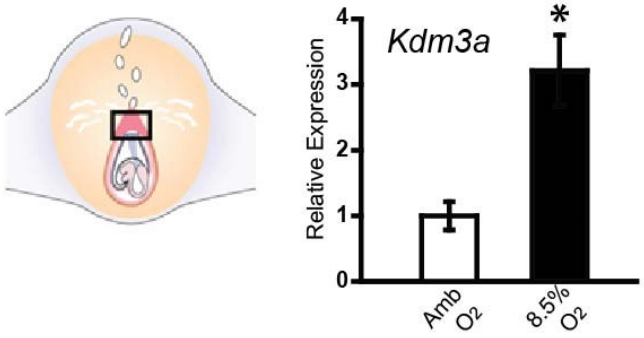
Kdm3a
Relative Expression
4
3
2
1
0
*
Amb O2
8.5% O2

B

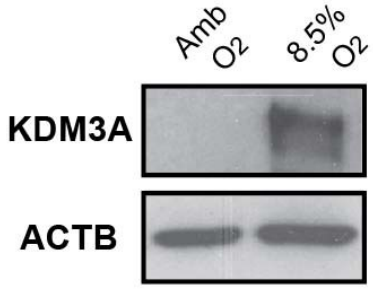
Amb O2
8.5% O2
KDM3A
ACTB

C

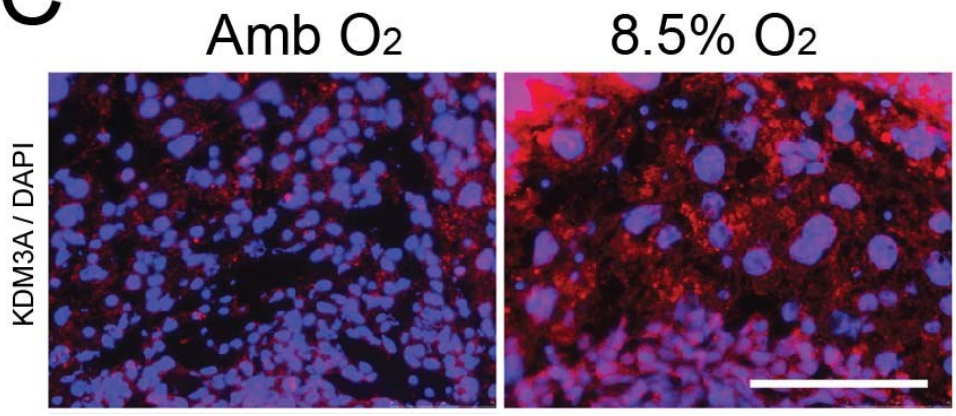
Amb O2
8.5% O2
KDM3A / DAPI

Fig. 3.6. Hypoxia exposure upregulates *Mmp12, Ppp1r3c in vivo*. Rats were exposed to 8.5% oxygen for 24 h beginning on d8.5 and sacrificed on gestation d9.5. Gestation d9.5 ectoplacental cone tissues were dissected, RNA extracted, and hypoxia responsive genes *Mmp12* and *Ppp1r3c* were measured by qRT-PCR. qRT-PCR measurements (SYBR Green) were performed using the ΔΔCT method). 18S rRNA served as an internal control. Asterisks indicate significant differences among groups (n=5; $P<0.05$; Mann-Whitney Rank Sum Test).

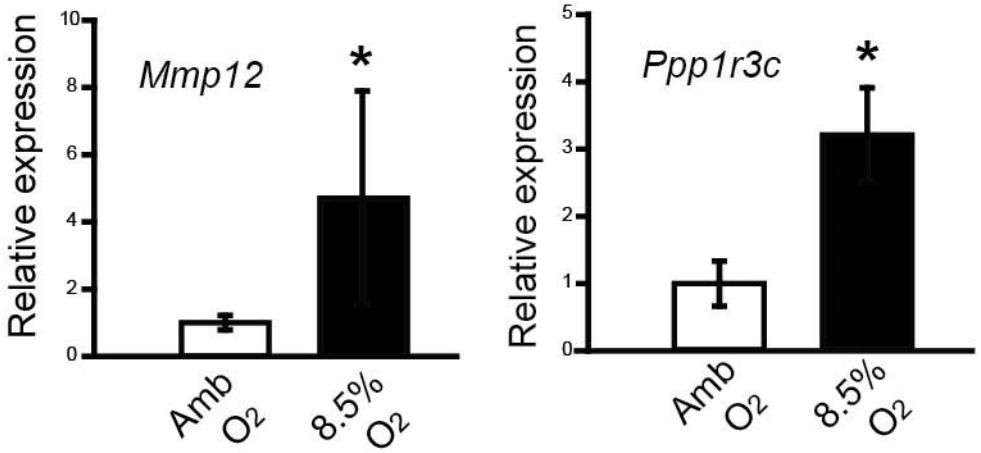
Relative expression
10
8
6
4
2
0
Mmp12
*
Amb O2
8.5% O2
Relative expression
5
4
3
2
1
0
Ppp1r3c
*
Amb O2
8.5% O2

Fig. 3.7. Regulation of KDM3A expression during trophoblast differentiation. A) *In vitro* **Kdm3a** expression in rat TS cells during the course of differentiation induced by mitogen withdrawal. qRT-PCR measurements (SYBR Green) were performed using the ΔΔCT method). 18S rRNA served as an internal control. Asterisks indicate significant differences among groups (n=5; P<0.05; Student's t Test). **B)** Western blot analysis of *in vitro* KDM3A expression in rat TS cells during the course of differentiation induced by mitogen withdrawl. **C)** *In vivo* developmental expression of KDM3A in placenta from gestation d9.5 to d13.5. qRT-PCR – representative experiments performed in triplicate and evaluated by analysis of variance and Tukey's Test (*P<0.05, comparisons with d9.5). **D)** Western blot analysis of KDM3A during placental development. **E)** Immunolocalisation of KDM3A on placentation sites from gestation d9.5 to d13.5. Scale bar: 0.125 mm.

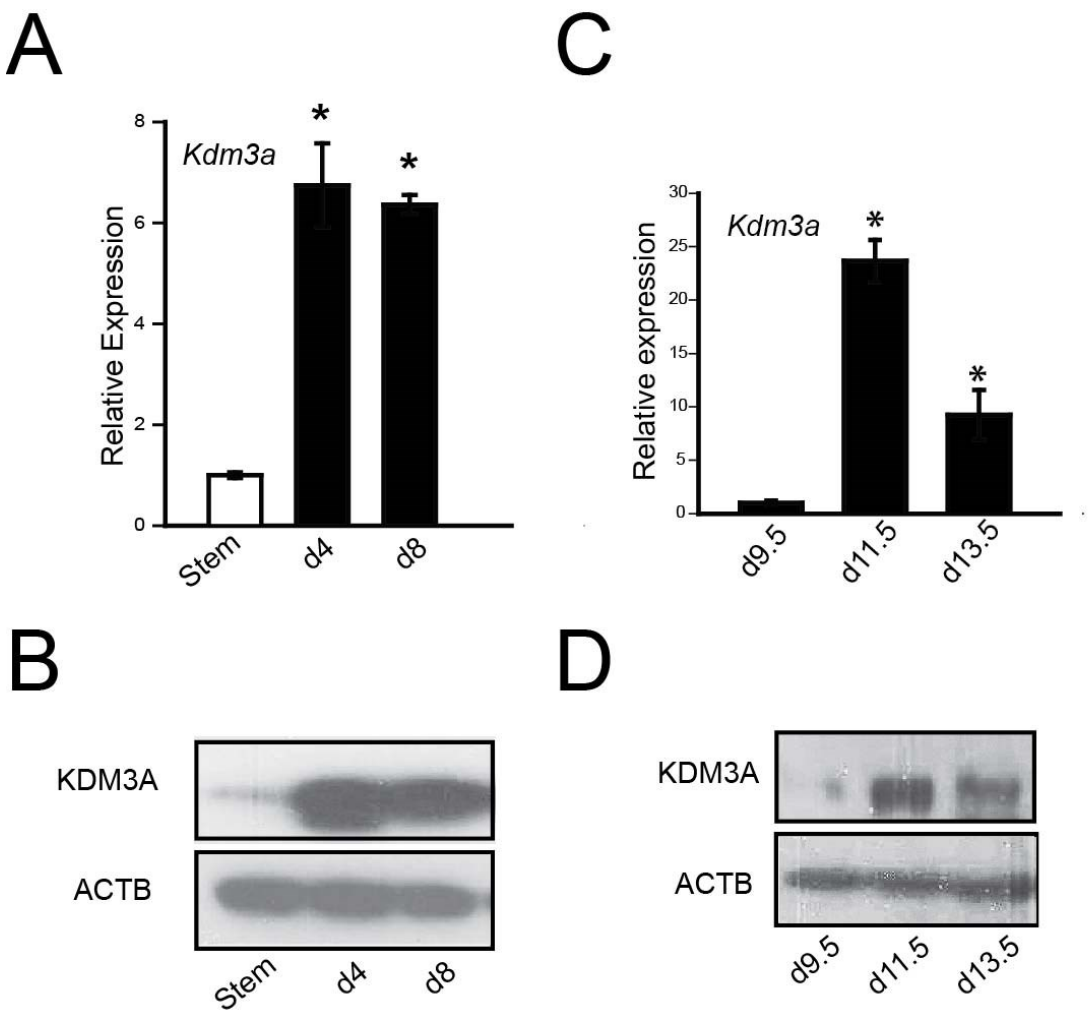
A
Kdm3a
Relative Expression
8
6
4
2
0
*
*
Stem
d4
d8
C
Kdm3a
Relative expression
30
25
20
15
10
5
0
*
*
d9.5
d11.5
d13.5
B
KDM3A
ACTB
Stem
d4
d8
D
KDM3A
ACTB
d9.5
d11.5
d13.5

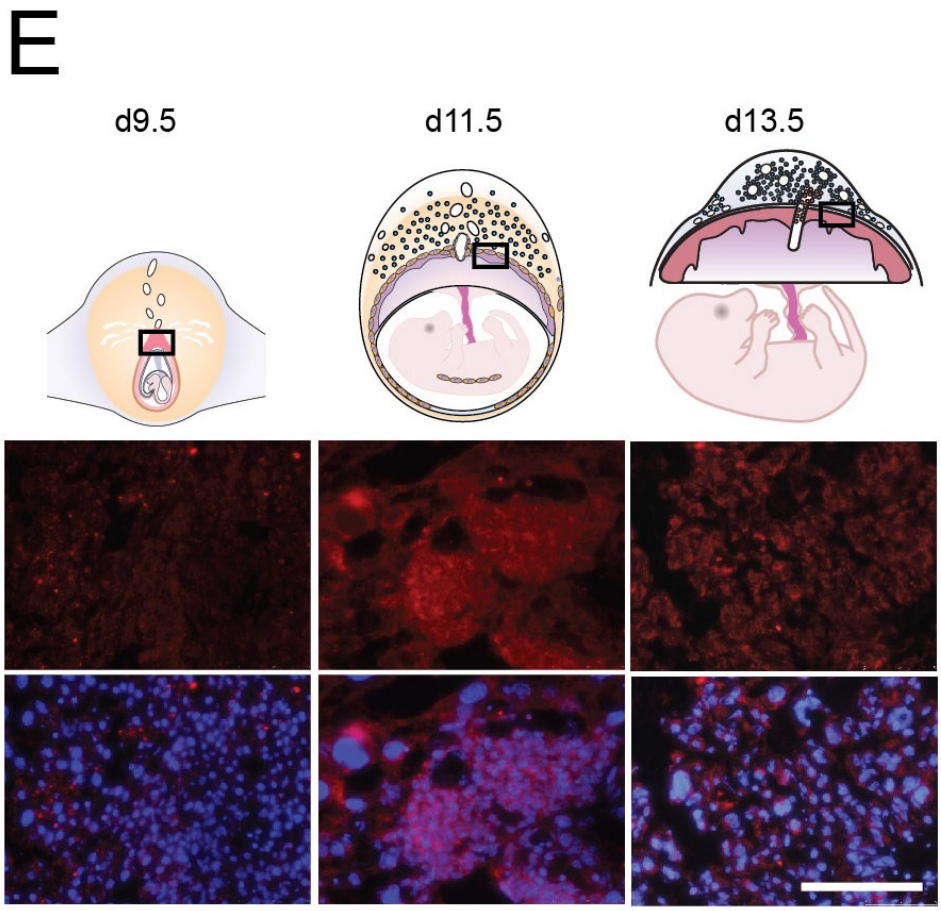
E
d9.5
d11.5
d13.5

unaffected by KDM3A manipulation (**Fig. 3.10**). A complementary experiment was performed to examine the regulatory role of KDM3A on gene expression independent of hypoxia. Ectopic expression of KDM3A significantly upregulated *Mmp12* and *Ppp1r3c* gene expression in TS cells grown in ambient conditions; however, this treatment was ineffective in altering *Il33* transcript levels (**Fig 3.11**). Thus, KDM3A is an effective intermediary controlling the expression of a subset of TS cell genes regulated by hypoxia/HIF signaling. The dependence on KDM3A is not the same for all KDM3A responsive genes.

KDM3A regulates hypoxia-activated trophoblast cell invasion.

Hypoxia is an effective activator of invasive trophoblast lineage development (Chakraborty et al., 2011; Rosario et al., 2008). We next explored whether KDM3A was involved in development of the hypoxia-activated invasive trophoblast lineage. Two model systems were evaluated: i) TS cell invasion through Matrigel chambers; ii) blastocyst outgrowths (Ain et al., 2003b; Armant et al., 1986; Chakraborty et al., 2011; Peters et al., 1999). Exposure to low oxygen stimulates TS cell acquisition of an invasive phenotype and penetration through the extracellular matrix and the outward migration and spreading of trophoblast cells from attached blastocysts. KDM3A knockdown significantly decreased hypoxia-stimulated trophoblast invasion through Matrigel chambers and blastocyst outgrowth (**Fig. 3.12 A &B**). Ectopic expression of KDM3A in TS cells grown under ambient conditions significantly increased their movement through Matrigel chambers (**Fig. 3.12 C**). Collectively, these results indicate that KDM3A is a key regulator of TS cell adaptations to hypoxia, including gene expression and their acquisition of an invasive phenotype.

Fig. 3.8. KDM3A expression in human placentation. **A)** Hypoxia stimulates KDM3A expression in human trophoblast. BeWo trophoblast cells were incubated for 24 h in ambient O_2 (21%) or low O_2 (0.5%). qRT-PCR for KDM3A, representative experiment performed in triplicate and evaluated by Student's t test. **B)** Western blot analysis for KDM3A expression. **C)** Immunolocalization of KDM3A on human placentation sites. Scale bar: 100μm.

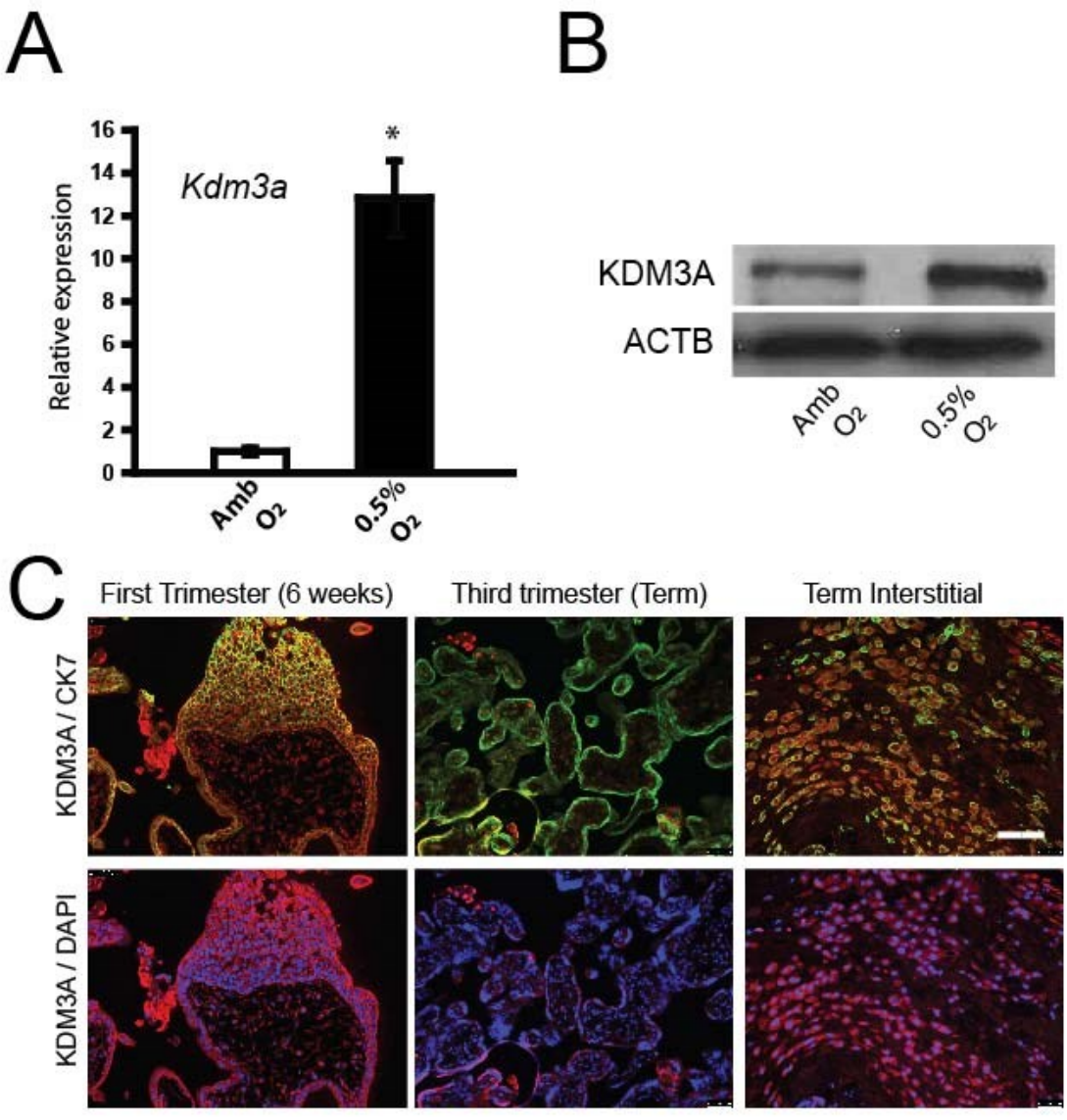
A
B
C
Kdm3a
Relative expression
16
14
12
10
8
6
4
2
0
*
Amb O2
0.5% O2
KDM3A
ACTB
Amb O2
0.5% O2
First Trimester (6 weeks)
Third trimester (Term)
Term Interstitial
KDM3A / CK7
KDM3A / DAPI

Fig. 3.9. Knockdown of KDM3A in rat TS cells. TS cells maintained in stem cell conditions were exposed to low oxygen (0.5%) for 24 h in the presence of Control (Cntrl) shRNA or *Kdm3a* shRNA-1& 2. **A**) qRT-PCR analysis for *Kdm3a* in TS cells exposed to ambient or low oxygen and control shRNA or *Kdm3a* shRNAs. qRT-PCR measurements (SYBR Green) were performed using the ΔΔCTmethod). 18S rRNA served as an internal control. All experiments were performed in triplicate. Asterisks indicate significant differences among groups ($P<0.05$; analysis of variance with Tukey's Test for comparisons). **B**) Western blot analysis for TS cells exposed to ambient or low oxygen and control shRNA or *Kdm3a* shRNAs.

A

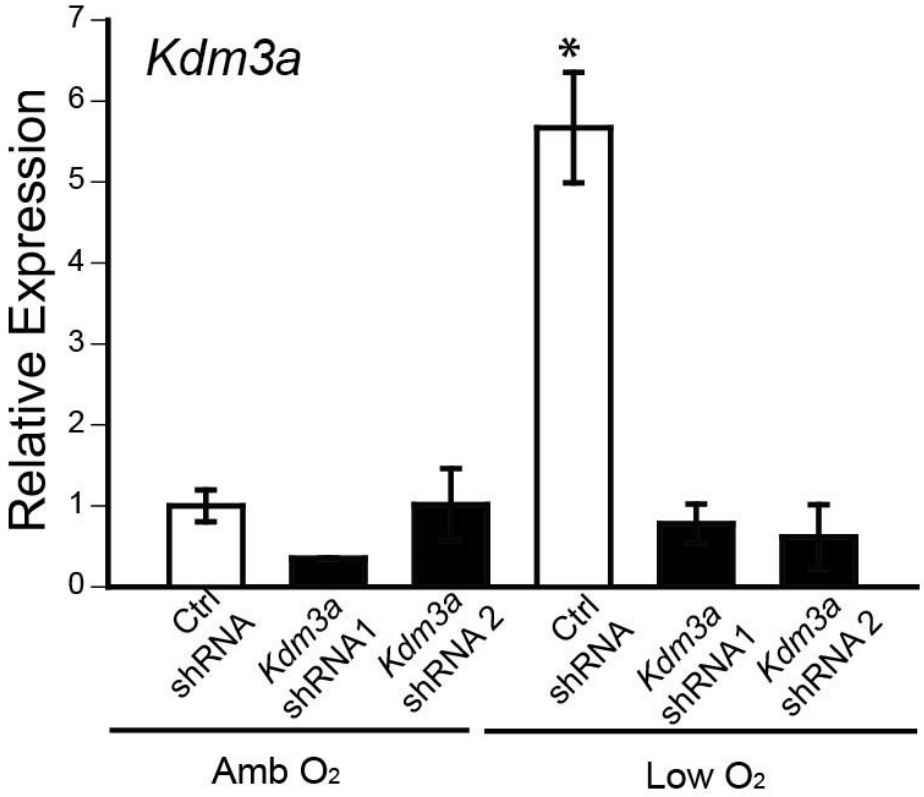
Kdm3a
Relative Expression
7
6
5
4
3
2
1
0
*
Ctrl shRNA
Kdm3a shRNA1
Kdm3a shRNA 2
Ctrl shRNA
Kdm3a shRNA1
Kdm3a shRNA 2
Amb O2
Low O2

B

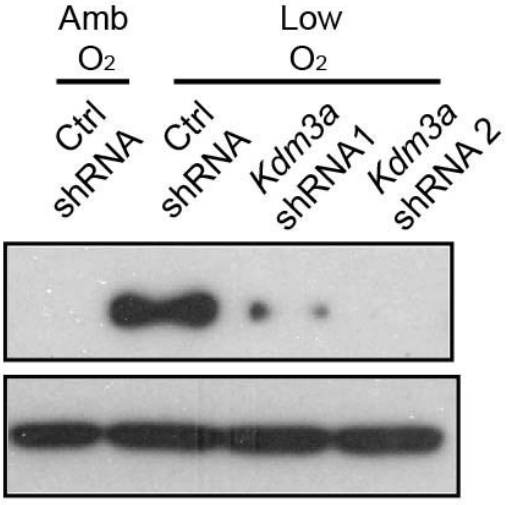
Amb O2
Low O2
Ctrl shRNA
Ctrl shRNA
Kdm3a shRNA1
Kdm3a shRNA 2

Fig. 3.10. Expression of hypoxia dependent KDM3A responsive genes. . A) qRT-PCR analyses for *Kdm3a* responsive upregulated genes . TS cells exposed to ambient or low oxygen and control shRNA or *Kdm3a* shRNA-1. All experiments were performed in triplicate. Asterisks indicate significant differences among groups (P<0.05 analysis of variance with Student-Newman-Keuls method for comparisons). **B)** qRT-PCR analyses for *Kdm3a* responsive downregulated genes . TS cells exposed to ambient or low oxygen and control shRNA or *Kdm3a* shRNA-1. All experiments were performed in triplicate. Asterisks indicate significant differences among groups (P<0.05 analysis of variance with Student-Newman-Keuls method for comparisons; # indicates P<,0.05 between control shRNA group in ambient conditions and control shRNA group in hypoxic conditions).

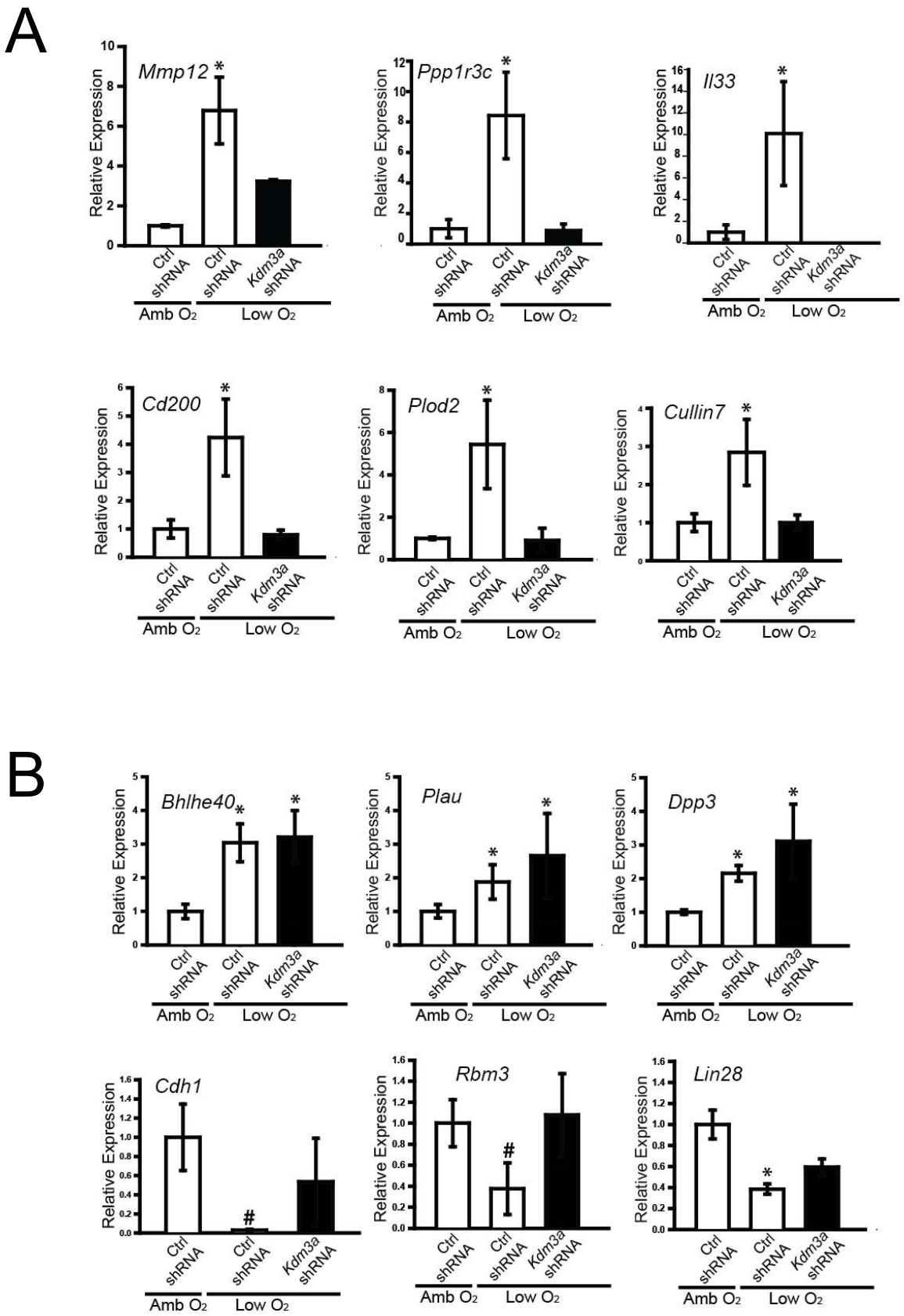
A
Mmp12
Ppp1r3c
Il33
Cd200
Plod2
Cullin7
Relative Expression
Ctrl shRNA
Kdm3a shRNA
Amb O2
Low O2
B
Bhlhe40
Plau
Dpp3
Cdh1
Rbm3
Lin28

Fig. 3.11.Ectopic expression of KDM3A in rat TS cells. **A)** TS cells were transfected with pcDNA3 or pcDNA3 expressing flag tagged *Kdm3a*. qRT-PCR analysis for *Kdm3a* in TS cells transfected with pcCDNA3 vector only or pcDNA3-*Kdm3a*. qRT-PCR measurements (SYBR Green) were performed using the ΔΔCTmethod. 18S rRNA served as an internal control. All experiments were performed in triplicate. Asterisks indicate significant differences among groups ($P<0.05$; Student's t Test for comparisons). **B)** Westren blot analysis for flag and KDM3A expression. **C)** qRT-PCR analysis for Ppp1r3c and Mmp12 in TS cells transfected with pcCDNA3 vector only or pcDNA3-Kdm3a. qRT-PCR measurements (SYBR Green) were performed using the ΔΔCTmethod. 18S rRNA served as an internal control. All experiments were performed in triplicate. Asterisks indicate significant differences among groups ($P<0.05$; Student's t Test for comparisons).

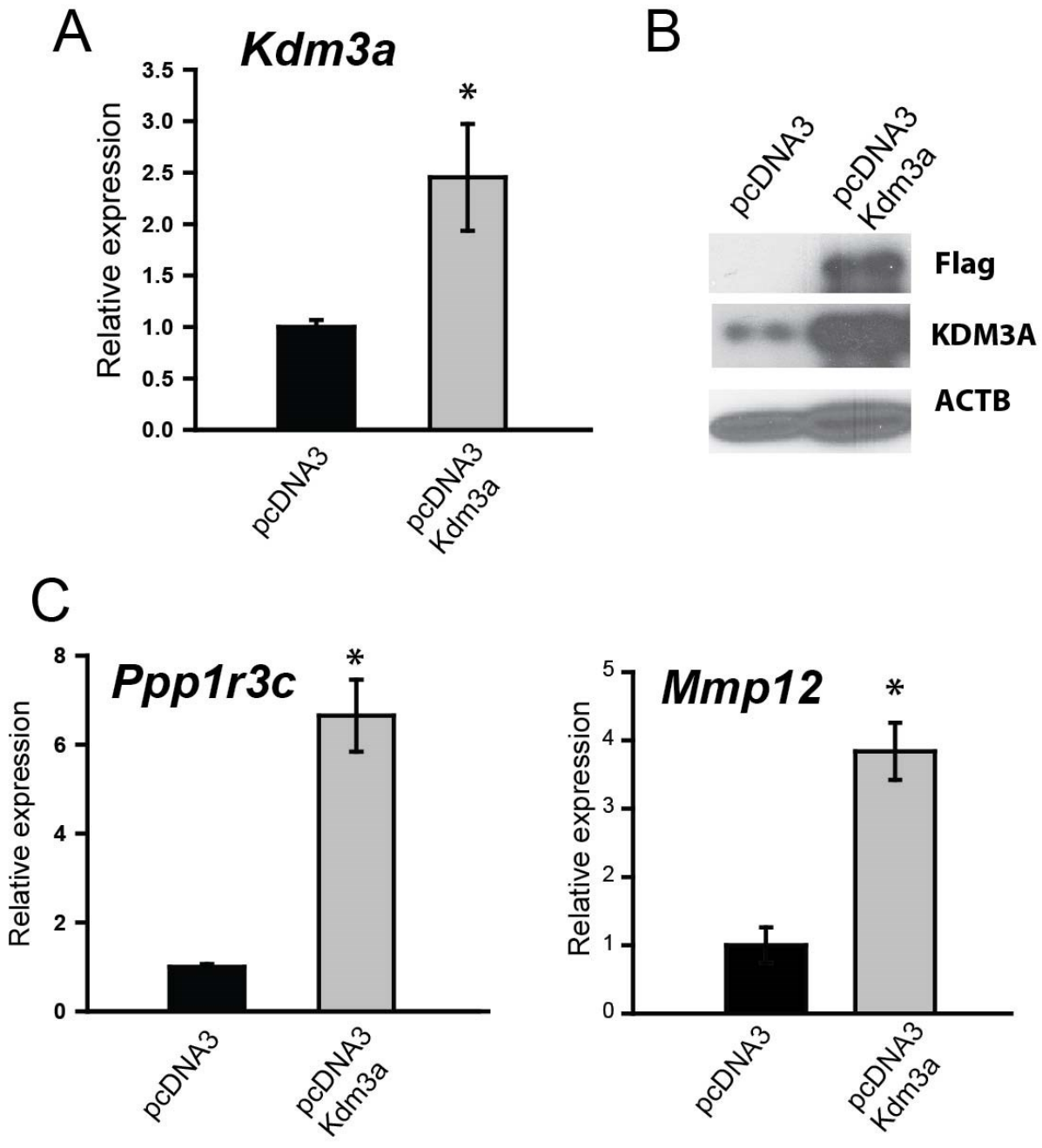
A
Kdm3a
Relative expression
3.5
3.0
2.5
2.0
1.5
1.0
0.5
0.0
*
pcDNA3
pcDNA3 Kdm3a
B
pcDNA3
pcDNA3 Kdm3a
Flag
KDM3A
ACTB
C
Ppp1r3c
Relative expression
8
6
4
2
0
*
pcDNA3
pcDNA3 Kdm3a
Mmp12
Relative expression
5
4
3
2
1
0
*
pcDNA3
pcDNA3 Kdm3a

Hypoxia-dependent histone modifications at the *Mmp12* locus

Several genes upregulated in low oxygen exposed TS cells are sensitive to KDM3A manipulation, including, *Mmp12*. MMP12 is a matrix metalloelastase that has been implicated in trophoblast-directed uterine spiral artery remodeling (Harris, 2010). KDM3A is a lysine demethylase with specificity for histone H3K9me1 and H3K9me2 (Yamane et al., 2006). Consequently, we next examined histone H3K9 methylation status within the proximal *Mmp12* promoter region and its susceptibility to regulation by hypoxia using a ChIP assay. Under low oxygen tensions, there was significant loss of enrichment of H3K9 mono and dimethyl groups at the proximal promoter region of *Mmp12* (**Fig. 3.13**). Such a change in the methylation landscape of histone H3K9 at the *Mmp12* locus is consistent with hypoxia-induced KDM3A expression and its known lysine demethylase activity.

Hypoxia-dependent global TS cell histone H3K9 methylation modifications

In other cell types, it has been shown that hypoxia exposure can influence H3K9 methylation status (Chen et al., 2006; Johnson et al., 2008). Such observations prompted us to evaluate the effects of hypoxia on global H3K9 methylation in TS cells. Western blots for H3K9 methylation modifications were performed using lysates harvested from TS cells exposed to ambient or hypoxic (0.5% oxygen for 24 h) conditions. Low oxygen exposure was associated with prominent decreases in global H3K9me1 and H3K9me2, whereas modest changes were observed for H3K9me3 (**Fig. 3.14 A**). Immunocytochemistry in TS cell populations was consistent with a hypoxia-driven global down regulation of H3K9me1 (**Fig 3.14 C**). Disruption of KDM3A partly obviated the global effects of hypoxia on H3K9me1 (**Fig. 3.14 B**).

Fig 3.12. KDM3A regulates hypoxia activated trophoblast invasion. A) Assessment of the effects of oxygen tension and KDM3A expression on TS cell invasion. Cells penetrating Matrigel-coated filters were counted after staining with Diff Quick. Representative images of TS cells from the following conditions are shown: control shRNA and exposure to ambient oxygen, control shRNA and exposure to low oxygen, and *Kdm3a*shRNA-1 &2 and exposure to low oxygen. The bar graph shows quantification of TS cell invasion. All experiments were performed in triplicate. Asterisks indicate significant differences among groups ($P<0.05$; analysis of variance with Tukey's Test for comparisons). **B)** Effects of oxygen tension and KDM3A expression on blastocyst outgrowth assay . The area of the outgrowth was measured using Image J software. Representative images of blastocyst outgrowths from the following conditions: control shRNA and exposure to ambient oxygen, control shRNA and exposure to low oxygen, and *Kdm3a*shRNA-1 &2 and exposure to low oxygen. The bar graph shows quantification of outgrowth area in mm^2 ($P<0.05$; analysis of variance with Tukey's Test for comparisons).. **C)** Assessment of the effects of ectopic KDM3A expression on TS cell invasion. Cells penetrating Matrigel-coated filters were counted after staining with Diff Quick. Representative images of TS cells from the following conditions are shown: pcDNA3 and pcDNA3 expressing flag tagged *Kdma3a* in ambient oxygen tensions. The bar graph shows quantification of TS cell invasion. Asterisks indicate significant differences among groups ($P<0.05$;Student's t Test).

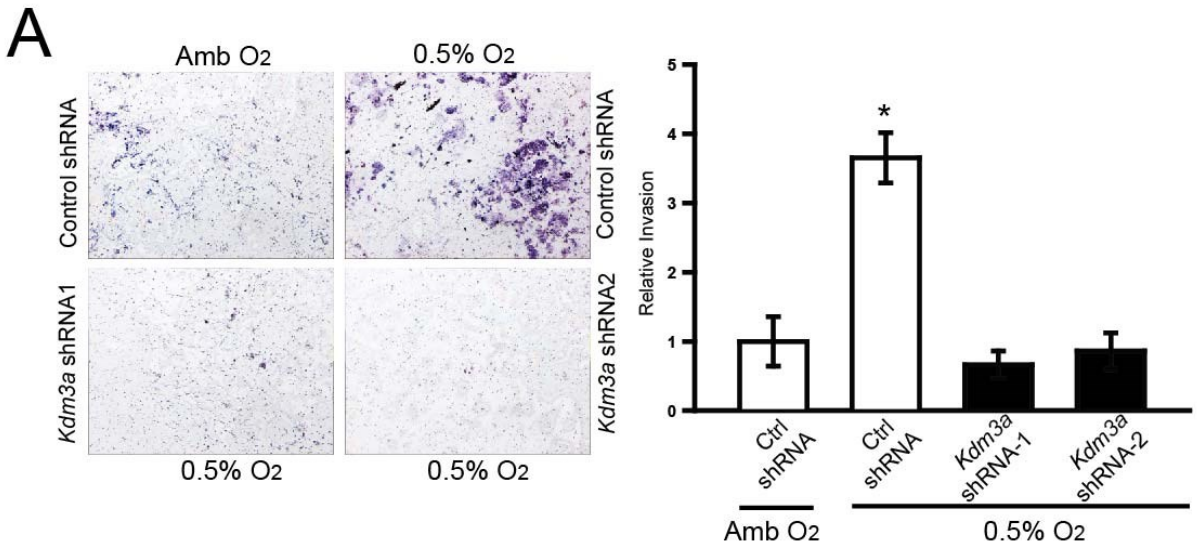
A
Amb O2
0.5% O2
Control shRNA
Kdm3a shRNA1
Control shRNA
Kdm3a shRNA2
0.5% O2
0.5% O2
Relative Invasion
*
Ctrl shRNA
Ctrl shRNA
Kdm3a shRNA-1
Kdm3a shRNA-2
Amb O2
0.5% O2

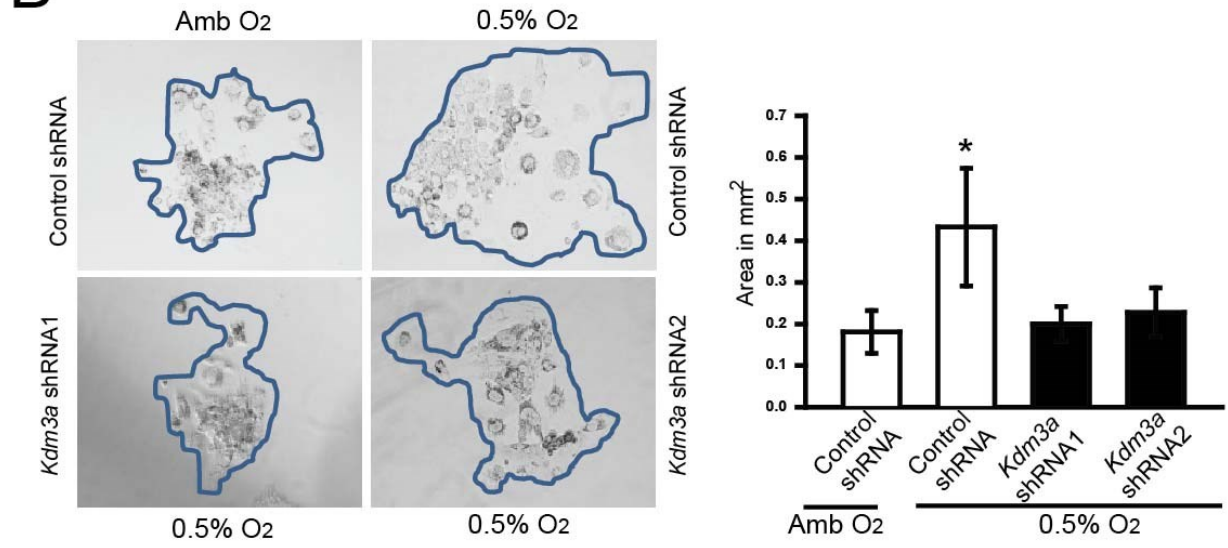
B
Amb O2
0.5% O2
Control shRNA
Kdm3a shRNA1
Control shRNA
Kdm3a shRNA2
0.5% O2
0.5% O2
Area in mm2
*
Control shRNA
Control shRNA
Kdm3a shRNA1
Kdm3a shRNA2
Amb O2
0.5% O2

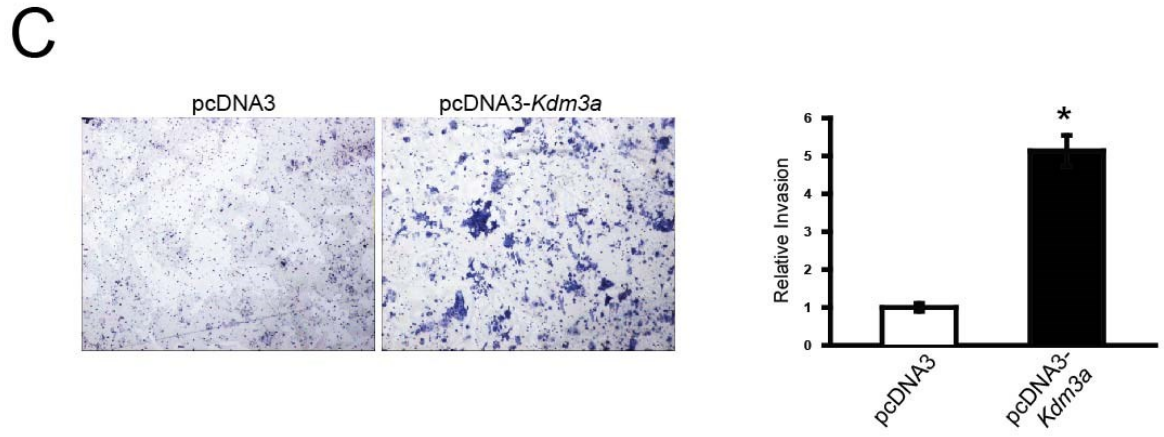
C
pcDNA3
pcDNA3-Kdm3a
Relative Invasion
*
pcDNA3
pcDNA3-Kdm3a

Complementary experiments were performed on E9.5 placentation sites of control and hypoxia exposed (8.5% O_2 for 24 h) rats. The *in vivo* findings are consistent with hypoxia-driven global changes in H3K9 methylation, especially H3K9me1 (**Fig. 3.14 D& E**).

In summary, our findings indicate that hypoxia has a global impact on chromatin reorganization in TS cells leading to the development of the invasive trophoblast cell lineage and places KDM3A within regulatory pathways controlling these events.

DISCUSSION

During development, the hemochorial placenta is constructed in response to stimuli present in the maternal environment and optimized to facilitate nutrient delivery to the fetus. Plasticity in placental organization is achieved via differential regulation of TS cell proliferation and differentiation. Among the myriad of potential signals emanating from the maternal environment, oxygen delivery plays a significant role. Eukaryotic ells have evolved mechanisms for adapting to exposure to low oxygen (Semenza, 2010). TS cells utilize these conserved hypoxia-signaling pathways to control placentation (Adelman et al., 2000; Cowden Dahl et al., 2005; Maltepe et al., 2005; Xie et al., 2011; Zhou et al., 2011). The proximal response of TS cells to hypoxia is differentiation into invasive trophoblast capable of targeting uterine spiral arteries with the goal of expanding nutrient flow to the placenta and fetus (Chakraborty et al., 2011; Rosario et al., 2008).

TS cell adaptations to hypoxia are hierarchically regulated. Low oxygen exposure elicits a broad spectrum of changes in the TS cell transcriptome highlighted by activation of genes

Fig. 3.13. ChIP analysis at *Mmp12* locus.ChIP analysis of H3K9me1 and H3K9me2 enrichment at rat *Mmp12* proximal promoter region (-500 to +1 bp) on sites A and B (described in materials and methods section) in rat TS cells exposed to ambient O_2 or 0.5% O_2. IgG was included as a negative control. Values significantly different are indicated (*, $P<0.05$).

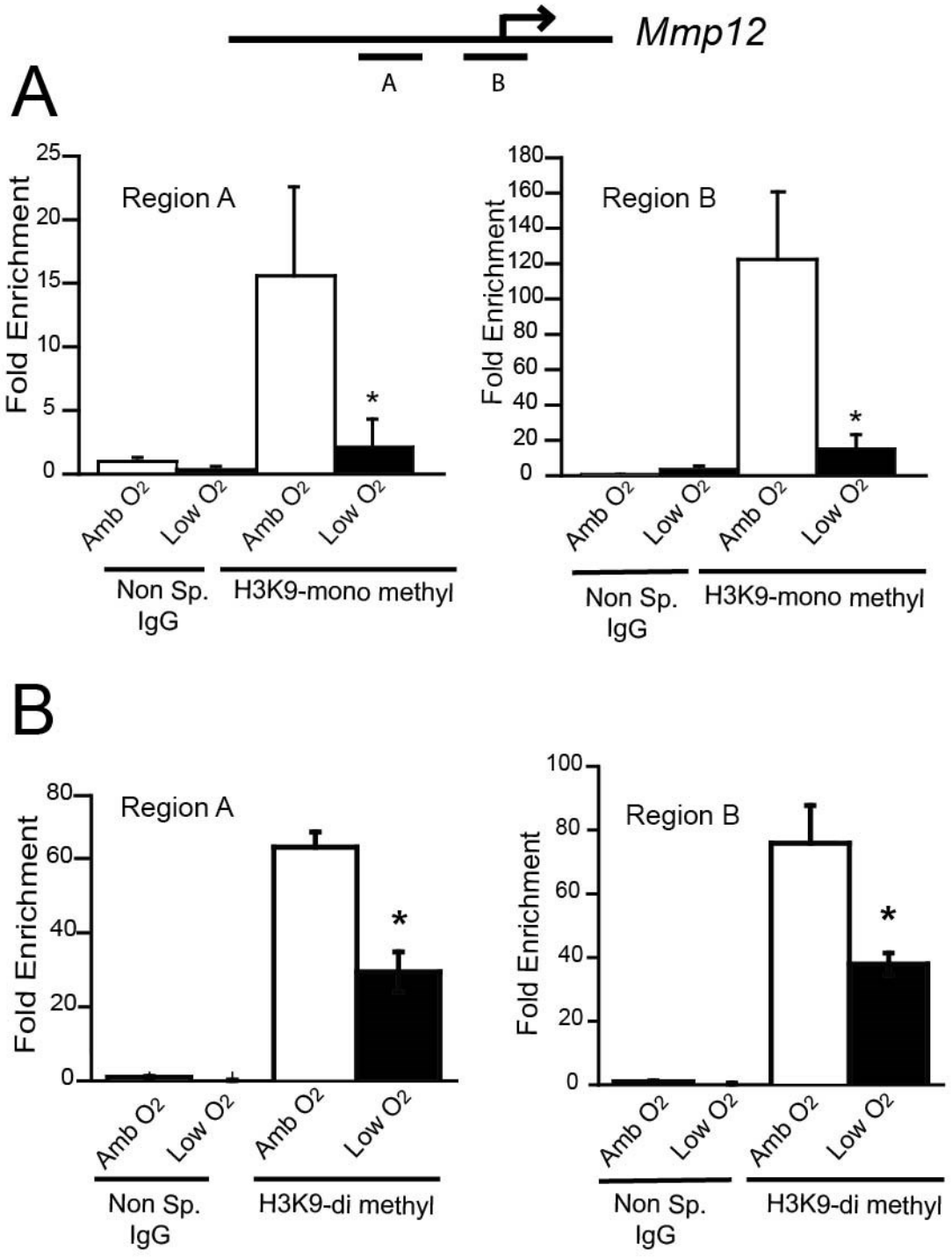
Mmp12
A
B
A
Region A
Fold Enrichment
25
20
15
10
5
0
*
Amb O2
Low O2
Amb O2
Low O2
Non Sp. IgG
H3K9-mono methyl
Region B
Fold Enrichment
180
160
140
120
100
80
60
40
20
0
*
Amb O2
Low O2
Amb O2
Low O2
Non Sp. IgG
H3K9-mono methyl
B
Region A
Fold Enrichment
80
60
40
20
0
*
Amb O2
Low O2
Amb O2
Low O2
Non Sp. IgG
H3K9-di methyl
Region B
Fold Enrichment
100
80
60
40
20
0
*
Amb O2
Low O2
Amb O2
Low O2
Non Sp. IgG
H3K9-di methyl

associated with cellular movement, invasion, and vascular remodeling. A subset of the hypoxia-induced changes in gene expression is dependent on HIF signaling, especially those genes activated by hypoxia. A subset of HIF-dependent genes is linked to the actions of KDM3A. Thus a path can be constructed from hypoxia to HIF activation to increases in KDM3A expression to alterations in the histone methylation status of genes promoting development of the invasive trophoblast lineage.

Hypoxia, HIF, and KDM3A have been implicated in regulating epithelial mesenchymal transition and cell invasion in disease states, including cancers (Guo et al., 2011; Krieg et al., 2010; Semenza, 2010; Yamada et al., 2012; Yamane et al., 2006; Yang et al., 2009). HIF binds to hypoxia response elements (HREs) at the *Kdm3a* locus and stimulates *Kdm3a* transcription (Krieg et al., 2010; Mimura et al., 2012). KDM3A targets histone H3K9me1 and H3K9me2 for demethylation and thus extending and amplifying HIF signaling (Krieg et al., 2010; Mimura et al., 2012). Histone H3K9me2 marks are associated with gene repression, and thus their removal is linked to gene activation (Li et al., 2007). Loss of the histone H3K9me2 and H3K9me1 modifications at the *Mmp12* locus correlate with increased *Mmp12* expression. MMP12 is a matrix metalloelastase expressed by invasive trophoblast and situated downstream of hypoxia, HIF, and KDM3A regulation, with actions on uterine spiral arteries facilitating nutrient delivery to extraembryonic and embryonic tissues (Harris, 2010).

KDM3A is specifically targeted to its sites of action within the genome. HIF1A can recruit KDM3A to some of its target genes, including the *Glut3* locus, resulting in H3K9me2 demethylation and transcriptional upregulation (Mimura et al., 2012). OCT1 is also linked to

Fig. 3.14. Effect of hypoxia signaling on global H3K9methylation status. A) Western blot analysis of rat TS cell exposed to ambient or 0.5% O_2 for H3K9me1, H3K9me2 and H3K9me3. **B)** Western blot analysis of TS cells under following conditions: Control shRNA and ambient O_2, Control shRNA and 0.5% O2, *Kdm3a* shRNA1 or *Kdm3a* shRNA2 and ambient O_2, and *Kdm3a* shRNA-1 or *Kdm3a* shRNA-2 and 0.5% O2 for H3K9me1, H3K9me2 and H3K9me3. C) Immunolocalisation of H3K9me1, H3K9me2 and H3K9me3 on cells exposed to ambient O_2 or 0.5%O_2. Cells are counterstained with pan cytokeratin. D) Rats were exposed to 8.5% oxygen for 24 h beginning on d8.5 and sacrificed on gestation d9.5. Gestation d9.5 ectoplacental cone tissues were dissected, protein lysates were prepared and used for western blot analyses of H3K9me1, H3K9me2 and H3K9me3. Total H3 and ACTB was used to detect equal protein loading. E) Immunolocalization of H3K9me1 and H3K9me2 on d9.5 placentation sites from animals housed in ambient O_2 tension or exposed to 8.5% O_2 for 24h.

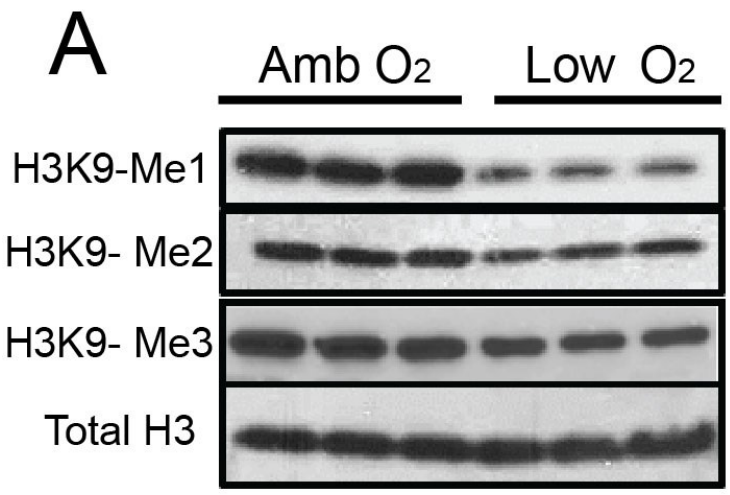
A
Amb O2
Low O2
H3K9-Me1
H3K9- Me2
H3K9- Me3
Total H3

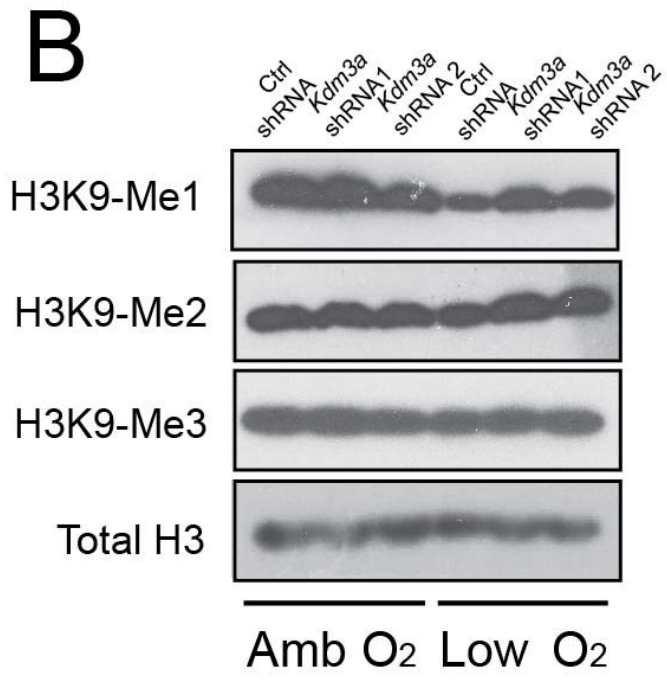
B
Ctrl shRNA
Kdm3a shRNA1
Kdm3a shRNA 2
Ctrl shRNA
Kdm3a shRNA1
Kdm3a shRNA 2
H3K9-Me1
H3K9-Me2
H3K9-Me3
Total H3
Amb O2
Low O2

C

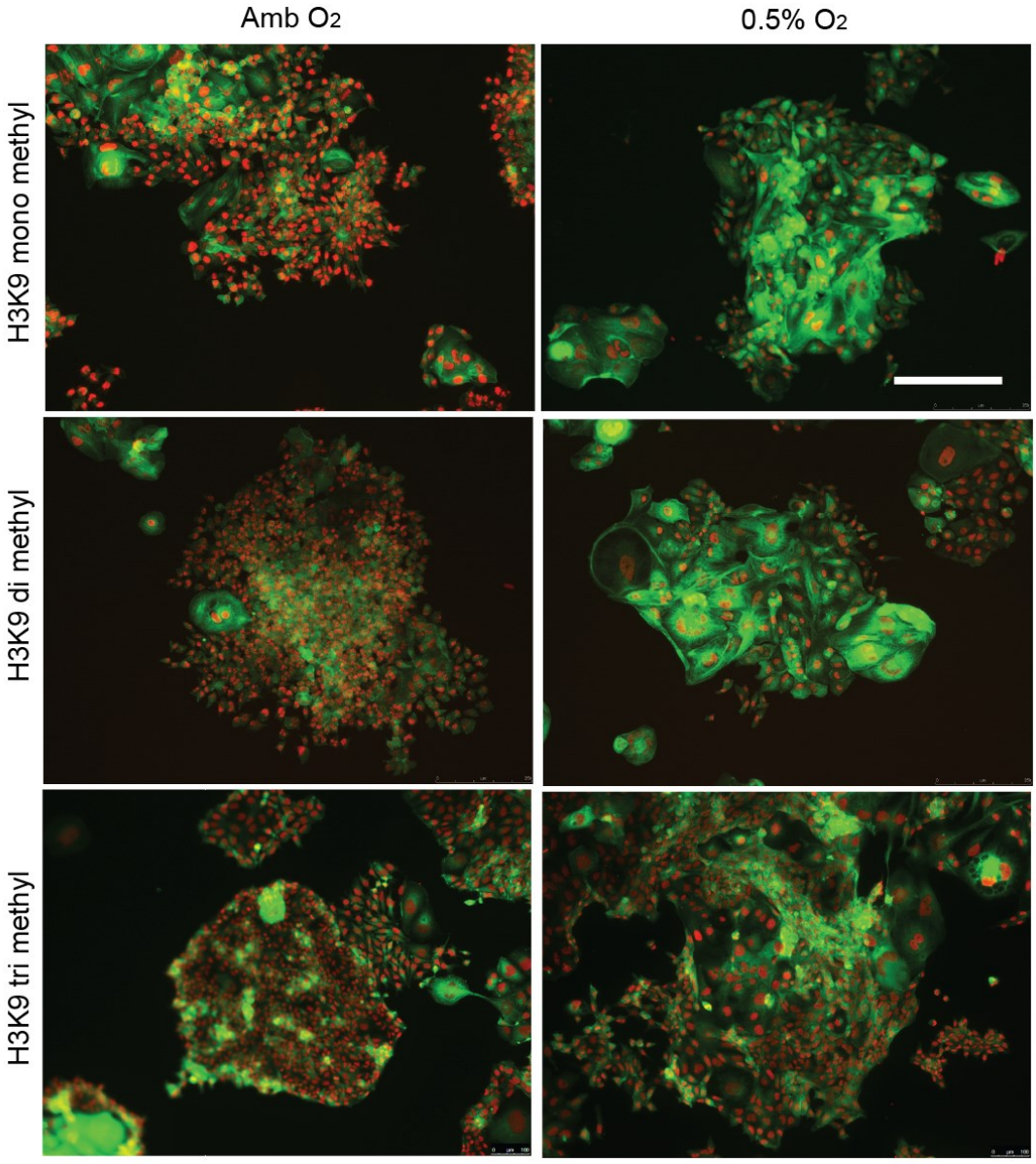

D

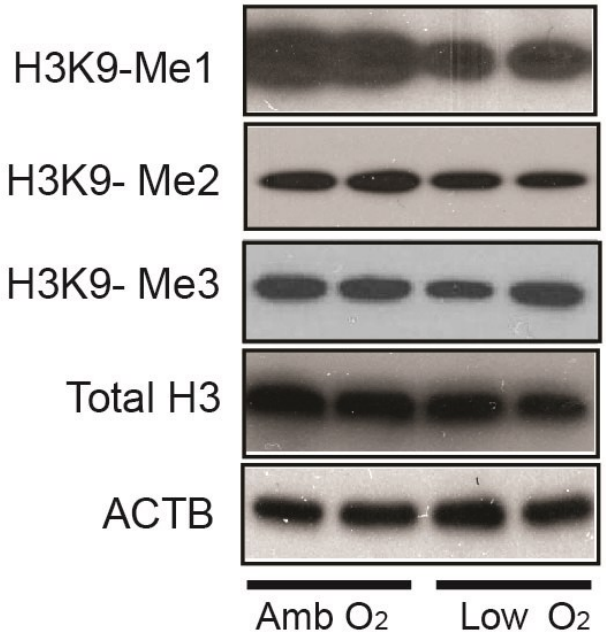

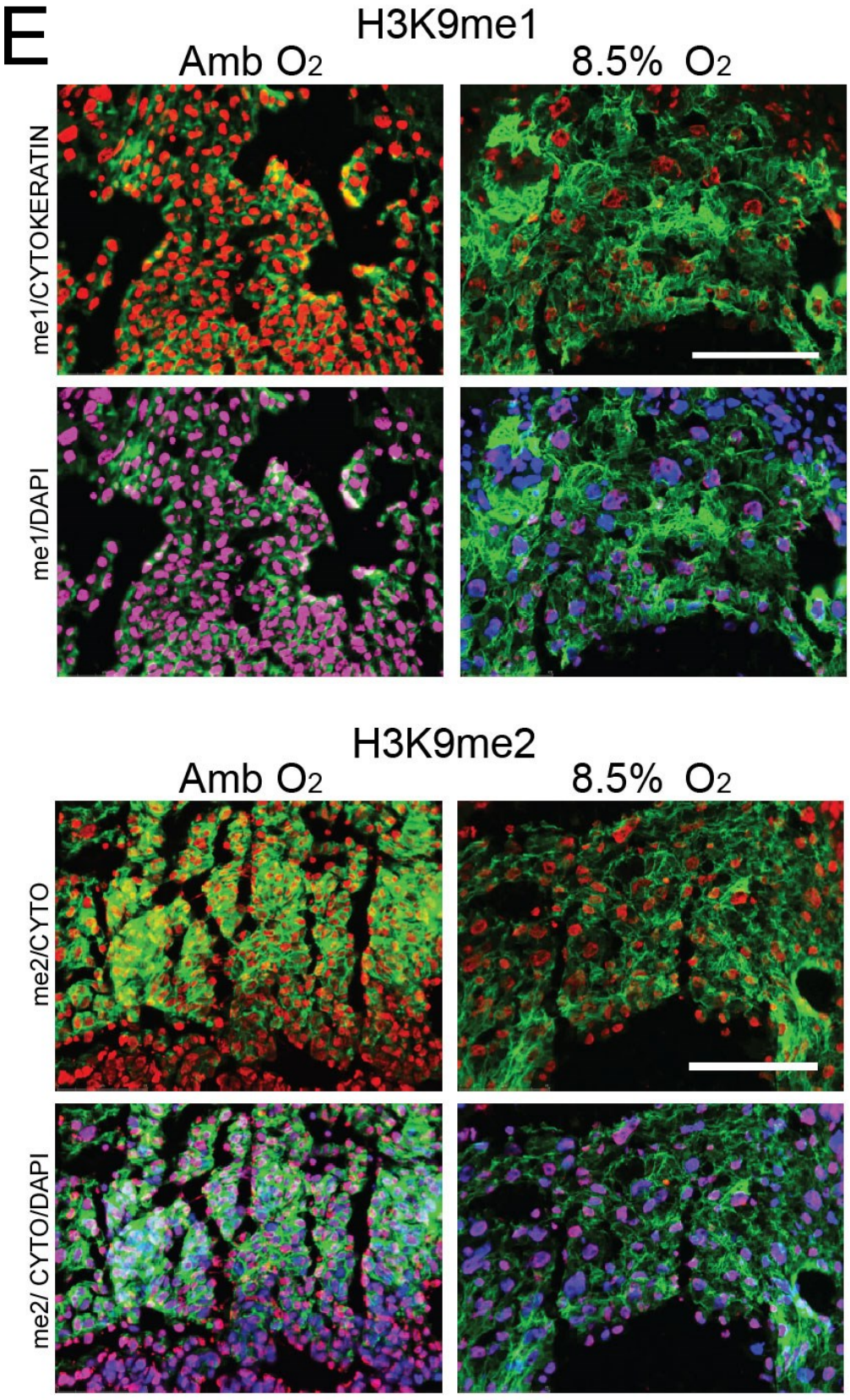
E
H3K9me1
Amb O2
8.5% O2
me1/CYTOKERATIN
me1/DAPI
H3K9me2
Amb O2
8.5% O2
me2/CYTO
me2/ CYTO/DAPI

KDM3A recruitment to target genes where KDM3A acts to remove repressive histone marks (Shakya et al., 2011). OCT1 has also been identified as a participant in the regulation of trophoblast lineage development (Sebastiano et al., 2010). KDM3A is also known to interact with nuclear receptors, including the androgen receptor, through an LXXLL motif (Yamane et al., 2006), providing a method of targeting to relevant loci. Although the androgen receptor does not appear to contribute to the regulation of trophoblast biology, other nuclear receptors such as PPARG and ESRRB have been linked to both trophoblast and hypoxia regulation (Ao et al., 2008; Parast et al., 2009; Rielland et al., 2008). In hypoxic TS cells, KDM3A may be delivered by HIF transcription factors to its gene targets in some instances, whereas arrival at other loci may be entirely independent of HIF (*Mmp12*, *Ppp1r3c*). This conclusion is based on the observed differential outcomes of *loss-of-function* and *gain-of-function* KDM3A manipulations in TS cells shown in this report. Elucidation of mechanisms controlling KDM3A arrival at its appropriate targets in the TS cell genome is an important future task.

Cells respond to hypoxia with global changes in histone modifications (Johnson et al., 2008; Melvin and Rocha, 2012). This epigenetic reorganization is postulated to establish a less compact chromatin environment, facilitating rapid transcriptional activation of genes and adaptations to hypoxic conditions. Consistent with such observations TS cells respond to hypoxia with global changes in histone H3K9me1 and H3K9me2. Recently H3K9me1 has achieved some prominence. Histone H3K9 methylation is a progressive event, wherein H3K9 monomethyl transferases deposit methyl groups on unmethylated histone H3K9 yielding H3K9me1 and H3K9me2 states. The H3K9 monomethylation mark serves as a recognition signal for SUV39H, an H3K9 methyl transferase, which can convert H3K9me1to a more

repressive H3K9me3 and bring about heterochromatic silencing (Towbin et al., 2012). Changes in histone H3K9 methylation, particularly H3K9 monomethylation, are also observed during chromatin assembly implicating its role in maintaining chromatin architecture (Jasencakova and Groth, 2010; Loyola et al., 2009). H3K9 methylation status and SUV39H have also been linked to development of the trophoblast lineage (Alder et al., 2010; Rugg-Gunn et al., 2010).

A role for KDM3A under hypoxic conditions may seem contradictory based on its known enzymatic properties. KDM3A is a α ketoglutarate-dependent dioxygenase and requires oxygen for enzymatic activity (Chen et al., 2006; Johnson et al., 2008). Our findings are consistent with Beyer and coworkers who observed the preservation of KDM3A histone demethylase activity in cells exposed to 0.5% oxygen (Beyer et al., 2008). Another α ketoglutarate-dependent dioxygenase and known regulator of HIF, HIF-asparaginyl hydroxylase, also retains its enzymatic function under low oxygen tensions (Stolze et al., 2004). Distribution of oxygen within intracellular compartments may be preserved to maintain enzymes that are critical for adaptations to hypoxia.

In summary, our observations connect hypoxia-dependent establishment of the invasive trophoblast lineage to an epigenetic modulator called KDM3A. HIF signaling serves as an essential intermediary in the process and key regulator of KDM3A expression. KDM3A acts on the epigenetic landscape of target loci controlling development of the invasive trophoblast lineage.

CHAPTER 4:

GENERAL DISCUSSION

I. Model

A summary of our research findings is presented in Figs. 4.1 and 4.2. Fig 4.1 illustrates the role of natural killer cells and hypoxia signaling in trophoblast lineage development. Uterine NK cells regulate vascular development, which impacts oxygen delivery and trophoblast lineage development, ultimately impacting the structural and functional organization of the chorioallantoic placenta.

Fig 4.2 depicts mechanisms of low oxygen signaling in trophoblast invasion. Low oxygen tensions stabilize HIF transcription factors which regulates expression of a number of genes involved in hypoxic adaptations. HIF mediated upregulation of histone demethylase KDM3A epigenetically regulates a subset of hypoxia responsive genes controlling development of the invasive trophoblast lineage.

II. NK Cells Modulate the Timing of Critical Events During Hemochorial Placentation

Strategies have been employed to investigate roles for NK cells during the establishment of pregnancy. These have included genetic mouse models possessing NK cell deficiencies (Croy et al., 2002) and systemic immunodepletion of NK cells using administration of antibodies to asialo GM1 during rat gestation (Chapter 2). The success of the immunodepletion approach is gestation-stage dependent and most effective when administered immediately prior to or concurrent with embryo implantation. From the mouse genetic models we learned that NK cells promote uterine spiral artery remodeling, including decreasing arterial smooth muscle wall thickness and increasing vessel lumen diameter(Guimond et al., 1997). NK cell immunodepletion in the rat results in striking changes in uterine spiral arteries, characterized

Fig. 4.1. Schematic diagram showing the role of NK cells and hypoxia/HIF signaling in the regulation of trophoblast cell differentiation. NK cells regulate uterine vascular development, which impacts oxygen delivery (ΔO_2) and trophoblast lineage decisions, regulating the organisation of the chorioallantoic placenta. Differentiated trophoblast lineages in the labyrinth zone include syncytial trophoblast. Differentiated trophoblast lineages in the junctional zone include trophoblast giant cells, spongiotrophoblast cells, glycogen cells and precursors for invasive trophoblast cells.

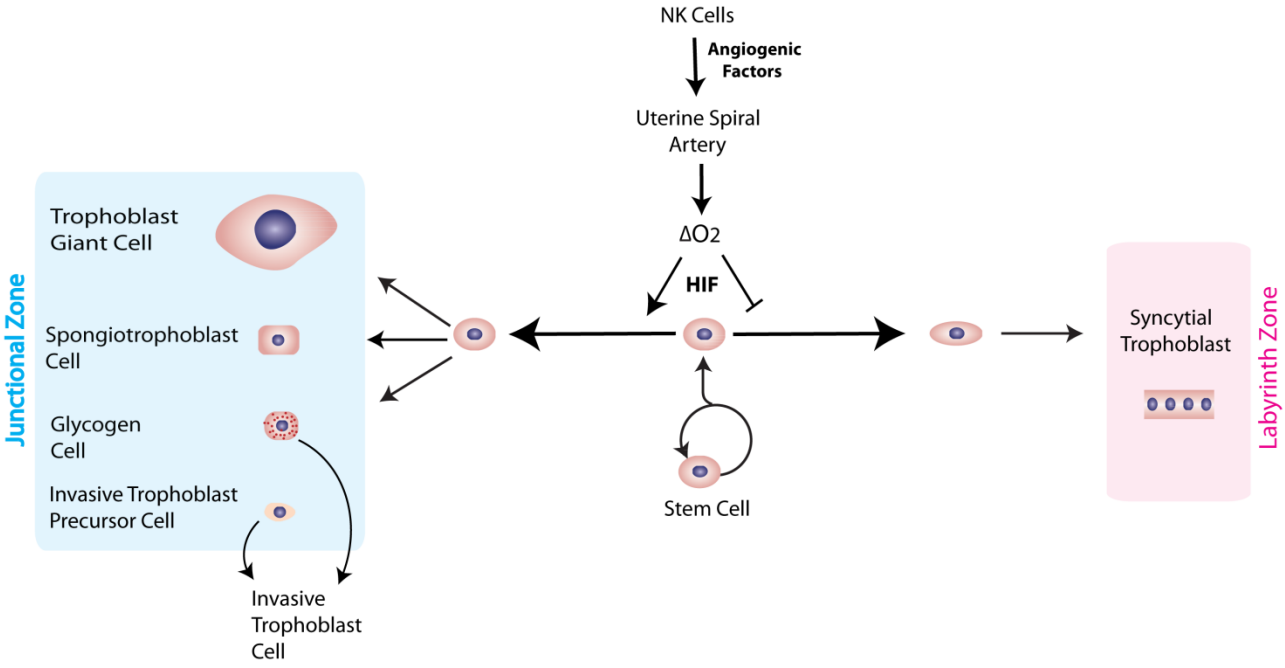
NK Cells
Angiogenic Factors
Uterine Spiral Artery
ΔO2
HIF
Stem Cell
Junctional Zone
Trophoblast Giant Cell
Spongiotrophoblast Cell
Glycogen Cell
Invasive Trophoblast Precursor Cell
Invasive Trophoblast Cell
Syncytial Trophoblast
Labyrinth Zone

Fig4.2. Schematic showing the mechanism of hypoxia signaling mediated KDM3A action and trophoblast invasion. Hypoxia signaling activates KDM3A expression which brings about epigenetic modifications of H3K9 methylation status affecting the invasive behavior of the rat trophoblast cells.

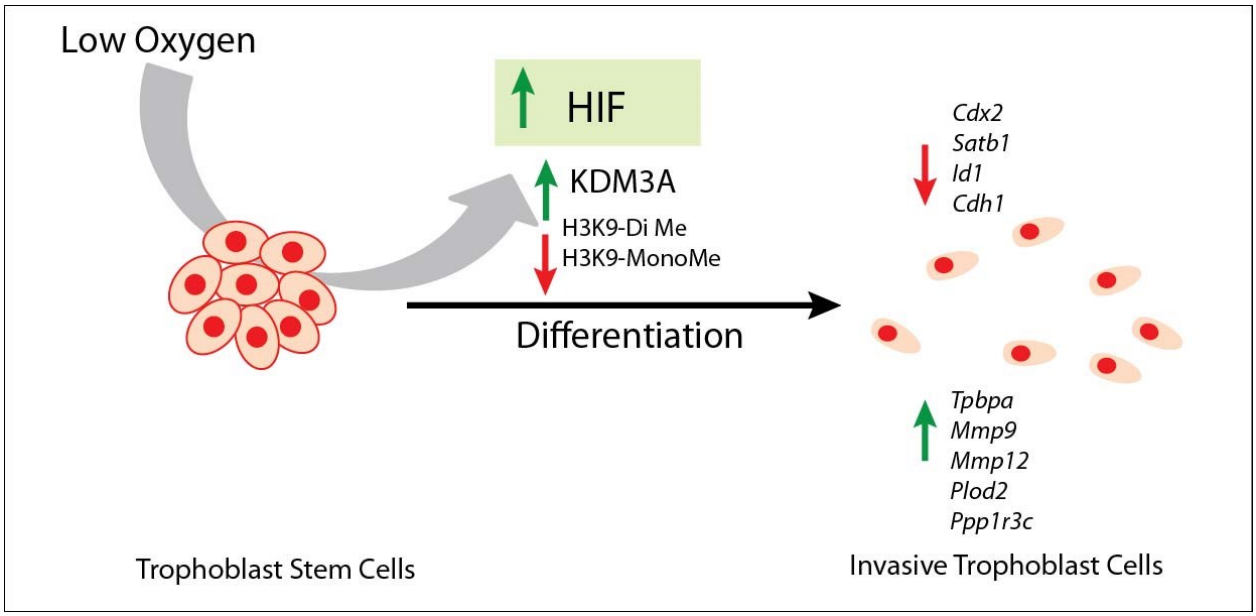
Low Oxygen
HIF
KDM3A
H3K9-Di Me
H3K9-MonoMe
Differentiation
Cdx2
Satb1
Id1
Cdh1
Tpbpa
Mmp9
Mmp12
Plod2
Ppp1r3c
Trophoblast Stem Cells
Invasive Trophoblast Cells

initially by a delay in uterine spiral artery development and progression toward the placenta and subsequently by an acceleration of endovascular invasive trophoblast cell movement and extensive uterine spiral artery remodeling. These physical changes include replacement of the endothelium with endovascular trophoblast cells, their acquisition of a pseudo-endothelial phenotype, the disappearance of smooth muscle cells in the tunica media of the modified uterine spiral artery, distention of uterine spiral artery lumen, and an increased capacity for blood delivery to the placenta. Thus, NK cells possess two apparently contradictory actions in establishing the hemochorial placenta: 1) they promote uterine spiral artery development and remodeling; and 2) they restrain trophoblast-directed uterine spiral artery remodeling. The relative impact of each action on uterine spiral artery remodeling is not equivalent. Invasive trophoblast-directed uterine spiral artery restructuring is far more extensive than NK cell-directed uterine spiral artery restructuring. It is apparent that these opposing efforts are interconnected in an important way. The presence of NK cells delays and reduces the magnitude of trophoblast-directed uterine spiral arterial modifications, which is viewed as a maternally protective adaptation.

Oxygen tension is a key mediator of NK cell actions at the placentation site

NK cells have profound effects on the organization of the placentation site, including the development and function of the invasive trophoblast cell lineage. These cells have been proposed to affect invasive trophoblast cells through their secretion of an assortment of cytokines/chemokines and via direct cell-cell interactions (Lash et al., 2010; Trowsdale and Moffett, 2008; Zhang et al., 2011). Some factors produced by NK cells stimulate invasive properties of trophoblast cells, whereas other NK cell-derived factors inhibit trophoblast invasion. These observations are based exclusively on *in vitro* experimentation and are difficult

to reconcile. A compelling hypothesis has also been proposed for direct NK cell-invasive trophoblast cell engagement (Chazara et al., 2011; Trowsdale and Moffett, 2008). NK cells possess surface receptors termed killer inhibitory receptors (KIRs), which specifically recognize histocompatibility antigens on the surface of trophoblast located at the maternal-fetal interface. This cell-cell interaction modifies NK cell and trophoblast cell function. Two observations support an involvement of NK cell-invasive trophoblast cell adhesion in hemochorial placentation: i) the existence of specific NK cell KIR receptor and histocompatibility antigen isoform combinations in successful pregnancies versus pregnancies afflicted with preeclampsia;(Chazara et al., 2011; Hiby et al., 2010; Hiby et al., 2004) and ii) the observation that endovascular trophoblast invasion and uterine spiral artery remodeling is affected by maternal and paternal histocompatibility antigen combinations (Madeja et al., 2011). These paracrine and cell-cell modes of NK cell action on trophoblast cells may be operative during the establishment of the hemochorial placenta; however, they are probably secondary to the more fundamental action of NK cells on uterine spiral artery development. The latter activities are likely mediated by a myriad of angiogenic and vasoactive factors secreted by NK cells (Zhang et al., 2011).

NK cells regulate uterine spiral artery development and in doing so control oxygen tension at the early placentation site. The absence of NK cells at the maternal-fetal interface results in a transient hypoxia. The effects of NK cell depletion on invasive trophoblast-directed uterine spiral artery remodeling can be mimicked by appropriately timed *in vivo* hypoxia exposure (Rosario et al., 2008). A critical developmental window of sensitivity to *in vivo* hypoxia exposure exists between E8.5 and E9.5 of rat pregnancy. This gestational interval represents a key developmental phase associated with commitment of trophoblast stem

(TS)/precursor cells to differentiated trophoblast cell lineages of the junctional zone versus the labyrinth zone. In addition to the robust extension of endovascular trophoblast invasion deep into the uterine spiral arteries in both NK cell depleted and maternal hypoxia *in vivo* models, the junctional zone also undergoes an expansion relative to the labyrinth zone (Rosario et al., 2008).

III. Hypoxia signaling in trophoblast invasion

TS cell populations are an excellent *in vitro* model system for elucidating mechanisms regulating differentiation (Asanoma et al., 2011; Tanaka et al., 1998). TS cell exposure to a range of oxygen tensions can differentially influence cell proliferation and differentiation (Adelman et al., 2000; Xie et al., 2011; Zhou et al., 2011). The impact of oxygen tension on development of invasive trophoblast lineages from TS cell populations has received little attention. Low oxygen tensions can promote differentiation of TS cells towards junctional zone trophoblast cell lineages. At least some of these hypoxia-stimulated actions are mediated by the HIF transcription factor complex (Adelman et al., 2000). Disruption of HIF signaling impairs TS cell responses to low oxygen and acquisition of an invasive phenotype. Whether these HIF actions are at specific gene loci controlling the invasive trophoblast cell lineage or are indirect through more widespread epigenetic modifications and how they differentially affect TS cell proliferation versus differentiation remain to be determined (Maltepe et al., 2005). Identifying the biology of specific hypoxia-sensitive and HIF target genes should provide insight into the regulatory machinery controlling the invasive trophoblast cell lineage.

Oxygen tension is an important stimulus for placentation. Oxygen tension at the maternal fetal interface changes throughout gestation and is dependent on placental development. Availability of oxygen and developmental variations of oxygen tension can have different

consequences depending on the stage of gestation. Low oxygen tension can be a developmental cue for placental organization and adaptive responses associated with placental development. Alternatively, it can also be a consequence of defective, pathological placentation wherein improper vascular remodeling results in poor placental perfusion and inefficient nutrient delivery. We utilized low oxygen tension as a developmental trigger to study hemochorial placentation and performed global TS cell gene expression analysis to identify targets of low oxygen exposure. We determined that hypoxia promotes a unique differentiated invasive trophoblast lineage, which is characterized by downregulation of trophoblast stem cell associated genes, loss of expression of genes involved cell contacts, upregulation of genes involved in extracellular matrix remodeling, cell movement, and vascular restructuring.

In this study we identified several genes regulated by HIF signaling. Knockdown of the HIF1B, the common binding partner for HIF1A and HIF2A affected hypoxia responses in TS cells. HIF1B has other binding partners so further studies should be conducted to study roles of HIF1A or HIF2A in TS cell adaptations to hypoxia. We envisage modest effects on disruption of HIF1A or HIF2A since it is known that they act on an overlapping set of target genes (Bracken et al., 2006; Hu et al., 2006a; Raval et al., 2005) . This conclusion is further supported from analysis of mouse placentation following mutation of HIF1A, HIF2A, or both HIF1A and HIF2A (Cowden Dahl et al., 2005). ChIP analysis with antibodies specific to HIF1A or HIF2 at known hypoxia responsive target genes such as *Kdm3a* and *Bhlhe40* or alternatively at a genome-wide view using ChIP seq.

Significance of the HIF targets

We have identified hypoxia signature of gene expression in rat TS cells. These genes are reflective of hypoxic adaptations and their functional roles in the process of invasion need to be evaluated. An emerging pattern of gene function in a subset of genes was related to various aspects of invasion. *Mmp12* (Harris, 2010), *Plod2* (Evens et al., 2010; Noda et al., 2012), *Mmp9* (Peters et al., 1999), *Loxl2* (Luo et al., 2012; Wong et al., 2012), *Cul7* (Fu et al., 2010) are known have prominent function of extra cellular matrix remodeling, invasion and metastses. We have observed significant downregulation of expression Cdh1 which is a hallmark of epithelial mesenchymal transition reported in a number of different cell types (Vicovac and Aplin, 1996). *Bhlhe40* (Hughes et al., 2004; Xie et al., 2011) and *Hand1* (Martindill et al., 2007) are trophoblast differentiation markers and are upregulated and downregulated, respectively in hypoxia exposed TS cells. Hand1 is a key transcription factor involved in the differentiation of trophoblast giant cell lineage (Hughes et al., 2004; Martindill et al., 2007). Consistent with the known function of HAND1, our results demonstrate that hypoxia drives TS cells toward a unique non-giant cell invasive lineage.

The significance of changes in the expression level of each of the genes listed above to acquisition of the invasive trophoblast lineage should be evaluated. Mouse models are potentially available; however, mouse and rat placentation are not equivalent processes. The mouse exhibits shallow trophoblast invasion, which differs dramatically from the extensive trophoblast invasion occurring in the human. Our research shows the importance of utilizing rat models to study trophoblast invasion and uterine spiral artery restructuring.Gene targeting of rat ES cells is a recent technique for generating rat models with a modest success rate (Tong et al., 2011). Other techniques include trophoblast specific knockdown of genes utilizing lentiviral shRNA

delivery(Lee et al., 2009), gene targeting via zinc finger nucleases (Geurts et al., 2009) and use of transposon systems to disrupt gene function (Lu et al., 2007).

Hypoxia dependent global epigenetic changes in rat TS cells

Our approach in trying to understand the molecular mechanisms underlying hypoxia signaling in trophoblast cells is built on the premise that TS cells developmentally experience low oxygen tensions, differentiate and move toward correcting the oxygen deficit. Thus transient exposures to low oxygen, especially *in vitro*, are potentially more physiologically relevant. Chronic exposure to extremely low oxygen tensions can generate pathological responses which will not be reflective of the adaptive response. In our experiments 0.5% oxygen tensions caused a unique differentiated lineage of trophoblast cells possessing an invasive phenotype. Along with the increased invasiveness, we also observed global changes in H3K9 methylation patterns. Biological significance associated with these dramatic global changes in histone marks needs to be deciphered. Genome wide locations of H3K9me1 and H3K9me2 methylation in ambient and hypoxia exposed TS cells will provide information regarding the possible regulatory roles of these histone marks. ChIP sequencing (seq) studies with antibodies to each histone mark will facilitate localization of relevant genomic regions and their correlation with potential regulatory mechanisms controlling adaptations to hypoxia and invasive trophoblast lineage development. A similar strategy has been used to dissect hippocampal gene networks controlling responses to stressors. Hippocampal H3 histone methylation, especially H3K9me3 is regulated by acute and chronic stress in the rat (Hunter et al., 2009). ChIP seq localized stress induced H3K9me3 enrichment to sites responsible for silencing endogenous retroviral elements (Hunter et al., 2012).

In our analysis we observed global changes in histone H3K9 methylation. Others have observed that hypoxia exposure results in global epigenetic changes in histone methylation and acetylation (Johnson et al., 2008). Expansions of repressive H3K27 trimethylation marks and activating H3K4 trimethylation marks following hypoxia have been observed. Parameters of hypoxia exposure (duration and concentration) and cell type should be considered in further investigations.

KDM3A as a mediator of hypoxia dependent adaptations in rat TS cells

Low oxygen tension stabilizes HIF transcription factors, which control cellular adaptations at a transcriptional level and through regulation of epigenetic modifiers. The latter represents a global mechanism of regulation extending the breadth of HIF influence. In TS cells KDM3A is rapidly upregulated in response to hypoxia in a HIF-dependent manner. KDM3A is a histone H3K9 demethylase and controls the expression of a subset of hypoxia/HIF responsive genes and development of the invasive trophoblast lineage. We expect that KDM3A directs differentiation through its actions at specific loci throughout the genome. Again a ChIP seq approach for identifying enrichment of KDM3A at specific genomic sites will be informative.

Histone H3K9me1 and H3K9me2 enrichment at the *Mmp12* locus in TS cells was influenced by hypoxia exposure. Whether this event is dependent upon the activities of KDM3A is unknown. Additionally, the breadth of KDM3A action on the distribution of genome-wide changes in H3K9me1 and H3K9me2 marks is unknown. Combining a ChIP seq analysis of histone H3K9 methylation with genome-wide KDM3A localization will help address this uncertainty.

Activation of HIF signaling pathways under low oxygen tensions upregulate a variety of other JmJc domain containing demethylases which include Kdm4b, Kdm4c, Jarid1b (Krieg et al., 2010; Pollard et al., 2008). These demethylases act on different histone methylation marks. Kdm4 family of demethylases act on H3K93me/2me and H3k363me/2me and Jarid1b acts on H3K4-2me/3me (Mosammaparast and Shi, 2010). Presumably these different JmJc domain containing demethylases possess unique as well as overlapping targets and contribute to a complex histone H3 methylome characteristic of cells undergoing adaptations to hypoxia. The conditions of our experimentation were not associated with dramatic changes in KDM4 or JARID1B demethylases.

IV. Relevance of our research to human placentation and human pregnancy disorders

Pregnancy associated disorders

There are a number of pregnancy associated disorders in humans which are associated with improper trophoblast development and differentiation leading to inadequate trophoblast invasion and vascular remodeling. Preclampsia syndrome is one of the most common placental pathology occurring in 3-5% of first pregnancies (Kanasaki and Kalluri, 2009). It is characterized by mild to severe maternal hypertension and proteinuria around midgestation and/or mild to severe intrauterine fetal growth restriction. Preeclampsia is one of the leading causes of maternal and fetal death during pregnancy. Poor traophoblast invasion leads to insufficient prefusion of the placenta which triggers placental hypoxia. This causes upregulation of placental anti-angiogenic factors like soluble Flt1 (Levine et al., 2004; Maynard et al., 2003) which results in the angiogenic factor imbalance and subsequent disruption of vascular

endothelium and maternal cardiovascular system (Maynard and Karumanchi, 2011; Powe et al., 2011). Possible cures include premature delivery of the baby and the placenta.

IUGR is another pregnancy associated disorder which is characterized by small for gestational age babies (Scifres and Nelson, 2009). Causes of the disease can be traced back to improper placental development as well as shallow trophoblast invasion leading to inefficient vascular remodeling. IUGR can result in developmentally growth retarded babies, disability and even fetal death. Research has shown that placental environment can play a huge role in determining adult life health disorders like hypertension, cardiovascular disease, renal diseases and diabetes to name a few (Barker, 2007; Thornburg et al., 2010a; Thornburg et al., 2010b).

Uterine NK cells and pregnancy associated disorders:

Recent studies have implicated role of decidual NK cells in vascular smooth muscle cell apoptosis(Fraser et al., 2012). Studies show in a co-culture *in vitro* model that decidual NK cells from normal pregnancies can initiate trophoblast invasion disrupting vascular endothelium, however when decidual NK cells obtained from high resistance pregnancies are co-cultured with trophoblast cells, impaired vascular remodeling and reduced invasiveness is observed. (Fraser et al.,2012). Peripheral NK cell number has been shown to stay unchanged in preeclamptic pregnancies, aberrant NK cell expression and increased NKG2A- and NKG2C surface receptors have been observed in preeclampsia (Bachmayer et al., 2009) .

NK cells exhibit a polarity in their production of cytokines during pregnancy. Similar to other types of immune cells, NK cells also shift from Th1 to Th2 cytokines as pregnancy progresses. Persistence of NK cell Th1 production (e.g. Tumor Necrosis Factor α) is associated with a higher incidence of abortions.

Elevated NK cell cytotoxicity is also associated with implantation failure after *in vitro* fertilization and embryo transfer and in women experiencing recurrent pregnancy loss(Fukui et al., 2011) . Correlations have been made between cell surface expression of receptors in peripheral NK cells and pregnancy outcomes. A significant decrease in the percentage of CD56bright/NKp46+ cells is detected in preeclamptic patients 3-4 months before the onset of preelampsia (Fukui et al., 2012).

Finally, increased numbers of uterine NK cells have been observed at the placental interface in preeclamptic (Reister et al., 2006) and IUGR (Williams et al., 2009) pregnancies. Furthermore, excessive LIF production by NK cells in preeclamptic pregnancies has been associated with reductions in matrix metalloprotease synthesis by extravillous trophoblast (Reister et al., 2006).

Hypoxia signaling and pregnancy associated disorders:

Role of HIF transcription factors in preeclampsia remains debatable. This is largely due to the fact that hypoxia signaling seems to be playing instructive role in shaping of the placenta during early gestation. The placenta develops under low oxygen tensions until the uterine maternal vasculature is remodeled by invading trophoblast cells (Rodesch et al., 1992). HIFA is highly expressed in early gestation trophoblast cells and is subsequently downregulated around 9 weeks of gestation (Caniggia et al., 2000). However this issue is complex. Failures in placentation caused by shallow trophoblast invasion result in impaired placental perfusion, and trigger chronic hypoxia signaling, which leads to pathogenesis.

HIF1A expression may be upregulated in preeclampsia. *HIF-1A* RNA expression in maternal plasma is increased in pregnant women with preeclampsia and IUGR (Ashur-Fabian et

al., 2012). A role for HIF-1A in the pathogenesis of preeclampsia has also been determined from investigation of placentation in women residing at high altitudes experiencing chronic hypoxia (Zamudio et al., 2007). Preelampsia incidence is higher in these women and their placentas show elevated HIF1A expression (Zamudio et al., 2007). A number of downstream effectors of HIF signaling involved in the pathogenesis of preeclampsia have been identified. Anti-angiogenic factors like Endothelin (Yamashita et al., 2001), sFlt1(Nevo et al., 2008; Nevo et al., 2006), Endoglin (Yinon et al., 2008) are hypoxia responsive and significantly upregulated in IUGR and preeclamptic placentas. Urocortin peptides are also HIF targets and elevated in preeclampsia (Imperatore et al., 2010). Urocortin peptides are known to be local regulators of myometrial contractility (Florio et al., 2004).

Stabilization is a key process regulating HIF activities. Early onset preeclamptic placentas exhibit decreased proteosomal degradation of HIF-1A (Rajakumar et al., 2006; Rajakumar et al., 2008). PHD2 and FIH are involved in stabilization and activation of HIF transcription factors and have been shown to be downregulated in early onset preeclampsia syndrome (Rolfo et al., 2010). Manifestation of the pathological features of preeclamptic disease is linked to an impaired ability of the trophoblast cells to respond and adapt to gestation dependent variations in oxygen tensions (Tal, 2012).

Hypoxia responsive invasion and vascular remodeling related genes in preeclampsia and IUGR

Several of the hypoxia responsive genes have been investigated in preeclampsia, including *Plau*, *Mmp9*, *Comt*, *Cul7*, *Cdh1*,*Fasl*,Glut1, *Vegfa*. PLAU is an established biomarker of Preeclampsia and complicated hypertensive pregnancies. Plasma concentrations of PLAU are

downregulated in severe preeclamptic pregnancies and IUGR (Koh et al., 1993; Lindoff and Astedt, 1994), as is cell surface PLAU activity (Graham and McCrae, 1996). Although the significance of MMP9 in the etiology of preeclampsia syndrome is unknown, increased MMP9 levels have been observed in preeclamptic placentas (Wang et al., 2010). Two methoxy estradiol (2ME) is generated by the enzymatic activities of COMT. Plasma concentrations of 2ME are low in preeclamptic pregnancies (Perez-Sepulveda et al., 2012; Seol et al., 2012). The Val158Met COMT polymorphism is associated with increased COMT activity and a decreased risk to develop preeclampsia, suggesting a protective role against preeclampsia. Conversely, a low COMT activity haplotype has been linked to higher risk of recurrent preeclampsia (Kanasaki et al., 2008; Roten et al., 2011).

The CUL7 gene is upregulated in IUGR and preeclampsia associated with IUGR, with extensive promoter hypomethylation observed in IUGR placentae (Gascoin-Lachambre et al., 2010). CDH1 plays an important role in cell-cell adhesion and epithelial to mesenchymal transitions. Variations in the expression of CDH1 and its repressor SNAIL are observed in preeclamptic placentas (Brown et al., 2005). FASL, a regulator of apoptosis, is significantly down regulated in placental villi of preeclamptia patients (Neale and Mor, 2005). Serum FASL concentrations have also been used as biomarker of the preeclampsia (Laskowska et al., 2006). IUGR is also associated with reduced glucose transport to the fetus and decreased expression of placental GLUT1 (Zamudio et al., 2010). In pregnancies with adverse outcomes, (gestational hypertension, small for gestational age and pre-term birth) reduced VEGF family of angiogenic factor mRNAs is observed (Andraweera et al., 2013). In a recent bioinformatics study accessing publicly available preeclampsia databases, VEGF family along with its receptors have found significant correlation with the disease (Tejera et al., 2012). Numerous polymorphisms

associated with VEGFA are correlated to pregnancies complicated with adverse outcomes (Andraweera et al., 2013; Andraweera et al., 2011).

KDM3A in the human placenta

Knowledge of the role of KDM3A in human trophoblast is limited. KDM3A can be localized in the first trimester trophoblast samples, particularly strong immunostaining was observed in the extravillous trophoblast columns (Chapter 3; **Fig 3.8C**). Its expression can also be observed in the Bewo cell line and upregulation of *Kdm3a* can be observed on hypoxia exposure both at transcript and protein levels (Chapter 3; **Fig 3.8 A&B**). Thorough investigations are needed to evaluate the role of KDM3A in human trophoblast cells. First trimester trophoblast may be the best choice to understand the role of KDM3A in the process of low oxygen signaling dependent trophoblast invasion. Although the potential for mechanistic studies on role of KDM3A in human placentation is limited, KDM3A expression, activity and polymorphisms can be investigated in normal as well as complicated pregnancy outcomes.

V. Overview of the importance of the work

We have identified the importance of maternal environment on development of placentation. Our work identified uterine NK cells as regulators of placentation, particularly fine tuning oxygen availability at the developing placentation site. Availability of oxygen acted as a developmental cue for the organization of chorioallantoic placentation and the process of invasive trophoblast lineage development. In the later part of the work, we have identified mechanisms underlying hypoxia signaling. These efforts started with gene profiling experiments in rat TS cells and led to the identification of KDM3A, a key mediator of hypoxia dependent epigenetic reorganisation and development of the invasive trophoblast lineage. This knowledge

derived from the rat placentation model can be utilized to elucidate specific mechanisms underlying regulation of hemochorial placentation in normal and pathologic pregnancies.

REFERENCES

Abell, A.N., Jordan, N.V., Huang, W., Prat, A., Midland, A.A., Johnson, N.L., Granger, D.A., Mieczkowski, P.A., Perou, C.M., Gomez, S.M., Li, L., Johnson, G.L., 2011. MAP3K4/CBP-regulated H2B acetylation controls epithelial-mesenchymal transition in trophoblast stem cells. Cell stem cell 8, 525-537.

Adamson, S.L., Lu, Y., Whiteley, K.J., Holmyard, D., Hemberger, M., Pfarrer, C., Cross, J.C., 2002. Interactions between trophoblast cells and the maternal and fetal circulation in the mouse placenta. Dev Biol 250, 358-373.

Adelman, D.M., Gertsenstein, M., Nagy, A., Simon, M.C., Maltepe, E., 2000. Placental cell fates are regulated *in vivo* by HIF-mediated hypoxia responses. Genes Dev 14, 3191-3203.

Ain, R., Canham, L.N., Soares, M.J., 2003a. Gestation stage-dependent intrauterine trophoblast cell invasion in the rat and mouse: novel endocrine phenotype and regulation. Dev Biol 260, 176-190.

Ain, R., Konno, T., Canham, L.N., Soares, M.J., 2006. Phenotypic analysis of the rat placenta. Methods Mol Med 121, 295-313.

Ain, R., Soares, M.J., 2004. Is the metrial gland really a gland? J Reprod Immunol 61, 129-131.

Ain, R., Tash, J.S., Soares, M.J., 2003b. Prolactin-like protein-A is a functional modulator of natural killer cells at the maternal-fetal interface. Molecular and cellular endocrinology 204, 65-74.

Ain, R., Trinh, M.L., Soares, M.J., 2004. Interleukin-11 signaling is required for the differentiation of natural killer cells at the maternal-fetal interface. Dev Dyn 231, 700-708.

Alam, S.M., Konno, T., Dai, G., Lu, L., Wang, D., Dunmore, J.H., Godwin, A.R., Soares, M.J., 2007. A uterine decidual cell cytokine ensures pregnancy-dependent adaptations to a physiological stressor. Development 134, 407-415.

Alder, O., Lavial, F., Helness, A., Brookes, E., Pinho, S., Chandrashekran, A., Arnaud, P., Pombo, A., O'Neill, L., Azuara, V., 2010. Ring1B and Suv39h1 delineate distinct chromatin states at bivalent genes during early mouse lineage commitment. Development 137, 2483-2492.

Alsat, E., Wyplosz, P., Malassine, A., Guibourdenche, J., Porquet, D., Nessmann, C., Evain-Brion, D., 1996. Hypoxia impairs cell fusion and differentiation process in human cytotrophoblast, *in vitro*. J Cell Physiol 168, 346-353.

Andraweera, P.H., Dekker, G.A., Dissanayake, V.H., Bianco-Miotto, T., Jayasekara, R.W., Roberts, C.T., 2013. Vascular endothelial growth factor family gene polymorphisms in preeclampsia in Sinhalese women in Sri-Lanka. The journal of maternal-fetal & neonatal medicine : the official journal of the European Association of Perinatal Medicine, the Federation of Asia and Oceania Perinatal Societies, the International Society of Perinatal Obstet 26, 532-536.

Andraweera, P.H., Dekker, G.A., Thompson, S.D., Nowak, R.C., Zhang, J.V., McCowan, L.M., North, R.A., Roberts, C.T., 2011. Association of vascular endothelial growth factor +936 C/T single-nucleotide polymorphism with pregnancies complicated by small-for-gestational-age babies. Archives of pediatrics & adolescent medicine 165, 1123-1130.

Ao, A., Wang, H., Kamarajugadda, S., Lu, J., 2008. Involvement of estrogen-related receptors in transcriptional response to hypoxia and growth of solid tumors. Proc Natl Acad Sci U S A 105, 7821-7826.

Apps, R., Sharkey, A., Gardner, L., Male, V., Trotter, M., Miller, N., North, R., Founds, S., Moffett, A., 2011. Genome-wide expression profile of first trimester villous and extravillous human trophoblast cells. Placenta 32, 33-43.

Armant, D.R., Kaplan, H.A., Lennarz, W.J., 1986. Fibronectin and laminin promote *in vitro* attachment and outgrowth of mouse blastocysts. Dev Biol 116, 519-523.

Asanoma, K., Kubota, K., Chakraborty, D., Renaud, S.J., Wake, N., Fukushima, K., Soares, M.J., Rumi, M.A., 2012. SATB homeobox proteins regulate trophoblast stem cell renewal and differentiation. J Biol Chem 287, 2257-2268.

Asanoma, K., Rumi, M.A., Kent, L.N., Chakraborty, D., Renaud, S.J., Wake, N., Lee, D.S., Kubota, K., Soares, M.J., 2011. FGF4-dependent stem cells derived from rat blastocysts differentiate along the trophoblast lineage. Dev Biol 351, 110-119.

Ashkar, A.A., Black, G.P., Wei, Q., He, H., Liang, L., Head, J.R., Croy, B.A., 2003. Assessment of requirements for IL-15 and IFN regulatory factors in uterine NK cell differentiation and function during pregnancy. J Immunol 171, 2937-2944.

Ashkar, A.A., Croy, B.A., 2001. Functions of uterine natural killer cells are mediated by interferon gamma production during murine pregnancy. Semin Immunol 13, 235-241.

Ashkar, A.A., Di Santo, J.P., Croy, B.A., 2000. Interferon gamma contributes to initiation of uterine vascular modification, decidual integrity, and uterine natural killer cell maturation during normal murine pregnancy. J Exp Med 192, 259-270.

Ashton, S.V., Whitley, G.S., Dash, P.R., Wareing, M., Crocker, I.P., Baker, P.N., Cartwright, J.E., 2005. Uterine spiral artery remodeling involves endothelial apoptosis induced by extravillous trophoblasts through Fas/FasL interactions. Arteriosclerosis, thrombosis, and vascular biology 25, 102-108.

Ashur-Fabian, O., Yerushalmi, G.M., Mazaki-Tovi, S., Steinberg, D.M., Goldshtein, I., Yackobovitch-Gavan, M., Schiff, E., Amariglio, N., Rechavi, G., 2012. Cell free expression of hif1alpha and p21 in maternal peripheral blood as a marker for preeclampsia and fetal growth restriction. PloS one 7, e37273.

Bachmayer, N., Sohlberg, E., Sundstrom, Y., Hamad, R.R., Berg, L., Bremme, K., Sverremark-Ekstrom, E., 2009. Women with pre-eclampsia have an altered NKG2A and NKG2C receptor expression on peripheral blood natural killer cells. American journal of reproductive immunology 62, 147-157.

Barber, E.M., Pollard, J.W., 2003. The uterine NK cell population requires IL-15 but these cells are not required for pregnancy nor the resolution of a Listeria monocytogenes infection. J Immunol 171, 37-46.

Barker, D.J., 2007. The origins of the developmental origins theory. Journal of internal medicine 261, 412-417.

Barlozzari, T., Herberman, R.B., Reynolds, C.W., 1987. Inhibition of pluripotent hematopoietic stem cells of bone marrow by large granular lymphocytes. Proc Natl Acad Sci U S A 84, 7691-7695.

Barlozzari, T., Leonhardt, J., Wiltrout, R.H., Herberman, R.B., Reynolds, C.W., 1985. Direct evidence for the role of LGL in the inhibition of experimental tumor metastases. J Immunol 134, 2783-2789.

Benita, Y., Kikuchi, H., Smith, A.D., Zhang, M.Q., Chung, D.C., Xavier, R.J., 2009. An integrative genomics approach identifies Hypoxia Inducible Factor-1 (HIF-1)-target genes that form the core response to hypoxia. Nucleic acids research 37, 4587-4602.

Beyer, S., Kristensen, M.M., Jensen, K.S., Johansen, J.V., Staller, P., 2008. The histone demethylases JMJD1A and JMJD2B are transcriptional targets of hypoxia-inducible factor HIF. J Biol Chem 283, 36542-36552.

Bilban, M., Tauber, S., Haslinger, P., Pollheimer, J., Saleh, L., Pehamberger, H., Wagner, O., Knofler, M., 2010. Trophoblast invasion: assessment of cellular models using gene expression signatures. Placenta 31, 989-996.

Bracken, C.P., Fedele, A.O., Linke, S., Balrak, W., Lisy, K., Whitelaw, M.L., Peet, D.J., 2006. Cell-specific regulation of hypoxia-inducible factor (HIF)-1alpha and HIF-2alpha stabilization and transactivation in a graded oxygen environment. J Biol Chem 281, 22575-22585.

Brown, L.M., Lacey, H.A., Baker, P.N., Crocker, I.P., 2005. E-cadherin in the assessment of aberrant placental cytotrophoblast turnover in pregnancies complicated by pre-eclampsia. Histochemistry and cell biology 124, 499-506.

Bruick, R.K., McKnight, S.L., 2001. A conserved family of prolyl-4-hydroxylases that modify HIF. Science 294, 1337-1340.

Bulmer, J.N., Lash, G.E., 2005. Human uterine natural killer cells: a reappraisal. Mol Immunol 42, 511-521.

Bulmer, J.N., Williams, P.J., Lash, G.E., 2010. Immune cells in the placental bed. The International journal of developmental biology 54, 281-294.

Burnett, T.G., Hunt, J.S., 2000. Nitric oxide synthase-2 and expression of perforin in uterine NK cells. J Immunol 164, 5245-5250.

Burnett, T.G., Tash, J.S., Hunt, J.S., 2002. Investigation of the role of nitric oxide synthase 2 in pregnancy using mutant mice. Reproduction 124, 49-57.

Burton, G.J., 2009. Oxygen, the Janus gas; its effects on human placental development and function. J Anat 215, 27-35.

Burton, G.J., Jaunaiux, E., 2001. Maternal vascularisation of the human placenta: does the embryo develop in a hypoxic environment? Gynecol Obstet Fertil 29, 503-508.

Caluwaerts, S., Vercruysse, L., Luyten, C., Pijnenborg, R., 2005. Endovascular trophoblast invasion and associated structural changes in uterine spiral arteries of the pregnant rat. Placenta 26, 574-584.

Caniggia, I., Mostachfi, H., Winter, J., Gassmann, M., Lye, S.J., Kuliszewski, M., Post, M., 2000. Hypoxia-inducible factor-1 mediates the biological effects of oxygen on human trophoblast differentiation through TGFbeta(3). J Clin Invest 105, 577-587.

Cartwright, J.E., Keogh, R.J., Tissot van Patot, M.C., 2007. Hypoxia and placental remodelling. Advances in experimental medicine and biology 618, 113-126.

Chakraborty, D., Rumi, M.A., Konno, T., Soares, M.J., 2011. Natural killer cells direct hemochorial placentation by regulating hypoxia-inducible factor dependent trophoblast lineage decisions. Proc Natl Acad Sci U S A 108, 16295-16300.

Chazara, O., Xiong, S., Moffett, A., 2011. Maternal KIR and fetal HLA-C: a fine balance. J Leukoc Biol 90, 703-716.

Chen, H., Yan, Y., Davidson, T.L., Shinkai, Y., Costa, M., 2006. Hypoxic stress induces dimethylated histone H3 lysine 9 through histone methyltransferase G9a in mammalian cells. Cancer research 66, 9009-9016.

Christofferson, R.H., 1993. Comments on the direction of blood flow in the central placental vessel in the rat. Teratology 47, 1-9.

Coan, P.M., Conroy, N., Burton, G.J., Ferguson-Smith, A.C., 2006. Origin and characteristics of glycogen cells in the developing murine placenta. Dev Dyn 235, 3280-3294.

Cowden Dahl, K.D., Fryer, B.H., Mack, F.A., Compernolle, V., Maltepe, E., Adelman, D.M., Carmeliet, P., Simon, M.C., 2005. Hypoxia-inducible factors 1alpha and 2alpha regulate trophoblast differentiation. Mol Cell Biol 25, 10479-10491.

Crocker, I.P., Wareing, M., Ferris, G.R., Jones, C.J., Cartwright, J.E., Baker, P.N., Aplin, J.D., 2005. The effect of vascular origin, oxygen, and tumour necrosis factor alpha on trophoblast invasion of maternal arteries *in vitro*. J Pathol 206, 476-485.

Croy, B.A., Ashkar, A.A., Minhas, K., Greenwood, J.D., 2000. Can murine uterine natural killer cells give insights into the pathogenesis of preeclampsia? J Soc Gynecol Investig 7, 12-20.

Croy, B.A., Chantakru, S., Esadeg, S., Ashkar, A.A., Wei, Q., 2002. Decidual natural killer cells: key regulators of placental development (a review). J Reprod Immunol 57, 151-168.

Croy, B.A., He, H., Esadeg, S., Wei, Q., McCartney, D., Zhang, J., Borzychowski, A., Ashkar, A.A., Black, G.P., Evans, S.S., Chantakru, S., van den Heuvel, M., Paffaro, V.A., Jr., Yamada, A.T., 2003. Uterine natural killer cells: insights into their cellular and molecular biology from mouse modelling. Reproduction 126, 149-160.

Croy, B.A., Luross, J.A., Guimond, M.J., Hunt, J.S., 1996. Uterine natural killer cells: insights into lineage relationships and functions from studies of pregnancies in mutant and transgenic mice. Nat Immun 15, 22-33.

Damsky, C.H., Fisher, S.J., 1998. Trophoblast pseudo-vasculogenesis: faking it with endothelial adhesion receptors. Current opinion in cell biology 10, 660-666.

Davies, J., Glasser, S.R., 1968. Histological and fine structural observations on the placenta of the rat. Acta anatomica 69, 542-608.

De Oliveira, L.G., Lash, G.E., Murray-Dunning, C., Bulmer, J.N., Innes, B.A., Searle, R.F., Sass, N., Robson, S.C., 2010. Role of interleukin 8 in uterine natural killer cell regulation of extravillous trophoblast cell invasion. Placenta 31, 595-601.

Dosiou, C., Giudice, L.C., 2005. Natural killer cells in pregnancy and recurrent pregnancy loss: endocrine and immunologic perspectives. Endocrine reviews 26, 44-62.

Dunwoodie, S.L., 2009. The role of hypoxia in development of the Mammalian embryo. Developmental cell 17, 755-773.

Ema, M., Hirota, K., Mimura, J., Abe, H., Yodoi, J., Sogawa, K., Poellinger, L., Fujii-Kuriyama, Y., 1999. Molecular mechanisms of transcription activation by HLF and HIF1alpha in response to hypoxia: their stabilization and redox signal-induced interaction with CBP/p300. EMBO J 18, 1905-1914.

Enders, A.C., Welsh, A.O., 1993. Structural interactions of trophoblast and uterus during hemochorial placenta formation. J Exp Zool 266, 578-587.

Epstein, A.C., Gleadle, J.M., McNeill, L.A., Hewitson, K.S., O'Rourke, J., Mole, D.R., Mukherji, M., Metzen, E., Wilson, M.I., Dhanda, A., Tian, Y.M., Masson, N., Hamilton, D.L., Jaakkola, P., Barstead, R., Hodgkin, J., Maxwell, P.H., Pugh, C.W., Schofield, C.J., Ratcliffe, P.J., 2001. C. elegans EGL-9 and mammalian homologs define a family of dioxygenases that regulate HIF by prolyl hydroxylation. Cell 107, 43-54.

Erlebacher, A., 2010. Immune surveillance of the maternal/fetal interface: controversies and implications. Trends in endocrinology and metabolism: TEM 21, 428-434.

Evens, A.M., Sehn, L.H., Farinha, P., Nelson, B.P., Raji, A., Lu, Y., Brakman, A., Parimi, V., Winter, J.N., Schumacker, P.T., Gascoyne, R.D., Gordon, L.I., 2010. Hypoxia-inducible factor-1 {alpha} expression predicts superior survival in patients with diffuse large B-cell lymphoma treated with R-CHOP. Journal of clinical oncology : official journal of the American Society of Clinical Oncology 28, 1017-1024.

Fischer, B., Bavister, B.D., 1993. Oxygen tension in the oviduct and uterus of rhesus monkeys, hamsters and rabbits. Journal of reproduction and fertility 99, 673-679.

Florio, P., Vale, W., Petraglia, F., 2004. Urocortins in human reproduction. Peptides 25, 1751-1757.

Fraser, R., Whitley, G.S., Johnstone, A.P., Host, A.J., Sebire, N.J., Thilaganathan, B., Cartwright, J.E., 2012. Impaired decidual natural killer cell regulation of vascular remodelling in early human pregnancies with high uterine artery resistance. J Pathol.

Fryer, B.H., Simon, M.C., 2006. Hypoxia, HIF and the placenta. Cell Cycle 5, 495-498.

Fu, J., Lv, X., Lin, H., Wu, L., Wang, R., Zhou, Z., Zhang, B., Wang, Y.L., Tsang, B.K., Zhu, C., Wang, H., 2010. Ubiquitin ligase cullin 7 induces epithelial-mesenchymal transition in human choriocarcinoma cells. J Biol Chem 285, 10870-10879.

Fu, L., Chen, L., Yang, J., Ye, T., Chen, Y., Fang, J., 2012. HIF-1alpha-induced histone demethylase JMJD2B contributes to the malignant phenotype of colorectal cancer cells via an epigenetic mechanism. Carcinogenesis 33, 1664-1673.

Fukui, A., Funamizu, A., Yokota, M., Yamada, K., Nakamua, R., Fukuhara, R., Kimura, H., Mizunuma, H., 2011. Uterine and circulating natural killer cells and their roles in women with recurrent pregnancy loss, implantation failure and preeclampsia. J Reprod Immunol 90, 105-110.

Fukui, A., Yokota, M., Funamizu, A., Nakamua, R., Fukuhara, R., Yamada, K., Kimura, H., Fukuyama, A., Kamoi, M., Tanaka, K., Mizunuma, H., 2012. Changes of NK cells in preeclampsia. American journal of reproductive immunology 67, 278-286.

Gardner, R.L., Papaioannou, V.E., Barton, S.C., 1973. Origin of the ectoplacental cone and secondary giant cells in mouse blastocysts reconstituted from isolated trophoblast and inner cell mass. J Embryol Exp Morphol 30, 561-572.

Gascoin-Lachambre, G., Buffat, C., Rebourcet, R., Chelbi, S.T., Rigourd, V., Mondon, F., Mignot, T.M., Legras, E., Simeoni, U., Vaiman, D., Barbaux, S., 2010. Cullins in human intra-uterine growth restriction: expressional and epigenetic alterations. Placenta 31, 151-157.

Genbacev, O., Joslin, R., Damsky, C.H., Polliotti, B.M., Fisher, S.J., 1996. Hypoxia alters early gestation human cytotrophoblast differentiation/invasion *in vitro* and models the placental defects that occur in preeclampsia. J Clin Invest 97, 540-550.

Genbacev, O., Zhou, Y., Ludlow, J.W., Fisher, S.J., 1997. Regulation of human placental development by oxygen tension. Science 277, 1669-1672.

Georgiades, P., Ferguson-Smith, A.C., Burton, G.J., 2002. Comparative developmental anatomy of the murine and human definitive placentae. Placenta 23, 3-19.

Geurts, A.M., Cost, G.J., Freyvert, Y., Zeitler, B., Miller, J.C., Choi, V.M., Jenkins, S.S., Wood, A., Cui, X., Meng, X., Vincent, A., Lam, S., Michalkiewicz, M., Schilling, R., Foeckler, J., Kalloway, S., Weiler, H., Menoret, S., Anegon, I., Davis, G.D., Zhang, L., Rebar, E.J., Gregory, P.D., Urnov, F.D., Jacob, H.J., Buelow, R., 2009. Knockout rats via embryo microinjection of zinc-finger nucleases. Science 325, 433.

Gnarra, J.R., Ward, J.M., Porter, F.D., Wagner, J.R., Devor, D.E., Grinberg, A., Emmert-Buck, M.R., Westphal, H., Klausner, R.D., Linehan, W.M., 1997. Defective placental vasculogenesis causes embryonic lethality in VHL-deficient mice. Proc Natl Acad Sci U S A 94, 9102-9107.

Graham, C.H., McCrae, K.R., 1996. Altered expression of gelatinase and surface-associated plasminogen activator activity by trophoblast cells isolated from placentas of preeclamptic patients. Am J Obstet Gynecol 175, 555-562.

Graham, C.H., Postovit, L.M., Park, H., Canning, M.T., Fitzpatrick, T.E., 2000. Adriana and Luisa Castellucci award lecture 1999: role of oxygen in the regulation of trophoblast gene expression and invasion. Placenta 21, 443-450.

Gu, Y.Z., Hogenesch, J.B., Bradfield, C.A., 2000. The PAS superfamily: sensors of environmental and developmental signals. Annu Rev Pharmacol Toxicol 40, 519-561.

Gu, Y.Z., Moran, S.M., Hogenesch, J.B., Wartman, L., Bradfield, C.A., 1998. Molecular characterization and chromosomal localization of a third alpha-class hypoxia inducible factor subunit, HIF3alpha. Gene Expr 7, 205-213.

Guimond, M.J., Luross, J.A., Wang, B., Terhorst, C., Danial, S., Croy, B.A., 1997. Absence of natural killer cells during murine pregnancy is associated with reproductive compromise in TgE26 mice. Biol Reprod 56, 169-179.

Guo, X., Shi, M., Sun, L., Wang, Y., Gui, Y., Cai, Z., Duan, X., 2011. The expression of histone demethylase JMJD1A in renal cell carcinoma. Neoplasma 58, 153-157.

Hanna, J., Goldman-Wohl, D., Hamani, Y., Avraham, I., Greenfield, C., Natanson-Yaron, S., Prus, D., Cohen-Daniel, L., Arnon, T.I., Manaster, I., Gazit, R., Yutkin, V., Benharroch, D., Porgador, A., Keshet, E., Yagel, S., Mandelboim, O., 2006. Decidual NK cells regulate key developmental processes at the human fetal-maternal interface. Nat Med 12, 1065-1074.

Hanna, J., Mandelboim, O., 2007. When killers become helpers. Trends Immunol 28, 201-206.

Harris, L.K., 2010. Review: Trophoblast-vascular cell interactions in early pregnancy: how to remodel a vessel. Placenta 31 Suppl, S93-98.

Harris, L.K., Smith, S.D., Keogh, R.J., Jones, R.L., Baker, P.N., Knofler, M., Cartwright, J.E., Whitley, G.S., Aplin, J.D., 2010. Trophoblast- and vascular smooth muscle cell-derived MMP-12 mediates elastolysis during uterine spiral artery remodeling. The American journal of pathology 177, 2103-2115.

Hayashi, M., Sakata, M., Takeda, T., Tahara, M., Yamamoto, T., Okamoto, Y., Minekawa, R., Isobe, A., Ohmichi, M., Tasaka, K., Murata, Y., 2005. Up-regulation of c-met protooncogene product expression through hypoxia-inducible factor-1alpha is involved in trophoblast invasion under low-oxygen tension. Endocrinology 146, 4682-4689.

Head, J.R., 1996. Uterine natural killer cells during pregnancy in rodents. Nat Immun 15, 7-21.
Herzog, M., Josseaux, E., Dedeurwaerder, S., Calonne, E., Volkmar, M., Fuks, F., 2012. The histone demethylase Kdm3a is essential to progression through differentiation. Nucleic acids research 40, 7219-7232.

Hiby, S.E., Apps, R., Sharkey, A.M., Farrell, L.E., Gardner, L., Mulder, A., Claas, F.H., Walker, J.J., Redman, C.W., Morgan, L., Tower, C., Regan, L., Moore, G.E., Carrington, M., Moffett, A., 2010. Maternal activating KIRs protect against human reproductive failure mediated by fetal HLA-C2. J Clin Invest 120, 4102-4110.

Hiby, S.E., Walker, J.J., O'Shaughnessy K, M., Redman, C.W., Carrington, M., Trowsdale, J., Moffett, A., 2004. Combinations of maternal KIR and fetal HLA-C genes influence the risk of preeclampsia and reproductive success. J Exp Med 200, 957-965.

Ho-Chen, J.K., Ain, R., Alt, A.R., Wood, J.G., Gonzalez, N.C., Soares, M.J., 2006. Hypobaric hypoxia as a tool to study pregnancy-dependent responses at the maternal-fetal interface. Methods Mol Med 122, 427-434.

Ho-Chen, J.K., Bustamante, J.J., Soares, M.J., 2007. Prolactin-like protein-f subfamily of placental hormones/cytokines: responsiveness to maternal hypoxia. Endocrinology 148, 559-565.

Hockel, M., Vaupel, P., 2001. Tumor hypoxia: definitions and current clinical, biologic, and molecular aspects. J Natl Cancer Inst 93, 266-276.

Hu, C.J., Iyer, S., Sataur, A., Covello, K.L., Chodosh, L.A., Simon, M.C., 2006a. Differential regulation of the transcriptional activities of hypoxia-inducible factor 1 alpha (HIF-1alpha) and HIF-2alpha in stem cells. Mol Cell Biol 26, 3514-3526.

Hu, Y., Dutz, J.P., MacCalman, C.D., Yong, P., Tan, R., von Dadelszen, P., 2006b. Decidual NK cells alter *in vitro* first trimester extravillous cytotrophoblast migration: a role for IFN-gamma. J Immunol 177, 8522-8530.

Hu, Y., Eastabrook, G., Tan, R., MacCalman, C.D., Dutz, J.P., von Dadelszen, P., 2010. Decidual NK cell-derived conditioned medium enhances capillary tube and network organization in an extravillous cytotrophoblast cell line. Placenta 31, 213-221.

Hu, Y., Tan, R., Maccalman, C.D., Eastabrook, G., Park, S.H., Dutz, J.P., von Dadelszen, P., 2008. IFN-gamma-mediated extravillous trophoblast outgrowth inhibition in first trimester explant culture: a role for insulin-like growth factors. Mol Hum Reprod.

Hughes, M., Dobric, N., Scott, I.C., Su, L., Starovic, M., St-Pierre, B., Egan, S.E., Kingdom, J.C., Cross, J.C., 2004. The Hand1, Stra13 and Gcm1 transcription factors override FGF signaling to promote terminal differentiation of trophoblast stem cells. Dev Biol 271, 26-37.

Hunt, J.S., Miller, L., Vassmer, D., Croy, B.A., 1997. Expression of the inducible nitric oxide synthase gene in mouse uterine leukocytes and potential relationships with uterine function during pregnancy. Biol Reprod 57, 827-836.

Hunt, J.S., Petroff, M.G., Burnett, T.G., 2000. Uterine leukocytes: key players in pregnancy. Semin Cell Dev Biol 11, 127-137.

Hunter, R.G., McCarthy, K.J., Milne, T.A., Pfaff, D.W., McEwen, B.S., 2009. Regulation of hippocampal H3 histone methylation by acute and chronic stress. Proc Natl Acad Sci U S A 106, 20912-20917.

Hunter, R.G., Murakami, G., Dewell, S., Seligsohn, M., Baker, M.E., Datson, N.A., McEwen, B.S., Pfaff, D.W., 2012. Acute stress and hippocampal histone H3 lysine 9 trimethylation, a retrotransposon silencing response. Proc Natl Acad Sci U S A 109, 17657-17662.

Ikawa, M., Yamada, S., Nakanishi, T., Okabe, M., 1999. Green fluorescent protein (GFP) as a vital marker in mammals. Current topics in developmental biology 44, 1-20.

Imperatore, A., Rolfo, A., Petraglia, F., Challis, J.R., Caniggia, I., 2010. Hypoxia and preeclampsia: increased expression of urocortin 2 and urocortin 3. Reproductive sciences 17, 833-843.

Ivan, M., Kondo, K., Yang, H., Kim, W., Valiando, J., Ohh, M., Salic, A., Asara, J.M., Lane, W.S., Kaelin, W.G., Jr., 2001. HIFalpha targeted for VHL-mediated destruction by proline hydroxylation: implications for O2 sensing. Science 292, 464-468.

Iwatsuki, K., Shinozaki, M., Sun, W., Yagi, S., Tanaka, S., Shiota, K., 2000. A novel secretory protein produced by rat spongiotrophoblast. Biol Reprod 62, 1352-1359.

Jaakkola, P., Mole, D.R., Tian, Y.M., Wilson, M.I., Gielbert, J., Gaskell, S.J., Kriegsheim, A., Hebestreit, H.F., Mukherji, M., Schofield, C.J., Maxwell, P.H., Pugh, C.W., Ratcliffe, P.J., 2001a. Targeting of HIF-alpha to the von Hippel-Lindau ubiquitylation complex by O2-regulated prolyl hydroxylation. Science 292, 468-472.

Jaakkola, P., Mole, D.R., Tian, Y.M., Wilson, M.I., Gielbert, J., Gaskell, S.J., von Kriegsheim, A., Hebestreit, H.F., Mukherji, M., Schofield, C.J., Maxwell, P.H., Pugh, C.W., Ratcliffe, P.J., 2001b. Targeting of HIF-alpha to the von Hippel-Lindau ubiquitylation complex by O2-regulated prolyl hydroxylation. Science 292, 468-472.

James, J.L., Stone, P.R., Chamley, L.W., 2006a. The effects of oxygen concentration and gestational age on extravillous trophoblast outgrowth in a human first trimester villous explant model. Hum Reprod 21, 2699-2705.

James, J.L., Stone, P.R., Chamley, L.W., 2006b. The regulation of trophoblast differentiation by oxygen in the first trimester of pregnancy. Hum Reprod Update 12, 137-144.

Jasencakova, Z., Groth, A., 2010. Restoring chromatin after replication: how new and old histone marks come together. Semin Cell Dev Biol 21, 231-237.

Jiang, B., Kamat, A., Mendelson, C.R., 2000. Hypoxia prevents induction of aromatase expression in human trophoblast cells in culture: potential inhibitory role of the hypoxia-inducible transcription factor Mash-2 (mammalian achaete-scute homologous protein-2). Mol Endocrinol 14, 1661-1673.

Johnson, A.B., Denko, N., Barton, M.C., 2008. Hypoxia induces a novel signature of chromatin modifications and global repression of transcription. Mutation research 640, 174-179.

Kadyrov, M., Schmitz, C., Black, S., Kaufmann, P., Huppertz, B., 2003. Pre-eclampsia and maternal anaemia display reduced apoptosis and opposite invasive phenotypes of extravillous trophoblast. Placenta 24, 540-548.

Kalkunte, S.S., Mselle, T.F., Norris, W.E., Wira, C.R., Sentman, C.L., Sharma, S., 2009. Vascular endothelial growth factor C facilitates immune tolerance and endovascular activity of human uterine NK cells at the maternal-fetal interface. J Immunol 182, 4085-4092.

Kanasaki, K., Kalluri, R., 2009. The biology of preeclampsia. Kidney international 76, 831-837.
Kanasaki, K., Palmsten, K., Sugimoto, H., Ahmad, S., Hamano, Y., Xie, L., Parry, S., Augustin, H.G., Gattone, V.H., Folkman, J., Strauss, J.F., Kalluri, R., 2008. Deficiency in catechol-O-methyltransferase and 2-methoxyoestradiol is associated with pre-eclampsia. Nature 453, 1117-1121.

Kaufmann, P., Black, S., Huppertz, B., 2003. Endovascular trophoblast invasion: implications for the pathogenesis of intrauterine growth retardation and preeclampsia. Biol Reprod 69, 1-7.

Kawazu, M., Saso, K., Tong, K.I., McQuire, T., Goto, K., Son, D.O., Wakeham, A., Miyagishi, M., Mak, T.W., Okada, H., 2011. Histone demethylase JMJD2B functions as a co-factor of estrogen receptor in breast cancer proliferation and mammary gland development. PloS one 6, e17830.

Kilburn, B.A., Wang, J., Duniec-Dmuchowski, Z.M., Leach, R.E., Romero, R., Armant, D.R., 2000. Extracellular matrix composition and hypoxia regulate the expression of HLA-G and integrins in a human trophoblast cell line. Biol Reprod 62, 739-747.

Ko, S.Y., Kang, H.Y., Lee, H.S., Han, S.Y., Hong, S.H., 2006. Identification of Jmjd1a as a STAT3 downstream gene in mES cells. Cell structure and function 31, 53-62.

Koh, S.C., Anandakumar, C., Montan, S., Ratnam, S.S., 1993. Plasminogen activators, plasminogen activator inhibitors and markers of intravascular coagulation in pre-eclampsia. Gynecologic and obstetric investigation 35, 214-221.

Konno, T., Rempel, L.A., Arroyo, J.A., Soares, M.J., 2007. Pregnancy in the brown Norway rat: a model for investigating the genetics of placentation. Biol Reprod 76, 709-718.

Krieg, A.J., Rankin, E.B., Chan, D., Razorenova, O., Fernandez, S., Giaccia, A.J., 2010.

Regulation of the histone demethylase JMJD1A by hypoxia-inducible factor 1 alpha enhances hypoxic gene expression and tumor growth. Mol Cell Biol 30, 344-353.

Kruse, A., Hallmann, R., Butcher, E.C., 1999. Specialized patterns of vascular differentiation antigens in the pregnant mouse uterus and the placenta. Biol Reprod 61, 1393-1401.

Kruse, A., Martens, N., Fernekorn, U., Hallmann, R., Butcher, E.C., 2002. Alterations in the expression of homing-associated molecules at the maternal/fetal interface during the course of pregnancy. Biol Reprod 66, 333-345.

Lash, G.E., Bulmer, J.N., 2011. Do uterine natural killer (uNK) cells contribute to female reproductive disorders? J Reprod Immunol 88, 156-164.

Lash, G.E., Hornbuckle, J., Brunt, A., Kirkley, M., Searle, R.F., Robson, S.C., Bulmer, J.N., 2007. Effect of low oxygen concentrations on trophoblast-like cell line invasion. Placenta 28, 390-398.

Lash, G.E., Otun, H.A., Innes, B.A., Kirkley, M., De Oliveira, L., Searle, R.F., Robson, S.C., Bulmer, J.N., 2006a. Interferon-gamma inhibits extravillous trophoblast cell invasion by a mechanism that involves both changes in apoptosis and protease levels. FASEB J 20, 2512-2518.

Lash, G.E., Robson, S.C., Bulmer, J.N., 2010. Review: Functional role of uterine natural killer (uNK) cells in human early pregnancy decidua. Placenta 31 Suppl, S87-92.

Lash, G.E., Schiessl, B., Kirkley, M., Innes, B.A., Cooper, A., Searle, R.F., Robson, S.C., Bulmer, J.N., 2006b. Expression of angiogenic growth factors by uterine natural killer cells during early pregnancy. J Leukoc Biol 80, 572-580.

Laskowska, M., Laskowska, K., Leszczynska-Gorzelak, B., Oleszczuk, J., 2006. Evaluation of the maternal and umbilical vein serum sFas/sFasL system in pregnancies complicated by preeclampsia with intrauterine growth retardation. European journal of obstetrics, gynecology, and reproductive biology 126, 155-159.

Lee, D.S., Rumi, M.A., Konno, T., Soares, M.J., 2009. *In vivo* genetic manipulation of the rat trophoblast cell lineage using lentiviral vector delivery. Genesis 47, 433-439.

Leno-Duran, E., Hatta, K., Bianco, J., Yamada, A.T., Ruiz-Ruiz, C., Olivares, E.G., Croy, B.A., 2010. Fetal-placental hypoxia does not result from failure of spiral arterial modification in mice. Placenta 31, 731-737.

Levine, R.J., Maynard, S.E., Qian, C., Lim, K.H., England, L.J., Yu, K.F., Schisterman, E.F., Thadhani, R., Sachs, B.P., Epstein, F.H., Sibai, B.M., Sukhatme, V.P., Karumanchi, S.A., 2004. Circulating angiogenic factors and the risk of preeclampsia. The New England journal of medicine 350, 672-683.

Li, B., Carey, M., Workman, J.L., 2007. The role of chromatin during transcription. Cell 128, 707-719.

Li, X.F., Charnock-Jones, D.S., Zhang, E., Hiby, S., Malik, S., Day, K., Licence, D., Bowen, J.M., Gardner, L., King, A., Loke, Y.W., Smith, S.K., 2001. Angiogenic growth factor messenger ribonucleic acids in uterine natural killer cells. J Clin Endocrinol Metab 86, 1823-1834.

Librach, C.L., Werb, Z., Fitzgerald, M.L., Chiu, K., Corwin, N.M., Esteves, R.A., Grobelny, D., Galardy, R., Damsky, C.H., Fisher, S.J., 1991. 92-kD type IV collagenase mediates invasion of human cytotrophoblasts. The Journal of cell biology 113, 437-449.

Lindoff, C., Astedt, B., 1994. Plasminogen activator of urokinase type and its inhibitor of placental type in hypertensive pregnancies and in intrauterine growth retardation: possible markers of placental function. Am J Obstet Gynecol 171, 60-64.

Liu, C.C., Young, J.D., 2001. Uterine natural killer cells in the pregnant uterus. Advances in immunology 79, 297-329.

Liu, Z., Zhou, S., Liao, L., Chen, X., Meistrich, M., Xu, J., 2010. Jmjd1a demethylase-regulated histone modification is essential for cAMP-response element modulator-regulated gene expression and spermatogenesis. J Biol Chem 285, 2758-2770.

Lockman, K., Taylor, J.M., Mack, C.P., 2007. The histone demethylase, Jmjd1a, interacts with the myocardin factors to regulate SMC differentiation marker gene expression. Circulation research 101, e115-123.

Loh, Y.H., Zhang, W., Chen, X., George, J., Ng, H.H., 2007. Jmjd1a and Jmjd2c histone H3 Lys 9 demethylases regulate self-renewal in embryonic stem cells. Genes Dev 21, 2545-2557.

Loyola, A., Tagami, H., Bonaldi, T., Roche, D., Quivy, J.P., Imhof, A., Nakatani, Y., Dent, S.Y., Almouzni, G., 2009. The HP1alpha-CAF1-SetDB1-containing complex provides H3K9me1 for Suv39-mediated K9me3 in pericentric heterochromatin. EMBO reports 10, 769-775.

Lu, B., Geurts, A.M., Poirier, C., Petit, D.C., Harrison, W., Overbeek, P.A., Bishop, C.E., 2007. Generation of rat mutants using a coat color-tagged Sleeping Beauty transposon system. Mammalian genome : official journal of the International Mammalian Genome Society 18, 338-346.

Luo, W., Chang, R., Zhong, J., Pandey, A., Semenza, G.L., 2012. Histone demethylase JMJD2C is a coactivator for hypoxia-inducible factor 1 that is required for breast cancer progression. Proc Natl Acad Sci U S A 109, E3367-3376.

Madeja, Z., Yadi, H., Apps, R., Boulenouar, S., Roper, S.J., Gardner, L., Moffett, A., Colucci, F., Hemberger, M., 2011. Paternal MHC expression on mouse trophoblast affects uterine vascularization and fetal growth. Proc Natl Acad Sci U S A 108, 4012-4017.

Majmundar, A.J., Wong, W.J., Simon, M.C., 2010. Hypoxia-inducible factors and the response to hypoxic stress. Molecular cell 40, 294-309.

Maltepe, E., Krampitz, G.W., Okazaki, K.M., Red-Horse, K., Mak, W., Simon, M.C., Fisher, S.J., 2005. Hypoxia-inducible factor-dependent histone deacetylase activity determines stem cell fate in the placenta. Development 132, 3393-3403.

Martindill, D.M., Risebro, C.A., Smart, N., Franco-Viseras Mdel, M., Rosario, C.O., Swallow, C.J., Dennis, J.W., Riley, P.R., 2007. Nucleolar release of Hand1 acts as a molecular switch to determine cell fate. Nature cell biology 9, 1131-1141.

Maynard, S.E., Karumanchi, S.A., 2011. Angiogenic factors and preeclampsia. Seminars in nephrology 31, 33-46.

Maynard, S.E., Min, J.Y., Merchan, J., Lim, K.H., Li, J., Mondal, S., Libermann, T.A., Morgan, J.P., Sellke, F.W., Stillman, I.E., Epstein, F.H., Sukhatme, V.P., Karumanchi, S.A., 2003. Excess placental soluble fms-like tyrosine kinase 1 (sFlt1) may contribute to endothelial dysfunction, hypertension, and proteinuria in preeclampsia. J Clin Invest 111, 649-658.

Melvin, A., Rocha, S., 2012. Chromatin as an oxygen sensor and active player in the hypoxia response. Cellular signalling 24, 35-43.

Mimura, I., Nangaku, M., Kanki, Y., Tsutsumi, S., Inoue, T., Kohro, T., Yamamoto, S., Fujita, T., Shimamura, T., Suehiro, J., Taguchi, A., Kobayashi, M., Tanimura, K., Inagaki, T., Tanaka, T., Hamakubo, T., Sakai, J., Aburatani, H., Kodama, T., Wada, Y., 2012. Dynamic change of chromatin conformation in response to hypoxia enhances the expression of GLUT3 (SLC2A3) by cooperative interaction of hypoxia-inducible factor 1 and KDM3A. Mol Cell Biol 32, 3018-3032.

Moffett-King, A., 2002. Natural killer cells and pregnancy. Nat Rev Immunol 2, 656-663.

Moffett, A., Loke, C., 2006a. Immunology of placentation in eutherian mammals. Nat Rev Immunol 6, 584-594.

Moffett, A., Loke, C., 2006b. Implantation, embryo-maternal interactions, immunology and modulation of the uterine environment -- a workshop report. Placenta 27 Suppl A, S54-55.

Monk, J.M., Leonard, S., McBey, B.A., Croy, B.A., 2005. Induction of murine spiral artery modification by recombinant human interferon-gamma. Placenta 26, 835-838.

Mosammaparast, N., Shi, Y., 2010. Reversal of histone methylation: biochemical and molecular mechanisms of histone demethylases. Annual review of biochemistry 79, 155-179.

Muller, H., Liu, B., Croy, B.A., Head, J.R., Hunt, J.S., Dai, G., Soares, M.J., 1999. Uterine natural killer cells are targets for a trophoblast cell-specific cytokine, prolactin-like protein A. Endocrinology 140, 2711-2720.

Murphy, S.P., Fast, L.D., Hanna, N.N., Sharma, S., 2005. Uterine NK cells mediate inflammation-induced fetal demise in IL-10-null mice. J Immunol 175, 4084-4090.

Murphy, S.P., Tayade, C., Ashkar, A.A., Hatta, K., Zhang, J., Croy, B.A., 2009. Interferon Gamma in Successful Pregnancies. Biol Reprod.

Myatt, L., 2006. Placental adaptive responses and fetal programming. The Journal of physiology 572, 25-30.

Neale, D.M., Mor, G., 2005. The role of Fas mediated apoptosis in preeclampsia. Journal of perinatal medicine 33, 471-477.

Nelson, D.M., Johnson, R.D., Smith, S.D., Anteby, E.Y., Sadovsky, Y., 1999. Hypoxia limits differentiation and up-regulates expression and activity of prostaglandin H synthase 2 in cultured trophoblast from term human placenta. Am J Obstet Gynecol 180, 896-902.

Nevo, O., Many, A., Xu, J., Kingdom, J., Piccoli, E., Zamudio, S., Post, M., Bocking, A., Todros, T., Caniggia, I., 2008. Placental expression of soluble fms-like tyrosine kinase 1 is increased in singletons and twin pregnancies with intrauterine growth restriction. J Clin Endocrinol Metab 93, 285-292.

Nevo, O., Soleymanlou, N., Wu, Y., Xu, J., Kingdom, J., Many, A., Zamudio, S., Caniggia, I., 2006. Increased expression of sFlt-1 in *in vivo* and *in vitro* models of human placental hypoxia is mediated by HIF-1. American journal of physiology. Regulatory, integrative and comparative physiology 291, R1085-1093.

Noda, T., Yamamoto, H., Takemasa, I., Yamada, D., Uemura, M., Wada, H., Kobayashi, S., Marubashi, S., Eguchi, H., Tanemura, M., Umeshita, K., Doki, Y., Mori, M., Nagano, H., 2012. PLOD2 induced under hypoxia is a novel prognostic factor for hepatocellular carcinoma after curative resection. Liver international : official journal of the International Association for the Study of the Liver 32, 110-118.

Nottke, A., Colaiacovo, M.P., Shi, Y., 2009. Developmental roles of the histone lysine demethylases. Development 136, 879-889.

Okada, Y., Scott, G., Ray, M.K., Mishina, Y., Zhang, Y., 2007. Histone demethylase JHDM2A is critical for Tnp1 and Prm1 transcription and spermatogenesis. Nature 450, 119-123.

Parast, M.M., Yu, H., Ciric, A., Salata, M.W., Davis, V., Milstone, D.S., 2009. PPARgamma regulates trophoblast proliferation and promotes labyrinthine trilineage differentiation. PloS one 4, e8055.

Parham, P., 2004. NK cells and trophoblasts: partners in pregnancy. J Exp Med 200, 951-955.
Pedersen, M.T., Helin, K., 2010. Histone demethylases in development and disease. Trends in cell biology 20, 662-671.

Peel, S., 1989. Granulated metrial gland cells. Adv Anat Embryol Cell Biol 115, 1-112.
Perez-Sepulveda, A., Torres, M.J., Valenzuela, F.J., Larrain, R., Figueroa-Diesel, H., Galaz, J., Nien, J.K., Serra, R., Michea, L., Illanes, S.E., 2012. Low 2-methoxyestradiol levels at the first trimester of pregnancy are associated with the development of pre-eclampsia. Prenatal diagnosis 32, 1053-1058.

Peters, T.J., Albieri, A., Bevilacqua, E., Chapman, B.M., Crane, L.H., Hamlin, G.P., Seiki, M., Soares, M.J., 1999. Differentiation-dependent expression of gelatinase B/matrix metalloproteinase-9 in trophoblast cells. Cell Tissue Res 295, 287-296.

Pijnenborg, R., Bland, J.M., Robertson, W.B., Dixon, G., Brosens, I., 1981a. The pattern of interstitial trophoblastic invasion of the myometrium in early human pregnancy. Placenta 2, 303-316.

Pijnenborg, R., Robertson, W.B., Brosens, I., Dixon, G., 1981b. Review article: trophoblast invasion and the establishment of haemochorial placentation in man and laboratory animals. Placenta 2, 71-91.

Pijnenborg, R., Vercruysse, L., Hanssens, M., 2006. The uterine spiral arteries in human pregnancy: facts and controversies. Placenta 27, 939-958.

Pollard, P.J., Loenarz, C., Mole, D.R., McDonough, M.A., Gleadle, J.M., Schofield, C.J., Ratcliffe, P.J., 2008. Regulation of Jumonji-domain-containing histone demethylases by hypoxia-inducible factor (HIF)-1alpha. The Biochemical journal 416, 387-394.

Powe, C.E., Levine, R.J., Karumanchi, S.A., 2011. Preeclampsia, a disease of the maternal endothelium: the role of antiangiogenic factors and implications for later cardiovascular disease. Circulation 123, 2856-2869.

Pringle, K.G., Kind, K.L., Thompson, J.G., Roberts, C.T., 2007. Complex interactions between hypoxia inducible factors, insulin-like growth factor-II and oxygen in early murine trophoblasts. Placenta 28, 1147-1157.

Qi, H.H., Sarkissian, M., Hu, G.Q., Wang, Z., Bhattacharjee, A., Gordon, D.B., Gonzales, M., Lan, F., Ongusaha, P.P., Huarte, M., Yaghi, N.K., Lim, H., Garcia, B.A., Brizuela, L., Zhao, K., Roberts, T.M., Shi, Y., 2010. Histone H4K20/H3K9 demethylase PHF8 regulates zebrafish brain and craniofacial development. Nature 466, 503-507.

Rajakumar, A., Doty, K., Daftary, A., Markovic, N., Conrad, K.P., 2006. Expression of von Hippel Lindau (pVHL) protein in placentae from normal pregnant women and women with preeclampsia. Placenta 27, 411-421.

Rajakumar, A., Michael, H.M., Daftary, A., Jeyabalan, A., Gilmour, C., Conrad, K.P., 2008. Proteasomal activity in placentas from women with preeclampsia and intrauterine growth restriction: implications for expression of HIF-alpha proteins. Placenta 29, 290-299.

Raval, R.R., Lau, K.W., Tran, M.G., Sowter, H.M., Mandriota, S.J., Li, J.L., Pugh, C.W., Maxwell, P.H., Harris, A.L., Ratcliffe, P.J., 2005. Contrasting properties of hypoxia-inducible factor 1 (HIF-1) and HIF-2 in von Hippel-Lindau-associated renal cell carcinoma. Mol Cell Biol 25, 5675-5686.

Red-Horse, K., Rivera, J., Schanz, A., Zhou, Y., Winn, V., Kapidzic, M., Maltepe, E., Okazaki, K., Kochman, R., Vo, K.C., Giudice, L., Erlebacher, A., McCune, J.M., Stoddart, C.A., Fisher, S.J., 2006. Cytotrophoblast induction of arterial apoptosis and lymphangiogenesis in an *in vivo* model of human placentation. J Clin Invest 116, 2643-2652.

Red-Horse, K., Zhou, Y., Genbacev, O., Prakobphol, A., Foulk, R., McMaster, M., Fisher, S.J., 2004. Trophoblast differentiation during embryo implantation and formation of the maternal-fetal interface. J Clin Invest 114, 744-754.

Redman, C.W., Sargent, I.L., 2005. Latest advances in understanding preeclampsia. Science 308, 1592-1594.

Reister, F., Kingdom, J.C., Ruck, P., Marzusch, K., Heyl, W., Pauer, U., Kaufmann, P., Rath, W., Huppertz, B., 2006. Altered protease expression by periarterial trophoblast cells in severe early-onset preeclampsia with IUGR. Journal of perinatal medicine 34, 272-279.

Rielland, M., Hue, I., Renard, J.P., Alice, J., 2008. Trophoblast stem cell derivation, cross-species comparison and use of nuclear transfer: new tools to study trophoblast growth and differentiation. Dev Biol 322, 1-10.

Roberts, R.M., Fisher, S.J., 2011. Trophoblast stem cells. Biol Reprod 84, 412-421.

Robins, J.C., Heizer, A., Hardiman, A., Hubert, M., Handwerger, S., 2007. Oxygen tension directs the differentiation pathway of human cytotrophoblast cells. Placenta 28, 1141-1146.

Rodesch, F., Simon, P., Donner, C., Jauniaux, E., 1992. Oxygen measurements in endometrial and trophoblastic tissues during early pregnancy. Obstet Gynecol 80, 283-285.

Rolfo, A., Many, A., Racano, A., Tal, R., Tagliaferro, A., Ietta, F., Wang, J., Post, M., Caniggia, I., 2010. Abnormalities in oxygen sensing define early and late onset preeclampsia as distinct pathologies. PloS one 5, e13288.

Rosario, G.X., Konno, T., Soares, M.J., 2008. Maternal hypoxia activates endovascular trophoblast cell invasion. Dev Biol 314, 362-375.

Roten, L.T., Fenstad, M.H., Forsmo, S., Johnson, M.P., Moses, E.K., Austgulen, R., Skorpen, F., 2011. A low COMT activity haplotype is associated with recurrent preeclampsia in a Norwegian population cohort (HUNT2). Mol Hum Reprod 17, 439-446.

Rugg-Gunn, P.J., Cox, B.J., Ralston, A., Rossant, J., 2010. Distinct histone modifications in stem cell lines and tissue lineages from the early mouse embryo. Proc Natl Acad Sci U S A 107, 10783-10790.

Samoszuk, M.K., Walter, J., Mechetner, E., 2004. Improved immunohistochemical method for detecting hypoxia gradients in mouse tissues and tumors. The journal of histochemistry and cytochemistry : official journal of the Histochemistry Society 52, 837-839.

Sarbassov, D.D., Ali, S.M., Sabatini, D.M., 2005a. Growing roles for the mTOR pathway. Current opinion in cell biology 17, 596-603.

Sarbassov, D.D., Guertin, D.A., Ali, S.M., Sabatini, D.M., 2005b. Phosphorylation and regulation of Akt/PKB by the rictor-mTOR complex. Science 307, 1098-1101.

Sargent, I.L., Borzychowski, A.M., Redman, C.W., 2006. NK cells and human pregnancy--an inflammatory view. Trends Immunol 27, 399-404.
Schofield, C.J., Ratcliffe, P.J., 2004. Oxygen sensing by HIF hydroxylases. Nat Rev Mol Cell Biol 5, 343-354.

Scifres, C.M., Nelson, D.M., 2009. Intrauterine growth restriction, human placental development and trophoblast cell death. The Journal of physiology 587, 3453-3458.

Sebastiano, V., Dalvai, M., Gentile, L., Schubart, K., Sutter, J., Wu, G.M., Tapia, N., Esch, D., Ju, J.Y., Hubner, K., Bravo, M.J., Scholer, H.R., Cavaleri, F., Matthias, P., 2010. Oct1 regulates trophoblast development during early mouse embryogenesis. Development 137, 3551-3560.

Semenza, G.L., 2000. HIF-1 and human disease: one highly involved factor. Genes Dev 14, 1983-1991.

Semenza, G.L., 2001. Hypoxia-inducible factor 1: oxygen homeostasis and disease pathophysiology. Trends Mol Med 7, 345-350.

Semenza, G.L., 2010. Oxygen homeostasis. Wiley interdisciplinary reviews. Systems biology and medicine 2, 336-361.

Seol, H.J., Cho, G.J., Oh, M.J., Kim, H.J., 2012. 2-Methoxyoestradiol levels and placental catechol-O-methyltransferase expression in patients with late-onset preeclampsia. Archives of gynecology and obstetrics.

Shakya, A., Kang, J., Chumley, J., Williams, M.A., Tantin, D., 2011. Oct1 is a switchable, bipotential stabilizer of repressed and inducible transcriptional states. J Biol Chem 286, 450-459.
Simmons, D.G., Cross, J.C., 2005. Determinants of trophoblast lineage and cell subtype specification in the mouse placenta. Dev Biol 284, 12-24.

Simon, M.C., Keith, B., 2008. The role of oxygen availability in embryonic development and stem cell function. Nat Rev Mol Cell Biol 9, 285-296.
Smith, S.D., Dunk, C.E., Aplin, J.D., Harris, L.K., Jones, R.L., 2009. Evidence for immune cell involvement in decidual spiral arteriole remodeling in early human pregnancy. The American journal of pathology 174, 1959-1971.

Stolze, I.P., Tian, Y.M., Appelhoff, R.J., Turley, H., Wykoff, C.C., Gleadle, J.M., Ratcliffe, P.J., 2004. Genetic analysis of the role of the asparaginyl hydroxylase factor inhibiting hypoxia-inducible factor (FIH) in regulating hypoxia-inducible factor (HIF) transcriptional target genes [corrected]. J Biol Chem 279, 42719-42725.

Strobl-Mazzulla, P.H., Sauka-Spengler, T., Bronner-Fraser, M., 2010. Histone demethylase JmjD2A regulates neural crest specification. Developmental cell 19, 460-468.

Takeda, K., Ho, V.C., Takeda, H., Duan, L.J., Nagy, A., Fong, G.H., 2006. Placental but not heart defects are associated with elevated hypoxia-inducible factor alpha levels in mice lacking prolyl hydroxylase domain protein 2. Mol Cell Biol 26, 8336-8346.

Takemori, K., Okamura, H., Kanzaki, H., Koshida, M., Konishi, I., 1984. Scanning electron microscopy study on corrosion cast of rat uterine vasculature during the first half of pregnancy. J Anat 138 (Pt 1), 163-173.

Takemori, K., Okamura, H., Kanzaki, H., Koshida, M., Konishi, I., Mori, T., 1985. Scanning electron microscopy study on corrosion casts of rat uterine vasculature during the second half of pregnancy and post partum. J Anat 142, 21-31.

Tal, R., 2012. The role of hypoxia and hypoxia-inducible factor-1Alpha in preeclampsia pathogenesis. Biol Reprod 87, 134.

Tanaka, S., Kunath, T., Hadjantonakis, A.K., Nagy, A., Rossant, J., 1998. Promotion of trophoblast stem cell proliferation by FGF4. Science 282, 2072-2075.

Tateishi, K., Okada, Y., Kallin, E.M., Zhang, Y., 2009. Role of Jhdm2a in regulating metabolic gene expression and obesity resistance. Nature 458, 757-761.

Tejera, E., Bernardes, J., Rebelo, I., 2012. Preeclampsia: a bioinformatics approach through protein-protein interaction networks analysis. BMC systems biology 6, 97.

Thornburg, K.L., O'Tierney, P.F., Louey, S., 2010a. Review: The placenta is a programming agent for cardiovascular disease. Placenta 31 Suppl, S54-59.

Thornburg, K.L., Shannon, J., Thuillier, P., Turker, M.S., 2010b. In utero life and epigenetic predisposition for disease. Advances in genetics 71, 57-78.

Tong, C., Huang, G., Ashton, C., Li, P., Ying, Q.L., 2011. Generating gene knockout rats by homologous recombination in embryonic stem cells. Nature protocols 6, 827-844.

Towbin, B.D., Gonzalez-Aguilera, C., Sack, R., Gaidatzis, D., Kalck, V., Meister, P., Askjaer, P., Gasser, S.M., 2012. Step-wise methylation of histone H3K9 positions heterochromatin at the nuclear periphery. Cell 150, 934-947.

Trowsdale, J., Moffett, A., 2008. NK receptor interactions with MHC class I molecules in pregnancy. Semin Immunol 20, 317-320.

Tuuli, M.G., Longtine, M.S., Nelson, D.M., 2011. Review: Oxygen and trophoblast biology--a source of controversy. Placenta 32 Suppl 2, S109-118.

Uy, G.D., Downs, K.M., Gardner, R.L., 2002. Inhibition of trophoblast stem cell potential in chorionic ectoderm coincides with occlusion of the ectoplacental cavity in the mouse. Development 129, 3913-3924.

Vanharanta, S., Shu, W., Brenet, F., Hakimi, A.A., Heguy, A., Viale, A., Reuter, V.E., Hsieh, J.J., Scandura, J.M., Massague, J., 2013. Epigenetic expansion of VHL-HIF signal output drives multiorgan metastasis in renal cancer. Nat Med 19, 50-56.

Vercruysse, L., Caluwaerts, S., Luyten, C., Pijnenborg, R., 2006. Interstitial trophoblast invasion in the decidua and mesometrial triangle during the last third of pregnancy in the rat. Placenta 27, 22-33.

Verrier, L., Vandromme, M., Trouche, D., 2011. Histone demethylases in chromatin cross-talks. Biology of the cell / under the auspices of the European Cell Biology Organization 103, 381-401.

Vicovac, L., Aplin, J.D., 1996. Epithelial-mesenchymal transition during trophoblast differentiation. Acta anatomica 156, 202-216.

Wang, C., Tanaka, T., Nakamura, H., Umesaki, N., Hirai, K., Ishiko, O., Ogita, S., Kaneda, K., 2003. Granulated metrial gland cells in the murine uterus: localization, kinetics, and the functional role in angiogenesis during pregnancy. Microscopy research and technique 60, 420-429.

Wang, C., Umesaki, N., Nakamura, H., Tanaka, T., Nakatani, K., Sakaguchi, I., Ogita, S., Kaneda, K., 2000. Expression of vascular endothelial growth factor by granulated metrial gland cells in pregnant murine uteri. Cell Tissue Res 300, 285-293.

Wang, G.L., Jiang, B.H., Rue, E.A., Semenza, G.L., 1995. Hypoxia-inducible factor 1 is a basic-helix-loop-helix-PAS heterodimer regulated by cellular O2 tension. Proc Natl Acad Sci U S A 92, 5510-5514.

Wang, G.L., Semenza, G.L., 1995. Purification and characterization of hypoxia-inducible factor 1. J Biol Chem 270, 1230-1237.

Wang, Z., Lu, S., Liu, C., Zhao, B., Pei, K., Tian, L., Ma, X., 2010. Expressional and epigenetic alterations of placental matrix metalloproteinase 9 in preeclampsia. Gynecological

endocrinology: the official journal of the International Society of Gynecological Endocrinology 26, 96-102.

Wellmann, S., Bettkober, M., Zelmer, A., Seeger, K., Faigle, M., Eltzschig, H.K., Buhrer, C., 2008. Hypoxia upregulates the histone demethylase JMJD1A via HIF-1. Biochemical and biophysical research communications 372, 892-897.

Wen, B., Wu, H., Shinkai, Y., Irizarry, R.A., Feinberg, A.P., 2009. Large histone H3 lysine 9 dimethylated chromatin blocks distinguish differentiated from embryonic stem cells. Nature genetics 41, 246-250.

Whitley, G.S., Cartwright, J.E., 2010. Cellular and molecular regulation of spiral artery remodelling: lessons from the cardiovascular field. Placenta 31, 465-474.

Wiemers, D.O., Ain, R., Ohboshi, S., Soares, M.J., 2003. Migratory trophoblast cells express a newly identified member of the prolactin gene family. J Endocrinol 179, 335-346.

Wiesener, M.S., Jurgensen, J.S., Rosenberger, C., Scholze, C.K., Horstrup, J.H., Warnecke, C., Mandriota, S., Bechmann, I., Frei, U.A., Pugh, C.W., Ratcliffe, P.J., Bachmann, S., Maxwell, P.H., Eckardt, K.U., 2003. Widespread hypoxia-inducible expression of HIF-2alpha in distinct cell populations of different organs. FASEB J 17, 271-273.

Williams, P.J., Bulmer, J.N., Searle, R.F., Innes, B.A., Robson, S.C., 2009. Altered decidual leucocyte populations in the placental bed in pre-eclampsia and foetal growth restriction: a comparison with late normal pregnancy. Reproduction 138, 177-184.

Wong, C.C., Zhang, H., Gilkes, D.M., Chen, J., Wei, H., Chaturvedi, P., Hubbi, M.E., Semenza, G.L., 2012. Inhibitors of hypoxia-inducible factor 1 block breast cancer metastatic niche formation and lung metastasis. Journal of molecular medicine 90, 803-815

Xie, Y., Awonuga, A.O., Zhou, S., Puscheck, E.E., Rappolee, D.A., 2011. Interpreting the stress response of early mammalian embryos and their stem cells. International review of cell and molecular biology 287, 43-95.

Yamada, D., Kobayashi, S., Yamamoto, H., Tomimaru, Y., Noda, T., Uemura, M., Wada, H., Marubashi, S., Eguchi, H., Tanemura, M., Doki, Y., Mori, M., Nagano, H., 2012. Role of the hypoxia-related gene, JMJD1A, in hepatocellular carcinoma: clinical impact on recurrence after hepatic resection. Annals of surgical oncology 19 Suppl 3, S355-364.

Yamane, K., Toumazou, C., Tsukada, Y., Erdjument-Bromage, H., Tempst, P., Wong, J., Zhang, Y., 2006. JHDM2A, a JmjC-containing H3K9 demethylase, facilitates transcription activation by androgen receptor. Cell 125, 483-495.

Yamashita, K., Discher, D.J., Hu, J., Bishopric, N.H., Webster, K.A., 2001. Molecular regulation of the endothelin-1 gene by hypoxia. Contributions of hypoxia-inducible factor-1, activator protein-1, GATA-2, AND p300/CBP. J Biol Chem 276, 12645-12653.

Yang, J., Ledaki, I., Turley, H., Gatter, K.C., Montero, J.C., Li, J.L., Harris, A.L., 2009. Role of hypoxia-inducible factors in epigenetic regulation via histone demethylases. Annals of the New York Academy of Sciences 1177, 185-197.

Yinon, Y., Nevo, O., Xu, J., Many, A., Rolfo, A., Todros, T., Post, M., Caniggia, I., 2008. Severe intrauterine growth restriction pregnancies have increased placental endoglin levels: hypoxic regulation via transforming growth factor-beta 3. The American journal of pathology 172, 77-85.

Zamudio, S., 2003. The placenta at high altitude. High altitude medicine & biology 4, 171-191.

Zamudio, S., Torricos, T., Fik, E., Oyala, M., Echalar, L., Pullockaran, J., Tutino, E., Martin, B., Belliappa, S., Balanza, E., Illsley, N.P., 2010. Hypoglycemia and the origin of hypoxia-induced reduction in human fetal growth. PloS one 5, e8551.

Zamudio, S., Wu, Y., Ietta, F., Rolfo, A., Cross, A., Wheeler, T., Post, M., Illsley, N.P.,

Caniggia, I., 2007. Human placental hypoxia-inducible factor-1alpha expression correlates with clinical outcomes in chronic hypoxia *in vivo*. The American journal of pathology 170, 2171-2179.

Zhang, J., Chen, Z., Smith, G.N., Croy, B.A., 2011. Natural killer cell-triggered vascular transformation: maternal care before birth? Cellular & molecular immunology 8, 1-11.

Zhou, S., Xie, Y., Puscheck, E.E., Rappolee, D.A., 2011. Oxygen levels that optimize TSC culture are identified by maximizing growth rates and minimizing stress. Placenta 32, 475-481.

Zhou, Y., Chiu, K., Brescia, R.J., Combs, C.A., Katz, M.A., Kitzmiller, J.L., Heilbron, D.C., Fisher, S.J., 1993. Increased depth of trophoblast invasion after chronic constriction of the lower aorta in rhesus monkeys. Am J Obstet Gynecol 169, 224-229.

Zhou, Y., Fisher, S.J., Janatpour, M., Genbacev, O., Dejana, E., Wheelock, M., Damsky, C.H., 1997. Human cytotrophoblasts adopt a vascular phenotype as they differentiate. A strategy for successful endovascular invasion? J Clin Invest 99, 2139-2151.

APPENDICES

APPENDIX A

Table A1.1. Genes associated with the biopathways analyzed by Ingenuity Pathway Analysis

Category	Functions annotations	p- value	Predicted activation state	Activation Z score	Molecules
Cell Cycle	segregation of chromosomes	3.66E-06	Decreased	-2.138	BUB1 (includes EG:100307076),CCNA2,CCNB1,CCNB2,CIT,DDX11/DDX12P,EBNA1BP2,ECT2,ESPL1,GPSM2,KIF2C,NCAPD2,NCAPD3,PLK1,PTTG1,SKA2,SPC25 (includes EG:100144563),SYCP3,TOP2A,ZW10
Cellular Assembly and Organization	segregation of chromosomes	3.66E-06	Decreased	-2.138	BUB1 (includes EG:100307076),CCNA2,CCNB1,CCNB2,CIT,DDX11/DDX12P,EBNA1BP2,ECT2,ESPL1,GPSM2,KIF2C,NCAPD2,NCAPD3,PLK1,PTTG1,SKA2,SPC25 (includes EG:100144563),SYCP3,TOP2A,ZW10
DNA Replication, Recombination, and Repair	segregation of chromosomes	3.66E-06	Decreased	-2.138	BUB1 (includes EG:100307076),CCNA2,CCNB1,CCNB2,CIT,DDX11/DDX12P,EBNA1BP2,ECT2,ESPL1,GPSM2,KIF2C,NCAPD2,NCAPD3,PLK1,PTTG1,SKA2,SPC25 (includes EG:100144563),SYCP3,TOP2A,ZW10
Cellular Growth and Proliferation	proliferation of cells	3.01E-05	Decreased	-2.553	AATF,ACACA,ACTN1,ADAM15,ADM,AFAP1L1,AK4,AKT1S1,ALKBH1,ANP32A,APBB2,APEX1,APPL1,ARID5B,ARIH2,ATF4,ATF6,ATIC,AURKA,B4GALT6,BARX1,BBC3,BCAT1,BCCIP,BCL3,BCL6,BCR,BHLHE40,BHLHE41,BMP4,BMPR1A,BMPR2,BNIP3,BSG,BTG2,BUB1 (includes EG:100307076),BYSL,C10orf54,C14orf169,CASP6,CBLB,CCDC92,CCNA2,CCNB1,CCNG1,CCNG2,CCNI,CD164,CD82,CDC20 (includes EG:107995),CDCA8,CDCP1,CDH1,CDKN1B,CHCHD6,CHEK1,CITED2,CLDN15,CLDN4,CLK1,CLTC,COMMD5,COMT,CREM (includes EG:12916),CTSF,CUL7,CYP20A1,DDB1,DDIT3,DDX11/DDX12P,DDX21,DDX56,DHPS,DNAJB1,DNAJB2,DNAJB6,DNM1L,DUSP1,E2F5,E2F8,EBNA1BP2,ECT2,EFEMP2,EFNA1,EFS,EGLN1,EGLN3,EGR1,EIF2AK4,EIF2B1,EIF4EBP1,EIF4G2,ELF3,ELL,EMP3,EOMES,EPS8,ERO1L,ERRFI1,ESPL1,ETV5,EXOSC2,EXOSC4,EXOSC9,F11R,FABP3,FASLG,FASN,FBLN1,FKBP5,FLOT2,FOXO4,FRMD6,FRS2,FTSJ3,GADD45A,GADD45B,GCAT,GCLC,GFER,GIPC1,GNG2,GNL3,GPI,GPNMB,GRB2,GSS,GTPBP4,H2AFX,H2AFY,HAND1,HBP1,HDAC5,HDAC6,HELLS,HES6,HEXB,HIF1A,HK1,HK2,HNRNPAB,HS6ST1,HSP90B1,HSPA1A/HSPA1B,HYAL2,ID1,ID2,ID3,IER3,IGF2BP3,IGFBP2,IL11RA,IL23A,IL33,IL6ST,INSIG1,IRF

					2,ITGA3,ITGA7,IVNS1ABP,JUN,KIA A0101,KIF20A,KIF2C,KLF4,KPNA2,K SR1,LAMC1,LIN28A,LMNB1,LMNB2, LTBP1,MAD1L1,MAFF,MAGED2,MA P3K1,MAP3K7 (includes EG:26409),MAP3K8,MAPK14,MAPT, MFSD12,MGAT1,MIF,MLLT3,MMP12 ,MMP9,MN1,MSX1,MT1E,MT1H,MT HFD1,MYBBP1A,MYC,MYCL1,NAE1 ,NAMPT,NASP,NCOA3,NDE1 (includes EG:54820),NDUFAF4,NF2,NOA1,NOL 8,NOLC1,NOP2,NOTCH2,NPDC1,NPY ,NQO1,NRF1,NTAN1,NUB1,NUBP1,N UDC,OSTF1,PAK1IP1,PAWR,PDCD4, PDGFA,PDIA3,PDXK,PGK1,Phb,PHC1 ,PHLDA2,PI4KA,PIK3CA,PLAT,PLAU ,PLIN3,PLK1,PNPT1,POLD4,POMGN T1,PPAN,PPAT,PPM1D,PPP2R1B,PRD X3,PREB,PRG2,PRKCD,PRMT1,PRPF 4B,PSAP,PSMB10,PSMC4,PSMC5,PS ME3,PTHLH,PTTG1,Pvr,RAD51,RAF1 ,RALB,RASD1,RBBP7,RBM3,RBM38, Rbpj,RBPJ,RHOB,RNF139,RNF2,RNF4 ,RORA,RRM2,S1PR1,SATB1,SCAMP2 ,SCPEP1,SDC1 (includes EG:20969),SENP1,SERPINH1,SET,SF3 B3,SFN,SHMT1,SLC2A1,SLC9A3R1,S MAD2,SMARCB1,SMC3,SOS1,SPHK1 ,SRC,SREBF1,SRSF2,SRSF3,SRSF5,SS BP1,SSBP3,STMN1,STRN,SURF4,TA CC1,TBP,TBRG4,TCOF1,TERF1,TES, TFAP2A,TFPI,TFRC,TGM2 (includes EG:21817),THOC1,TIMELESS,TJP2,T NFRSF12A,TOB1,TOP2A,TSC22D1,T SPAN31,TSPO,TTC5,TUSC2,TXNL1,T YMS,UBE2C,UHRF2,UPP1,USP10,UT P20,VAMP8,VDAC1,VEGFA,VHL,VL DLR,WDR12,WDR77,WIPF1,WNK2, WTAP,WWTR1,YPEL3,ZFP36L2,ZNF 259
Cellular Growth and Proliferation	cytostasis	1.20E-03	Decreased	-2.483	ANP32A,BCL6,BCR,BHLHE40,BMP4, BMPR1A,BMPR2,CASP6,CDCA8,CD H1,CDKN1B,EGR1,GPI,HBP1,HDAC6 ,HSPA1A/HSPA1B,ID1,ID2,IRF2,JUN, LTBP1,MAD1L1,MAPK14,MIF,MYC, NF2,NQO1,PRMT1,RAF1,RBPJ,SMAD 2,SMC3,SRC,TFAP2A,TOP2A,TTC5
Cellular Growth and Proliferation	proliferation of lung cancer cell lines	1.77E-03	Decreased	-2.300	BBC3,CDCA8,CDCP1,CHEK1,ECT2,E RRFI1,H2AFY,HK1,HK2,ID1,MAP3K7 (includes EG:26409),MAPK14,MYC,NASP,NCO A3,NOTCH2,PIK3CA,PLK1,POLD4,P RKCD,RAF1,RASD1,RHOB,SET,STM N1,TSPO,TUSC2,WDR12
Cellular Development	proliferation of lung cancer cell lines	1.77E-03	Decreased	-2.300	BBC3,CDCA8,CDCP1,CHEK1,ECT2,E RRFI1,H2AFY,HK1,HK2,ID1,MAP3K7 (includes EG:26409),MAPK14,MYC,NASP,NCO A3,NOTCH2,PIK3CA,PLK1,POLD4,P RKCD,RAF1,RASD1,RHOB,SET,STM N1,TSPO,TUSC2,WDR12

Cellular Growth and Proliferation	proliferation of tumor cell lines	2.71E-03	Decreased	-2.431	AATF,ACACA,ADAM15,ADM,AKT1S1,APEX1,ARIH2,AURKA,BBC3,BCCIP,BCL6,BCR,BMP4,BMPR1A,BMPR2,BNIP3,BSG,BTG2,BUB1 (includes EG:100307076),C14orf169,CCNA2,CCNG2,CDCA8,CDCP1,CDH1,CDKN1B,CHCHD6,CHEK1,CREM (includes EG:12916),CUL7,DDX21,DUSP1,E2F5,E2F8,ECT2,EFNA1,EGR1,ELF3,EPS8,ERRFI1,FASN,FKBP5,FRMD6,GADD45A,GCAT,GRB2,GTPBP4,H2AFY,HAND1,HBP1,HDAC5,HES6,HIF1A,HK1,HK2,ID1,ID2,IER3,IGF2BP3,IGFBP2,IL23A,IL6ST,ITGA7,JUN,KIAA0101,KIF20A,KLF4,KPNA2,MAD1L1,MAP3K7 (includes EG:26409),MAPK14,MFSD12,MIF,MLLT3,MMP9,MYBBP1A,MYC,NASP,NCOA3,NDUFAF4,NF2,NOTCH2,NPY,NUB1,NUBP1,PDCD4,PDIA3,PHC1,PIK3CA,PLAT,PLAU,PLK1,PNPT1,POLD4,PRKCD,PRMT1,PRPF4B,PTHLH,PTTG1,RAD51,RAF1,RALB,RASD1,RHOB,RNF4,RORA,RRM2,SENP1,SET,SFN,SLC2A1,SLC9A3R1,SMARCB1,SPHK1,SRC,SREBF1,SRSF2,SRSF3,SRSF5,SSBP1,STMN1,TERF1,TES,TFAP2A,THOC1,TSPO,TUSC2,TYMS,UBE2C,VEGFA,VHL,WDR12,WWTR1
Cellular Development	proliferation of tumor cell lines	2.71E-03	Decreased	-2.431	AATF,ACACA,ADAM15,ADM,AKT1S1,APEX1,ARIH2,AURKA,BBC3,BCCIP,BCL6,BCR,BMP4,BMPR1A,BMPR2,BNIP3,BSG,BTG2,BUB1 (includes EG:100307076),C14orf169,CCNA2,CCNG2,CDCA8,CDCP1,CDH1,CDKN1B,CHCHD6,CHEK1,CREM (includes EG:12916),CUL7,DDX21,DUSP1,E2F5,E2F8,ECT2,EFNA1,EGR1,ELF3,EPS8,ERRFI1,FASN,FKBP5,FRMD6,GADD45A,GCAT,GRB2,GTPBP4,H2AFY,HAND1,HBP1,HDAC5,HES6,HIF1A,HK1,HK2,ID1,ID2,IER3,IGF2BP3,IGFBP2,IL23A,IL6ST,ITGA7,JUN,KIAA0101,KIF20A,KLF4,KPNA2,MAD1L1,MAP3K7 (includes EG:26409),MAPK14,MFSD12,MIF,MLLT3,MMP9,MYBBP1A,MYC,NASP,NCOA3,NDUFAF4,NF2,NOTCH2,NPY,NUB1,NUBP1,PDCD4,PDIA3,PHC1,PIK3CA,PLAT,PLAU,PLK1,PNPT1,POLD4,PRKCD,PRMT1,PRPF4B,PTHLH,PTTG1,RAD51,RAF1,RALB,RASD1,RHOB,RNF4,RORA,RRM2,SENP1,SET,SFN,SLC2A1,SLC9A3R1,SMARCB1,SPHK1,SRC,SREBF1,SRSF2,SRSF3,SRSF5,SSBP1,STMN1,TERF1,TES,TFAP2A,THOC1,TSPO,TUSC2,TYMS,UBE2C,VEGFA,VHL,WDR12,WWTR1
Cellular Growth and Proliferation	cytostasis of tumor cell lines	5.90E-03	Decreased	-2.587	BCL6,BCR,BHLHE40,BMP4,BMPR1A,CDCA8,CDH1,CDKN1B,EGR1,GPI,IRF2,LTBP1,MAPK14,NQO1,PRMT1,RBPJ,SMAD2,TOP2A,TTC5

Cell Death and Survival	cell death of cancer cells	9.40E-03	Increased	2.102	AKT1S1,BIK,BMP4,BOK,CASP6,CDH1,CDKN1B,CHEK1,DDIT3,EGLN3,EIF2AK3,FASLG,FASN,FOXO4,HIF1A,JUN,MAP3K1,MAPK14,MMP9,MYC,NCOA3,PAWR,PLK1,PRKCD,RAF1,RALB,SPHK1,TFAP2A,VEGFA,VHL
Tumor Morphology	cell death of cancer cells	9.40E-03	Increased	2.102	AKT1S1,BIK,BMP4,BOK,CASP6,CDH1,CDKN1B,CHEK1,DDIT3,EGLN3,EIF2AK3,FASLG,FASN,FOXO4,HIF1A,JUN,MAP3K1,MAPK14,MMP9,MYC,NCOA3,PAWR,PLK1,PRKCD,RAF1,RALB,SPHK1,TFAP2A,VEGFA,VHL
Post-Translational Modification	ubiquitination of protein	1.06E-02	Increased	2.213	ARIH1,ARIH2,BAG5,CDC34,DDB1,DNAJB2,FBXO22,FBXO6,GCLC,GTPBP4,HDAC6,HSPBP1,MAP3K1,MAPT,NDFIP2,NUB1,PLK1,PSMC4,RLIM,RNF13,RNF139,RNF4,UBE2C,UBE2T,UBE4B,UBR1 (includes EG:197131),UBR2 (includes EG:224826),UHRF2,VHL,WWP1
Cardiovascular Disease	damage of artery	1.12E-02	Decreased	-2.000	EFEMP2,PLAT,PLAU,PLOD1
Cell Cycle	contact growth inhibition of tumor cell lines	1.25E-02	Decreased	-2.287	BMP4,BMPR1A,CDH1,EGR1,GPI,LTBP1,MAPK14,SMAD2,TOP2A,TTC5
Cellular Growth and Proliferation	contact growth inhibition of tumor cell lines	1.25E-02	Decreased	-2.287	BMP4,BMPR1A,CDH1,EGR1,GPI,LTBP1,MAPK14,SMAD2,TOP2A,TTC5
Cell-To-Cell Signaling and Interaction	contact growth inhibition of tumor cell lines	1.25E-02	Decreased	-2.287	BMP4,BMPR1A,CDH1,EGR1,GPI,LTBP1,MAPK14,SMAD2,TOP2A,TTC5
Developmental Disorder	craniofacial abnormality	1.40E-02	Decreased	-2.402	ALKBH1,BMPR1A,CITED2,GADD45A,GDF1,HSD17B2,INSIG1,INSIG2,JMJD6,LAMC1,LMNB1,LMNB2,MSX1,ORC1 (includes EG:18392),ORC6 (includes EG:23594),PDGFA,RAF1,RBPJ,RGMA,SMAD2,SOS1,SPHK1,TCOF1,TFAP2A
Connective Tissue Disorders	craniofacial abnormality	1.40E-02	Decreased	-2.402	ALKBH1,BMPR1A,CITED2,GADD45A,GDF1,HSD17B2,INSIG1,INSIG2,JMJD6,LAMC1,LMNB1,LMNB2,MSX1,ORC1 (includes EG:18392),ORC6 (includes EG:23594),PDGFA,RAF1,RBPJ,RGMA,SMAD2,SOS1,SPHK1,TCOF1,TFAP2A
Skeletal and Muscular Disorders	craniofacial abnormality	1.40E-02	Decreased	-2.402	ALKBH1,BMPR1A,CITED2,GADD45A,GDF1,HSD17B2,INSIG1,INSIG2,JMJD6,LAMC1,LMNB1,LMNB2,MSX1,ORC1 (includes EG:18392),ORC6 (includes EG:23594),PDGFA,RAF1,RBPJ,RGMA,SMAD2,SOS1,SPHK1,TCOF1,TFAP2A
Cellular Development	differentiation of stem cells	1.86E-02	Decreased	-2.263	BHLHE41,BMP4,EIF4G2,HIF1A,HSP90B1,ID2,ID3,IL6ST,JUN,KLF4,LIN28A,MLLT11,MSX1,MYC,RBPJ,RNF2,S1PR1,SFN,SMARCB1,VEGFA,WNT4,WWTR1

Cell Cycle	cytokinesis	2.71E-02	Decreased	-2.534	AURKA,CCNB1,CCNG1,CDC20 (includes EG:107995),CIT,ECT2,GADD45A,IVNS1ABP,KIF20A,KIF23,PLK1,RALB,RHOB,SETD8,SRC,SSRP1,TOP2A
Cellular Movement	cytokinesis	2.71E-02	Decreased	-2.534	AURKA,CCNB1,CCNG1,CDC20 (includes EG:107995),CIT,ECT2,GADD45A,IVNS1ABP,KIF20A,KIF23,PLK1,RALB,RHOB,SETD8,SRC,SSRP1,TOP2A
Cell Death and Survival	apoptosis of keratinocyte cancer cell lines	3.04E-02	Increased	2.186	BCL3,FASLG,IER3,NQO1,RHOB
Cellular Movement	invasion of epithelial cell lines	3.04E-02	Increased	2.201	CDH1,IER3,ITGA3,MMP9,PLAU

Fig.A1.1 Selective canonical pathways analyzed by Ingenuity Pathway Analysis. The bar graph represents a subset of significantly represented canonical signaling pathways when rat TS cells are exposed to 0.5% O_2analyzed by Ingenuity Pathway analysis.

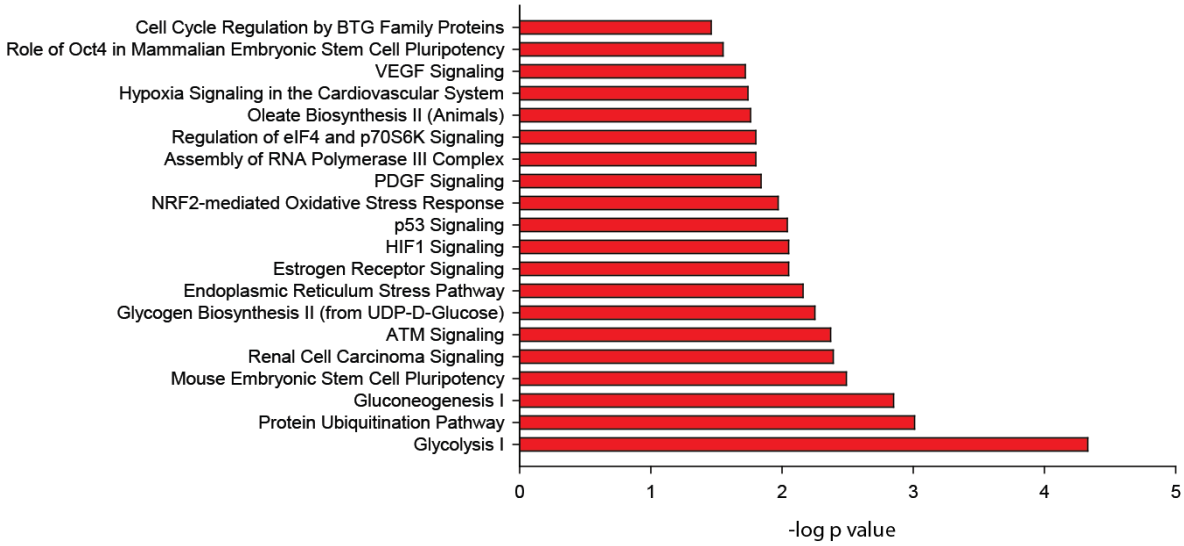
Cell Cycle Regulation by BTG Family Proteins
Role of Oct4 in Mammalian Embryonic Stem Cell Pluripotency
VEGF Signaling
Hypoxia Signaling in the Cardiovascular System
Oleate Biosynthesis II (Animals)
Regulation of eIF4 and p70S6K Signaling
Assembly of RNA Polymerase III Complex
PDGF Signaling
NRF2-mediated Oxidative Stress Response
p53 Signaling
HIF1 Signaling
Estrogen Receptor Signaling
Endoplasmic Reticulum Stress Pathway
Glycogen Biosynthesis II (from UDP-D-Glucose)
ATM Signaling
Renal Cell Carcinoma Signaling
Mouse Embryonic Stem Cell Pluripotency
Gluconeogenesis I
Protein Ubiquitination Pathway
Glycolysis I
0
1
2
3
4
5
-log p value

Table A1.2. Genes represented in canonical pathways by Ingenuity Pathway Analysis.

Ingenuity Canonical Pathways	-log(p-value)	Ratio	Molecules
Glycolysis I	4.33E00	2E-01	PGK1,Eno1/Eno1-ps1,GPI,PGAM1,ENO2,ALDOA,PFKL,Tpi1 (includes others),ALDOC
Protein Ubiquitination Pathway	3.01E00	1.23E-01	USP24,PSMA3,ANAPC1/LOC100286979,CDC20 (includes EG:107995),HSPA1A/HSPA1B,PSMB10,UBR2 (includes EG:224826),UBR1 (includes EG:197131),DNAJC3,DNAJB2,PSMB8,USP39,PSMC5,USP48,HSP90B1,PSMC6,USP10,DNAJB1,USP15,UBE4B,USP27X,PSMC4,THOP1,USP1,DNAJB9,DNAJC11,PSME1,DNAJC5,PSMD12,CDC34,DNAJB6,VHL,UBE2C
Gluconeogenesis I	2.85E00	1.4E-01	PGK1,Eno1/Eno1-ps1,GPI,PGAM1,ENO2,ALDOA,ALDOC
Mouse Embryonic Stem Cell Pluripotency	2.49E00	1.52E-01	IL6ST,RAF1,ID2,PIK3CA,BMP4,GRB2,RRAS,BMPR2,ID3,MYC,ID1,MAPK14,MAP3K7 (includes EG:26409),BMPR1A,SOS1
Renal Cell Carcinoma Signaling	2.39E00	1.62E-01	VEGFA,RAF1,PIK3CA,JUN,SLC2A1,GRB2,RRAS,SOS1,EGLN3,HIF1A,RAP1A,VHL
ATM Signaling	2.37E00	1.8E-01	RAD51,SMC3,JUN,GADD45B,MAPK14,GADD45A,H2AFX,CCNB2,ATF4,CHEK1,CCNB1
Glycogen Biosynthesis II (from UDP-D-Glucose)	2.25E00	2.5E-01	GYS1,GYG1,GBE1
Endoplasmic Reticulum Stress Pathway	2.16E00	2.78E-01	DNAJC3,ATF4,ATF6,EIF2S1,EIF2AK3
Estrogen Receptor Signaling	2.05E00	1.32E-01	RAF1,SRC,TAF11 (includes EG:309638),GRB2,GTF2F2,RRAS,TBP,MED21,GTF2F1,TAF13 (includes EG:310784),NCOA3,MED27,THRAP3,SOS1,POLR2I,TAF2 (includes EG:170844),MED10,GTF2H3
HIF1α Signaling	2.05E00	1.39E-01	PIK3CA,SLC2A1,RRAS,HIF1A,SLC2A3,VEGFA,EGLN1,JUN,MAPK14,EGLN3,MMP12,APEX1,MMP9,MMP17,VHL
p53 Signaling	2.04E00	1.35E-01	PIK3CA,GADD45B,C12orf5,CHEK1,CCNG1,CASP6,JUN,MAPK14,GADD45A,STAG1,BBC3,GNL3,SFN
NRF2-mediated Oxidative Stress Response	1.97E00	1.2E-01	RAF1,PIK3CA,RRAS,MAP3K1,NQO1,DNAJC3,GCLC,DNAJB2,DNAJB9,MAFF,DNAJC11,JUN,DNAJC5,MAPK14,MAP3K7 (includes EG:26409),PRKCD,ATF4,CDC34,DNAJB6,DNAJB1,GCLM,FKBP5,EIF2AK3
PDGF Signaling	1.84E00	1.41E-01	MYC,RAF1,SRC,PIK3CA,JUN,GRB2,RRAS,PDGFA,MAP3K1,SOS1,SPHK1,INPP5K
Assembly of RNA Polymerase III Complex	1.8E00	2.5E-01	GTF3C4,GTF3C3,TBP,GTF3A
Regulation of eIF4 and p70S6K Signaling	1.8E00	1.03E-01	RAF1,PIK3CA,GRB2,RRAS,EIF2B3,EIF4G3,PAIP2,ITGA3,EIF2S1,EIF4EBP1,RPS24,MAPK14,EIF4G2,EIF1AX,PPM1J,SOS1,EIF2B1,PPP2R1B
Oleate Biosynthesis II (Animals)	1.76E00	1.58E-01	SCD,UFSP2,Scd2

Hypoxia Signaling in the Cardiovascular System	1.74E00	1.52E-01	VEGFA,P4HB,HSP90B1,JUN,NQO1,ATF4,HIF1A,CDC34,VHL,UBE2C
VEGF Signaling	1.72E00	1.31E-01	RAF1,PIK3CA,GRB2,RRAS,EIF2B3,HIF1A,EIF2S1,VEGFA,EIF1AX,SOS1,EIF2B1,SFN,ACTN1
Role of Oct4 in Mammalian Embryonic Stem Cell Pluripotency	1.55E00	1.56E-01	CASP6,KDM5B,TDH,PCGF6,PHC1,SH3GLB1,FBXO15
Cell Cycle Regulation by BTG Family Proteins	1.46E00	1.67E-01	PRMT1,PPM1J,BTG2,E2F5,PPP2R1B,CCRN4L
Cardiomyocyte Differentiation via BMP Receptors	1.45E00	2E-01	BMP4,BMPR1A,MAP3K7 (includes EG:26409),BMPR2
PI3K/AKT Signaling	1.41E00	1.04E-01	RAF1,PIK3CA,GRB2,RRAS,ITGA3,EIF4EBP1,HSP90B1,GYS1,PPM1J,SOS1,MAP3K8,CDKN1B,INPP5K,SFN,PPP2R1B
ERK/MAPK Signaling	1.29E00	9.71E-02	SRC,RAF1,PIK3CA,PLA2G12A,GRB2,RRAS,PPP1R3C,ITGA3,RAP1A,EIF4EBP1,KSR1,MYC,ELF3,PPP1R10,DUSP1,PRKCD,PPM1J,SOS1,ATF4,PPP2R1B
ErbB2-ErbB3 Signaling	1.28E00	1.33E-01	MYC,RAF1,PIK3CA,JUN,GRB2,RRAS,SOS1,CDKN1B
Cell Cycle: G2/M DNA Damage Checkpoint Regulation	1.27E00	1.46E-01	GADD45A,TOP2A,CCNB2,PLK1,SFN,CHEK1,CCNB1
BMP signaling pathway	1.25E00	1.25E-01	RAF1,JUN,BMP4,MAPK14,BMPR1A,GRB2,RRAS,MAP3K7 (includes EG:26409),SOS1,BMPR2
TGF-β Signaling	1.24E00	1.24E-01	SMAD2,RAF1,JUN,BMP4,MAPK14,BMPR1A,GRB2,RRAS,MAP3K7 (includes EG:26409),SOS1,BMPR2
AMPK Signaling	1.21E00	9.64E-02	CAB39,SRC,PIK3CA,CPT1A,PFKL,PPM1D,EIF4EBP1,GYS1,MAPK14,PPM1J,FASN,AK4,ACACA,HLTF,PPP2R1B,PPAT
Cyclins and Cell Cycle Regulation	1.18E00	1.12E-01	HDAC6,CCNA2,RAF1,PPM1J,E2F5,CCNB2,CDKN1B,PPP2R1B,HDAC5,CCNB1
Assembly of RNA Polymerase II Complex	1.13E00	1.25E-01	TAF11 (includes EG:309638),TBP,GTF2F1,TAF13 (includes EG:310784),TAF2 (includes EG:170844),POLR2I,GTF2H3
tRNA Charging	1.11E00	7.41E-02	TARS2,MARS2,DARS,HARS,HARS2,FARSB
Fatty Acid β-oxidation I	1.1E00	1.11E-01	ECI2,AUH (includes EG:11992),SLC27A1,SLC27A3,ECI1
Ceramide Signaling	1.08E00	1.14E-01	RAF1,PIK3CA,JUN,RRAS,PPM1J,MAP3K1,SPHK1,S1PR1,PPP2R1B,KSR1
Hereditary Breast Cancer Signaling	9.95E-01	1.02E-01	PIK3CA,GADD45B,RRAS,HDAC5,CHEK1,CCNB1,RAD51,HDAC6,GADD45A,H2AFX,SFN,HLTF,POLR2I
p38 MAPK Signaling	9.8E-01	1.03E-01	IL33,IL1R2,MYC,MAPK14,PLA2G12A,DDIT3,DUSP1,MAP3K7 (includes EG:26409),MAPT,ATF4,FASLG,IRAK2
Aldosterone Signaling in Epithelial Cells	9.76E-01	9.52E-02	RAF1,PIK3CA,HSPA1A/HSPA1B,PDIA3,DNAJC3,DNAJB2,DNAJB9,DNAJC11,HSP90B1,DNAJC5,DUSP1,PRKCD,SOS1,DNAJB6,DNAJB1,PI4KA

Endometrial Cancer Signaling	9.67E-01	1.23E-01	MYC,RAF1,PIK3CA,CDH1,GRB2,RRAS,SOS1
Paxillin Signaling	9.66E-01	9.91E-02	SRC,ITGAE,PIK3CA,MAPK14,GRB2,RRAS,SOS1,ITGA3,ITGA7,ACTN1,GIT2
Glioblastoma Multiforme Signaling	9.58E-01	9.15E-02	RAF1,SRC,PIK3CA,GRB2,RRAS,PDGFA,PDIA3,NF2,MYC,RHOB,PRKCD,SOS1,E2F5,WNT4,CDKN1B
PTEN Signaling	9.46E-01	9.63E-02	FOXO4,RAF1,PIK3CA,SHARPIN,GRB2,RRAS,BMPR2,ITGA3,BMPR1A,SOS1,INPP5K,CDKN1B,FASLG
Glucose and Glucose-1-phosphate Degradation	9.3E-01	9.09E-02	HK1,PGM1
Role of NANOG in Mammalian Embryonic Stem Cell Pluripotency	9.13E-01	9.65E-02	IL6ST,RAF1,PIK3CA,RIF1 (includes EG:295602),BMP4,BMPR1A,GRB2,RRAS,SOS1,BMPR2,WNT4
14-3-3-mediated Signaling	9.04E-01	1.03E-01	RAF1,SRC,PIK3CA,JUN,GRB2,RRAS,PDIA3,PRKCD,MAPT,CDKN1B,SFN,AKT1S1
Transcriptional Regulatory Network in Embryonic Stem Cells	8.58E-01	1.25E-01	RIF1 (includes EG:295602),KAT6A,HAND1,EOMES,SET
Glycogen Degradation II	8.3E-01	1.25E-01	PGM1,PYGL
Sertoli Cell-Sertoli Cell Junction Signaling	8.19E-01	8.72E-02	RAF1,SRC,TJP2,CLDN15,RRAS,MAP3K1,ITGA3,MPP6 (includes EG:35343),F11R,CDH1,JUN,MAPK14,CLDN4,MAP3K7 (includes EG:26409),MAP3K8,ACTN1,PVRL2
Cell Cycle: G1/S Checkpoint Regulation	7.97E-01	1.06E-01	HDAC6,MYC,PAK1IP1,E2F5,GNL3,CDKN1B,HDAC5
Chronic Myeloid Leukemia Signaling	7.95E-01	9.52E-02	HDAC6,MYC,RAF1,PIK3CA,GRB2,RRAS,SOS1,E2F5,CDKN1B,HDAC5
VEGF Family Ligand-Receptor Interactions	7.83E-01	9.52E-02	VEGFA,RAF1,PIK3CA,PLA2G12A,GRB2,RRAS,PRKCD,SOS1
FLT3 Signaling in Hematopoietic Progenitor Cells	6.8E-01	1.05E-01	RAF1,PIK3CA,MAPK14,GRB2,RRAS,SOS1,ATF4,EIF4EBP1
Molecular Mechanisms of Cancer	6.14E-01	7.69E-02	RAF1,PIK3CA,BMP4,APH1B,BMPR2,HIF1A,CHEK1,MYC,CASP6,JUN,RHOB,BBC3,BMPR1A,MAP3K7 (includes EG:26409),SOS1,E2F5,FASLG,SMAD2,SRC,RRAS,GRB2,RALB,AURKA,RAP1A,CDH1,MAPK14,PRKCD,RBPJ,CDKN1B
Lipid Antigen Presentation by CD1	6.1E-01	8.7E-02	PDIA3,PSAP
Fatty Acid Activation	6.1E-01	1.05E-01	SLC27A1,SLC27A3
Leukocyte Extravasation Signaling	5.48E-01	8.12E-02	SRC,PIK3CA,CLDN15,RAP1A,F11R,WIPF1,MAPK14,CLDN4,PRKCD,FER,MMP12,CTTN,ACTN1,MMP9,MMP17,ARHGAP8/PRR5-ARHGAP8
Glioma Signaling	5.38E-01	8.04E-02	RAF1,PIK3CA,Calm1 (includes others),GRB2,RRAS,PDGFA,PRKCD,SOS1,E2F5
FAK Signaling	5.29E-01	7.92E-02	RAF1,SRC,PIK3CA,GRB2,RRAS,SOS1,ITGA3,GIT2

Arsenate Detoxification I (Glutaredoxin)	5.17E-01	5E-02	GLRX2
Prostate Cancer Signaling	5.1E-01	8.16E-02	RAF1,PIK3CA,HSP90B1,GRB2,RRAS,SOS1,ATF4,CDKN1B
LPS-stimulated MAPK Signaling	4.8E-01	8.54E-02	RAF1,PIK3CA,JUN,MAPK14,RRAS,MAP3K7 (includes EG:26409),PRKCD
Germ Cell-Sertoli Cell Junction Signaling	4.75E-01	7.93E-02	SRC,PIK3CA,RRAS,MAP3K1,ITGA3,CDH1,MAPK14,RHOB,MAP3K7 (includes EG:26409),FER,MAP3K8,ACTN1,PVRL2
ErbB Signaling	4.74E-01	9.2E-02	RAF1,PIK3CA,JUN,MAPK14,GRB2,RRAS,PRKCD,SOS1
Breast Cancer Regulation by Stathmin1	4.73E-01	7.73E-02	RAF1,PIK3CA,Calm1 (includes others),GRB2,RRAS,PPP1R3C,GNB4,STMN1,PPP1R10,PPM1J,PRKCD,SOS1,E2F5,GNG2,CDKN1B,PPP2R1B
Colorectal Cancer Metastasis Signaling	4.73E-01	7.39E-02	IL6ST,SMAD2,SRC,PIK3CA,GRB2,RRAS,MYC,VEGFA,GNB4,APPL1,CDH1,JUN,RHOB,SOS1,WNT4,GNG2,MMP12,MMP9,MMP17
Mechanisms of Viral Exit from Host Cells	4.69E-01	8.89E-02	PRKCD,SH3GLB1,LMNB2,LMNB1
Acute Myeloid Leukemia Signaling	4.62E-01	8.54E-02	MYC,RAF1,PIK3CA,GRB2,RRAS,SOS1,EIF4EBP1

Table A2.1. Genes upregulated on hypoxia exposure

Affymetrix ID	Gene Title	Gene Symbol	Ave amb sig int	Ave hypox sig int	hypox/ amb
1373108_at	protein phosphatase 1, regulatory (inhibitor) subunit 3C	Ppp1r3c	40	1668	**41.298**
1373685_at	ankyrin repeat domain 37	Ankrd37	177	4762	**26.832**
1380804_at	---	---	44	709	**16.012**
1368530_at	matrix metallopeptidase 12	Mmp12	76	937	**12.277**
1372897_at	procollagen lysine, 2-oxoglutarate 5-dioxygenase 2	Plod2	186	2100	**11.303**
1377190_at	---	---	370	3196	**8.635**
1395153_at	claudin 15	Cldn15	207	1698	**8.219**
1369415_at	basic helix-loop-helix family, member e40	Bhlhe40	71	580	**8.198**
1389659_at	cytotoxic T lymphocyte-associated protein 2 alpha	Ctla2a	1720	13531	**7.867**
1379483_at	Basic helix-loop-helix family, member e40	Bhlhe40	77	588	**7.654**
1370975_at	lysine (K)-specific demethylase 3A	Kdm3a	559	4013	**7.180**
1371824_at	adenylate kinase 3-like 1	Ak3l1	327	2303	**7.042**
1368674_at	phosphorylase, glycogen, liver	Pygl	1668	11366	**6.813**
1368025_at	DNA-damage-inducible transcript 4	Ddit4	1434	9702	**6.766**
1386998_at	aldolase C, fructose-bisphosphate	Aldoc	533	3501	**6.572**
1391640_at	---	---	177	1158	**6.545**
1387455_a_at	very low density lipoprotein receptor	Vldlr	144	940	**6.514**
1394948_at	---	---	151	975	**6.445**
1394259_at	claudin 15	Cldn15	85	550	**6.444**
1398350_at	hypothetical protein LOC100364588	LOC100364588	709	4468	**6.300**
1398120_at	---	---	81	505	**6.213**
1389265_at	glucan (1,4-alpha-), branching enzyme 1	Gbe1	724	4437	**6.125**
1389611_at	very low density lipoprotein receptor	Vldlr	145	881	**6.061**
1370954_at	prolyl 4-hydroxylase, alpha polypeptide I	P4ha1	2424	13537	**5.584**
1370341_at	enolase 2, gamma, neuronal	Eno2	689	3838	**5.571**
1376845_at	interferon, alpha-inducible protein 27 like 2B	Ifi27l2b	2412	13329	**5.526**
1389230_at	---	---	794	4342	**5.466**
1376850_a_at	chemokine (C-C motif) ligand 27	Ccl27	176	954	**5.421**
1375455_at	guanylate cyclase activator 1a (retina)	Guca1a	171	924	**5.396**

1373554_at	---	---	225	1213	**5.380**
1369961_at	phosphatidic acid phosphatase type 2A	Ppap2a	665	3550	**5.335**
1367507_at	nudix (nucleoside diphosphate linked moiety X)-type motif 22	Nudt22	825	4315	**5.230**
1397918_at	---	---	592	3095	**5.225**
1391458_at	N-myc downstream regulated gene 1	Ndrg1	310	1600	**5.165**
1378930_a_at	---	---	500	2584	**5.165**
1391932_at	similar to hypothetical protein MGC47256	RGD1308694	137	702	**5.139**
1368079_at	pyruvate dehydrogenase kinase, isozyme 1	Pdk1	1139	5832	**5.119**
1389581_at	interleukin 33	Il33	1643	8300	**5.052**
1394548_at	carboxypeptidase M	Cpm	106	522	**4.926**
1367950_at	solute carrier family 22 (organic cation/carnitine transporter), member 5	Slc22a5	143	699	**4.883**
1387908_at	RAS, dexamethasone-induced 1	Rasd1	621	3030	**4.882**
1371434_at	hypothetical protein LOC691807	LOC691807	3601	16897	**4.692**
1382475_at	---	---	156	727	**4.674**
1376653_at	putative homeodomain transcription factor 1	Phtf1	483	2249	**4.654**
1390502_at	similar to RIKEN cDNA 1700025G04 gene	RGD1309104	438	2015	**4.596**
1379611_at	---	---	121	548	**4.520**
1390943_at	similar to chromosome 1 open reading frame 63	RGD1359529	118	526	**4.453**
1391756_at	rCG54026-like /// rCG54026-like	LOC100362394 /// LOC100365991	7829	34762	**4.440**
1369670_at	Cd200 molecule	Cd200	4598	20384	**4.434**
1378006_at	---	---	361	1577	**4.365**
1393690_at	insulin induced gene 2	Insig2	529	2268	**4.285**
1393240_at	EGF-containing fibulin-like extracellular matrix protein 2	Efemp2	136	584	**4.280**
1373970_at	interleukin 33	Il33	1373	5741	**4.182**
1373558_at	---	---	133	554	**4.164**
1387964_a_at	ERO1-like (S. cerevisiae)	Ero1l	516	2149	**4.162**
1369006_at	hexokinase 2	Hk2	452	1838	**4.063**
1373291_at	---	---	184	741	**4.029**
1396239_at	similar to RIKEN cDNA 2310008H04	RGD1566036	812	3265	**4.022**
1373979_at	---	---	549	2198	**4.004**
1370081_a_at	vascular endothelial growth factor A	Vegfa	150	595	**3.976**
1376593_at	---	---	394	1561	**3.960**
1384002_at	ATPase, class VI, type 11B	Atp11b	165	653	**3.946**
1372341_at	solute carrier family 25,	Slc25a36	655	2540	**3.878**

	member 36				
1392603_at	---	---	358	1380	**3.853**
1375182_at	---	---	175	673	**3.846**
1373807_at	vascular endothelial growth factor A	Vegfa	463	1777	**3.841**
1371953_at	cyclin G2	Ccng2	353	1336	**3.779**
1367966_at	dipeptidylpeptidase 3 /// similar to Dipeptidyl-peptidase 3 (Dipeptidyl-peptidase III) (DPP III)	Dpp3 /// LOC678760	2133	8034	**3.766**
1370884_at	sepiapterin reductase (7,8-dihydrobiopterin:NADP+ oxidoreductase)	Spr	473	1766	**3.737**
1382476_x_at	---	---	155	578	**3.723**
1384098_at	ring finger protein 125	Rnf125	1023	3798	**3.712**
1394940_at	family with sequence similarity 46, member A	Fam46a	178	657	**3.687**
1367942_at	acid phosphatase 5, tartrate resistant	Acp5	869	3157	**3.633**
1387805_at	BCL2/adenovirus E1B interacting protein 3	Bnip3	2779	10006	**3.600**
1389207_at	EGL nine homolog 1 (C. elegans)	Egln1	1659	5967	**3.596**
1368254_a_at	sphingosine kinase 1	Sphk1	176	622	**3.541**
1367894_at	insulin induced gene 1	Insig1	831	2942	**3.541**
1389075_at	---	---	613	2161	**3.525**
1387180_at	interleukin 1 receptor, type II	Il1r2	898	3143	**3.499**
1367789_at	solute carrier family 27 (fatty acid transporter), member 1	Slc27a1	690	2409	**3.490**
1369310_at	brain abundant, membrane attached signal protein 1	Basp1	275	959	**3.489**
1392706_at	---	---	208	723	**3.482**
1376642_at	XK, Kell blood group complex subunit-related family, member 8	Xkr8	187	640	**3.417**
1369473_at	phosphoglucomutase 1	Pgm1	338	1143	**3.378**
1388634_at	phosphoglucomutase 1	Pgm1	1096	3679	**3.356**
1386721_at	zinc finger protein 503	Znf503	473	1585	**3.354**
1374544_at	platelet receptor Gi24	MGC112715	1655	5543	**3.349**
1387769_a_at	inhibitor of DNA binding 3	Id3	214	717	**3.344**
1369393_at	mitogen-activated protein kinase kinase kinase 8	Map3k8	370	1227	**3.320**
1379368_at	B-cell CLL/lymphoma 6	Bcl6	228	755	**3.311**
1374224_at	eukaryotic translation initiation factor 2 alpha kinase 4	Eif2ak4	1545	5035	**3.258**
1389789_at	Max dimerization protein 1	Mxd1	300	977	**3.257**
1375230_at	---	---	3341	10854	**3.249**
1371692_at	myeloid/lymphoid or mixed-lineage leukemia (trithorax homolog, Drosophila); translocated to, 11	Mllt11	483	1568	**3.247**

1374004_at	prolyl endopeptidase-like	Prepl	824	2657	**3.225**
1370517_at	neuronal pentraxin 1	Nptx1	381	1227	**3.222**
1383519_at	Hexokinase 2	Hk2	5174	16532	**3.195**
1379057_at	hypothetical protein LOC683460	LOC683460	484	1547	**3.192**
1376941_at	Williams-Beuren syndrome chromosome region 16 homolog (human)	Wbscr16	897	2849	**3.176**
1376030_at	ArfGAP with coiled-coil, ankyrin repeat and PH domains 1	Acap1	366	1161	**3.169**
1374310_at	protein phosphatase 1J	Ppm1j	392	1239	**3.163**
1372652_at	forkhead box O4	Foxo4	306	966	**3.159**
1390391_at	---	---	635	1989	**3.130**
1389530_at	solute carrier family 35, member E1	Slc35e1	1189	3705	**3.117**
1390203_at	---	---	298	925	**3.110**
1392905_at	Guanine nucleotide binding protein (G protein), gamma 2	Gng2	632	1951	**3.088**
1387587_at	Fas ligand (TNF superfamily, member 6)	Faslg	1033	3183	**3.083**
1389986_at	---	---	625	1902	**3.041**
1388440_at	anterior pharynx defective 1 homolog B (C. elegans)	Aph1b	672	2041	**3.038**
1376877_at	CUB domain containing protein 1	Cdcp1	927	2792	**3.010**
1368305_at	caspase 6	Casp6	3361	9936	**2.957**
1379251_at	---	---	602	1779	**2.955**
1396737_at	structural maintenance of chromosomes flexible hinge domain containing 1	Smchd1	235	694	**2.955**
1368247_at	heat shock 70kD protein 1A /// heat shock 70kD protein 1B (mapped)	Hspa1a /// Hspa1b	2104	6216	**2.954**
1382255_at	---	---	778	2286	**2.939**
1372610_at	prolyl 4-hydroxylase, alpha polypeptide II	P4ha2	1655	4819	**2.911**
1381335_at	---	---	1094	3130	**2.860**
1372328_at	kinesin light chain 4	Klc4	374	1068	**2.859**
1374105_at	HIG1 hypoxia inducible domain family, member 1A	Higd1a	348	984	**2.832**
1370912_at	heat shock 70kD protein 1A	Hspa1a	761	2149	**2.825**
1389377_at	insulin induced gene 2	Insig2	657	1856	**2.823**
1390433_at	regulator of chromosome condensation (RCC1) and BTB (POZ) domain containing protein 1	Rcbtb1	280	789	**2.816**
1371394_x_at	---	---	7377	20683	**2.804**
1387389_at	receptor (G protein-coupled) activity modifying protein 3	Ramp3	321	901	**2.803**
1368871_at	mitogen activated protein kinase kinase kinase 1	Map3k1	269	754	**2.803**
1393246_at	zinc finger, MYND-type	Zmynd10	329	921	**2.799**

	containing 10				
1374446_at	TCDD-inducible poly(ADP-ribose) polymerase	Tiparp	505	1396	**2.766**
1397247_at	CUB domain containing protein 1	Cdcp1	472	1304	**2.762**
1393214_at	---	---	3193	8814	**2.760**
1368012_at	telomerase associated protein 1	Tep1	308	846	**2.752**
1380682_at	mex3 homolog B (C. elegans)	Mex3b	265	727	**2.748**
1372844_at	ephrin A1	Efna1	448	1229	**2.746**
1377869_at	CCR4 carbon catabolite repression 4-like (S. cerevisiae)	Ccrn4l	724	1983	**2.739**
1374693_at	poly (ADP-ribose) polymerase family, member 16	Parp16	1128	3075	**2.725**
1376481_at	a disintegrin-like and metalloprotease (reprolysin type) with thrombospondin type 1 motif, 9	Adamts9	254	690	**2.713**
1385168_at	similar to receptor-interacting factor 1	RGD1306520	510	1379	**2.702**
1389615_at	Der1-like domain family, member 1	Derl1	2203	5936	**2.695**
1384080_at	---	---	293	788	**2.689**
1378800_at	---	---	224	600	**2.681**
1368641_at	wingless-type MMTV integration site family, member 4	Wnt4	318	850	**2.676**
1388714_at	elongation factor RNA polymerase II	Ell	1382	3698	**2.675**
1369874_at	G protein-coupled receptor 1	Gpr1	323	862	**2.669**
1395268_at	WW domain containing E3 ubiquitin protein ligase 1	Wwp1	790	2108	**2.668**
1367912_at	latent transforming growth factor beta binding protein 1	Ltbp1	240	640	**2.663**
1372691_at	uridine phosphorylase 1	Upp1	826	2198	**2.662**
1384164_at	---	---	479	1274	**2.662**
1376076_at	hypoxia-inducible protein 2-like	LOC100361568	5202	13829	**2.658**
1369166_at	matrix metallopeptidase 9	Mmp9	2703	7183	**2.657**
1398706_at	---	---	2818	7462	**2.648**
1387017_at	squalene epoxidase	Sqle	525	1385	**2.639**
1387201_at	ring finger protein 138	Rnf138	1162	3049	**2.625**
1371360_at	N-myc downstream regulated gene 1	Ndrg1	8284	21738	**2.624**
1371392_at	glucose phosphate isomerase	Gpi	8155	21272	**2.608**
1379397_at	RAR-related orphan receptor alpha	Rora	260	677	**2.607**
1373812_at	cyclin-dependent kinase inhibitor 1B	Cdkn1b	1488	3880	**2.607**
1398273_at	ephrin A1	Efna1	283	737	**2.600**
1385068_at	---	---	238	615	**2.583**
1393252_at	---	---	286	737	**2.583**
1389439_at	---	---	563	1452	**2.579**

1376990_at	---	---	655	1688	**2.577**
1398364_at	similar to chromosome 1 open reading frame 63	RGD1359529	1438	3691	**2.567**
1384743_at	---	---	347	888	**2.563**
1370062_at	HIG1 hypoxia inducible domain family, member 1A	Higd1a	6757	17284	**2.558**
1383498_at	---	---	364	922	**2.530**
1389297_at	ERO1-like (S. cerevisiae)	Ero1l	10334	26140	**2.529**
1389652_at	---	---	771	1947	**2.526**
1373494_at	breakpoint cluster region	Bcr	1932	4879	**2.526**
1370264_at	spectrin repeat containing, nuclear envelope 1	Syne1	242	602	**2.489**
1372295_at	nuclear prelamin A recognition factor	Narf	281	700	**2.486**
1380547_at	chloride channel 3	Clcn3	540	1335	**2.474**
1371624_at	zinc finger CCCH-type containing 7B	Zc3h7b	377	926	**2.459**
1380229_at	v-maf musculoaponeurotic fibrosarcoma oncogene homolog F (avian)	Maff	730	1796	**2.459**
1388471_at	t-complex 11 (mouse) like 2	Tcp11l2	239	587	**2.457**
1368146_at	dual specificity phosphatase 1	Dusp1	3861	9486	**2.457**
1377719_a_at	---	---	948	2327	**2.454**
1369628_at	synaptic vesicle glycoprotein 2b	Sv2b	1213	2966	**2.446**
1382325_at	glycine C-acetyltransferase (2-amino-3-ketobutyrate-coenzyme A ligase)	Gcat	938	2294	**2.445**
1386888_at	eukaryotic translation initiation factor 4E binding protein 1	Eif4ebp1	4417	10788	**2.443**
1397179_at	similar to DIP13 alpha	RGD1309388	368	898	**2.440**
1384082_at	---	---	702	1714	**2.440**
1383302_at	DnaJ (Hsp40) homolog, subfamily B, member 1	Dnajb1	893	2169	**2.430**
1390688_at	DEAD (Asp-Glu-Ala-Asp) box polypeptide 50	Ddx50	1401	3400	**2.427**
1392453_at	chloride channel 3	Clcn3	576	1388	**2.408**
1368899_at	bone morphogenetic protein receptor, type IA	Bmpr1a	322	774	**2.399**
1389138_at	---	---	2746	6557	**2.388**
1378232_at	chloride channel 3	Clcn3	361	860	**2.386**
1390394_at	similar to CG3570-PA	LOC500034	549	1308	**2.381**
1393131_at	FLT3-interacting zinc finger 1	Fiz1	1497	3555	**2.376**
1392516_a_at	StAR-related lipid transfer (START) domain containing 4	Stard4	341	807	**2.366**
1370848_at	solute carrier family 2 (facilitated glucose transporter), member 1	Slc2a1	11103	26256	**2.365**
1368965_at	solute carrier family 16, member 3 (monocarboxylic acid transporter 4)	Slc16a3	3530	8336	**2.361**
1386978_at	BCL2/adenovirus E1B interacting protein 3-like	Bnip3l	3293	7749	**2.353**

1367898_at	BCL2/adenovirus E1B interacting protein 3-like	Bnip3l	3917	9209	**2.351**
1393887_at	choline phosphotransferase 1	Chpt1	850	1989	**2.341**
1376965_at	---	---	467	1091	**2.335**
1368147_at	dual specificity phosphatase 1	Dusp1	250	583	**2.331**
1371993_at	copine III	Cpne3	351	817	**2.328**
1373533_at	---	---	2315	5386	**2.327**
1398275_at	matrix metallopeptidase 9	Mmp9	4525	10473	**2.314**
1374296_at	---	---	1424	3290	**2.310**
1370249_at	translocator protein	Tspo	3253	7442	**2.287**
1369737_at	cAMP responsive element modulator	Crem	224	512	**2.284**
1368826_at	catechol-O-methyltransferase	Comt	330	752	**2.279**
1377029_at	---	---	402	916	**2.279**
1388409_at	zinc finger CCCH-type containing 7B	Zc3h7b	296	673	**2.276**
1372179_at	hippocalcin-like 1	Hpcal1	3553	8080	**2.274**
1379601_at	alkB, alkylation repair homolog 5 (E. coli)	Alkbh5	547	1245	**2.274**
1374610_at	---	---	1288	2929	**2.273**
1379676_a_at	deoxyribonuclease 1-like 1	Dnase1l1	273	621	**2.270**
1399154_at	lysine (K)-specific demethylase 2A	Kdm2a	742	1675	**2.257**
1383161_a_at	---	---	1516	3421	**2.256**
1372518_at	fibulin 1	Fbln1	589	1328	**2.255**
1383447_at	ets variant 5	Etv5	511	1151	**2.254**
1391935_at	eukaryotic translation initiation factor 4E member 3	Eif4e3	678	1525	**2.250**
1368174_at	EGL nine homolog 3 (C. elegans)	Egln3	859	1930	**2.246**
1368488_at	nuclear factor, interleukin 3 regulated	Nfil3	344	769	**2.232**
1379680_at	---	---	511	1140	**2.231**
1370220_at	serine carboxypeptidase 1	Scpep1	4913	10941	**2.227**
1370719_a_at	chloride channel CLIC-like 1	Clcc1	365	813	**2.225**
1390830_at	hypothetical protein LOC499602	LOC499602	266	591	**2.224**
1394576_at	---	---	247	548	**2.222**
1380130_at	---	---	256	569	**2.221**
1372340_at	methionine adenosyltransferase II, beta	Mat2b	1387	3076	**2.218**
1393373_at	opsin 3	Opn3	243	539	**2.217**
1398981_at	TP53 regulated inhibitor of apoptosis 1	Triap1	2156	4771	**2.213**
1393990_at	zinc finger protein 503	Znf503	292	645	**2.207**
1367900_at	glycogenin 1	Gyg1	379	837	**2.206**
1387361_s_at	phosphoglycerate kinase 1	Pgk1	14135	31173	**2.205**
1382802_x_at	---	---	1225	2700	**2.205**

1372006_at	---	---	3265	7176	**2.198**
1392221_at	---	---	453	994	**2.196**
1396051_at	---	---	325	711	**2.192**
1378400_at	family with sequence similarity 122B	Fam122b	1079	2364	**2.190**
1398287_at	plasminogen activator, urokinase	Plau	3427	7506	**2.190**
1380855_at	---	---	586	1277	**2.181**
1372140_at	coiled-coil domain containing 28A	Ccdc28a	330	719	**2.177**
1386909_a_at	voltage-dependent anion channel 1	Vdac1	3544	7691	**2.170**
1394479_at	arylformamidase	Afmid	426	921	**2.162**
1389580_at	helicase-like transcription factor	Hltf	312	673	**2.156**
1383224_at	par-6 (partitioning defective 6) homolog beta (C. elegans)	Pard6b	1196	2578	**2.156**
1373023_at	---	---	290	622	**2.147**
1385405_at	ADAM metallopeptidase domain 23	Adam23	270	579	**2.147**
1379649_at	glycosyltransferase 8 domain containing 3	Glt8d3	490	1048	**2.139**
1378204_at	---	---	239	512	**2.138**
1375673_at	---	---	682	1458	**2.137**
1369590_a_at	DNA-damage inducible transcript 3	Ddit3	639	1366	**2.137**
1380410_at	---	---	420	898	**2.136**
1385925_at	---	---	359	767	**2.135**
1387614_at	synaptonemal complex protein 3	Sycp3	645	1374	**2.130**
1374478_at	similar to RIKEN cDNA 2610528J11	RGD1305347	270	574	**2.125**
1388874_at	metastasis suppressor 1	Mtss1	949	2016	**2.124**
1383228_at	---	---	932	1981	**2.124**
1383306_at	---	---	1233	2608	**2.115**
1388532_at	similar to hypothetical protein	RGD1310571	1791	3786	**2.114**
1389857_at	WW domain binding protein 5	Wbp5	2154	4539	**2.107**
1396099_at	tetraspanin 33	Tspan33	279	589	**2.106**
1370845_at	ectonucleoside triphosphate diphosphohydrolase 2	Entpd2	794	1669	**2.104**
1367650_at	tubulointerstitial nephritis antigen-like 1	Tinagl1	4653	9784	**2.103**
1377042_at	polycomb group ring finger 5	Pcgf5	2606	5465	**2.097**
1396300_at	arylformamidase	Afmid	270	566	**2.096**
1379703_at	DENN/MADD domain containing 3	Dennd3	366	766	**2.096**
1387249_at	BCL2-interacting killer (apoptosis-inducing)	Bik	253	529	**2.095**
1376996_at	---	---	472	987	**2.091**
1398294_at	actinin, alpha 1	Actn1	544	1135	**2.086**
1391450_at	lysyl oxidase-like 2	Loxl2	1232	2567	**2.084**

1376304_at	---	---	3218	6701	**2.082**
1388464_at	similar to cullin 7	LOC680835	3510	7309	**2.082**
1368279_at	myeloid/lymphoid or mixed-lineage leukemia (trithorax homolog, Drosophila); translocated to, 3	Mllt3	1343	2797	**2.082**
1367601_at	Cbp/p300-interacting transactivator, with Glu/Asp-rich carboxy-terminal domain, 2	Cited2	2659	5519	**2.075**
1389539_at	Similar to DIP13 alpha	RGD1309388	772	1600	**2.073**
1390192_at	solute carrier family 27 (fatty acid transporter), member 3	Slc27a3	354	730	**2.064**
1376159_at	GDNF-inducible zinc finger protein 1	Gzf1	998	2059	**2.063**
1383034_at	RING1 and YY1 binding protein	Rybp	2331	4807	**2.062**
1383227_at	similar to ADP-ribosylation factor-like 1	LOC688311	1754	3615	**2.061**
1377720_x_at	---	---	1949	4008	**2.057**
1387116_at	DnaJ (Hsp40) homolog, subfamily B, member 9	Dnajb9	880	1808	**2.053**
1373673_at	---	---	1019	2086	**2.047**
1376436_at	lysM and putative peptidoglycan-binding domain-containing protein 3-like	LOC100360174 /// Lysmd3	632	1292	**2.043**
1391148_at	---	---	332	678	**2.043**
1375916_at	protein-L-isoaspartate (D-aspartate) O-methyltransferase domain containing 2	Pcmtd2	302	614	**2.038**
1389544_at	translocase of outer mitochondrial membrane 7 homolog (yeast)	Tomm7	7907	16095	**2.035**
1371791_at	surfeit 4	Surf4	1021	2077	**2.035**
1383910_at	---	---	1739	3533	**2.032**
1386934_at	solute carrier family 6 (neurotransmitter transporter, creatine), member 8	Slc6a8	738	1498	**2.030**
1372822_at	---	---	1566	3173	**2.027**
1398247_at	lon peptidase 1, mitochondrial	Lonp1	3779	7659	**2.026**
1395745_at	---	---	484	980	**2.024**
1372706_at	hexosaminidase B	Hexb	2257	4567	**2.023**
1379462_at	kinase suppressor of ras 1	Ksr1	617	1246	**2.020**
1368689_at	gap junction protein, beta 5	Gjb5	1719	3466	**2.016**
1390423_at	MYC binding protein 2	Mycbp2	1399	2813	**2.011**
1389419_at	---	---	1561	3137	**2.009**
1376522_at	---	---	260	522	**2.004**
1381400_at	---	---	296	593	**2.003**
1382400_at	rearranged L-myc fusion	Rlf	594	1189	**2.002**
1376724_at	---	---	269	538	**2.002**
1391253_at	---	---	343	686	**1.999**

1389169_at	progesterone receptor membrane component 2	Pgrmc2	259	518	**1.997**
1383110_at	kelch-like 24 (Drosophila)	Klhl24	329	657	**1.997**
1395973_at	---	---	482	961	**1.995**
1378925_at	cAMP responsive element modulator	Crem	843	1682	**1.995**
1391183_at	golgi associated PDZ and coiled-coil motif containing	Gopc	315	627	**1.990**
1374625_at	hairy and enhancer of split 6 (Drosophila)	Hes6	406	806	**1.987**
1367602_at	Cbp/p300-interacting transactivator, with Glu/Asp-rich carboxy-terminal domain, 2	Cited2	6718	13346	**1.987**
1375011_at	---	---	585	1160	**1.983**
1372016_at	growth arrest and DNA-damage-inducible, beta	Gadd45b	1453	2879	**1.982**
1375368_at	phosphoglycolate phosphatase	Pgp	1251	2478	**1.982**
1390396_at	eukaryotic translation initiation factor 4E member 3	Eif4e3	916	1808	**1.974**
1367796_at	mannosyl (alpha-1,3-)-glycoprotein beta-1,2-N-acetylglucosaminyltransferase	Mgat1	341	673	**1.973**
1388945_at	similar to 1300014I06Rik protein	RGD1311307	1423	2805	**1.971**
1395267_at	---	---	332	655	**1.971**
1371027_at	Cas-Br-M (murine) ecotropic retroviral transforming sequence b	Cblb	506	998	**1.970**
1388038_at	attractin	Atrn	452	890	**1.970**
1399166_a_at	B-cell CLL/lymphoma 7B	Bcl7b	426	839	**1.969**
1398411_at	---	---	18739	36896	**1.969**
1382404_at	---	---	1674	3294	**1.968**
1391346_at	transcription factor 25 (basic helix-loop-helix)	Tcf25	256	503	**1.967**
1394012_at	---	---	633	1243	**1.964**
1388539_at	plakophilin 2	Pkp2	3225	6334	**1.964**
1374722_at	C1q and tumor necrosis factor related protein 1	C1qtnf1	306	599	**1.961**
1388900_at	RGD1566118	RGD1566118	2412	4729	**1.961**
1367706_at	voltage-dependent anion channel 1	Vdac1	7131	13980	**1.960**
1370073_at	DnaJ (Hsp40) homolog, subfamily C, member 3	Dnajc3	1323	2593	**1.959**
1383058_at	---	---	409	800	**1.958**
1371988_at	mannosidase, alpha, class 1A, member 1	Man1a1	533	1042	**1.956**
1374254_a_at	transmembrane protein 205	Tmem205	571	1115	**1.951**
1381470_at	---	---	2058	3993	**1.940**
1389196_at	hypothetical protein LOC681367	LOC681367	1018	1974	**1.939**
1375910_at	CDC42 effector protein (Rho GTPase binding) 3	Cdc42ep3	573	1112	**1.939**

1367609_at	macrophage migration inhibitory factor	Mif	8516	16503	**1.938**
1390792_a_at	---	---	434	838	**1.931**
1371094_at	LIM homeobox 2	Lhx2	332	640	**1.930**
1398561_at	interferon regulatory factor 2	Irf2	363	701	**1.930**
1369562_at	hippocalcin-like 1	Hpcal1	1071	2065	**1.928**
1387747_at	gap junction protein, beta 3	Gjb3	2664	5126	**1.924**
1375341_at	transmembrane protein 189	Tmem189	589	1133	**1.923**
1375723_at	---	---	874	1679	**1.922**
1388705_at	selenoprotein M	Selm	947	1819	**1.921**
1396199_at	hypothetical protein LOC690326	LOC690326	326	626	**1.920**
1373624_at	---	---	1728	3318	**1.920**
1377043_at	---	---	274	526	**1.920**
1392475_at	activating transcription factor 6	Atf6	1704	3271	**1.919**
1371113_a_at	transferrin receptor	Tfrc	3361	6450	**1.919**
1379770_at	choline phosphotransferase 1	Chpt1	447	858	**1.919**
1375948_at	AlkB, alkylation repair homolog 5 (E. coli)	Alkbh5	1215	2332	**1.919**
1375652_at	signal sequence receptor, gamma	Ssr3	2294	4393	**1.915**
1383631_at	similar to Oligosaccharyl transferase 3 CG7748-PA	RGD1311563	1948	3730	**1.915**
1387130_at	solute carrier family 39 (iron-regulated transporter), member 1	Slc40a1	1263	2417	**1.914**
1389189_at	actinin, alpha 1	Actn1	7382	14123	**1.913**
1376415_at	mitochondrial ribosome recycling factor	Mrrf	671	1284	**1.912**
1374581_at	Der1-like domain family, member 1	Derl1	2295	4384	**1.911**
1370199_at	nucleobindin 1	Nucb1	3104	5921	**1.908**
1371467_at	similar to RIKEN cDNA 0610007P06	LOC293103	4963	9463	**1.907**
1389648_at	receptor-interacting serine-threonine kinase 4	Ripk4	411	782	**1.906**
1392923_at	---	---	274	522	**1.906**
1372136_at	Tetraspanin 14	Tspan14	7648	14573	**1.905**
1374632_at	jumonji domain containing 6	Jmjd6	1473	2804	**1.903**
1374204_at	WD repeat and SOCS box-containing 1	Wsb1	2139	4066	**1.901**
1399012_at	transmembrane protein 59	Tmem59	3130	5951	**1.901**
1383327_at	programmed cell death 4	Pdcd4	799	1520	**1.901**
1390982_at	chromatin assembly factor 1, subunit B (p60)	Chaf1b	953	1812	**1.900**
1372950_at	blocked early in transport 1 homolog (S. cerevisiae) like	Bet1l	387	734	**1.896**
1393823_at	polymerase (DNA directed), eta	Polh	267	506	**1.896**
1368407_at	heparanase	Hpse	265	503	**1.895**

1389528_s_at	Jun oncogene	Jun	1635	3085	**1.887**
1368549_at	HMG-box transcription factor 1	Hbp1	484	913	**1.886**
1372029_at	mannose-6-phosphate receptor binding protein 1	M6prbp1	3084	5815	**1.885**
1376501_at	Rho GTPase activating protein 8	Arhgap8	738	1390	**1.884**
1369813_at	DnaJ (Hsp40) homolog, subfamily C, member 5	Dnajc5	378	711	**1.884**
1389023_at	Similar to Oligosaccharyl transferase 3 CG7748-PA	RGD1311563	6919	13006	**1.880**
1371635_at	transmembrane protein, adipocyte asscociated 1	Tpra1	435	817	**1.879**
1373600_at	glycosyltransferase 8 domain containing 3	Glt8d3	3690	6931	**1.878**
1383183_at	---	---	369	694	**1.878**
1387798_a_at	complement component (3b/4b) receptor 1-like	Cr1l	3838	7202	**1.876**
1383028_at	carnitine deficiency-associated gene expressed in ventricle 3 homolog (mouse)	Cdv3	607	1139	**1.876**
1387675_at	plasminogen activator, urokinase	Plau	12417	23261	**1.873**
1393492_at	---	---	467	875	**1.873**
1367807_at	procollagen-lysine 1, 2-oxoglutarate 5-dioxygenase 1	Plod1	2507	4694	**1.873**
1374911_at	oxidative stress responsive gene	RGD1303142	1008	1886	**1.871**
1389787_at	PTK7 protein tyrosine kinase 7	Ptk7	3019	5648	**1.871**
1391494_at	---	---	549	1025	**1.869**
1388662_at	---	---	375	701	**1.866**
1377022_at	abhydrolase domain containing 10	Abhd10	1266	2363	**1.866**
1391481_at	---	---	4582	8547	**1.865**
1372863_at	MYC binding protein 2	Mycbp2	2688	5010	**1.864**
1372364_a_at	N-terminal asparagine amidase	Ntan1	2458	4580	**1.863**
1369986_at	hydroxyacyl glutathione hydrolase	Hagh	809	1508	**1.863**
1380265_at	small nuclear RNA activating complex, polypeptide 1	Snapc1	1375	2560	**1.862**
1381969_at	---	---	2549	4743	**1.861**
1369220_at	dynamin 1-like	Dnm1l	417	774	**1.859**
1388404_at	RNA polymerase 1-3	Rpo1-3	4934	9165	**1.857**
1389973_a_at	surfeit 4	Surf4	1161	2157	**1.857**
1378032_at	nuclear factor of kappa light polypeptide gene enhancer in B-cells inhibitor, zeta	Nfkbiz	5190	9639	**1.857**
1374404_at	Jun oncogene	Jun	320	593	**1.855**
1367743_at	phosphofructokinase, liver	Pfkl	356	660	**1.854**
1387081_at	reticulocalbin 2, EF-hand calcium binding domain	Rcn2	15287	28280	**1.850**
1373590_at	stomatin	Stom	441	816	**1.850**
1373373_at	---	---	2214	4091	**1.847**

1383167_at	---	---	424	784	**1.847**
1373376_at	---	---	2049	3783	**1.846**
1371981_at	Down syndrome critical region gene 3	Dscr3	2300	4245	**1.846**
1382534_at	---	---	757	1396	**1.844**
1388772_at	LSM8 homolog, U6 small nuclear RNA associated (S. cerevisiae)	Lsm8	1125	2075	**1.844**
1388680_at	C1GALT1-specific chaperone 1	C1galt1c1	313	576	**1.840**
1379283_at	---	---	2513	4618	**1.837**
1367635_at	prolyl 4-hydroxylase, beta polypeptide	P4hb	18538	34058	**1.837**
1374121_at	---	---	5986	10997	**1.837**
1367914_at	epithelial membrane protein 3	Emp3	2265	4154	**1.834**
1395248_at	ER degradation enhancer, mannosidase alpha-like 1	Edem1	597	1095	**1.834**
1399022_at	CDC-like kinase 1	Clk1	2414	4426	**1.833**
1379347_at	---	---	837	1532	**1.831**
1383019_at	---	---	297	544	**1.831**
1383226_at	zinc finger protein X-linked	Zfx	1375	2518	**1.831**
1370957_at	interleukin 6 signal transducer	Il6st	1295	2371	**1.831**
1389258_at	ring finger protein 138	Rnf138	723	1323	**1.829**
1388370_at	cyclin I	Ccni	4894	8933	**1.825**
1382024_at	DnaJ (Hsp40) homolog, subfamily B, member 6 /// similar to DnaJ homolog subfamily B member 6 (Heat shock protein J2) (HSJ-2) (MRJ) (mDj4)	Dnajb6 /// LOC690183	7774	14185	**1.825**
1372739_at	tetraspanin 31	Tspan31	2477	4516	**1.823**
1369738_s_at	cAMP responsive element modulator	Crem	295	538	**1.822**
1382128_at	---	---	382	695	**1.822**
1377345_at	---	---	1880	3424	**1.821**
1376230_at	transmembrane protein 82	Tmem82	283	516	**1.821**
1373810_at	phospholipase A2, group XIIA	Pla2g12a	1299	2360	**1.817**
1387521_at	programmed cell death 4	Pdcd4	656	1193	**1.817**
1373499_at	growth arrest specific 5	Gas5	7819	14192	**1.815**
1376878_at	similar to RIKEN cDNA 2310022B05	RGD1559896	419	760	**1.814**
1385426_at	coiled-coil domain containing 109B	Ccdc109b	290	525	**1.812**
1386886_at	CD164 molecule, sialomucin	Cd164	14031	25426	**1.812**
1371819_at	histone deacetylase 5	Hdac5	566	1026	**1.811**
1389780_at	tissue factor pathway inhibitor (lipoprotein-associated coagulation inhibitor)	Tfpi	1926	3488	**1.811**
1373106_at	zinc finger protein 36, C3H type-like 2	Zfp36l2	1335	2411	**1.806**

1392547_at	hypothetical LOC302884	MGC105649	716	1291	**1.804**
1371854_at	---	---	2905	5241	**1.804**
1395980_at	---	---	282	509	**1.803**
1392937_at	cyclin I	Ccni	665	1197	**1.800**
1372244_at	calcium binding protein 39	Cab39	3599	6477	**1.800**
1372717_at	---	---	1722	3098	**1.799**
1373781_a_at	suprabasin	Sbsn	15415	27714	**1.798**
1376410_at	matrix metallopeptidase 17	Mmp17	526	945	**1.796**
1378180_at	dCMP deaminase	Dctd	913	1640	**1.796**
1367519_at	oxysterol binding protein-like 2	Osbpl2	904	1622	**1.794**
1383080_at	---	---	2671	4789	**1.793**
1383328_x_at	programmed cell death 4	Pdcd4	1190	2132	**1.792**
1373459_at	serine/threonine kinase 11 interacting protein	Stk11ip	670	1200	**1.791**
1389014_at	nicotinamide phosphoribosyltransferase	Nampt	2117	3789	**1.790**
1398961_at	similar to ring finger protein 13	LOC681578	442	792	**1.790**
1373759_at	---	---	344	616	**1.790**
1372379_at	---	---	672	1202	**1.789**
1391723_at	---	---	552	985	**1.785**
1394614_at	glucosamine (N-acetyl)-6-sulfatase	Gns	311	554	**1.780**
1376805_at	---	---	2719	4839	**1.780**
1378010_at	---	---	282	500	**1.772**
1392627_x_at	---	---	23574	41740	**1.771**
1390420_at	carboxypeptidase X (M14 family), member 1	Cpxm1	307	543	**1.770**
1367603_at	triosephosphate isomerase 1	Tpi1	13223	23397	**1.769**
1372980_at	tetraspanin 33	Tspan33	693	1223	**1.766**
1388426_at	sterol regulatory element binding transcription factor 1	Srebf1	447	788	**1.765**
1369788_s_at	Jun oncogene	Jun	647	1142	**1.765**
1388789_at	Similar to hypothetical protein MGC17943	RGD1563325	1353	2386	**1.764**
1383099_at	GC-rich promoter binding protein 1	Gpbp1	290	512	**1.764**
1389558_at	similar to CG3570-PA	LOC500034	760	1337	**1.760**
1373149_at	yippee-like 3 (Drosophila)	Ypel3	606	1065	**1.759**
1399039_at	similar to DnaJ (Hsp40) homolog, subfamily B, member 10 isoform 2	LOC689593	674	1184	**1.757**
1377704_at	male-specific lethal 2 homolog (Drosophila)	Msl2	343	602	**1.756**
1389681_at	poliovirus receptor-related 2	Pvrl2	985	1730	**1.756**
1387770_at	interferon, alpha-inducible protein 27	Ifi27	945	1659	**1.756**
1393730_at	ADAM metallopeptidase with thrombospondin type 1 motif, 4	Adamts4	686	1204	**1.756**
1389710_at	Son of sevenless homolog 1	Sos1	2517	4418	**1.756**

	(Drosophila)				
1367529_at	Der1-like domain family, member 1	Derl1	1897	3329	**1.755**
1382415_at	arginine/serine-rich coiled-coil 2	Rsrc2	963	1689	**1.754**
1383357_a_at	RELT-like 1	Rell1	1596	2798	**1.754**
1368080_at	response gene to complement 32	Rgc32	456	800	**1.753**
1368235_at	CDC-like kinase 3	Clk3	748	1309	**1.751**
1369725_at	ArfGAP with dual PH domains 2	Adap2	1616	2827	**1.749**
1393345_at	---	---	1398	2445	**1.749**
1371926_at	---	---	2436	4254	**1.747**
1385668_at	hypothetical protein LOC683460	LOC683460	413	720	**1.744**
1389077_at	Golgi transport 1 homolog B (S. cerevisiae)	Golt1b	392	684	**1.743**
1368881_at	blocked early in transport 1 homolog (S. cerevisiae)	Bet1	445	775	**1.742**
1383840_at	chondroitin sulfate N-acetylgalactosaminyltransferase 1	Csgalnact1	571	994	**1.741**
1372733_at	---	---	491	854	**1.739**
1390524_at	ring finger protein 12	Rnf12	2736	4752	**1.737**
1390145_at	Dmx-like 2	Dmxl2	401	697	**1.736**
1389435_at	Family with sequence similarity 114, member A1	Fam114a1	458	795	**1.735**
1383474_at	interleukin-1 receptor-associated kinase 2	Irak2	347	600	**1.731**
1398906_at	sedlin-like	LOC287274	3911	6768	**1.731**
1396128_at	GC-rich promoter binding protein 1	Gpbp1	938	1623	**1.730**
1382199_at	---	---	730	1262	**1.730**
1377948_at	ankyrin repeat and zinc finger domain containing 1	Ankzf1	394	679	**1.725**
1372243_at	calcium binding protein 39	Cab39	2460	4242	**1.724**
1398596_at	natural killer tumor recognition sequence-like	LOC100364165	1129	1946	**1.723**
1384584_at	---	---	636	1095	**1.723**
1392118_at	---	---	296	508	**1.719**
1383730_at	Tetratricopeptide repeat domain 9C	Ttc9c	734	1262	**1.719**
1383162_at	---	---	1425	2447	**1.718**
1391271_at	neuron navigator 2	Nav2	297	510	**1.717**
1367729_at	ornithine aminotransferase (gyrate atrophy)	Oat	1305	2238	**1.715**
1374174_at	---	---	305	523	**1.713**
1388388_at	male-enhanced antigen 1	Mea1	4334	7421	**1.712**
1381124_at	---	---	1451	2482	**1.711**
1388777_at	signal sequence receptor, gamma	Ssr3	4558	7794	**1.710**
1391505_x_at	---	---	20110	34383	**1.710**

1370381_at	proline-rich nuclear receptor coactivator 1	Pnrc1	1706	2917	**1.709**
1390926_at	zinc finger, SWIM-type containing 3	Zswim3	328	561	**1.709**
1383326_a_at	programmed cell death 4	Pdcd4	1028	1755	**1.707**
1367648_at	insulin-like growth factor binding protein 2	Igfbp2	1252	2135	**1.705**
1398601_at	spire homolog 1 (Drosophila)	Spire1	525	896	**1.705**
1374541_at	glycogen synthase 1, muscle	Gys1	1583	2698	**1.704**
1380077_at	---	---	316	538	**1.703**
1383624_at	similar to hypothetical protein LOC284018 isoform b	RGD1565033	421	717	**1.702**
1367800_at	plasminogen activator, tissue	Plat	3064	5213	**1.702**
1394815_at	Similar to RIKEN cDNA 9030409E16	RGD1559505	1014	1723	**1.699**
1374185_at	thioredoxin domain containing 11	Txndc11	901	1530	**1.699**
1395662_at	---	---	486	826	**1.699**
1371894_at	Glucosamine (N-acetyl)-6-sulfatase	Gns	3003	5096	**1.697**
1370318_at	phosphatidylinositol 4-kinase, catalytic, alpha	Pi4ka	1056	1791	**1.696**
1373983_at	arginine/serine-rich coiled-coil 2	Rsrc2	3790	6425	**1.695**
1389840_at	splicing factor 3b, subunit 1	Sf3b1	2734	4634	**1.695**
1392508_at	exoribonuclease 1	Eri1	326	552	**1.694**
1385959_at	Son of sevenless homolog 1 (Drosophila)	Sos1	449	761	**1.694**
1382993_at	Bcl-2 binding component 3	Bbc3	728	1233	**1.694**
1386394_at	---	---	7503	12705	**1.693**
1374232_at	phosphoinositide-3-kinase, catalytic, alpha polypeptide	Pik3ca	367	621	**1.693**
1370820_at	F-box protein 6	Fbxo6	3096	5234	**1.690**
1390117_at	---	---	413	698	**1.690**
1367617_at	aldolase A, fructose-bisphosphate	Aldoa	21018	35465	**1.687**
1374884_at	protein phosphatase 1D Mg-depend. δ isoform	Ppm1d	610	1030	**1.687**
1388750_at	transferrin receptor	Tfrc	13186	22237	**1.686**
1382379_at	ring finger protein 138	Rnf138	1325	2232	**1.685**
1373519_at	---	---	597	1005	**1.685**
1368206_at	acyl-CoA thioesterase 8	Acot8	654	1102	**1.684**
1383213_at	epidermal growth factor receptor pathway substrate 8	Eps8	600	1010	**1.684**
1383829_at	bobby sox homolog (Drosophila)	Bbx	1971	3319	**1.684**
1372246_at	osteoclast stimulating factor 1	Ostf1	3268	5501	**1.683**
1373950_at	zinc finger protein 496	Znf496	1178	1983	**1.683**
1387135_at	a disintegrin and metallopeptidase domain 15 (metargidin)	Adam15	413	694	**1.680**
1388628_at	transmembrane emp24 protein	Tmed3	539	906	**1.680**

	transport domain containing 3				
1376779_at	forkhead box O1	Foxo1	302	506	**1.678**
1372171_at	polyhomeotic-like 1 (Drosophila)	Phc1	438	735	**1.678**
1367764_at	cyclin G1	Ccng1	8705	14605	**1.678**
1386995_at	BTG family, member 2	Btg2	6275	10522	**1.677**
1389742_at	---	---	1786	2991	**1.675**
1390938_at	Rho GTPase activating protein 28	Arhgap28	573	960	**1.674**
1380474_at	Lysyl oxidase-like 2	Loxl2	389	651	**1.674**
1390769_at	Ribose-phosphate pyrophosphokinase I -like	LOC314140	5057	8462	**1.673**
1383724_at	heparan sulfate 2-O-sulfotransferase 1	Hs2st1	463	774	**1.673**
1382721_at	gametogenetin binding protein 2	Ggnbp2	2551	4266	**1.673**
1384323_at	proteasome (prosome, macropain) 26S subunit, ATPase, 6	Psmc6	5487	9177	**1.672**
1388618_at	nidogen 2	Nid2	2069	3457	**1.671**
1386976_at	Cd82 molecule	Cd82	1983	3312	**1.671**
1374800_at	---	---	2712	4528	**1.670**
1373569_at	---	---	1083	1808	**1.669**
1388468_at	CDC42 small effector 1	Cdc42se1	2280	3805	**1.669**
1384452_at	Zinc finger, CCHC domain containing 7	Zcchc7	777	1296	**1.668**
1382891_at	Ubiquitin specific peptidase 27, X-linked	Usp27x	404	674	**1.667**
1367699_at	SH3-domain GRB2-like 1	Sh3gl1	1298	2161	**1.665**
1392789_at	solute carrier family 25, member 36	Slc25a36	313	520	**1.664**
1370355_at	stearoyl-Coenzyme A desaturase 1	Scd1	715	1189	**1.663**
1374252_at	centrosomal protein 110kDa	Cep110	343	570	**1.662**
1373887_at	---	---	1439	2389	**1.660**
1385829_at	obscurin-like 1	Obsl1	602	997	**1.657**
1388271_at	metallothionein 2A	Mt2A	12994	21519	**1.656**
1374948_at	transmembrane protein 106A	Tmem106a	735	1217	**1.656**
1383667_at	RUN domain containing 1	Rundc1	491	813	**1.655**
1390109_at	---	---	5993	9917	**1.655**
1373258_at	cathepsin F	Ctsf	742	1227	**1.653**
1395346_at	angio-associated, migratory cell protein	Aamp	1565	2587	**1.653**
1367575_at	enolase 1, (alpha)	Eno1	16782	27706	**1.651**
1367516_at	distrobrevin binding protein 1	Dtnbp1	847	1396	**1.649**
1373775_at	Negative regulator of ubiquitin-like proteins 1	Nub1	310	511	**1.647**
1376994_at	---	---	360	593	**1.646**
1386229_at	corepressor interacting with RBPJ, 1	Cir1	578	952	**1.646**

1399069_at	---	---	1187	1952	**1.644**
1375421_a_at	praja 2, RING-H2 motif containing	Pja2	1668	2742	**1.644**
1370859_at	protein disulfide isomerase family A, member 6	Pdia6	11161	18340	**1.643**
1368947_at	growth arrest and DNA-damage-inducible, alpha	Gadd45a	611	1004	**1.643**
1392887_at	---	---	549	901	**1.643**
1372569_at	four and a half LIM domains 3	Fhl3	1322	2171	**1.642**
1389248_at	galactokinase 1	Galk1	7308	11996	**1.641**
1384312_at	iroquois homeobox 1	Irx1	508	833	**1.640**
1373844_at	protein phosphatase methylesterase 1	Ppme1	1073	1758	**1.639**
1367810_at	solute carrier family 6 (neurotransmitter transporter, creatine), member 8	Slc6a8	461	756	**1.639**
1398768_at	retinoblastoma binding protein 7	Rbbp7	15188	24883	**1.638**
1384423_at	5-nucleotidase, cytosolic II-like	LOC100364597	546	895	**1.638**
1390412_at	solute carrier family 39 (iron-regulated transporter), member 1	Slc40a1	661	1083	**1.637**
1372846_at	cytochrome b, ascorbate dependent 3	Cybasc3	889	1454	**1.636**
1376862_at	ubiquitination factor E4B	Ube4b	3818	6246	**1.636**
1390209_at	synaptogyrin 3	Syngr3	697	1139	**1.635**
1383222_at	---	---	740	1209	**1.635**
1377213_at	---	---	1176	1922	**1.634**
1385436_at	transmembrane channel-like 4	Tmc4	312	510	**1.634**
1392575_at	Zinc finger protein 654	Znf654	447	731	**1.634**
1383543_at	golgi transport 1 homolog B (S. cerevisiae)	Golt1b	357	583	**1.634**
1392985_at	ariadne ubiquitin-conjugating enzyme E2 binding protein homolog 1 (Drosophila)	Arih1	768	1255	**1.633**
1397224_at	ATPase, Ca++ transporting, plasma membrane 1	Atp2b1	429	700	**1.632**
1392754_at	ADAM metallopeptidase domain 8	Adam8	1458	2379	**1.632**
1382007_at	SH3-domain GRB2-like endophilin B1	Sh3glb1	3005	4901	**1.631**
1379260_at	headcase homolog (Drosophila)	Heca	503	820	**1.630**
1385314_at	---	---	606	987	**1.629**
1391051_at	---	---	8981	14626	**1.629**
1390249_at	similar to human chromosome 15 open reading frame 39	RGD1305464	1301	2118	**1.628**
1368751_at	potassium voltage-gated channel, delayed-rectifier, subfamily S, member 3	Kcns3	482	785	**1.627**
1389565_at	---	---	367	597	**1.627**
1390205_at	---	---	830	1349	**1.626**
1382466_at	small nuclear ribonucleoprotein	Snrnp48	914	1485	**1.624**

	48k (U11/U12)				
1383239_at	zinc finger, CCHC domain containing 7	Zcchc7	952	1546	**1.623**
1368076_at	von Hippel-Lindau tumor suppressor	Vhl	3218	5222	**1.623**
1373902_at	ribosomal modification protein rimK-like family member B	Rimklb	789	1280	**1.621**
1395928_at	---	---	355	576	**1.621**
1374863_at	retinol binding protein 7, cellular	Rbp7	2391	3874	**1.620**
1398975_at	angio-associated, migratory cell protein	Aamp	4809	7787	**1.619**
1382348_at	dihydroorotate dehydrogenase	Dhodh	346	561	**1.618**
1373225_at	---	---	4190	6777	**1.617**
1387156_at	hydroxysteroid (17-beta) dehydrogenase 2	Hsd17b2	3090	4995	**1.616**
1383894_at	---	---	339	548	**1.616**
1375548_at	similar to RIKEN cDNA 4732418C07	RGD1310351	2561	4137	**1.616**
1374543_at	---	---	1508	2436	**1.615**
1377167_at	---	---	885	1430	**1.615**
1383361_at	DnaJ (Hsp40) homolog, subfamily B, member 6	Dnajb6	17171	27730	**1.615**
1371237_a_at	metallothionein 1a	Mt1a	15874	25632	**1.615**
1387001_at	v-ral simian leukemia viral oncogene homolog B (ras related; GTP binding protein)	Ralb	4096	6613	**1.615**
1391205_at	HEAT repeat containing 2	Heatr2	1002	1617	**1.614**
1373996_at	gene trap locus F3b	Gtlf3b	1015	1638	**1.613**
1382020_at	sperm associated antigen 9	Spag9	654	1055	**1.612**
1371547_at	C10 protein	LOC100362005	4685	7553	**1.612**
1387114_at	protein kinase C, delta	Prkcd	904	1458	**1.612**
1398359_at	ring finger protein 181	Rnf181	1627	2621	**1.611**
1372710_at	blocked early in transport 1 homolog (S. cerevisiae)	Bet1	1260	2030	**1.610**
1372377_at	DEAD (Asp-Glu-Ala-Asp) box polypeptide 41	Ddx41	736	1184	**1.610**
1393342_at	---	---	1749	2814	**1.609**
1376763_at	---	---	349	561	**1.609**
1391167_at	---	---	2305	3707	**1.608**
1371540_at	keratinocyte associated protein 2	Krtcap2	2393	3848	**1.608**
1375640_at	FK506 binding protein 9	Fkbp9	1757	2824	**1.607**
1391422_at	DnaJ (Hsp40) homolog, subfamily B, member 6	Dnajb6	1036	1664	**1.607**
1371766_at	---	---	958	1540	**1.607**
1370427_at	platelet-derived growth factor alpha polypeptide	Pdgfa	2835	4547	**1.604**
1392541_at	gamma-glutamyl cyclotransferase	Ggct	571	915	**1.602**
1372551_at	Fas-activated serine/threonine	Fastk	489	783	**1.602**

	kinase				
1371666_at	---	---	2418	3871	**1.601**
1382385_at	proteasome (prosome, macropain) 26S subunit, ATPase, 6	Psmc6	1344	2150	**1.600**
1372773_at	neural proliferation, differentiation and control, 1	Npdc1	496	793	**1.600**
1386540_at	---	---	548	877	**1.600**
1369929_at	prosaposin	Psap	10514	16815	**1.599**
1371648_at	damage-specific DNA binding protein 1	Ddb1	8886	14206	**1.599**
1398795_at	aspartyl-tRNA synthetase	Dars	3838	6136	**1.599**
1389705_at	recombination activating gene 1 activating protein 1	Rag1ap1	692	1106	**1.598**
1371373_at	ring finger protein 181	Rnf181	2519	4024	**1.597**
1370347_at	PDZ and LIM domain 7	Pdlim7	1308	2090	**1.597**
1382556_a_at	similar to DIP13 alpha	RGD1309388	684	1092	**1.597**
1384478_at	myeloid/lymphoid or mixed-lineage leukemia (trithorax homolog, Drosophila); translocated to, 3	Mllt3	473	755	**1.595**
1374144_at	---	---	639	1020	**1.595**
1388503_at	EP300 interacting inhibitor of differentiation 1	Eid1	1061	1692	**1.594**
1375003_at	serine (or cysteine) peptidase inhibitor, clade B, member 6a	Serpinb6a	4303	6857	**1.594**
1370331_at	interleukin 11 receptor, alpha chain 1	Il11ra1	633	1008	**1.593**
1389409_at	testis derived transcript	Tes	1638	2605	**1.591**
1374572_at	GATS protein-like 3	Gatsl3	1651	2626	**1.591**
1376797_at	CSRP2 binding protein	Csrp2bp	496	788	**1.590**
1395147_at	---	---	413	657	**1.590**
1376352_at	---	---	1339	2127	**1.589**
1367643_at	basigin	Bsg	15648	24857	**1.588**
1389570_at	inositol polyphosphate-5-phosphatase K	Inpp5k	452	717	**1.588**
1368321_at	early growth response 1	Egr1	1067	1691	**1.585**
1374560_at	proline-rich coiled-coil 1	Prrc1	325	515	**1.585**
1388391_at	NADH dehydrogenase (ubiquinone) 1 alpha subcomplex, 1	Ndufa1	8209	13003	**1.584**
1382056_at	splicing factor, arginine/serine-rich 11	Sfrs11	1932	3059	**1.584**
1373454_at	similar to RIKEN cDNA 0610037P05	RGD1305823	2103	3331	**1.584**
1378705_at	SET domain containing 5	Setd5	1615	2557	**1.584**
1383596_at	ISY1 splicing factor homolog (S. cerevisiae)	Isy1	736	1165	**1.583**
1392598_at	---	---	2161	3420	**1.582**
1383269_at	ring finger protein 2	Rnf2	2186	3458	**1.582**
1374507_at	ubiquitination factor E4B	Ube4b	1754	2771	**1.580**

1382797_at	similar to 1500019C06Rik protein	RGD1560433	409	647	**1.580**
1393136_at	transmembrane protein 57	Tmem57	718	1135	**1.579**
1379497_at	---	---	21766	34372	**1.579**
1390201_at	RAP1A, member of RAS oncogene family	Rap1a	592	935	**1.579**
1374622_at	---	---	1984	3132	**1.579**
1387085_at	phosphoribosyl pyrophosphate synthetase 1	Prps1	688	1085	**1.577**
1376848_at	---	---	575	907	**1.577**
1385252_at	tripartite motif-containing 6	Trim6	485	764	**1.576**
1369963_at	platelet-activating factor acetylhydrolase, isoform 1b, subunit 3	Pafah1b3	679	1071	**1.576**
1373922_at	---	---	334	526	**1.576**
1372093_at	Max interactor 1-like /// MAX interactor 1	LOC100360898 /// Mxi1	724	1141	**1.576**
1390234_at	splicing factor 3b, subunit 1	Sf3b1	10929	17208	**1.575**
1387367_at	golgi apparatus protein 1	Glg1	526	829	**1.574**
1368326_at	eukaryotic translation initiation factor 2 alpha kinase 3	Eif2ak3	579	912	**1.574**
1386929_at	hexokinase 1	Hk1	786	1237	**1.574**
1384489_at	lysine (K)-specific demethylase 2A	Kdm2a	458	720	**1.573**
1384163_at	---	---	2117	3328	**1.572**
1390842_at	transcription factor AP-2, alpha	Tcfap2a	2545	3998	**1.571**
1398641_at	pleckstrin homology domain-containing, family A (phosphoinositide binding specific) member 3	Plekha3	1999	3139	**1.570**
1388722_at	DnaJ (Hsp40) homolog, subfamily B, member 1	Dnajb1	1492	2341	**1.569**
1382312_at	AT rich interactive domain 5B (Mrf1 like)	Arid5b	1729	2712	**1.568**
1388942_at	---	---	874	1371	**1.568**
1388563_at	GC-rich promoter binding protein 1	Gpbp1	4241	6645	**1.567**
1384272_at	---	---	368	577	**1.567**
1382283_at	WAS/WASL interacting protein family, member 1	Wipf1	968	1516	**1.566**
1372552_at	acyl-Coenzyme A binding domain containing 3	Acbd3	1793	2807	**1.566**
1372509_at	hypothetical protein LOC687192	LOC687192	443	694	**1.566**
1373977_at	Kinesin family member 5C	Kif5c	714	1117	**1.565**
1373141_at	ariadne homolog 2 (Drosophila)	Arih2	677	1059	**1.565**
1377649_at	---	---	342	535	**1.564**
1398788_at	protein disulfide isomerase family A, member 3	Pdia3	10329	16149	**1.563**
1394854_at	telomeric repeat binding factor (NIMA-interacting) 1	Terf1	487	761	**1.563**
1374052_at	Family with sequence similarity 160, member B1	Fam160b1	429	670	**1.562**

1389298_at	---	---	1341	2094	**1.561**
1369879_a_at	transmembrane BAX inhibitor motif containing 6	Tmbim6	5353	8350	**1.560**
1374670_at	Similar to hypothetical protein MGC20700	RGD1307722	472	737	**1.560**
1372769_at	ligatin	Lgtn	1079	1683	**1.559**
1385953_at	myeloid/lymphoid or mixed-lineage leukemia (trithorax homolog, Drosophila); translocated to, 3	Mllt3	1146	1785	**1.558**
1368101_at	calmodulin 3	Calm3	2375	3698	**1.557**
1378294_at	F-box and leucine-rich repeat protein 12	Fbxl12	1260	1961	**1.557**
1368936_at	thioredoxin-like 1	Txnl1	5705	8881	**1.557**
1376006_at	---	---	1356	2110	**1.556**
1384122_at	---	---	1171	1823	**1.556**
1370937_a_at	integrin, alpha 7	Itga7	564	878	**1.556**
1383155_at	family with sequence similarity 117, member B	Fam117b	835	1299	**1.556**
1382970_at	similar to ubiquitin protein ligase E3 component n-recognin 2	LOC363188	465	723	**1.555**
1374725_at	Moloney leukemia virus 10	Mov10	518	805	**1.555**
1387690_at	caspase 3	Casp3	351	545	**1.555**
1372132_at	CNDP dipeptidase 2 (metallopeptidase M20 family)	Cndp2	1187	1846	**1.555**
1374917_at	SEC63 homolog (S. cerevisiae)	Sec63	379	588	**1.553**
1371616_at	---	---	3483	5407	**1.552**
1382743_at	Intermediate filament family orphan 2	Iffo2	682	1058	**1.552**
1383201_at	---	---	2626	4069	**1.550**
1383687_at	---	---	824	1277	**1.549**
1395064_at	similar to 4930429A08Rik protein	RGD1564943	747	1156	**1.548**
1392785_at	---	---	1482	2294	**1.548**
1388587_at	immediate early response 3	Ier3	9552	14782	**1.548**
1367486_at	ADP-ribosylation factor GTPase activating protein 2	Arfgap2	597	923	**1.547**
1398787_at	Ras homolog enriched in brain	Rheb	6305	9753	**1.547**
1384508_at	---	---	491	759	**1.546**
1391012_at	family with sequence similarity 83, member F	Fam83f	1346	2081	**1.546**
1390134_at	---	---	717	1109	**1.546**
1390141_at	methylenetetrahydrofolate dehydrogenase (NADP+ dependent) 1-like	Mthfd1l	855	1322	**1.546**
1390347_at	---	---	336	519	**1.545**
1379315_at	Ras association (RalGDS/AF-6) domain family (N-terminal) member 7	Rassf7	669	1033	**1.544**
1389444_at	Zinc finger, DHHC-type containing 20	Zdhhc20	922	1423	**1.544**

1371611_at	exostoses (multiple) 2	Ext2	1050	1620	**1.543**
1371579_at	Similar to signal peptidase complex subunit 3 homolog	LOC680782	4904	7564	**1.543**
1376843_at	bone morphogenetic protein receptor, type II (serine/threonine kinase)	Bmpr2	1567	2415	**1.542**
1389364_at	Nedd4 family interacting protein 2	Ndfip2	2880	4440	**1.542**
1370007_at	protein disulfide isomerase family A, member 4	Pdia4	4427	6824	**1.542**
1389071_at	EH domain binding protein 1-like 1	Ehbp1l1	716	1103	**1.540**
1367660_at	fatty acid binding protein 3, muscle and heart	Fabp3	14644	22540	**1.539**
1368486_at	insulin receptor substrate 3	Irs3	331	509	**1.538**
1367873_at	ATPase, H+ transporting, lysosomal accessory protein 1	Atp6ap1	2257	3471	**1.538**
1393019_at	---	---	334	514	**1.538**
1387279_at	F11 receptor	F11r	4526	6958	**1.537**
1399026_at	poly(A) binding protein interacting protein 2	Paip2	6584	10116	**1.536**
1377691_at	SEC22 vesicle trafficking protein homolog B (S. cerevisiae)	Sec22b	3002	4611	**1.536**
1371310_s_at	serine (or cysteine) peptidase inhibitor, clade H, member 1	Serpinh1	1280	1965	**1.536**
1367668_a_at	stearoyl-CoA desaturase (delta-9-desaturase)	Scd	2369	3636	**1.535**
1373458_at	brain expressed gene 4	Bex4	5599	8593	**1.535**
1393824_at	Similar to RIKEN cDNA 9030409E16	RGD1559505	1215	1864	**1.535**
1380445_at	---	---	454	697	**1.534**
1370305_at	Yip1 interacting factor homolog (S. cerevisiae)	Yif1	774	1188	**1.534**
1382873_at	CTTNBP2 N-terminal like	Cttnbp2nl	478	734	**1.534**
1378990_at	---	---	384	589	**1.534**
1379724_at	pleckstrin homology-like domain, family B, member 2	Phldb2	405	621	**1.533**
1388071_x_at	RT1 class Ib, locus EC2	RT1-EC2	1172	1797	**1.533**
1389598_at	ceroid-lipofuscinosis, neuronal 6	Cln6	3675	5635	**1.533**
1390185_at	decapping enzyme, scavenger	Dcps	615	943	**1.533**
1367744_at	melanoma antigen, family D, 2	Maged2	453	693	**1.532**
1388883_at	polymerase (DNA-directed), delta 4	Pold4	665	1018	**1.531**
1376086_at	UFM1-specific peptidase 2	Ufsp2	2669	4084	**1.530**
AFFX-r2-Bs-thr-3_s_at	---	---	800	1223	**1.530**
1382568_at	---	---	550	842	**1.529**
1390419_a_at	tumor suppressor candidate 3	Tusc3	1044	1596	**1.529**
1379850_at	proteasome (prosome, macropain) 26S subunit, ATPase, 6	Psmc6	4805	7344	**1.528**
1388729_at	Harvey rat sarcoma virus oncogene, subgroup R	Rras	1085	1659	**1.528**

1374736_at	---	---	694	1061	**1.528**
1383643_at	similar to UPF0197 protein C11orf10 homolog	RGD1560328	3475	5308	**1.527**
1372237_at	---	---	781	1193	**1.527**
1379302_at	recombination signal binding protein for immunoglobulin kappa J region	Rbpj	720	1100	**1.527**
1373208_at	---	---	772	1179	**1.527**
1376062_at	syndecan 1	Sdc1	1592	2430	**1.527**
1398879_at	transmembrane protein 66	Tmem66	1987	3028	**1.524**
1372149_at	AU RNA binding protein/enoyl-coenzyme A hydratase	Auh	1552	2364	**1.523**
1373117_at	ubiquitin-like with PHD and ring finger domains 2	Uhrf2	2719	4140	**1.523**
1376347_at	lysine (K)-specific demethylase 5B	Kdm5b	1278	1945	**1.522**
1378743_at	similar to Peptidyl-prolyl cis-trans isomerase NIMA-interacting 4 (Rotamase Pin4) (PPIase Pin4)	LOC684441	455	692	**1.522**
1390789_at	acyl-Coenzyme A dehydrogenase family, member 11	Acad11	835	1269	**1.521**
1398842_at	clathrin, heavy chain (Hc)	Cltc	10800	16424	**1.521**
1373788_at	solute carrier family 41, member 1	Slc41a1	534	812	**1.521**
1398922_at	---	---	1101	1674	**1.520**
1391006_at	---	---	363	552	**1.520**
1368511_at	basic helix-loop-helix family, member e41	Bhlhe41	2212	3363	**1.520**
1389529_at	Family with sequence similarity 168, member A	Fam168a	359	545	**1.520**
1376200_at	hypothetical LOC316976	MGC72974	1136	1727	**1.520**
1373250_at	---	---	3497	5312	**1.519**
1375184_at	---	---	371	564	**1.518**
1370255_at	surfactant protein C	Sftpc	478	725	**1.518**
1386864_at	phosphoglycerate mutase 1 (brain)	Pgam1	21892	33225	**1.518**
1370375_at	glutaminase 2 (liver, mitochondrial)	Gls2	646	980	**1.517**
1384865_at	---	---	962	1459	**1.517**
1371769_at	secretory carrier membrane protein 2	Scamp2	750	1138	**1.517**
1371610_at	---	---	1905	2891	**1.517**
1374903_at	glucosaminyl (N-acetyl) transferase 2, I-branching enzyme	Gcnt2	2051	3110	**1.517**
1383116_at	asparagine-linked glycosylation 13 homolog (S. cerevisiae)	Alg13	1202	1823	**1.516**
1398776_at	ribophorin II	Rpn2	6286	9531	**1.516**
1388331_at	heat shock protein 90kDa beta (Grp94), member 1	Hsp90b1	11970	18145	**1.516**

1372893_at	Yip1 domain family, member 1	Yipf1	1696	2571	**1.516**
1388904_at	hypothetical protein Dd25	Dd25	749	1135	**1.516**
1398909_at	hypothetical LOC301124	LOC301124	2272	3441	**1.515**
1380095_at	WAP four-disulfide core domain 6A	Wfdc6a	956	1448	**1.515**
1382427_at	CGG triplet repeat binding protein 1	Cggbp1	986	1493	**1.514**
1388531_at	progesterone receptor membrane component 2	Pgrmc2	1081	1633	**1.511**
1388407_at	family with sequence similarity 195, member B	Fam195b	1210	1827	**1.511**
1389526_at	EFR3 homolog A (S. cerevisiae)	Efr3a	686	1036	**1.510**
1373413_at	transmembrane protein 128	Tmem128	1656	2499	**1.509**
1371780_at	KDEL (Lys-Asp-Glu-Leu) endoplasmic reticulum protein retention receptor 2	Kdelr2	4995	7538	**1.509**
1367867_at	growth factor, augmenter of liver regeneration	Gfer	1916	2892	**1.509**
1372804_at	MMR_HSR1 domain containing protein RGD1359460	RGD1359460	901	1360	**1.509**
1374092_at	WW domain containing transcription regulator 1	Wwtr1	534	806	**1.508**
1382317_at	epidermal growth factor receptor pathway substrate 8	Eps8	795	1198	**1.507**
1387642_at	Interleukin 23, alpha subunit p19	Il23a	2603	3921	**1.506**
1369452_a_at	phosphatidylinositol binding clathrin assembly protein	Picalm	450	678	**1.505**
1374202_at	---	---	519	782	**1.505**
1367783_at	GABA(A) receptor-associated protein like 2	Gabarapl2	2480	3732	**1.505**
1383590_at	chondroitin sulfate N-acetylgalactosaminyltransferase 1	Csgalnact1	1752	2635	**1.504**
1391880_at	---	---	2970	4464	**1.503**
1390032_at	RNA binding motif, single stranded interacting protein 2	Rbms2	2081	3127	**1.503**
1387903_at	praja 2, RING-H2 motif containing	Pja2	1259	1888	**1.500**
1378094_at	---	---	845	1268	**1.500**
1372272_at	Hypothetical protein LOC692032	LOC692032	1142	1712	**1.500**

Table A2.2: Genes downregulated by hypoxia

Affymetrix ID	Gene Title	Gene Symbol	Ave amb sig int	Ave hypox sig int	amb/ hypox
1393128_at	G patch domain containing 4	Gpatch4	567	83	**-6.843**
1377114_at	---	---	9144	1601	**-5.713**
1386947_at	cadherin 1	Cdh1	1789	373	**-4.792**
1382186_a_at	G patch domain containing 4	Gpatch4	580	143	**-4.048**
1387988_at	hydroxy-delta-5-steroid dehydrogenase, 3 beta- and steroid delta-isomerase 6	Hsd3b6	8204	2183	**-3.758**
1388781_at	---	---	663	188	**-3.536**
1378958_at	coiled-coil domain containing 86	Ccdc86	815	236	**-3.456**
1371350_at	methionine adenosyltransferase II, alpha	Mat2a	3430	995	**-3.446**
1371583_at	RNA binding motif (RNP1, RRM) protein 3	Rbm3	7243	2142	**-3.381**
1373536_at	---	---	8159	2567	**-3.179**
1374945_at	tRNA methyltransferase 61 homolog A (S. cerevisiae)	Trmt61a	565	178	**-3.171**
1370288_a_at	tropomyosin 1, alpha	Tpm1	692	219	**-3.165**
1387028_a_at	inhibitor of DNA binding 1	Id1	4684	1489	**-3.147**
1374777_at	hypothetical protein LOC502894	LOC502894	847	269	**-3.145**
1382381_at	---	---	2315	751	**-3.082**
1388194_at	dihydrolipoamide S-acetyltransferase	Dlat	727	242	**-3.005**
1377461_at	---	---	684	232	**-2.951**
1385066_a_at	---	---	617	210	**-2.940**
1386586_at	PAK1 interacting protein 1	Pak1ip1	1687	578	**-2.920**
1378003_at	leucine rich repeat containing 8 family, member B	Lrrc8b	1673	584	**-2.866**
1377627_at	UTP20, small subunit (SSU) processome component, homolog (yeast)	Utp20	759	265	**-2.857**
1389554_at	---	---	1077	378	**-2.854**
1382275_at	PAK1 interacting protein 1	Pak1ip1	2458	866	**-2.840**
1376098_a_at	---	---	2542	899	**-2.829**
1379380_at	sprouty homolog 1, antagonist of FGF signaling (Drosophila)	Spry1	503	178	**-2.818**
1387776_at	transglutaminase 2, C polypeptide	Tgm2	676	240	**-2.816**
1375551_at	coiled-coil domain containing 86	Ccdc86	784	279	**-2.809**
1372789_at	zinc finger protein 637	Zfp637	1076	389	**-2.763**
1380611_at	FK506 binding protein 5	Fkbp5	1318	479	**-2.750**
1371840_at	sphingosine-1-phosphate receptor 1	S1pr1	1110	404	**-2.745**
1388473_at	---	---	521	190	**-2.742**
1378106_at	pleckstrin homology-like domain, family A, member 2	Phlda2	6380	2333	**-2.735**

1389690_at	similar to RIKEN cDNA 2410146L05	RGD1311103	1531	562	**-2.723**
1377021_at	tRNA methyltransferase 6 homolog (S. cerevisiae)	Trmt6	783	289	**-2.714**
1380523_at	F-box protein 15	Fbxo15	4157	1534	**-2.711**
1383675_at	similar to Protein KIAA0690	LOC679127	1203	444	**-2.711**
1375911_at	hypothetical protein LK44	RGD735140	528	198	**-2.663**
1386910_a_at	APEX nuclease (multifunctional DNA repair enzyme) 1	Apex1	1583	595	**-2.660**
1386946_at	carnitine palmitoyltransferase 1a, liver	Cpt1a	911	343	**-2.657**
1372510_at	sulfiredoxin 1 homolog (S. cerevisiae)	Srxn1	1431	543	**-2.638**
1372326_at	Solute carrier family 2 (facilitated glucose transporter), member 3	Slc2a3	1064	405	**-2.628**
1371765_at	histone cluster 3, H2a	Hist3h2a	620	236	**-2.628**
1392514_at	brix domain containing 1	Bxdc1	2148	818	**-2.625**
1373944_at	---	---	654	252	**-2.595**
1374857_at	GAR1 ribonucleoprotein homolog (yeast)	Gar1	2825	1095	**-2.580**
1370287_a_at	tropomyosin 1, alpha	Tpm1	1858	721	**-2.575**
1373068_at	interferon-related developmental regulator 2	Ifrd2	1412	548	**-2.575**
1391889_at	---	---	596	232	**-2.570**
1391306_at	---	---	1021	399	**-2.561**
1374340_at	---	---	1236	483	**-2.558**
1383747_at	epithelial cell transforming sequence 2 oncogene	Ect2	3596	1423	**-2.527**
1383301_at	hypothetical protein LOC498154	LOC498154	772	307	**-2.516**
1386668_a_at	similar to Protein KIAA0690	LOC679127	627	250	**-2.509**
1391063_at	kinesin family member 23	Kif23	965	385	**-2.508**
1387232_at	bone morphogenetic protein 4	Bmp4	2195	889	**-2.468**
1377708_at	hypothetical protein LOC499339	LOC499339	2274	925	**-2.457**
1390579_at	similar to RIKEN cDNA 1810029B16	RGD1305222	2369	967	**-2.450**
1370366_at	translocase of inner mitochondrial membrane 10 homolog (yeast)	Timm10	2608	1067	**-2.444**
1378214_at	---	---	697	287	**-2.433**
1370346_at	cyclin B1	Ccnb1	3901	1605	**-2.431**
1388178_at	nuclear receptor coactivator 3	Ncoa3	803	333	**-2.414**
1371775_at	---	---	642	266	**-2.413**
1379337_at	FAST kinase domains 2	Fastkd2	1608	671	**-2.396**
1395603_at	RGD1565487	RGD1565487	1096	458	**-2.394**
1392385_at	Nuclear receptor coactivator 3	Ncoa3	1438	601	**-2.393**
1389532_at	Nebulette	Nebl	1420	594	**-2.389**
1391905_at	PWP2 periodic tryptophan protein homolog (yeast)	Pwp2	678	284	**-2.386**
1378112_at	MYST histone acetyltransferase	Myst3	1291	543	**-2.379**
1383685_at	HEAT repeat containing 1	Heatr1	1075	452	**-2.377**
1376206_at	Similar to TSG118.1	RGD1565096	2158	913	**-2.364**

1379526_at	---	---	967	409	**-2.363**
1367926_at	prohibitin	Phb	555	236	**-2.348**
1393904_at	lin-28 homolog (C. elegans)	Lin28	775	331	**-2.342**
1388560_at	WD repeat domain 77	Wdr77	5005	2143	**-2.336**
1377760_at	nucleolar complex associated 4 homolog (S. cerevisiae)	Noc4l	946	406	**-2.333**
1395376_at	DEAD/H (Asp-Glu-Ala-Asp/His) box polypeptide 11 (CHL1-like helicase homolog, S. cerevisiae)	Ddx11	1583	679	**-2.330**
1387268_at	polymerase (RNA) I polypeptide B	Polr1b	879	377	**-2.328**
1374288_at	FtsJ homolog 3 (E. coli)	Ftsj3	1723	741	**-2.325**
1381428_a_at	---	---	574	247	**-2.325**
1385020_at	hypothetical protein LOC499339	LOC499339	654	282	**-2.317**
1374836_at	ribosomal RNA processing 9, small subunit (SSU) processome component, homolog (yeast)	Rrp9	938	406	**-2.314**
1389384_at	NADH dehydrogenase (ubiquinone) 1 alpha subcomplex, assembly factor 4	Ndufaf4	2274	983	**-2.313**
1381217_at	tRNA methyltransferase 6 homolog (S. cerevisiae)	Trmt6	822	356	**-2.310**
1391754_at	2 ' -5 ' oligoadenylate synthetase 1I	Oas1i	545	236	**-2.308**
1392542_at	CDC42 small effector 2	Cdc42se2	1703	738	**-2.308**
1374716_at	ribosomal RNA processing 15 homolog (S. cerevisiae)	Rrp15	1048	455	**-2.304**
1388804_at	---	---	673	292	**-2.302**
1368508_at	proteasome subunit alpha type-3-like /// proteasome (prosome, macropain) subunit, alpha type 3 /// proteasome subunit alpha type 3-like	LOC100361067 /// Psma3 /// Psma3l	735	321	**-2.291**
1387154_at	neuropeptide Y	Npy	1622	710	**-2.285**
1377387_a_at	endothelin-converting enzyme 2 /// endothelin converting enzyme 2-like	Ece2 /// LOC100363561	570	250	**-2.285**
1379719_at	---	---	2483	1089	**-2.280**
1372498_at	cytokine induced apoptosis inhibitor 1	Ciapin1	2966	1305	**-2.273**
1372997_at	similar to Protein C22orf13 homolog	LOC687713	954	420	**-2.272**
1372116_at	mitochondrial ribosomal protein S2	Mrps2	2216	978	**-2.266**
1369943_at	transglutaminase 2, C polypeptide	Tgm2	2566	1135	**-2.261**
1393817_at	---	---	568	251	**-2.261**
1373897_at	Lamin B1	Lmnb1	5326	2369	**-2.248**
1386669_at	similar to Protein KIAA0690	LOC679127	542	241	**-2.247**
1368402_at	dynein, cytoplasmic 1 light intermediate chain 2	Dync1li2	2476	1104	**-2.243**
1371919_at	nudix (nucleoside diphosphate linked moiety X)-type motif 19	Nudt19	661	295	**-2.242**
1382592_at	coiled-coil domain containing 99	Ccdc99	818	366	**-2.238**
1385073_at	mCG146312-like	LOC100363331	5005	2240	**-2.235**
1374921_at	regulator of telomere elongation helicase 1	Rtel1	874	392	**-2.233**
1390384_at	H2A histone family, member X	H2afx	1081	484	**-2.232**

1386711_a_at	DnaJ (Hsp40) homolog, subfamily C, member 11	Dnajc11	628	282	**-2.231**
1389609_at	transmembrane 7 superfamily member 3	Tm7sf3	950	427	**-2.228**
1387895_s_at	cell division cycle 20 homolog (S. cerevisiae)	Cdc20	1292	581	**-2.225**
1387950_at	nuclear import 7 homolog (S. cerevisiae)	Nip7	4829	2171	**-2.225**
1377166_at	Amyotrophic lateral sclerosis 2 (juvenile) homolog (human)	Als2	560	253	**-2.214**
1387793_at	solute carrier family 9 (sodium/hydrogen exchanger), member 3 regulator 1	Slc9a3r1	2046	926	**-2.211**
1389282_at	Integrin, alpha 3	Itga3	957	433	**-2.209**
1378120_at	mRNA turnover 4 homolog (S. cerevisiae)	Mrto4	744	337	**-2.206**
1391461_at	similar to hypothetical protein	RGD1306576	1063	483	**-2.200**
1370177_at	poliovirus receptor	PVR	3313	1506	**-2.200**
1371303_at	L-threonine dehydrogenase	Tdh	1046	476	**-2.199**
1390036_at	solute carrier family 16, member 6 (monocarboxylic acid transporter 7)	Slc16a6	2160	985	**-2.193**
1398333_at	---	---	1484	679	**-2.186**
1385086_at	budding uninhibited by benzimidazoles 1 homolog (S. cerevisiae)	Bub1	2652	1216	**-2.180**
1382065_at	---	---	799	368	**-2.174**
1387076_at	hypoxia-inducible factor 1, alpha subunit (basic helix-loop-helix transcription factor)	Hif1a	9614	4424	**-2.173**
1375937_a_at	centromere protein T	Cenpt	565	260	**-2.173**
1395595_at	Mki67 (FHA domain) interacting nucleolar phosphoprotein	Mki67ip	1692	780	**-2.168**
1375895_at	rCG34104-like	LOC100360406	4762	2205	**-2.159**
1373625_at	serine hydroxymethyltransferase 1 (soluble)	Shmt1	1045	485	**-2.154**
1388136_at	translocase of inner mitochondrial membrane 9 homolog (yeast)	Timm9	1277	593	**-2.152**
1388582_at	proteasome (prosome, macropain) activator subunit 3	Psme3	1422	661	**-2.151**
1376065_at	RRS1 ribosome biogenesis regulator homolog (S. cerevisiae)	Rrs1	1172	545	**-2.150**
1391415_at	partner of NOB1 homolog (S. cerevisiae)	Pno1	2660	1242	**-2.141**
1377625_at	tRNA methyltransferase 6 homolog (S. cerevisiae)	Trmt6	897	420	**-2.135**
1373573_at	PP3111 protein	Pp3111	1393	653	**-2.135**
1368588_at	DEAD (Asp-Glu-Ala-Asp) box polypeptide 52	Ddx52	1089	510	**-2.134**
1382972_at	UTP15, U3 small nucleolar ribonucleoprotein,	Utp15	503	236	**-2.133**
1372467_at	heparan sulfate 6-O-sulfotransferase 1	Hs6st1	576	270	**-2.129**
1383323_at	DSN1, MIND kinetochore complex component, homolog (S. cerevisiae)	Dsn1	505	237	**-2.128**
1374501_at	---	---	4575	2153	**-2.125**
1376681_at	ribosomal RNA processing 8,	Rrp8	591	278	**-2.123**

	methyltransferase, homolog (yeast)				
1374227_at	tetratricopeptide repeat domain 27	Ttc27	825	389	**-2.123**
1374415_at	polymerase (RNA) III (DNA directed) polypeptide E	Polr3e	585	276	**-2.122**
1371622_at	DPH1 homolog (S. cerevisiae) /// candidate tumor suppressor in ovarian cancer 2	Dph1 /// Ovca2	1370	646	**-2.121**
1367632_at	glutamate-ammonia ligase (glutamine synthetase)	Glul	1430	674	**-2.120**
1372539_at	---	---	1140	538	**-2.118**
1372177_at	molybdenum cofactor synthesis 2	Mocs2	2815	1334	**-2.111**
1398264_at	solute carrier family 30 (zinc transporter), member 2	Slc30a2	2729	1294	**-2.109**
1388482_at	family with sequence similarity 129, member B	Fam129b	2302	1092	**-2.108**
1388340_at	NS5A (hepatitis C virus) transactivated protein 9	Ns5atp9	1285	610	**-2.105**
1370180_at	nudix (nucleoside diphosphate linked moiety X)-type motif 4	Nudt4	2340	1116	**-2.097**
1374152_at	WD repeat domain 46	Wdr46	553	264	**-2.096**
1372629_at	coronin, actin binding protein, 2B	Coro2b	919	439	**-2.095**
1373871_at	suppressor of Ty 7 (S. cerevisiae)-like	Supt7l	1669	797	**-2.093**
1368870_at	inhibitor of DNA binding 2	Id2	899	430	**-2.092**
1373564_at	3-hydroxyisobutyryl-Coenzyme A hydrolase	Hibch	952	455	**-2.091**
1391555_at	---	---	537	257	**-2.089**
1385344_at	---	---	786	377	**-2.087**
1376811_a_at	cleavage and polyadenylation specific factor 6	Cpsf6	1235	594	**-2.078**
1383428_at	armadillo repeat containing 8	Armc8	655	316	**-2.077**
1384922_at	---	---	700	338	**-2.072**
1375849_at	RGM domain family, member A	Rgma	909	440	**-2.065**
1376267_at	---	---	1977	961	**-2.057**
1393684_at	helicase, lymphoid specific	Hells	635	309	**-2.055**
1372502_at	neurofibromin 2 (merlin)	Nf2	1309	637	**-2.054**
1372966_at	major facilitator superfamily domain containing 2	Mfsd2	2062	1005	**-2.052**
1388436_at	small nuclear ribonucleoprotein polypeptide A	Snrpa	1996	975	**-2.048**
1384149_at	coiled-coil domain containing 75	Ccdc75	875	427	**-2.048**
1373390_at	male-specific lethal 1 homolog (Drosophila)	Msl1	896	439	**-2.043**
1377889_at	URB1 ribosome biogenesis 1 homolog (S. cerevisiae)	Urb1	1089	533	**-2.041**
1379406_at	similar to chromosome 14 open reading frame 21	RGD1308396	749	367	**-2.039**
1384901_at	---	---	832	408	**-2.038**
1383168_at	hypothetical protein LOC688298	LOC688298	1386	681	**-2.036**
1382076_at	solute carrier family 37 (glycerol-3-phosphate transporter), member 1	Slc37a1	1379	678	**-2.035**
1373733_at	BCL2-related ovarian killer	Bok	1603	788	**-2.034**

1393964_at	reproductive homeobox 9-like /// reproductive homeobox 9	LOC100364002 /// Rhox9	733	361	**-2.033**
1375686_at	peptidylprolyl isomerase (cyclophilin)-like 3	Ppil3	3930	1939	**-2.027**
1367934_at	ribosomal protein L39	Rpl39	546	270	**-2.026**
1390272_at	DPH5 homolog (S. cerevisiae)	Dph5	862	426	**-2.023**
1370316_at	HSPA (heat shock 70kDa) binding protein, cytoplasmic cochaperone 1	Hspbp1	992	491	**-2.021**
1377937_at	mitochondrial ribosomal protein S14	Mrps14	1808	895	**-2.020**
1368811_at	lamin B1	Lmnb1	812	403	**-2.016**
1387123_at	cytochrome P450, family 17, subfamily a, polypeptide 1	Cyp17a1	1279	635	**-2.015**
1371513_at	---	---	2724	1354	**-2.012**
1392981_at	iroquois homeobox 4	Irx4	1922	956	**-2.011**
1368181_at	methylenetetrahydrofolate dehydrogenase (NADP+ dependent) 1, methenyltetrahydrofolate cyclohydrolase, formyltetrahydrofolate synthetase	Mthfd1	3308	1645	**-2.011**
1388425_at	OAF homolog (Drosophila)	Oaf	4773	2374	**-2.010**
1379699_at	---	---	967	482	**-2.005**
1373282_at	similar to mitochondrial carrier protein MGC4399	LOC691431	794	396	**-2.004**
1374737_at	tRNA splicing endonuclease 54 homolog (S. cerevisiae)	Tsen54	1041	520	**-2.001**
1373263_at	WD repeat domain 74	Wdr74	1382	691	**-1.999**
1389983_at	nucleolar complex associated 2 homolog (S. cerevisiae)	Noc2l	1569	786	**-1.997**
1373538_at	ubiquitin specific peptidase 1	Usp1	905	453	**-1.996**
1373272_at	pleckstrin homology domain containing, family A member 5	Plekha5	604	304	**-1.988**
1367911_at	isocitrate dehydrogenase 3 (NAD+) alpha	Idh3a	1557	783	**-1.988**
1374806_at	stratifin	Sfn	5271	2652	**-1.987**
1373629_at	solute carrier family 7 (cationic amino acid transporter, y+ system), member 6	Slc7a6	921	464	**-1.987**
1372645_at	presenilin associated, rhomboid-like	Parl	1789	901	**-1.986**
1398427_at	Myocyte enhancer factor 2D	Mef2d	1086	547	**-1.983**
1393320_at	UTP15, U3 small nucleolar ribonucleoprotein, homolog (S. cerevisiae)	Utp15	2191	1105	**-1.982**
1375071_at	nucleoporin 133	Nup133	1568	791	**-1.982**
1372506_at	proteasome (prosome, macropain) activator	Psme3	2483	1254	**-1.979**
1389200_at	bystin-like	Bysl	2101	1064	**-1.975**
1382071_at	Nuclear respiratory factor 1	Nrf1	601	304	**-1.975**
1392454_at	zinc finger, HIT type 6	Znhit6	936	474	**-1.974**
1374223_at	---	---	677	343	**-1.974**
1375908_at	myelin protein zero-like 2	Mpzl2	788	400	**-1.971**
1367701_at	receptor (G protein-coupled) activity modifying protein 2	Ramp2	561	285	**-1.969**

1372879_at	AKT1 substrate 1 (proline-rich)	Akt1s1	1156	588	**-1.967**
1382903_at	zinc finger, ZZ-type containing 3	Zzz3	959	488	**-1.966**
1373181_at	actin filament associated protein 1-like 1	Afap1l1	1937	986	**-1.965**
1379858_at	methyltransferase like 2	Mettl2	1080	550	**-1.964**
1376214_at	methylmalonic aciduria (cobalamin deficiency) cblC type, with homocystinuria	Mmachc	1144	583	**-1.963**
1389472_at	methyltransferase like 13	Mettl13	606	309	**-1.962**
1375442_at	M-phase phosphoprotein 10 (U3 small nucleolar ribonucleoprotein)	Mphosph10	1491	760	**-1.961**
1372043_at	mRNA turnover 4 homolog (S. cerevisiae)	Mrto4	2703	1381	**-1.957**
1389253_at	vanin 1	Vnn1	514	263	**-1.957**
1385765_at	---	---	893	457	**-1.955**
1374569_at	glutamate-rich WD repeat containing 1	Grwd1	1387	710	**-1.954**
1379582_a_at	cyclin A2	Ccna2	4615	2363	**-1.953**
1368308_at	myelocytomatosis oncogene	Myc	1906	976	**-1.952**
1373784_at	chaperonin containing Tcp1, subunit 8 (theta)	Cct8	1567	803	**-1.950**
1371881_at	zinc finger, HIT type 2	Znhit2	539	276	**-1.949**
1389380_at	folylpolyglutamate synthase	Fpgs	811	416	**-1.948**
1372793_at	single-stranded DNA binding protein 1	Ssbp1	1344	690	**-1.948**
1374458_at	---	---	1103	566	**-1.947**
1399146_at	dolichol kinase	Dolk	702	361	**-1.943**
1393009_at	Friend virus susceptibility 1	Fv1	527	272	**-1.939**
1372876_at	selenophosphate synthetase 2	Sephs2	928	479	**-1.937**
1375901_at	DEAD (Asp-Glu-Ala-Asp) box polypeptide 21	Ddx21	7539	3892	**-1.937**
1378629_at	SATB homeobox 1	Satb1	9707	5011	**-1.937**
1371352_at	high mobility group nucleosomal binding domain 2	Hmgn2	3272	1691	**-1.935**
1379417_at	midasin homolog (yeast)	Mdn1	914	473	**-1.932**
1378976_x_at	---	---	827	428	**-1.931**
1372764_at	similar to density-regulated protein /// similar to density-regulated protein	LOC687565 /// LOC689601	4684	2431	**-1.927**
1385089_at	Grainyhead-like 1 (Drosophila)	Grhl1	582	302	**-1.927**
1394639_at	CDC42 small effector 2	Cdc42se2	546	284	**-1.925**
1373445_at	nucleolar protein 8	Nol8	769	399	**-1.925**
1373439_at	---	---	3530	1838	**-1.921**
1383889_at	---	---	821	428	**-1.920**
1378508_at	slingshot homolog 1 (Drosophila)	Ssh1	627	327	**-1.918**
1388668_at	---	---	1368	713	**-1.917**
1377287_at	methionyl-tRNA synthetase 2, mitochondrial	Mars2	892	466	**-1.915**
1398319_at	---	---	3079	1611	**-1.912**
1376519_at	brain protein 16	Brp16	522	274	**-1.907**

1371839_at	splicing factor, arginine/serine-rich 2	Sfrs2	3174	1665	**-1.907**
1396191_at	Eukaryotic translation initiation factor 5B	Eif5b	899	471	**-1.906**
1388132_at	splicing factor proline/glutamine rich (polypyrimidine tract binding protein associated)	Sfpq	2690	1412	**-1.905**
1372312_at	LTV1 homolog (S. cerevisiae)	Ltv1	1797	944	**-1.904**
1382290_at	methyltransferase like 10	Mettl10	721	379	**-1.903**
1393085_at	MIT, microtubule interacting and transport, domain containing 1	Mitd1	662	348	**-1.902**
1372302_at	family with sequence similarity 82, member A2	Fam82a2	1071	564	**-1.900**
1376018_at	Lamin B2	Lmnb2	922	486	**-1.898**
1371897_at	phosphatidic acid phosphatase type 2 domain containing 3	Ppapdc3	1541	813	**-1.895**
1380243_at	similar to CG14803-PA	RGD1304693	833	440	**-1.893**
1383752_at	NOP2 nucleolar protein homolog (yeast)	Nop2	1315	695	**-1.891**
1369932_a_at	v-raf-leukemia viral oncogene 1	Raf1	1176	623	**-1.888**
1395044_at	Hypothetical protein LOC688832	LOC688832	8653	4597	**-1.882**
1367478_at	HtrA serine peptidase 2	Htra2	1269	674	**-1.882**
1383169_at	---	---	3009	1600	**-1.880**
1389391_at	solute carrier family 35, member E3	Slc35e3	1206	643	**-1.875**
1367525_at	thyroid hormone receptor associated protein 3	Thrap3	2128	1135	**-1.874**
1389625_at	coiled-coil-helix-coiled-coil-helix domain containing 4	Chchd4	1325	708	**-1.871**
1371035_at	general transcription factor III A	Gtf3a	2056	1099	**-1.870**
1390392_at	transmembrane protein 185B	Tmem185b	2128	1138	**-1.870**
1374920_at	---	---	3161	1692	**-1.868**
1368681_at	parathyroid hormone-like hormone	Pthlh	2683	1437	**-1.867**
1390888_a_at	HemK methyltransferase family member 1	Hemk1	789	423	**-1.867**
1373001_at	coiled-coil-helix-coiled-coil-helix domain containing 4	Chchd4	2441	1308	**-1.866**
1390848_at	RNA binding motif protein 19	Rbm19	518	277	**-1.866**
1374323_at	BRCA2 and CDKN1A interacting protein	Bccip	2984	1600	**-1.865**
1384124_at	---	---	1886	1012	**-1.863**
1377661_at	fibroblast growth factor receptor substrate 2	Frs2	1236	664	**-1.863**
1389162_at	NFU1 iron-sulfur cluster scaffold homolog (S. cerevisiae)	Nfu1	1263	678	**-1.862**
1382727_at	rCG47764-like	LOC100362342	639	343	**-1.862**
1367834_at	spermidine synthase	Srm	1466	787	**-1.862**
1388925_at	sirtuin (silent mating type information regulation 2 homolog) 5 (S. cerevisiae)	Sirt5	879	473	**-1.859**
1370940_at	tight junction protein 2	Tjp2	1489	802	**-1.858**
1388397_at	EBNA1 binding protein 2	Ebna1bp2	6076	3271	**-1.858**

1383118_at	transmembrane protein 209	Tmem209	1540	830	**-1.855**
1381822_x_at	rCG32187-like	LOC100365491	609	329	**-1.855**
1385727_at	FGFR1 oncogene partner 2	Fgfr1op2	955	515	**-1.854**
1373452_at	RNA terminal phosphate cyclase-like 1	Rcl1	1549	835	**-1.854**
1368132_at	transducer of ErbB-2.1	Tob1	1127	608	**-1.854**
1384230_at	similar to keratinocytes associated protein 3	LOC683980	646	349	**-1.854**
1389521_at	influenza virus NS1A binding protein	Ivns1abp	3293	1779	**-1.852**
1390035_at	similar to hypothetical protein MGC29875; novel putative protein similar to YIL091C yeast hypothetical 84 kD protein from SGA1-KTR7	LOC305076	796	430	**-1.850**
1387826_at	similar to pyridoxal (pyridoxine, vitamin B6) kinase	RGD1566085	595	322	**-1.850**
1367987_at	arginyl aminopeptidase (aminopeptidase B)	Rnpep	3317	1793	**-1.850**
1389862_at	nucleolar protein 12	Nol12	693	375	**-1.850**
1370191_at	antizyme inhibitor 1	Azin1	2018	1093	**-1.845**
1383380_at	ribonuclease P/MRP 38 subunit (human)	Rpp38	1149	623	**-1.845**
1378191_at	nuclear cap binding protein subunit 1, 80kDa	Ncbp1	586	318	**-1.845**
1368517_at	single stranded DNA binding protein 3	Ssbp3	853	463	**-1.844**
1379488_at	TP53 regulating kinase	Trp53rk	962	522	**-1.843**
1393701_at	debranching enzyme homolog 1 (S. cerevisiae)	Dbr1	521	283	**-1.843**
1398482_at	B-cell CLL/lymphoma 3	Bcl3	1527	829	**-1.843**
1398458_at	WNK lysine deficient protein kinase 2	Wnk2	2772	1508	**-1.838**
1392499_at	phosphoribosylformylglycinamidine synthase	Pfas	1490	811	**-1.837**
1393848_at	ribonucleotide reductase M2	Rrm2	6189	3371	**-1.836**
1383632_at	---	---	2563	1398	**-1.834**
1367759_at	H1 histone family, member 0	H1f0	7282	3975	**-1.832**
1389758_at	transcriptional adaptor 2 (ADA2 homolog, yeast)-like	Tada2l	673	368	**-1.831**
1388400_at	cell division cycle 34 homolog (S. cerevisiae)	Cdc34	5115	2794	**-1.830**
1371503_at	nucleotide binding protein 1	Nubp1	1193	652	**-1.830**
1392511_at	TAF2 RNA polymerase II, TATA box binding protein (TBP)-associated factor	Taf2	1709	935	**-1.828**
1374063_at	splicing factor, arginine/serine-rich 3	Sfrs3	9501	5199	**-1.828**
1387206_at	UDP-Gal:betaGlcNAc beta 1,4-galactosyltransferase, polypeptide 6	B4galt6	1220	668	**-1.827**
1373722_at	kinesin family member 20A	Kif20a	1409	772	**-1.825**
1370886_a_at	kinesin light chain 1	Klc1	912	500	**-1.824**
1392999_at	neuropilin (NRP) and tolloid (TLL)-like 2	Neto2	2593	1423	**-1.823**
1378937_at	---	---	511	281	**-1.822**

1372526_at	folliculin	Flcn	889	488	**-1.822**
1394095_at	gypsy retrotransposon integrase 1	Gin1	1106	607	**-1.822**
1387847_at	G protein-coupled receptor 98	Gpr98	591	325	**-1.821**
1377268_at	similar to RIKEN cDNA 1200014M14	RGD1310597	554	305	**-1.820**
1371901_at	---	---	626	344	**-1.820**
1388709_at	WD repeat domain 43	Wdr43	1058	582	**-1.819**
1385522_at	origin recognition complex, subunit 1-like (yeast)	Orc1l	1254	690	**-1.818**
1374005_at	coiled-coil domain containing 51	Ccdc51	524	289	**-1.816**
1375532_at	---	---	922	508	**-1.814**
1368436_at	nuclear distribution gene C homolog (A. nidulans)	Nudc	5709	3147	**-1.814**
1378264_at	Nuclear autoantigenic sperm protein (histone-binding)	Nasp	1964	1083	**-1.814**
1373440_at	LYR motif containing 2	Lyrm2	1425	786	**-1.813**
1377676_at	nuclear casein kinase and cyclin-dependent kinase substrate 1	Nucks1	4872	2687	**-1.813**
1368187_at	glycoprotein (transmembrane) nmb	Gpnmb	2280	1258	**-1.813**
1369499_at	thymidylate synthetase	Tyms	912	503	**-1.812**
1377658_at	actin filament associated protein 1-like 1	Afap1l1	614	339	**-1.811**
1374452_at	phosphodiesterase 9A	Pde9a	570	315	**-1.810**
1377060_at	methylcrotonoyl-Coenzyme A carboxylase 2 (beta)	Mccc2	1129	624	**-1.810**
1391282_at	similar to dJ55C23.6 gene product	RGD1306962	659	364	**-1.809**
1383961_a_at	DnaJ (Hsp40) homolog, subfamily C, member 11	Dnajc11	851	471	**-1.809**
1388641_at	phosphoribosylglycinamide formyltransferase	Gart	1491	825	**-1.808**
1398980_at	suppressor of Ty 16 homolog (S. cerevisiae)	Supt16h	2956	1638	**-1.805**
1370345_at	cyclin B1	Ccnb1	3131	1735	**-1.805**
1377833_at	RAP1 interacting factor homolog (yeast)	Rif1	874	484	**-1.805**
1377383_at	embryonal Fyn-associated substrate	Efs	2151	1192	**-1.804**
1372483_at	zinc finger protein 469	Zfp469	627	348	**-1.803**
1370311_at	eukaryotic translation initiation factor 2B, subunit 1 alpha	Eif2b1	1633	907	**-1.800**
1389065_at	RNA binding motif protein 34	Rbm34	887	493	**-1.800**
1367746_a_at	flotillin 2	Flot2	571	317	**-1.799**
1389041_at	Vac14 homolog (S. cerevisiae)	Vac14	667	371	**-1.799**
1379317_a_at	programmed cell death 11	Pdcd11	2816	1566	**-1.798**
1390574_at	---	---	852	474	**-1.797**
1398809_at	nudE nuclear distribution gene E homolog 1 (A. nidulans)	Nde1	1284	715	**-1.797**
1399029_at	ubiquitin specific peptidase 48	Usp48	780	434	**-1.796**
1382886_at	---	---	673	375	**-1.794**
1376261_at	BCL2-associated athanogene 5	Bag5	1166	650	**-1.793**

1376211_a_at	potassium channel tetramerisation domain containing 6	Kctd6	656	366	**-1.792**
1375270_at	---	---	1014	566	**-1.792**
1381252_at	exoribonuclease 2	Eri2	524	292	**-1.792**
1376001_at	polymerase (RNA) I polypeptide E	Polr1e	1327	741	**-1.791**
1382672_a_at	fer (fms/fps related) protein kinase, testis specific 2	Fert2	752	420	**-1.791**
1371658_at	COX4 neighbor	Cox4nb	2265	1265	**-1.791**
1374177_at	TAF13 RNA polymerase II, TATA box binding protein (TBP)-associated factor	Taf13	3434	1918	**-1.790**
1370297_at	polo-like kinase 1 (Drosophila)	Plk1	1235	690	**-1.790**
1390481_a_at	ubiquitin-conjugating enzyme E2T (putative)	Ube2t	961	538	**-1.786**
1392983_at	proteasome (prosome, macropain) 26S subunit, non-ATPase, 12	Psmd12	2688	1505	**-1.786**
1370300_at	prolactin regulatory element binding	Preb	977	548	**-1.782**
1383186_at	similar to RIKEN cDNA 1600013K19	RGD1307749	620	348	**-1.782**
1376690_at	mediator complex subunit 21	Med21	3103	1743	**-1.780**
1376687_at	ubiquitin specific peptidase 1	Usp1	2061	1158	**-1.780**
1395652_at	glycosyltransferase-like 1B	Gyltl1b	589	331	**-1.780**
1389800_at	PWWP domain containing 2B	Pwwp2b	1465	823	**-1.779**
1382052_at	---	---	969	545	**-1.779**
1382161_at	M-phase phosphoprotein 10 (U3 small nucleolar ribonucleoprotein)	Mphosph10	1425	801	**-1.778**
1367683_at	karyopherin alpha 2	Kpna2	7530	4236	**-1.778**
1399077_at	Metaxin 1	Mtx1	2840	1598	**-1.777**
1384185_at	similar to RIKEN cDNA 2410016O06	RGD1307704	1109	625	**-1.775**
1382174_at	---	---	2858	1610	**-1.775**
1374577_at	transforming growth factor beta regulator 4	Tbrg4	1844	1040	**-1.774**
1389197_at	KTEL (Lys-Tyr-Glu-Leu) containing 1	Ktelc1	3579	2018	**-1.773**
1386928_at	branched chain aminotransferase 2, mitochondrial	Bcat2	668	377	**-1.773**
1375432_at	similar to exosome component 1	LOC679140	2136	1205	**-1.772**
1377172_at	G-protein signaling modulator 2 (AGS3-like, C. elegans)	Gpsm2	1041	588	**-1.771**
1386897_at	protein arginine methyltransferase 1	Prmt1	6446	3640	**-1.771**
1371608_at	mitochondrial ribosomal protein S34	Mrps34	1112	628	**-1.771**
1383253_at	---	---	1669	944	**-1.769**
1376832_at	---	---	1345	760	**-1.769**
1377844_at	prostaglandin reductase 2	Ptgr2	1419	803	**-1.768**
1374886_at	BCS1-like (yeast)	Bcs1l	1006	569	**-1.768**
1370370_at	hyaluronoglucosaminidase 2	Hyal2	966	546	**-1.768**
1376039_at	aurora kinase A	Aurka	1703	963	**-1.768**
1380009_at	vaccinia related kinase 1	Vrk1	2004	1134	**-1.767**
1373721_at	histidyl-tRNA synthetase 2-like	Hars2l	1066	603	**-1.767**

1367659_s_at	dodecenoyl-Coenzyme A delta isomerase (3,2 trans-enoyl-Coenzyme A isomerase)	Dci	826	468	**-1.767**
1394568_at	similar to DNA segment, Chr 10, Wayne State University 102, expressed	RGD1563365	1237	700	**-1.766**
1389073_at	receptor accessory protein 4	Reep4	679	385	**-1.766**
1397551_at	DEAD (Asp-Glu-Ala-Asp) box polypeptide 27	Ddx27	1048	594	**-1.765**
1390558_at	staufen, RNA binding protein, homolog 2 (Drosophila)	Stau2	638	361	**-1.765**
1369962_at	5-aminoimidazole-4-carboxamide ribonucleotide formyltransferase/IMP cyclohydrolase	Atic	5142	2914	**-1.764**
1374799_at	non-SMC condensin I complex, subunit D2	Ncapd2	529	300	**-1.764**
1374538_at	protein O-linked mannose beta1,2-N-acetylglucosaminyltransferase	Pomgnt1	1200	681	**-1.763**
1398916_at	aurora kinase A interacting protein 1	Aurkaip1	2439	1383	**-1.763**
1376084_a_at	extra spindle pole bodies homolog 1 (S. cerevisiae)	Espl1	1512	859	**-1.761**
1386867_at	brain protein 44-like	Brp44l	6886	3911	**-1.761**
1390151_at	hypothetical protein LOC683034	LOC683034	570	324	**-1.760**
1372672_at	quinolinate phosphoribosyltransferase	Qprt	1257	715	**-1.759**
1374119_at	E74-like factor 3	Elf3	622	354	**-1.758**
1369642_at	platelet-activating factor acetylhydrolase, isoform 1b, subunit 2	Pafah1b2	1162	662	**-1.757**
1393202_a_at	Insulin-like growth factor 2 mRNA binding protein 3	Igf2bp3	1825	1039	**-1.756**
1376869_at	---	---	564	321	**-1.756**
1373917_at	Eukaryotic translation termination factor 1	Etf1	4049	2306	**-1.756**
1370893_at	acetyl-coenzyme A carboxylase alpha	Acaca	1330	758	**-1.755**
1388985_at	hypothetical LOC100361467	LOC100361467	3865	2202	**-1.755**
1372414_at	---	---	1047	597	**-1.754**
1387633_at	proteoglycan 2, bone marrow	Prg2	1421	810	**-1.754**
1369084_a_at	BCL2-related ovarian killer	Bok	642	366	**-1.753**
1383514_s_at	NMDA receptor regulated 1	Narg1	1866	1065	**-1.753**
1371838_at	splicing factor, arginine/serine-rich 2	Sfrs2	8898	5077	**-1.752**
1375540_at	CDKN2A interacting protein N-terminal like	Cdkn2aipnl	1170	669	**-1.750**
1380303_at	similar to Serine/threonine-protein kinase Haspin (Haploid germ cell-specific nuclear protein kinase) (Germ cell-specific gene 2 protein)	LOC687827	648	370	**-1.750**
1388806_at	tetratricopeptide repeat domain 5	Ttc5	649	371	**-1.749**
1370294_a_at	cell division cycle 20 homolog (S. cerevisiae)	Cdc20	1350	772	**-1.749**
1379525_at	cardiolipin synthase 1	Crls1	799	457	**-1.749**
1383108_at	TAF13 RNA polymerase II, TATA box binding protein (TBP)-associated factor	Taf13	1814	1038	**-1.748**

1378896_at	solute carrier family 30 (zinc transporter), member 2	Slc30a2	1789	1023	**-1.748**
1387779_at	MYB binding protein (P160) 1a	Mybbp1a	2251	1288	**-1.747**
1390839_at	PQ loop repeat containing 3	Pqlc3	2614	1497	**-1.746**
1372592_at	histone deacetylase 6	Hdac6	999	573	**-1.744**
1399010_at	COP9 constitutive photomorphogenic homolog subunit 7A (Arabidopsis)	Cops7a	1484	851	**-1.744**
1373929_at	mitochondrial ribosomal protein S7	Mrps7	2343	1344	**-1.744**
1371976_at	similar to RIKEN cDNA 9530058B02	RGD1311273	1494	857	**-1.744**
1372259_at	DEK oncogene	Dek	2121	1217	**-1.743**
1367780_at	pituitary tumor-transforming 1	Pttg1	2659	1526	**-1.742**
1377624_at	GTP-binding protein 10 (putative)	Gtpbp10	534	307	**-1.742**
1385024_at	cutC copper transporter homolog (E.coli)	Cutc	569	327	**-1.741**
1376703_at	nucleoporin 37	Nup37	3660	2102	**-1.741**
1373927_at	HMG box domain containing 4	Hmgxb4	801	460	**-1.741**
1372271_at	RNA binding motif protein 38	Rbm38	1486	855	**-1.738**
1373283_at	---	---	611	352	**-1.738**
1370128_at	heart and neural crest derivatives expressed 1	Hand1	533	307	**-1.737**
1374483_at	---	---	502	289	**-1.737**
1375042_at	asparagine-linked glycosylation 8, alpha-1,3-glucosyltransferase homolog (S. cerevisiae)	Alg8	1008	581	**-1.736**
1389038_at	eukaryotic translation termination factor 1	Etf1	4061	2340	**-1.736**
1373496_at	makorin ring finger protein 1	Mkrn1	1182	682	**-1.734**
1376040_at	signal-induced proliferation-associated 1 like 2	Sipa1l2	6509	3753	**-1.734**
1383290_at	serine peptidase inhibitor, Kunitz type 1	Spint1	988	570	**-1.734**
1373649_at	similar to COX10 homolog, cytochrome c oxidase assembly protein, heme A: farnesyltransferase	LOC687381 /// LOC691853	837	483	**-1.734**
1376321_at	family with sequence similarity 38, member A	Fam38a	1075	620	**-1.733**
1380148_at	---	---	1816	1048	**-1.733**
1397708_at	hypothetical LOC288978	LOC288978	582	336	**-1.732**
1383821_at	---	---	570	329	**-1.732**
1374318_at	BRCA1/BRCA2-containing complex, subunit 3	Brcc3	4757	2748	**-1.731**
1379626_at	SATB homeobox 1	Satb1	11491	6656	**-1.726**
1368032_at	nucleolar and coiled-body phosphoprotein 1	Nolc1	3361	1947	**-1.726**
1371322_at	laminin, gamma 1	Lamc1	1785	1034	**-1.726**
1388089_a_at	ring finger protein 4	Rnf4	1568	910	**-1.724**
1375863_a_at	similar to Gamma-tubulin complex component 4 (GCP-4)	RGD1306924	552	320	**-1.723**
1394884_s_at	single-stranded DNA binding protein 1	Ssbp1	2113	1227	**-1.722**
1398383_at	cytochrome b-561	Cyb561	814	473	**-1.722**

1372327_at	myelin expression factor 2	Myef2	1267	736	**-1.721**
1379407_at	IMP4, U3 small nucleolar ribonucleoprotein, homolog (yeast)	Imp4	1015	591	**-1.718**
1383799_at	G protein-coupled receptor 98	Gpr98	969	564	**-1.718**
1388484_at	ubiquitin-conjugating enzyme E2C	Ube2c	2745	1598	**-1.718**
1393346_at	coiled-coil domain containing 125	Ccdc125	1689	984	**-1.717**
1371600_at	protein kinase inhibitor, gamma	Pkig	923	538	**-1.716**
1368522_at	timeless homolog (Drosophila)	Timeless	1031	601	**-1.716**
1368233_at	general transcription factor IIF, polypeptide 2	Gtf2f2	1108	646	**-1.716**
1372250_at	dysbindin (dystrobrevin binding protein 1) domain containing 2	Dbndd2	1819	1061	**-1.714**
1370353_at	translocase of inner mitochondrial membrane 22 homolog (yeast)	Timm22	739	431	**-1.713**
1389566_at	cyclin B2	Ccnb2	2744	1603	**-1.712**
1386971_at	protein phosphatase 1, regulatory subunit 10	Ppp1r10	1011	591	**-1.712**
1395144_at	adherens junction associated protein 1	Ajap1	524	306	**-1.711**
1380448_at	alkB, alkylation repair homolog (E. coli)	Alkbh	2998	1754	**-1.709**
1374642_at	zinc finger protein 64	Zfp64	1238	724	**-1.709**
1372348_at	AP2 associated kinase 1	Aak1	543	318	**-1.706**
1379514_at	---	---	863	506	**-1.706**
1389217_at	RFNG O-fucosylpeptide 3-beta-N-acetylglucosaminyltransferase	Rfng	596	350	**-1.703**
1372391_at	Ribosomal protein L7-like 1	Rpl7l1	5845	3433	**-1.703**
1374597_at	cDNA sequence BC034664-like	LOC100363003	565	332	**-1.702**
1371717_at	mitofusin 1	Mfn1	1424	837	**-1.701**
1372916_at	Mitochondrial ribosomal protein S27	Mrps27	672	395	**-1.701**
1379261_at	spindle and kinetochore associated complex subunit 2	Ska2	526	309	**-1.701**
1398931_at	similar to CG12935-PA	LOC686289	909	535	**-1.699**
1387062_a_at	CHK1 checkpoint homolog (S. pombe)	Chek1	614	362	**-1.699**
1377410_at	E2F transcription factor 8	E2f8	1280	754	**-1.698**
1385222_at	eomesodermin homolog (Xenopus laevis)	Eomes	2016	1187	**-1.698**
1386870_at	glutamate-ammonia ligase (glutamine synthetase)	Glul	1577	929	**-1.698**
1373077_at	CDKN2A interacting protein N-terminal like	Cdkn2aipnl	1701	1002	**-1.697**
1383322_at	RAS-like family 11 member B	Rasl11b	1454	857	**-1.697**
1387260_at	Kruppel-like factor 4 (gut)	Klf4	1830	1079	**-1.696**
1372486_at	---	---	1855	1094	**-1.696**
1370323_at	thimet oligopeptidase 1	Thop1	813	480	**-1.696**
1372522_at	arginine and glutamate rich 1	Arglu1	4752	2803	**-1.695**
1377797_at	EMG1 nucleolar protein homolog (S. cerevisiae)	Emg1	1817	1072	**-1.694**
1371928_at	cell division cycle associated 8	Cdca8	1873	1105	**-1.694**

1372501_at	---	---	2877	1699	**-1.694**
1374892_at	spermidine/spermine N1-acetyltransferase family member 2	Sat2	929	549	**-1.694**
1371813_at	HIRA interacting protein 3	Hirip3	871	514	**-1.693**
1387071_a_at	microtubule-associated protein tau	Mapt	1076	636	**-1.693**
1377838_at	similar to RIKEN cDNA 0610039J04	RGD1562218	552	326	**-1.693**
1396000_at	---	---	656	387	**-1.692**
1394005_s_at	mediator complex subunit 21	Med21	799	472	**-1.692**
1387599_a_at	NAD(P)H dehydrogenase, quinone 1	Nqo1	13155	7784	**-1.690**
1393729_at	neuropilin (NRP) and tolloid (TLL)-like 2	Neto2	926	548	**-1.690**
1370030_at	glutamate cysteine ligase, modifier subunit	Gclm	1621	959	**-1.690**
1398384_at	exosome component 9	Exosc9	1009	597	**-1.689**
1389056_at	TRM1 tRNA methyltransferase 1 homolog (S. cerevisiae)	Trmt1	1115	660	**-1.689**
1367591_at	peroxiredoxin 3	Prdx3	6700	3968	**-1.688**
1391220_at	ESF1, nucleolar pre-rRNA processing protein, homolog (S. cerevisiae)	Esf1	2465	1460	**-1.688**
1385104_at	embryonal Fyn-associated substrate	Efs	751	445	**-1.688**
1388547_at	claudin 4	Cldn4	3358	1990	**-1.687**
1367708_a_at	fatty acid synthase	Fasn	1719	1019	**-1.687**
1376010_at	PRP4 pre-mRNA processing factor 4 homolog B (yeast)	Prpf4b	784	465	**-1.686**
1389025_at	TAF11 RNA polymerase II, TATA box binding protein (TBP)-associated factor	Taf11	1054	626	**-1.686**
1388182_at	DNA primase, p49 subunit	Prim1	4291	2546	**-1.686**
1370004_at	H2A histone family, member Y	H2afy	5067	3006	**-1.685**
1398902_at	similar to mKIAA0664 protein	RGD1307222	1459	866	**-1.685**
1376219_at	Probable phospholipid-transporting ATPase ID-like	LOC100364800	1467	871	**-1.685**
1382923_at	synaptotagmin binding, cytoplasmic RNA interacting protein	Syncrip	2128	1264	**-1.683**
1381759_at	RGD1565975	RGD1565975	741	440	**-1.682**
1372058_at	---	---	1244	739	**-1.682**
1376451_at	KRIT1, ankyrin repeat containing	Krit1	1928	1146	**-1.682**
1379530_at	---	---	3928	2337	**-1.680**
1376407_a_at	LSM7 homolog, U6 small nuclear RNA associated (S. cerevisiae)	Lsm7	1628	969	**-1.680**
1391921_at	RNA guanylyltransferase and 5'-phosphatase	Rngtt	1237	736	**-1.680**
1372620_at	acidic (leucine-rich) nuclear phosphoprotein 32 family, member E	Anp32e	3016	1796	**-1.679**
1389279_at	---	---	2968	1769	**-1.678**
1389969_at	translocase of outer mitochondrial membrane 40 homolog (yeast)	Tomm40	2767	1650	**-1.677**
1371565_at	KTI12 homolog, chromatin associated (S. cerevisiae)	Kti12	1297	773	**-1.677**
1388509_at	---	---	939	560	**-1.676**

1368302_at	msh homeobox 1	Msx1	2079	1241	**-1.675**
1372454_at	similar to RIKEN cDNA 2210016L21 gene	RGD1311899	884	528	**-1.675**
1372324_at	zinc finger, HIT type 3	Znhit3	1000	598	**-1.673**
1389015_at	FUN14 domain containing 2	Fundc2	1457	871	**-1.672**
1372046_at	general transcription factor IIIC, polypeptide 3	Gtf3c3	674	403	**-1.672**
1373583_at	---	---	737	441	**-1.672**
1382215_at	similar to Transcription initiation factor TFIID 105 kDa subunit (TAFII-105)	RGD1562997	571	342	**-1.672**
1376202_at	UDP-GlcNAc:betaGal beta-1,3-N-acetylglucosaminyltransferase 1	B3gnt1	753	450	**-1.671**
1388158_at	HLA-B associated transcript 1	Bat1	1888	1131	**-1.670**
1374014_at	neutral sphingomyelinase (N-SMase) activation associated factor	Nsmaf	543	325	**-1.670**
1372558_at	NMDA receptor regulated 1	Narg1	4566	2736	**-1.669**
1379652_at	similar to kinesin-like protein (103.5 kD) (klp-6)	RGD1559696	873	523	**-1.668**
1371809_at	mitochondrial ribosomal protein S18B	Mrps18b	4723	2831	**-1.668**
1384224_at	---	---	667	400	**-1.666**
1389357_at	MORC family CW-type zinc finger 2	Morc2	658	395	**-1.664**
1390021_at	histone cluster 1, H2bh	Hist1h2bh	859	516	**-1.664**
1389030_a_at	V-src sarcoma (Schmidt-Ruppin A-2) viral oncogene homolog (avian)	Src	1398	841	**-1.663**
1387219_at	adrenomedullin	Adm	10054	6044	**-1.663**
1370309_a_at	heterogeneous nuclear ribonucleoprotein A/B	Hnrnpab	12760	7674	**-1.663**
1383185_at	---	---	1458	877	**-1.662**
1399031_at	DET1 and DDB1 associated 1	Dda1	761	458	**-1.661**
1390494_at	ribosomal protein S24	Rps24	579	349	**-1.661**
1380490_at	similar to Importin-8 (Imp8) (Ran-binding protein 8) (RanBP8)	LOC686774	5557	3346	**-1.661**
1373682_at	DEAD (Asp-Glu-Ala-Asp) box polypeptide 51	Ddx51	635	383	**-1.661**
1388448_at	CDC42 small effector 2	Cdc42se2	4291	2584	**-1.661**
1381749_at	---	---	1559	939	**-1.659**
1395552_s_at	ankyrin repeat domain 13C	Ankrd13c	724	437	**-1.659**
1373451_at	ribonuclease H2, subunit B	Rnaseh2b	714	431	**-1.659**
1371704_at	DEAD (Asp-Glu-Ala-Asp) box polypeptide 23	Ddx23	1636	986	**-1.659**
1370327_at	COMM domain containing 5	Commd5	977	589	**-1.659**
1385856_at	RIO kinase 1 (yeast)	Riok1	814	491	**-1.659**
1382515_at	cleavage and polyadenylation specific factor 2	Cpsf2	760	458	**-1.658**
1373080_at	poly (A) polymerase alpha	Papola	7389	4456	**-1.658**
1395642_at	nucleolar protein 9	Nol9	1277	770	**-1.658**
1386857_at	stathmin 1	Stmn1	2712	1638	**-1.656**
1372661_at	transducin (beta)-like 3	Tbl3	900	543	**-1.656**

1390791_at	growth arrest-specific 2 like 1	Gas2l1	577	349	**-1.654**
1383652_at	jagunal homolog 1 (Drosophila)	Jagn1	1510	913	**-1.654**
1367624_at	activating transcription factor 4 (tax-responsive enhancer element B67)	Atf4	9907	5991	**-1.654**
1373959_at	protein phosphatase 2 (formerly 2A), regulatory subunit A, beta isoform	Ppp2r1b	1426	864	**-1.651**
1373516_at	ribosomal RNA processing 1 homolog B (S. cerevisiae)	Rrp1b	1717	1040	**-1.651**
1390996_at	zinc finger, FYVE domain containing 20	Zfyve20	517	313	**-1.651**
1367818_at	coenzyme Q3 homolog, methyltransferase (S. cerevisiae)	Coq3	1211	734	**-1.650**
1398759_at	TSC22 domain family, member 1	Tsc22d1	3142	1905	**-1.650**
1372415_at	general transcription factor IIH, polypeptide 3	Gtf2h3	737	447	**-1.649**
1370008_at	PSMC3 interacting protein	Psmc3ip	762	463	**-1.648**
1372218_at	WD repeat domain 12	Wdr12	2052	1246	**-1.648**
1396187_at	DEAD (Asp-Glu-Ala-Asp) box polypeptide 21	Ddx21	702	426	**-1.648**
1390779_at	---	---	515	313	**-1.647**
1387055_at	NEDD8 activating enzyme E1 subunit 1	Nae1	1044	635	**-1.645**
1372150_at	ubiquitin specific peptidase 10	Usp10	2552	1551	**-1.645**
1374159_at	ALS2 C-terminal like	Als2cl	2144	1303	**-1.645**
1388990_at	Mki67 (FHA domain) interacting nucleolar phosphoprotein	Mki67ip	2181	1326	**-1.645**
1389145_at	CDC42 effector protein (Rho GTPase binding) 2	Cdc42ep2	679	413	**-1.644**
1369958_at	ras homolog gene family, member B	Rhob	4390	2671	**-1.644**
1376440_at	ring finger protein 139	Rnf139	745	453	**-1.644**
1374972_at	TBC1 domain family, member 2	Tbc1d2	510	310	**-1.643**
1370304_at	translocase of inner mitochondrial membrane 17 homolog A (yeast)	Timm17a	6773	4123	**-1.643**
1373364_at	eukaryotic translation initiation factor 4 gamma, 3	Eif4g3	1373	836	**-1.643**
1373668_at	polymerase (RNA) II (DNA directed) polypeptide I	Polr2i	3532	2150	**-1.643**
1398362_at	Notch homolog 2 (Drosophila)	Notch2	3194	1944	**-1.643**
1368992_a_at	splicing factor, arginine/serine-rich 5	Sfrs5	2762	1681	**-1.642**
1371453_at	phenylalanyl-tRNA synthetase, beta subunit	Farsb	2975	1812	**-1.642**
1396013_at	leucine zipper-EF-hand containing transmembrane protein 1	Letm1	726	442	**-1.642**
1374579_at	similar to RIKEN cDNA E230015L20 gene	RGD1560873	637	388	**-1.640**
1382509_at	CCR4-NOT transcription complex, subunit 6	Cnot6	1926	1174	**-1.640**
1382856_at	XRCC6 binding protein 1	Xrcc6bp1	741	452	**-1.640**
1389471_at	translocase of outer mitochondrial membrane 34	Tomm34	832	508	**-1.639**
1389760_at	polycomb group ring finger 6	Pcgf6	2185	1333	**-1.638**
1399020_at	family with sequence similarity 40, member A	Fam40a	968	591	**-1.638**

1389241_at	similar to ubiquitin-protein ligase E3-alpha	RGD1562326	1442	880	**-1.638**
1368470_at	gamma-glutamyl hydrolase (conjugase, folylpolygammaglutamyl hydrolase)	Ggh	1488	909	**-1.638**
1376567_at	MAD1 mitotic arrest deficient-like 1 (yeast)	Mad1l1	528	322	**-1.638**
1390111_at	family with sequence similarity 91, member A1	Fam91a1	2215	1354	**-1.636**
1380062_at	membrane protein, palmitoylated 6 (MAGUK p55 subfamily member 6)	Mpp6	2045	1250	**-1.635**
1372478_at	CKLF-like MARVEL transmembrane domain containing 7	Cmtm7	638	391	**-1.633**
1395781_at	V-myc myelocytomatosis viral oncogene homolog 1, lung carcinoma derived (avian)	Mycl1	721	442	**-1.632**
1379300_at	carbohydrate sulfotransferase 2	Chst2	577	354	**-1.632**
1389525_at	ring finger protein 149	Rnf149	521	319	**-1.632**
1390918_at	growth hormone regulated TBC protein 1	Grtp1	1210	742	**-1.632**
1392161_at	ATP synthase mitochondrial F1 complex assembly factor 1	Atpaf1	509	312	**-1.631**
1385781_at	excision repair cross-complementing rodent repair deficiency complementation group 6 - like	Ercc6l	529	325	**-1.630**
1374851_at	mediator complex subunit 29	Med29	1344	825	**-1.629**
1372523_at	glutamate-cysteine ligase, catalytic subunit	Gclc	1435	882	**-1.627**
1378477_a_at	formin homology 2 domain containing 1	Fhod1	604	371	**-1.627**
1376201_at	methyltransferase 10 domain containing	Mett10d	730	449	**-1.627**
1388537_at	4-nitrophenylphosphatase domain and non-neuronal SNAP25-like protein homolog 1 (C. elegans)	Nipsnap1	740	455	**-1.626**
1378110_at	---	---	797	490	**-1.626**
1369970_at	vesicle-associated membrane protein 8	Vamp8	1165	717	**-1.625**
1374905_at	---	---	505	311	**-1.625**
1379909_at	G kinase anchoring protein 1	Gkap1	4894	3011	**-1.625**
1390989_at	motile sperm domain containing 2	Mospd2	598	368	**-1.625**
1370365_at	glutathione synthetase	Gss	1648	1014	**-1.625**
1371785_at	tumor necrosis factor receptor superfamily, member 12a	Tnfrsf12a	1891	1164	**-1.625**
1375022_at	AFG3(ATPase family gene 3)-like 2 (yeast)	Afg3l2	707	435	**-1.624**
1373353_at	bromodomain and PHD finger containing, 1	Brpf1	857	528	**-1.623**
1377299_at	nuclear autoantigenic sperm protein (histone-binding)	Nasp	2841	1750	**-1.623**
1375928_at	SET domain containing (lysine methyltransferase) 8	Setd8	2137	1316	**-1.623**
1382736_at	---	---	1297	800	**-1.623**
1389013_at	ribosomal protein L7-like 1	Rpl7l1	4261	2627	**-1.622**
1398935_at	---	---	1839	1134	**-1.622**
1375970_at	---	---	1057	652	**-1.622**

1380260_at	BARX homeobox 1	Barx1	739	456	**-1.621**
1389792_at	small optic lobes homolog (Drosophila)	Solh	1120	691	**-1.621**
1378551_at	cytochrome P450, family 20, subfamily a, polypeptide 1	Cyp20a1	511	315	**-1.619**
1389151_at	a disintegrin and metallopeptidase domain 19 (meltrin beta)	Adam19	740	457	**-1.618**
1395948_at	---	---	1272	786	**-1.618**
1382175_at	Wilms tumor 1 associated protein	Wtap	1067	659	**-1.618**
1388901_at	FK506 binding protein 5	Fkbp5	1026	634	**-1.618**
1392488_at	AMME chromosomal region gene 1-like	Ammecr1l	895	553	**-1.617**
1390020_at	Oxoglutarate (alpha-ketoglutarate) dehydrogenase (lipoamide)	Ogdh	1862	1152	**-1.617**
1373702_at	l(3)mbt-like 2 (Drosophila)	L3mbtl2	676	418	**-1.617**
1383626_at	zinc finger protein 259	Zfp259	579	358	**-1.617**
1389897_at	COP9 constitutive photomorphogenic homolog subunit 7A (Arabidopsis)	Cops7a	1218	754	**-1.616**
1372261_at	---	---	715	443	**-1.616**
1398439_a_at	origin recognition complex, subunit 6 like (yeast)	Orc6l	1152	713	**-1.616**
1370460_at	ubiquitin specific peptidase 15	Usp15	1036	642	**-1.615**
1399075_at	mitogen activated protein kinase kinase kinase 7	Map3k7	1857	1151	**-1.613**
1374964_at	dipeptidylpeptidase 8	Dpp8	527	327	**-1.612**
1373061_at	sorting nexin 17	Snx17	515	320	**-1.611**
1383240_at	---	---	2664	1654	**-1.611**
1389247_at	polymerase (RNA) III (DNA directed) polypeptide A	Polr3a	711	442	**-1.610**
1389537_at	Treacher Collins-Franceschetti syndrome 1 homolog (human)	Tcof1	569	354	**-1.609**
1373093_at	ERBB receptor feedback inhibitor 1	Errfi1	10183	6336	**-1.607**
1367833_at	proteasome (prosome, macropain) 26S subunit, ATPase, 5	Psmc5	3451	2148	**-1.607**
1380960_at	coronin, actin binding protein 2A	Coro2a	967	602	**-1.607**
1385268_at	coiled-coil domain containing 93	Ccdc93	587	366	**-1.605**
1398254_at	renin binding protein	Renbp	527	329	**-1.605**
1375767_at	pleckstrin homology domain containing, family G (with RhoGef domain) member 3	Plekhg3	700	436	**-1.604**
1387294_at	SH3-domain binding protein 5 (BTK-associated)	Sh3bp5	2073	1292	**-1.604**
1398371_at	coiled-coil domain containing 132	Ccdc132	1262	787	**-1.604**
1373913_at	polyribonucleotide nucleotidyltransferase 1	Pnpt1	1400	873	**-1.604**
1389263_at	retinoic acid induced 14	Rai14	2649	1652	**-1.604**
1391604_at	non-SMC condensin II complex, subunit D3	Ncapd3	1005	627	**-1.603**
1373213_at	synaptosomal-associated protein 29	Snap29	997	622	**-1.602**
1379656_a_at	---	---	3458	2159	**-1.602**
1388609_at	pleckstrin homology domain containing, family M (with RUN	Plekhm2	619	387	**-1.601**

	domain) member 2				
1372019_at	mediator complex subunit 10	Med10	2465	1540	**-1.601**
1389616_at	---	---	661	413	**-1.601**
1379715_at	similar to CG9346-PA	RGD1307882	1499	936	**-1.600**
1369641_at	platelet-activating factor acetylhydrolase, isoform 1b, subunit 2	Pafah1b2	996	623	**-1.600**
1386344_at	Ankylosis, progressive homolog (mouse)	Ankh	634	396	**-1.600**
1382082_at	nuclear transcription factor-Y beta	Nfyb	572	357	**-1.599**
1379980_at	---	---	763	478	**-1.599**
1377400_at	HIV-1 Rev binding protein 2	Hrb2	1473	922	**-1.598**
1388117_at	small nuclear ribonucleoprotein polypeptides B and B1	Snrpb	5415	3390	**-1.598**
1389053_at	Required for meiotic nuclear division 1 homolog (S. cerevisiae)	Rmnd1	1445	905	**-1.596**
1395560_at	---	---	594	372	**-1.596**
1395516_at	arginine and glutamate rich 1	Arglu1	1113	697	**-1.596**
1388567_at	THUMP domain containing 1	Thumpd1	1392	872	**-1.596**
1371336_at	hematological and neurological expressed 1	Hn1	6328	3967	**-1.595**
1372108_at	Pentatricopeptide repeat domain 3	Ptcd3	2603	1632	**-1.595**
1375979_at	---	---	764	479	**-1.595**
1379903_at	---	---	1768	1109	**-1.595**
1367720_at	aminolevulinate, delta-, dehydratase	Alad	2571	1613	**-1.594**
1394567_at	quiescin Q6 sulfhydryl oxidase 2	Qsox2	792	497	**-1.593**
1368612_at	integrin, beta 4	Itgb4	532	334	**-1.593**
1372540_at	ubiquitin-like domain containing CTD phosphatase 1	Ublcp1	2829	1776	**-1.593**
1376930_at	mitochondrial ribosomal protein L51	Mrpl51	1655	1039	**-1.592**
1387458_at	ring finger protein 4	Rnf4	1321	830	**-1.592**
1392746_x_at	La ribonucleoprotein domain family, member 1	Larp1	1107	696	**-1.592**
1380909_at	solute carrier family 25 (mitochondrial carrier, phosphate carrier), member 24	Slc25a24	3536	2222	**-1.591**
1373744_at	anaphase promoting complex subunit 1	Anapc1	895	563	**-1.591**
1389137_at	Citron	Cit	901	567	**-1.591**
1393341_at	---	---	639	402	**-1.590**
1372808_at	methylenetetrahydrofolate dehydrogenase (NADP+ dependent) 2, methenyltetrahydrofolate cyclohydrolase	Mthfd2	3489	2194	**-1.590**
1371670_at	exosome component 4	Exosc4	1958	1232	**-1.590**
1377945_at	DEAD (Asp-Glu-Ala-Asp) box polypeptide 18	Ddx18	1499	943	**-1.589**
1398337_at	Similar to RIKEN cDNA 9430077D24 gene	LOC290341	1423	896	**-1.588**
1370869_at	branched chain aminotransferase 1, cytosolic	Bcat1	2818	1774	**-1.588**

1374326_at	peter pan homolog (Drosophila)	Ppan	1382	870	**-1.587**
1376316_at	origin recognition complex, subunit 6 like (yeast)	Orc6l	1375	867	**-1.587**
1388790_at	coenzyme Q5 homolog, methyltransferase (S. cerevisiae)	Coq5	694	437	**-1.587**
1390534_at	structural maintenance of chromosomes 5	Smc5	2099	1322	**-1.587**
1392902_at	ESF1, nucleolar pre-rRNA processing protein, homolog (S. cerevisiae)	Esf1	1452	916	**-1.586**
1370526_at	integrin, alpha E	Itgae	982	620	**-1.586**
1371980_at	ATPase family, AAA domain containing 3A	Atad3a	511	322	**-1.586**
1372677_at	deoxyhypusine hydroxylase/monooxygenase	Dohh	1320	833	**-1.585**
1377709_at	---	---	17119	10805	**-1.584**
1377506_at	growth differentiation factor 1 /// LAG1 homolog, ceramide synthase 1	Gdf1 /// Lass1	2410	1522	**-1.584**
1374687_at	---	---	2672	1688	**-1.583**
1372988_at	CCR4-NOT transcription complex, subunit 10	Cnot10	1034	653	**-1.583**
1394554_at	---	---	801	506	**-1.582**
1370162_at	protein phosphatase 4, regulatory subunit 1	Ppp4r1	1436	907	**-1.582**
1380408_at	---	---	1584	1002	**-1.581**
1376357_at	ankyrin repeat and IBR domain containing 1	Ankib1	2005	1268	**-1.581**
1393142_at	centrosomal protein 70kDa	Cep70	572	362	**-1.581**
1373527_at	rCG48622-like	LOC100362920	943	597	**-1.580**
1387900_at	CDP-diacylglycerol--inositol 3-phosphatidyltransferase (phosphatidylinositol synthase)	Cdipt	1650	1044	**-1.580**
1398342_at	tumor suppressor candidate 2	Tusc2	1220	772	**-1.580**
1372628_at	adaptor-related protein complex AP-4, sigma 1	Ap4s1	1445	915	**-1.579**
1376177_at	family with sequence similarity 117, member A	Fam117a	619	392	**-1.579**
1390415_at	thyroid hormone receptor interactor 13	Trip13	1793	1136	**-1.579**
1377868_at	G protein-coupled receptor associated sorting protein 2	Gprasp2	541	343	**-1.578**
1370386_at	RuvB-like 1 (E. coli)	Ruvbl1	1483	940	**-1.578**
1368967_at	eukaryotic translation initiation factor 2B, subunit 3 gamma	Eif2b3	1217	771	**-1.577**
1390250_x_at	Probable phospholipid-transporting ATPase ID-like	LOC100364800	933	592	**-1.576**
1374568_at	similar to mKIAA1737 protein	RGD1309492	578	367	**-1.576**
1388736_at	coiled-coil domain containing 43	Ccdc43	653	414	**-1.576**
1384605_at	---	---	977	620	**-1.576**
1370437_at	nucleoporin like 1	Nupl1	1456	924	**-1.576**
1371907_at	ADP-ribosylation-like factor 6 interacting protein 4	Arl6ip4	1519	964	**-1.575**
1373980_at	similar to XPA binding protein 1	LOC688393	708	449	**-1.575**
1375506_at	aarF domain containing kinase 5	Adck5	934	593	**-1.574**

1371697_at	patatin-like phospholipase domain containing 2	Pnpla2	614	390	**-1.573**
1371563_at	regulator of chromosome condensation 2	Rcc2	726	461	**-1.573**
1368702_at	PRKC, apoptosis, WT1, regulator	Pawr	1456	926	**-1.573**
1374938_at	ZW10, kinetochore associated, homolog (Drosophila)	Zw10	897	570	**-1.573**
1378299_at	---	---	815	518	**-1.573**
1369063_at	acidic (leucine-rich) nuclear phosphoprotein 32 family, member A	Anp32a	8332	5299	**-1.572**
1388154_at	E2F transcription factor 5	E2f5	1271	808	**-1.572**
1395625_at	---	---	2074	1319	**-1.572**
1380186_at	---	---	604	384	**-1.571**
1389131_at	cytosolic 5-nucleotidase III-like protein-like /// 5'-nucleotidase, cytosolic III-like	LOC100364937 /// Nt5c3l	725	462	**-1.571**
1375216_at	poliovirus receptor-related 2	Pvrl2	1302	829	**-1.571**
1398955_at	COP9 constitutive photomorphogenic homolog subunit 8 (Arabidopsis)	Cops8	8167	5200	**-1.571**
1385118_at	eukaryotic translation initiation factor 2, subunit 1 alpha	Eif2s1	818	521	**-1.570**
1393745_at	origin recognition complex, subunit 3-like (yeast)	Orc3l	575	367	**-1.569**
1373178_at	---	---	3038	1936	**-1.569**
1389963_at	p55 protein	LOC652956	615	392	**-1.569**
1371489_at	---	---	6520	4160	**-1.567**
1393154_at	---	---	1211	773	**-1.567**
1372932_at	ribosomal RNA processing 1 homolog (S. cerevisiae)	Rrp1	1373	876	**-1.567**
1376298_at	UPF3 regulator of nonsense transcripts homolog B (yeast)	Upf3b	896	572	**-1.567**
1373389_at	acyl-Coenzyme A dehydrogenase family, member 9	Acad9	956	610	**-1.566**
1370421_a_at	cullin-associated and neddylation-dissociated 2 (putative)	Cand2	710	454	**-1.566**
1393106_x_at	general transcription factor IIF, polypeptide 1	Gtf2f1	2230	1425	**-1.565**
1373760_at	threonyl-tRNA synthetase 2, mitochondrial (putative)	Tars2	717	458	**-1.565**
1371914_at	SWI/SNF related, matrix associated, actin dependent regulator of chromatin, subfamily b, member 1	Smarcb1	1183	756	**-1.564**
1381259_at	stromal antigen 1	Stag1	1113	712	**-1.564**
1377697_at	amyloid beta (A4) precursor protein-binding, family B, member 2	Apbb2	515	329	**-1.563**
1389668_at	SPC25, NDC80 kinetochore complex component, homolog (S. cerevisiae)	Spc25	2455	1572	**-1.562**
1374033_at	proteasome (prosome, macropain) subunit, beta type 10	Psmb10	624	399	**-1.562**
1383059_a_at	G kinase anchoring protein 1	Gkap1	2012	1289	**-1.561**
1392986_at	striatin, calmodulin binding protein	Strn	977	626	**-1.561**
1372462_at	acetyl-Coenzyme A acetyltransferase 2	Acat2	780	500	**-1.560**
1397508_at	DEAD (Asp-Glu-Ala-Asp) box polypeptide 18	Ddx18	587	376	**-1.560**

1370976_at	GTPase activating protein (SH3 domain) binding protein 1	G3bp1	6358	4077	**-1.559**
1379659_at	BMP-2 inducible kinase	Bmp2k	815	523	**-1.559**
1390889_at	hypothetical protein LOC691543	LOC691543	588	377	**-1.559**
1388908_at	peroxisomal D3,D2-enoyl-CoA isomerase	Peci	690	442	**-1.559**
1370432_at	POU class 3 homeobox 1	Pou3f1	1873	1203	**-1.558**
1383362_at	---	---	583	374	**-1.557**
1371924_at	olfactomedin-like 3	Olfml3	974	626	**-1.556**
1388954_at	similar to hypothetical protein MGC25461	RGD1306717	520	335	**-1.555**
1388773_at	tumor necrosis factor, alpha-induced protein 2	Tnfaip2	864	556	**-1.554**
1373241_at	Mitochondrial ribosomal protein L49	Mrpl49	3007	1935	**-1.554**
1372059_at	similar to RIKEN cDNA 2610528E23	RGD1309437	1696	1092	**-1.554**
1394597_at	DDHD domain containing 1	Ddhd1	1170	753	**-1.553**
1367883_at	survival motor neuron 1	Smn1	2276	1466	**-1.552**
1383625_a_at	zinc finger protein 259	Zfp259	2392	1541	**-1.552**
1385699_at	YTH domain family, member 1	Ythdf1	2544	1640	**-1.551**
1388621_at	mediator complex subunit 11	Med11	650	419	**-1.551**
1392906_at	ubiquitin-like 4	Ubl4	1013	654	**-1.549**
1388956_at	exportin 5	Xpo5	1109	716	**-1.548**
1382792_at	---	---	981	634	**-1.548**
1389344_at	ubiquitin specific peptidase 39	Usp39	1619	1046	**-1.548**
1383572_at	zinc finger, DHHC-type containing 6	Zdhhc6	2263	1462	**-1.547**
1368324_at	breast cancer 2	Brca2	607	392	**-1.547**
1372547_at	similar to RIKEN cDNA 2410002O22 gene	RGD1306583	2388	1543	**-1.547**
1376701_a_at	similar to 5930416I19Rik protein	MGC94282	1108	716	**-1.547**
1379348_at	exosome component 2	Exosc2	653	422	**-1.546**
1372186_a_at	topoisomerase (DNA) II alpha	Top2a	1554	1005	**-1.546**
1373194_at	LYR motif containing 2	Lyrm2	528	341	**-1.546**
1383744_at	---	---	1975	1278	**-1.546**
1391584_at	---	---	560	362	**-1.546**
1372688_at	exosome component 7	Exosc7	2602	1685	**-1.545**
1387924_at	neuronal guanine nucleotide exchange factor	Ngef	1018	659	**-1.545**
1372933_at	sirtuin 7 (silent mating type information regulation 2, homolog) 7 (S. cerevisiae)	Sirt7	510	330	**-1.544**
1384456_at	ubiquitin specific protease 24	Usp24	795	515	**-1.544**
1381986_at	Similar to neuron navigator 1	LOC685707	1232	798	**-1.544**
1383125_at	TRM2 tRNA methyltransferase 2 homolog A (S. cerevisiae)	Trmt2a	1166	755	**-1.544**
1377232_at	LIM and calponin homology domains 1	Limch1	607	393	**-1.543**
1367663_at	proteasome (prosome, macropain) activator subunit 1	Psme1	3299	2138	**-1.543**

1376423_at	F-box and leucine-rich repeat protein 19	Fbxl19	1435	930	**-1.542**
1382679_at	WD repeat domain 43	Wdr43	1467	952	**-1.542**
1392698_a_at	general transcription factor IIIC, polypeptide 4	Gtf3c4	1083	702	**-1.542**
1395533_at	histidyl-tRNA synthetase	Hars	600	390	**-1.540**
1370123_a_at	cortactin	Cttn	640	416	**-1.540**
1391190_at	trinucleotide repeat containing 6a	Tnrc6a	756	491	**-1.540**
1391552_at	---	---	710	462	**-1.538**
1373168_at	Similar to LEYDIG CELL TUMOR 10 KD PROTEIN	LOC288913	726	472	**-1.538**
1376149_at	---	---	1084	706	**-1.537**
1398977_at	---	---	1040	677	**-1.536**
1368065_at	GIPC PDZ domain containing family, member 1	Gipc1	567	369	**-1.536**
1371811_at	Bernardinelli-Seip congenital lipodystrophy 2 homolog (human)	Bscl2	672	437	**-1.535**
1385676_at	Cd2 (cytoplasmic tail) binding protein 2	Cd2bp2	524	342	**-1.535**
1370144_at	GTP binding protein 4 /// similar to Nucleolar GTP-binding protein 1 (Chronic renal failure gene protein) (GTP-binding protein NGB) /// similar to Nucleolar GTP-binding protein 1 (Chronic renal failure gene protein) (GTP-binding protein NGB) /// similar to Nucleolar GTP-binding protein 1 (Chronic renal failure gene protein) (GTP-binding protein NGB) /// similar to GTP-binding protein NGB	Gtpbp4 /// LOC683324 /// LOC689822 /// LOC689842 /// RGD1563564	1366	890	**-1.534**
1373908_at	---	---	1341	874	**-1.534**
1375701_at	methyltransferase 10 domain containing	Mett10d	1485	968	**-1.534**
1382035_at	TATA box binding protein	Tbp	1261	823	**-1.533**
1368330_at	apoptosis antagonizing transcription factor	Aatf	600	392	**-1.533**
1392467_at	inositol (myo)-1(or 4)-monophosphatase 2	Impa2	1112	726	**-1.532**
1390171_at	family with sequence similarity 76, member A	Fam76a	1639	1070	**-1.532**
1383578_at	RAD51 homolog (RecA homolog, E. coli) (S. cerevisiae)	Rad51	2883	1882	**-1.532**
1371071_at	guanine nucleotide binding protein (G protein), beta polypeptide 4	Gnb4	646	422	**-1.532**
1370303_at	solute carrier family 35, member A4	Slc35a4	1252	818	**-1.531**
1386918_a_at	sigma non-opioid intracellular receptor 1	Sigmar1	842	551	**-1.530**
1371889_at	solute carrier family 22, member 17	Slc22a17	1392	910	**-1.530**
1372014_at	mediator complex subunit 27	Med27	857	560	**-1.529**
1388108_at	ELOVL family member 6, elongation of long chain fatty acids (yeast)	Elovl6	507	332	**-1.528**
1376641_at	THO complex 1	Thoc1	724	474	**-1.528**
1382921_at	SDA1 domain containing 1	Sdad1	745	487	**-1.528**
1389315_at	G protein-coupled receptor kinase	Git2	938	614	**-1.527**

	interacting ArfGAP 2				
1374161_at	importin 11	Ipo11	1589	1040	**-1.527**
1368214_at	SMAD family member 2	Smad2	1612	1056	**-1.526**
1378860_at	---	---	1627	1066	**-1.526**
1372619_at	mitochondrial ribosomal protein L49	Mrpl49	1583	1037	**-1.526**
1383353_at	---	---	2718	1781	**-1.526**
1391410_at	---	---	1516	994	**-1.525**
1378591_at	---	---	809	531	**-1.524**
1388350_at	peroxisomal biogenesis factor 19	Pex19	2353	1545	**-1.523**
1373935_at	polymerase (DNA directed), delta 2, regulatory subunit	Pold2	1243	816	**-1.522**
1372460_at	---	---	6929	4551	**-1.522**
1372869_at	similar to GTP-binding protein NGB	RGD1563564	1412	928	**-1.522**
1379804_at	sorting nexin family member 27	Snx27	1003	659	**-1.522**
1367786_at	proteasome (prosome, macropain) subunit, beta type 8 (large multifunctional peptidase 7)	Psmb8	944	621	**-1.521**
1367697_at	mitogen activated protein kinase 14	Mapk14	2168	1425	**-1.521**
1375918_at	zinc finger protein 830	Znf830	998	656	**-1.521**
1398772_at	NSFL1 (p97) cofactor (p47)	Nsfl1c	2606	1715	**-1.520**
1390650_at	nucleoporin 85	Nup85	1100	724	**-1.520**
1389389_at	DEAD (Asp-Glu-Ala-Asp) box polypeptide 56	Ddx56	1132	745	**-1.519**
1383051_at	Synaptotagmin binding, cytoplasmic RNA interacting protein	Syncrip	1455	958	**-1.519**
1376602_a_at	F-box protein 22	Fbxo22	1922	1265	**-1.519**
1374764_at	NOP14 nucleolar protein homolog (yeast)	Nop14	1254	826	**-1.518**
1370340_x_at	tropomyosin 3, gamma	Tpm3	1849	1218	**-1.518**
1372076_at	hepatitis B virus x interacting protein	Hbxip	3257	2146	**-1.518**
1373978_at	nuclear cap binding protein subunit 1, 80kDa	Ncbp1	1567	1033	**-1.518**
1398869_at	proteasome (prosome, macropain) 26S subunit, ATPase, 4	Psmc4	2687	1771	**-1.517**
1390177_at	---	---	786	518	**-1.517**
1397628_at	similar to RIKEN cDNA 2900092E17	RGD1305592	978	645	**-1.516**
1372015_at	transforming, acidic coiled-coil containing protein 1	Tacc1	943	622	**-1.516**
1388837_at	solute carrier family 44, member 2	Slc44a2	1114	735	**-1.516**
1388953_at	guanine nucleotide binding protein-like 3 (nucleolar)	Gnl3	5310	3505	**-1.515**
1388803_at	deoxyhypusine synthase	Dhps	1150	759	**-1.515**
1383559_at	DEAD (Asp-Glu-Ala-Asp) box polypeptide 19a	Ddx19a	776	512	**-1.515**
1388570_at	coenzyme Q9 homolog (S. cerevisiae)	Coq9	3470	2291	**-1.515**
1388129_at	structure specific recognition protein 1	Ssrp1	4328	2859	**-1.514**
1373074_at	similar to RIKEN cDNA 2700002I20	RGD1307279	2767	1828	**-1.514**
1376212_at	programmed cell death 2-like	Pdcd2l	1097	725	**-1.513**

1392615_at	selenoprotein I	Seli	1211	800	**-1.513**
1373729_at	ATP synthase mitochondrial F1 complex assembly factor 1	Atpaf1	1345	889	**-1.513**
1387080_at	structural maintenance of chromosomes 3	Smc3	5299	3504	**-1.512**
1397520_at	eukaryotic translation initiation factor 4, gamma 2 /// similar to eukaryotic translation initiation factor 4 gamma, 2	Eif4g2 /// LOC678831	1481	980	**-1.512**
1376655_at	---	---	869	575	**-1.512**
1392618_at	---	---	1010	669	**-1.511**
1393098_at	lethal giant larvae homolog 2 (Drosophila)	Llgl2	883	585	**-1.511**
1371351_at	RNA polymerase 1-3	Rpo1-3	3461	2293	**-1.510**
1384042_at	---	---	923	613	**-1.508**
1372134_at	coiled-coil-helix-coiled-coil-helix domain containing 6	Chchd6	658	437	**-1.506**
1379476_at	nucleoporin 35	Nup35	1910	1268	**-1.506**
1389274_at	dephospho-CoA kinase domain containing	Dcakd	850	565	**-1.505**
1370950_at	phosphatidic acid phosphatase type 2B	Ppap2b	737	489	**-1.505**
1372887_at	scavenger receptor class F, member 2	Scarf2	552	367	**-1.505**
1389117_at	O-sialoglycoprotein endopeptidase	Osgep	893	593	**-1.504**
1368069_at	SHANK-associated RH domain interactor	Sharpin	665	442	**-1.504**
1368385_a_at	growth factor receptor bound protein 2	Grb2	4882	3247	**-1.504**
1374858_at	DEAH (Asp-Glu-Ala-His) box polypeptide 29	LOC100362324	1609	1070	**-1.504**
1371887_at	high mobility group box 3	Hmgb3	878	584	**-1.503**
1373875_at	similar to RIKEN cDNA 1190005P17	RGD1308261	1076	716	**-1.503**
1390543_at	---	---	818	544	**-1.503**
1374912_at	kinesin family member 2C	Kif2c	977	650	**-1.503**
1390509_a_at	mitochondrial ribosomal protein L51	Mrpl51	2719	1810	**-1.502**
1392417_s_at	rCG32187-like /// TP53 regulating kinase	LOC100365491 /// Trp53rk	700	466	**-1.501**
1372331_at	eukaryotic translation initiation factor 1A, Y-linked	Eif1ay	3636	2423	**-1.501**
1369785_at	phosphoribosyl pyrophosphate amidotransferase	Ppat	1032	688	**-1.501**
1373468_at	---	---	1725	1149	**-1.501**
1395421_at	immunoglobulin superfamily, DCC subclass, member 3	Igdcc3	1348	899	**-1.500**
1371967_at	mitochondrial ribosomal protein L16	Mrpl16	2213	1475	**-1.500**
1387918_at	tropomyosin 3, gamma	Tpm3	1747	1165	**-1.500**
1382117_at	SET domain containing 6	Setd6	532	354	**-1.500**

APPENDIX B

Curriculum Vitae

Damayanti Chakraborty

Personal Information:

Born: 3rd March; 1982, Calcutta, India

Present position: Graduate Student, Department of Pathology and Laboratory Medicine,
University of Kansas Medical Center

Contact Information:

Department of Pathology and Laboratory Medicine,
University of Kansas Medical Center
39th and Rainbow Boulevard
Kansas City, KS 66160
Laboratory Phone: (913) 588-5690
Administrative Office Phone: (913) 588-5774
Fax: (913) 588-8287
Email: dchakraborty@kumc.edu

Education:

B.S	2003	Physiology	Presidency College, Calcutta University, Calcutta, India
M.S	2005	Biochemistry	Calcutta University, Calcutta, India
Ph.D.	2006-2013	Pathology/ Reproductive Biology	Department of Pathology and Laboratory Medicine, University of Kansas Medical Center, Kansas City, Kansas

Awards:

1. American Heart Predoctoral Fellowship, January-2010 – December-2011.
2. Biomedical Training Research Program Fellowship, University of Kansas Medical Center, July-2009 – June-2010.
3. First position in Basic Science Session 3, Student Research Forum, April-2010.
4. University of Kansas Medical Center student travel award 2008, 2010, 2012.

5. Best poster award, 4th Annual Gilbert S. Greenwald Symposium on Reproduction, Kansas City, Missouri, October 5-6, 2007.
6. Best poster award in International Conference on Male reproduction and infertility, Bangalore, India, September 16-18, 2005.
7. Qualified for lectureship in National Eligibility Test (NET) conducted by University Grants Commission (U G C), India, 2005.
8. Awarded scholarship by Education Directorate, Government of West Bengal, India for merit in Bachelor of Science Examinations, 2005.

Research Interests:

I am very interested to study epigenetic regulation of cell fate decisions particularly histone modifications underlying the stem and differentiation states and how delicate balance of different histone modifying enzymes governs these phenomena.

Research Support:

1. Recipient of a Predoctoral Fellowship from the American Heart Association, AHA Identification No. 10PRE2640133, January 1, 2010 to December 31, 2012. Project Title: Role of natural killer cells in uteroplacental vascular adaptations.
2. Recipient of Biomedical Training Research Program Fellowship, University of Kansas Medical Center, July-2009 – Dec-2009. Project Title: Role of natural killer cells in uteroplacental adaptations.

Oral Presentations:

1. **Chakraborty D**, Rumi MAK, Konno T, Asanoma K, and Soares MJ. Natural killer cells direct hemochorial placentation. Society for Gynecologic Investigation, Florida, March 16-19, 2011
2. **Chakraborty D**, Rumi MAK, Konno T, Asanoma K, and Soares MJ. Natural killer cell directed uterine spiral artery remodeling impacts oxygen delivery and trophoblast lineage decisions. Oral presentation at the Gordon Research Conference on Reproductive Tract Biology, Proctor Academy, Andover, New Hampshire, Aug 15-20, 2010.
3. **Chakraborty D**, Rumi MAK, Konno T, Asanoma K, and Soares MJ. Role of natural killer cells in uteroplacental vascular adaptations. Student Research Forum, University of Kansas Medical Center, Kansas City, Kansas, April 15-16, 2010.

4. **Chakraborty D**, Konno T, and Soares MJ. Role of uterine natural killer cells in uteroplacental adaptations. Student Research Forum, University of Kansas Medical Center, Kansas City, Kansas, April 9-10, 2009.

Book Chapters:

1. Varghese AC, **Chakraborty D**, and Bhattacharyya AK. Cryopreservation of Ovarian Tissue. In "The Laboratory Manual of Assisted Reproductive Technology" Editor: Rao, K A , Jaypee Brothers Medical Publishers, New Delhi, Chapter 22; pp 256-268.
2. **Chakraborty D** and Kumar TR. Murine models for reproduction. In "Sourcebook of models for biomedical research" Editor: Conn, PM, Humana Press, New Jersey, Chapter 44; pp: 411-423, 2008.

Publications:

1. Soares MJ, **Chakraborty D**, Renaud SJ, Kubota K, Bu P, Konno T, and Rumi MA. Regulatory pathways controlling uterine spiral artery remodeling. Journal of Reproduction and Development, 2012; 58:283-87.
2. **Chakraborty D**, Rumi MA, and Soares MJ. NK cells, hypoxia and trophoblast cell differentiation., Cell Cycle. 2012 Jul 1;11(13):2427-30.
3. Soares MJ, **Chakraborty D**, Karim Rumi MA, Konno T, and Renaud SJ. Rat placentation: an experimental model for investigating the hemochorial maternal-fetal interface. Placenta. 2012 Apr;33(4):233-43.
4. Asanoma K, Kubota K, **Chakraborty D**, Renaud SJ, Wake N, Fukushima K, Soares MJ, and Rumi MAK. SATB homeobox proteins regulate trophoblast stem cell renewal and differentiation. J Biol Chem. 2012 Jan 13;287(3):2257-68.
5. **Chakraborty D**, Rumi MA, Konno T, and Soares MJ. Natural killer cells direct hemochorial placentation by regulating hypoxia-inducible factor dependent trophoblast lineage decisions. Proc Natl Acad Sci U S A. 2011 Sep 27;108(39):16295-300.
   Highlighted by: Biology of Reproduction
   http://www.biolreprod.org/content/early/2011/09/20/biolreprod.111.096537.abstract
   Faculty of 1000: http://f1000.com/13399011
   University of Kansas Medical Center: http://pa.kumc.edu/news-listing-page/illuminating-the-complexities-of-fetal-programming.html

6. Asanoma K, Rumi MAK, Kent LN, **Chakraborty D**, Renaud SJ, Wake N, Lee DS, Kubota K, and Soares MJ. FGF4-dependent stem cells derived from rat blastocysts differentiate along the trophoblast lineage. Dev Biol. 2011 Mar 1;351(1):110-9.

Abstracts Presented:

1. **Chakraborty D**, Rumi MA, Krieg AJ, and Soares MJ. Role of hypoxia signaling in trophoblast cell lineage commitment. Faseb Science Research Conference on Transcriptional Regulation During Cell Growth, Differentiation, and Development, Snowmass, Colorado July 15-20, 2012
2. Rumi MA, **Chakraborty D**, Asanoma K, Kubota K, Bu P, PhD, Renaud SJ, and Soares MJ. Transcriptional hierarchy of SATB homeobox proteins in trophoblast stem cells. Fetal Programming and Environmental Exposures: Implications for Prenatal Care and Pre-Term Birth. The New York Academy of Sciences, NY June 11-12, 2012.
3. **Chakraborty D**, Rumi MAK, Krieg AJ, and Soares MJ. Role of hypoxia signaling in trophoblast cell lineage commitment. Poster presented in 8th Annual Gilbert S. Greenwald Symposium on Reproduction, Kansas City Kansas, Missouri, 2011
4. Asanoma K, Kubota K, **Chakraborty D**, Renaud SJ, Soares MJ, and Rumi MA. SATB homeobox proteins regulate trophoblast stem cell renewal and differentiation. Poster presented in 8th Annual Gilbert S. Greenwald Symposium on Reproduction, Kansas City Kansas, Missouri, 2011.
5. Rumi MA, Kent LN, Lee DS, **Chakraborty D**, Konno T and Soares MJ. Rat placental lactogen II promoter directs trophoblast giant cell specific expression. Gordon Research Conference on Reproductive Tract Biology, Andover, New Hampshire. Aug 15-20, 2010
6. **Chakraborty D**, Konno T, Soares MJ. Uterine natural killer cells: Homing and their effects on rat placentation. Poster presented in fourth Annual Gilbert S. Greenwald Symposium on Reproduction, Kansas City, Missouri, October 9-11, 2008.
7. **Chakraborty D**, Konno T, and Soares MJ. Uterine natural killer cells: Homing and their effects on rat placentation. Poster presented in Gordon Research Conference on Reproductive Tract Biology, Proctor Academy, Andover, New Hampshire, August 3-8, 2008.
8. **Chakraborty D**, Konno T, and Soares MJ. Role of uterine natural killer cells in rat placentation. Oral presentation in Student Research Forum (SRF), University of Kansas Medical center, Kansas City, Kansas, April 11-12, 2008.

9. **Chakraborty D**, Konno T, and Soares MJ. Uterine natural killer cells: Their effects on rat placentation. Poster presented in fourth Annual Gilbert S. Greenwald Symposium on Reproduction, Kansas City, Missouri, October 5-6, 2007.

10. **Chakraborty D**, Varghese AC, Mukhopakhaya D, Bhattacharya SM, Bhattacharyya AK, and Agarwal A. Motility characteristics and DNA integrity of spermatozoa processed with different concentrations of reduced glutathione (GSH). Poster presented in 62nd annual meeting of ASRM, Louisiana, New Orleans, October 2006.

11. **Chakraborty D**, Varghese AC, and Bhattacharyya AK. Study on pronuclear morphology and cleavage kinetics as scoring criteria for selection of best embryo for transfer. Poster presented in International Conference on Male Reproduction and Infertility, Indian Institute of Science, Bangalore, India, September 16-18, 2005.